Exploring the Roles and Interplay of REST and USP15 in Cancer

Matthew Concannon

Thesis submitted in accordance with the requirements of the

University of Liverpool for the Degree of Doctor in Philosophy

August 2017

Exploring the Roles and Interplay of REST and USP15 in Cancer

Matthew Concannon

Abstract

Repressor Element-1 (RE-1) Silencing Transcription Factor (REST), through the actions of associated co-repression complexes, modifies chromatin with repressive epigenetic modifications. REST can regulate a myriad of genes that in part, restricts access to proteins expressed in neuronal cells. During the cell cycle REST is acutely degraded at the onset of mitosis, which is required for effective cell division. As cells exit mitosis, re-expression of REST protein is supported by co-translational deubiquitylation of USP15. The overarching aim of this project was to explore the relationship between REST and USP15 in lung cancer and during the cell cycle.

The expression of REST is differentially regulated in neuroendocrine cancers, with a known increase in a truncated isoform, REST4. In response to the finding of a novel protein coding REST transcript, I performed a quantitative assessment of REST expression in thoracic cancers. Simultaneously, I analysed the expression of USP15 and its isoforms. Interestingly, USP15 isoform 1 was markedly increased in neuroendocrine cancer cell lines. During the cell cycle, the truncated REST4 isoform was increased eight-fold during mitosis, which coincides with the degradation of full-length protein. The splicing factor proposed to regulate splicing of REST was not identified in the cell line.

The regulation of gene expression by full-length REST underpins its tumour suppressive function. The loss of REST elicits broad transcriptional changes and is complicated by intricate feedback loops of opposing mRNA and miRNAs. As such, the consequences of REST dysregulation or loss on the cellular proteome and systems are not well studied. Here, I addressed the consequences of the loss of REST in lung cancer, using a proteomic approach in combination with siRNA knockdown. The proteins responsive to REST or USP15 knockdown, were used to determine cellular pathways that could influence cellular physiology. The aim of which is to determine whether the loss of REST protein promotes the neuroendocrine phenotype or metastatic properties in lung cancer. As USP15, is a known regulator of REST protein expression, parallel proteomic studies were performed and correlated to determine the interplay of USP15 and REST.

USP15-mediated regulation of mitochondrial Complex I proteins, identified by proteomic analysis, suggested a potentially novel role for USP15. The downregulation of Complex I proteins and proposed dysfunction of mitochondrial Complex I was not apparent in high-glucose conditions. Future experiments are required to determine the extent of USP15 involvement.

Acknowledgments

Firstly, I would like to thank the Wellcome Trust for funding this research study and PhD and to the University of Liverpool for providing me with additional support which has helped me to get this far.

This thesis would not have been possible were it not for a number of very inspirational and supportive individuals. My sincere gratitude goes to my primary supervisor, Professor Judy Coulson for her continued patience, enthusiasm and encouragement, particularly when I was writing this thesis. My thanks also to my secondary supervisor, Professor Ian Prior for his objective insight. I will be forever grateful to both of you for helping me to achieve what I sometimes thought would be impossible.

I am fortunate to have worked in a lab filled with fantastic people. The hard-working and convivial atmosphere is something I will always cherish. I am especially grateful to Dr Andrew Fielding for being my lunch-mate, being a good listener and helping me avoid the rabbit holes of intellectual curiosity. I would like give a special mention to; Dr. Jenna Kenyani for organising some of the best fancy dress parties ever, Zohra Butt for her love of cake and Dr. Sarah Darling for making me feel so welcome. Thank you all for your ability to make me smile.

I cannot fail to mention my many friends Neil, Dorota, Rachael, Dr. Dr. Joe and Matheus, as well as everyone on the fifth floor, Ewan, Alice, Aitor, Emma, Fiona, Leah, Doug, Yvonne, Arnaud, Eri … et al.

Finally, my deep and sincere gratitude to my parents, Carole and Stephen for their unfailing belief in my ability and never ending supply of tea. To my siblings Robert and Hannah for always being there for me, no matter what. To the rest of my family for their continuous and unparalleled love, good old fashioned northern humour and common sense. I couldn't have done it without you.

CONTENTS

Abstract i
Acknowledgments ii
CONTENTS....1
List of Tables....7
List of Figures....8
List of Abbreviations....10

CHAPTER 1: INTRODUCTION....15
1.1 Regulation of Transcription....15
1.1.1 Basal Gene Expression....15
1.1.2 Sequence-Specific Transcription Factors....15
1.1.3 Transcriptional Co-Factors....16
1.1.3.1 Chromatin....16
1.1.3.2 Transcriptional Regulation by Histone Modifications....17
1.1.3.3 Transcriptional Regulation by ATP-Dependent Chromatin Remodelling....17
1.2 The Repressor Element -1 Silencing Transcription Factor (REST)....18
1.2.1 Discovery of REST....18
1.2.2 REST Molecular Biology and Cellular Function....19
1.2.2.1 Zinc Fingers and DNA binding....20
1.2.2.2 Nuclear Localisation: NLS and ZFs....21
1.2.2.3 Repression Domains and Repression Complexes....22
1.3 Regulation of REST Expression and Activity....24
1.3.1 Transcriptional Regulation of REST....25
1.3.2 Epigenetic Regulation of REST....26
1.3.3 Alternative Splicing of REST....27
1.3.4 Post-Translational Regulation of REST....28
1.3.4.1 Glycosylation....29
1.3.4.2 Phosphorylation....29
1.3.4.3 REST Ubiquitylation....31

1.4 REST Physiology and Pathology 32
1.4.1 REST Physiology 32
1.4.1.1 Neuronal Differentiation 32
1.4.1.2 Adult Tissue 33
1.4.1.3 Neuroendocrine Phenotype 34
1.4.2 REST Pathology 35
1.4.2.1 Adult Neurons 36
1.4.2.2 REST in Cancer: Oncogene or Tumour Suppressor 36
1.4.2.2.1 Genetic Causes of REST Dysfunction 37
1.4.2.2.2 Dysfunctional Alternative Splicing of REST 38
1.4.2.2.3 Post-Transcriptional Regulation of REST 39
1.5 Ubiquitylation: A Versatile Post-Translational Modification 39
1.5.1 Discovery of Ubiquitin 40
1.5.2 The Ubiquitylation Machinery: Writing the Ubiquitin Code 40
1.5.3 Diversity of the Ubiquitin Code 40
1.5.4 Reading the Ubiquitin Code 42
1.6 Deubiquitylation and Deubiquitylases 42
1.6.1 Deubiquitylases: Erasing the Ubiquitin Code 42
1.6.2 Ubiquitin Specific Peptidase 15 (USP15) 45
1.6.2.1 Domain Structure and Regulation of USP15 45
1.6.2.2 Cellular Roles of USP15 48
1.6.2.3 USP15 Association with Cancer 49
1.6.2.4 USP15 Role in the Reversible Ubiquitylation of REST 50
1.7 Project Aims 52
1.7.1 Chapter 3 52
1.7.2 Chapter 4 53
1.7.3 Chapter 5 53

CHAPTER 2: MATERIALS AND METHODS 54
2.1 Cell Biology 54
2.1.1 Reagents 54
2.1.2 Routine Cell Culture 54

2.1.3 Stable Isotope Labelling with Amino Acids in Cell Culture (SILAC) 58
2.1.4 Cell Synchronisation 58
2.1.5 siRNA Knockdown 60
2.1.6 Flow Cytometric Analysis of Cell Cycle....61
2.1.7 Measuring Cellular Bioenergetics 62
2.2 Molecular Biology 64
2.2.1 Reagents....64
2.2.2 RNA Extraction 65
2.2.3 Reverse Transcription Polymerase Chain Reaction (RT-PCR) ...66
2.2.3.1 Reverse Transcription 66
2.2.3.2 Endpoint RT-PCR 66
2.2.3.3 Quantitative Real-Time PCR (qRT-PCR) 68
2.2.4 Agarose Gel Electrophoresis 69
2.3 Protein Biochemistry 70
2.3.1 Reagents....70
2.3.2 Protein Extraction and Sample Preparation....70
2.3.3 SDS-PolyAcrylamide Gel Electrophoresis (SDS-PAGE) 71
2.3.4 Immunoblotting 72
2.3.5 Liquid Chromatography-Tandem Mass Spectroscopy (LC-MS/MMS) 74
2.3.5.1 1D PAGE and Sample Preparation....74
2.3.5.2 Liquid Chromatography (LC) and Tandem Mass Spectrometry (MS/MS) 75
2.3.5.3 Protein Assignments 76
2.4 Bioinformatics and Statistics 76
2.4.1 Statistical Analysis 76
2.4.2 Gene Ontology and Pathway Analysis....77

CHAPTER 3: REST AND USP15 EXPRESSION IN THORACIC CANCERS AND THROUGH THE CELL CYCLE....78
3.1 REST and USP15 Expression....78

3.1.1 Thoracic Cancers....78
3.1.2 Cell Cycle....79
3.2 Results....80
3.2.1 The Differential Expression of REST Splice Variants in Lung Cancer Cell Lines....80
3.2.2 Expression of REST-Regulators in Lung Cancer Cell Lines....86
3.2.3 USP15 Expression and Relationship with REST in Thoracic Cell Lines....90
3.2.4 Cell Cycle Profiles of REST and REST-Regulators....96
3.2.4.1 Protein Expression Profiles of REST and USP15....99
3.2.4.2 qRT-PCR Analysis of Deubiquitylase Regulators of REST....100
3.2.5 Differential Expression of REST Isoforms Through the Cell Cycle....102
3.3 Discussion....106
3.3.1 Expression of REST and USP15 in Thoracic Cancers....106
3.3.2 REST Expression During the Cell Cycle....108

CHAPTER 4: REST AND USP15-DEPENDENT PROTEOMES....110
4.1 The REST and USP15-Dependent Proteomes....110
4.1.1 Proteomic Analysis....110
4.1.2 A REST-Dependent Proteome....111
4.1.3 The USP15-Dependent Proteome....111
4.1.4 A USP15-REST Axis....112
4.2 Results....112
4.2.1 Experimental Design for Proteome Analysis....112
4.2.2 Protein Sampling and Reproducibility of Protein Identification....114
4.2.3 The USP15 and REST Responsive Proteomes....119
4.2.4 Cellular Functions of USP15 and REST-Responsive Proteins....122
4.2.5 Identification and Validation of Responsive Proteins....130
4.2.5.1 The Response of EGFR and VCL to USP15 Depletion....134
4.2.5.2 The Response of Integrins to REST Depletion....136
4.3 Discussion....138

4.3.1 Proteomic Analysis 138
4.3.2 REST 'omics' 140
4.3.3 GO Analysis of USP15 or REST-Dependent Proteomes.....141
4.3.3.1 REST and the Proteasome 142
4.3.3.2 REST and/or USP15 Responsive Proteins 142
4.3.4 REST and USP15-Dependent Actin Cytoskeletal Proteins 143
4.3.5 The USP15-Dependent Proteome 144

CHAPTER 5: THE USP15-MEDIATED REGULATION OF MITOCHONDRIAL PROTEINS 146
5.1 The USP15-Mediated Regulation of Mitochondrial Proteins 146
5.1.1 The Mitochondria 146
5.1.2 The Electron Transport Chain Complexes 146
5.1.3 Mitochondrial Protein Regulation 147
5.2 Response of Mitochondrial Proteins and Processes to USP15 and/or REST Depletion 148
5.2.1 Identifying Biological Processes of Mitochondrion-based siREST Responsive Proteins 151
5.2.2 Identifying Biological Processes of Mitochondrion-based siUSP15 Responsive Proteins 152
5.2.3. The Electron Transport Chain Response to USP15 Depletion .153
5.2.3.1 ETC Complex I Proteins are Selectively Reduced by siUSP15 153
5.2.3.1 Validation of siUSP15 Effect on Complex I Protein Expression 156
5.2.3.2. Bioenergetic Assessment of Cells in Response to USP15 Knockdown 162
5.3 Discussion 168
5.3.1 Complex I Dysfunction and NDUF Proteins 168
5.3.2 Potential Mechanisms of DUB Mediated Regulation of Mitochondrial Function and Proteins 171

5.3.2.1 DUB-mediated Regulation of Transcription and Upstream Signalling....171
5.3.2.2 USP15 Regulation of Protein Localisation....172
5.3.2.3 Ubiquitylation of Mitochondrial Proteins....173
5.3.2.4. DUBs and Mitochondrial Protein Quality Control and Degradation....173

CHAPTER 6: DISCUSSION....175
6.1 The Influence of REST Expression on Neuroendocrine Lung Cancer....175
6.2 REST Isoform Expression in Thoracic Cancers and During the Cell Cycle....177
6.2 USP15 Isoform Expression in Thoracic Cancer and During the Cell Cycle....180
6.3 A Proteomic Approach to Investigating New Roles for USP15 and REST in Lung Cancer....181
6.4 USP15-Regulation of Mitochondrial Complex I....184
Bibliography....187

List of Tables

Table 1.1 Ubiquitin Chain Linkages and Functions 41
Table 1.2 USP15 Protein Isoforms 46
Table 2.1 Cell Lines 56
Table 2.2 SILAC Amino Acids 58
Table 2.3 Details of siRNA oligonucleotides 61
Table 2.4. PCR Primers 67
Table 2.5. Primary Antibodies 73
Table 2.6. Secondary Fluorescent Antibodies 73

List of Figures

Figure 1.1 REST Protein Isoforms and Interactors 20
Figure 1.2 USP15 Protein Isoform 1 and Domains 46
Figure 1.3 Cell Cycle Dependent Ubiquitylation and Deubiquitylation of REST 51
Figure 2.1. Cell Cycle Synchronisation Regime 59
Figure 3.1. Validation of PCR Primers for REST Splice Variants..... 81
Figure 3.2. REST Splice Variant Expression in a Lung Cell Line Panel..... 83
Figure 3.3. Comparison of REST Splice Variant Expression between Neuroendocrine and Non-Neuroendocrine Cells 85
Figure 3.4. Validation of PCR Primers for REST Regulators and Dependent Transcript 88
Figure 3.5. REST Splicing Factor and REST-Dependent Transcript Expression in Thoracic Cells..... 89
Figure 3.6. Comparison of REST Transcripts with SRRM4 and SCG3..... 91
Figure 3.7. USP15 Transcript and Splice Variants in a Thoracic Cell Panel 94
Figure 3.8. USP15 Isoforms Expression Comparisons with REST Variants 95
Figure 3.9. Cell Cycle Synchronisation of A549 cells..... 97
Figure 3.10. REST and USP15 Protein Expression Throughout the Cell Cycle 100
Figure 3.11. qRT-PCR Analysis of REST Regulators Through the Cell Cycle 101
Figure 3.12. Increased REST4 Splicing During Mitosis 104
Figure 3.13. SRRM4 Primer Optimisation for A549 Cell Cycle Expression 105
Figure 4.1. SILAC Experiment Configuration 113
Figure 4.2. Peptide Sampling and Reproducibility of Protein Identification 116
Figure 4.3. Comparison of Protein Responses between Independent Experiments 118
Figure 4.4. Distribution of Responsive and Significant Proteins..... 120
Figure 4.5 Cross Correlation of siUSP15 and siREST Responsive Proteins 121

Figure 4.6. Gene Ontology Analysis of siUSP15 or siREST Responsive Proteins 123
Figure 4.7. Cellular Components Categories 125
Figure 4.8 Proteasome Protein Response to siREST Knockdown 127
Figure 4.9. Molecular Function and Biological Process GO Categories 129
Figure 4.10. Significant Actin-Associated Terms Respond Differently to siUSP15 and siREST 131
Figure 4.11. Validation of Selected Actin-Related Proteins Response to siUSP15 and siREST 133
Figure 4.12. Response of EGFR and VCL in an Independent USP15 Knockdown..... 135
Figure 4.13. Response of ITGA2 and ITGB1 in an Independent REST Knockdown..... 137
Figure 5.1. The Mitochondrion Protein Response to siRNA knockdown.... 149
Figure 5.2. The Electron Transport Chain (ETC) 154
Figure 5.3. Validation of NDUF Protein Changes..... 157
Figure 5.4. siRNA USP15 deconvolution of NDUF protein expression 160
Figure 5.5. Validation of NDUF knockdown using isoform specific siRNA. 161
Figure 5.6. Seahorse System and the Mitochondrial Stress Test 163
Figure 5.7. Seahorse Optimisation..... 165
Figure 5.8. siRNA knockdown effects on Mitochondrial Stress Test..... 167

List of Abbreviations

Abbreviation	Definition
ACN	Acetonitrile
ACTB	b-Actin
ALDH3A2	Aldehyde Dehydrogenase 3A2
AP-1	Activator Protein 1
APC	Adenomatous Polyposis Coli
ATM	Ataxia-Telangiectasia Mutated
ATP5	ATP Synthase Subunit F6
ATP6	Mitochondrially Encoded ATP Synthase 6
ATR	Rad3-Related
ATXN3	Ataxin-3
BAFs	BRG1 Associated Factors
BAP1	BRAC1 Associated Protein
BCA	Bicinchoninic Acid
BDNF	Brain Derived Neurotrophic Factor
BHC80	BRAF-HDAC Complex Protein 80
BMP	Bone Morphogenetic Protein
Bp	Base Pairs
BRAP	BRCA1-Associated Protein
BSA	Bovine Serum Albumin
C/EBP	CCAAT-Enhance-Binding Protein
CCN	Cyclin
cDNA	Complimentary DNA
CDYL	Chromodomain Y-like
CHIP	C-terminus of Heat Shock Cognate 70-Interacting Protein
ChIP-Seq	Chromatin Immunoprecipitation Sequencing
CID	Collison Induced Dissociation
CK1	Casein Kinase I
CK2	Casein Kinase II
COP9	Constitutive Photomorphogenesis 9
CoREST/RCOR1	REST Co-repressor 1
CPS1	Carbamoyl-Phosphate Synthase 1
Cq	Threshold Cycle
CREB	cAMP Responsive Element Binding
CRL	Cullin-RING Ligase
CSN	COP9 Signalosome
CYB5B	Cytochrome b5 Type B
DCNT1	Dynactin p150^{Glued}
DSP	Desmoplakin
DTT	Dithothreitol

DUB	Deubiquitylase
DUSP	Domain present in USPs
DYRK1A	Dual-Specificity Tyrosine Phosphorylation Regulated Kinase 1A
E1A	Early Region 1A Protein
E6AP	E6 Associated Protein
ECAR	Extracellular Acidification Rate
EGF	Epidermal Growth Factor
EGFR	Epidermal Growth Factor Receptor
EHMT2	Euchromatic Histone-Lysine N-methyltransferase
ELK1	ETS-domain Containing Protein 1
ERK	Extracellular Signal-Regulated Kinase
ESCs	Embryonic Stem Cells
ESI	Electrospray Ionisation
ETC	Electron Transport Chain
EZH2	Enchancer of Zeste Homolog 2
FCCP	Carbonyl cyanide 4-(trifluoromethoxy)phenylhydrazone
FSC/SSC	Forward Scatter/Side Scatter
GO	Gene Ontology
GTFs	General Transcription Factors
H3K4me1	Histone 3 Lysine 4 Mono-methylation
H3K9me3	Histone 9 Lysine 4 Tri-methlyation
HAP1	Huntingtin Associated Protein 1
HATs	Histone Acetylases
HCN2	Hyperpolarization-activated Cyclic Nucleotide-modulated Potassium Channel Protein 2
HDACs	Histone Deacetylases
HEK 293	Human Embryonic Kidney 293
HGF	Hepatocyte Growth Factor
HIPPI	Huntingtin Interacting Protein 1 Protein Interactor
HKDC1	Hexokinase Domain-Containing protein 1
HPV16	Human Papilloma Virus type 16
Hsc	Heat Shock Cognate
HTT	Huntingtin
IB1/JIP-1	Islet-Brain1/c-Jun amino-terminal kinase Interacting Protein-1
IKKB	Inhibitor of NF-kB Kinase b
IPI	International Protein Index
ITG	Integrin
JAMM	JAB1/MPN/MOV34
KCC2	K^+/Cl^- co-transporter
KDM5C	Lysine Specific Demethylase 5C
LACTB	Lactamase β

LC	Liquid Chromatography
LC/MS	Liquid Chromatography-tandem Mass Spectrometry
lincRNA	Long Intergenic Non-coding RNA
lncRNA	Long Non-coding RNA
LSD1/KDM1A	Lysine Specific Demythlase 1
Mad2	Mitotic Arrest Deficient 2
MAPK	Mitogen-Activated Protein Kinase
MDM2	Mouse Double Minute 2 Homolog
MECP2	Methyl-CpG Binding Protein 2
MEF	Mouse Embryonic Fibroblast
MEK	Mitogen Activated Protein Kinase Kinase
MINDY	Motif Interating with ubiquitin-containing novel DUB
miRNA	MicroRNA
MOPS	3-(N-morpholino) Propanesulfonic Acid
mRNA	Messenger RNA
MS/MS	Tandem Mass Spectrometry
NAD	Nicotinamide Adenine Dinucleotide
NCAM	Neuronal Cellular Adhesion Molecule
ncRNA	Non-coding RNA
NDUF	NADH:Ubiquinone Oxidoreductase Family
NE	Neuroendocrine
neuroD	Neurogenic Differentiation
NF-kB	Nuclear Factor Kappa B
NLS	Nuclear Localisation Signal
Non-NE	Non-neuroendocrine
NPC/C	Anaphase Promoting Complex/Cyclosome
NRSF	Neuron-Restrictive Silencing Factor
NSC/Ps	Neural Stem/Progenitor cells
NSCLC	Non-small Cell Lung Cancers
nSR100	Neuronal-specific SR-related Protein of 100kDa
NTRK2	Neurotrophic Receptor Tyrosine Kinase 2
OCR	Oxygen Consumption Rate
OTUs	Ovarian Tumour Proteases
PC12	Phenochromocytoma cell line
PCR	Polymerase Chain Reaction
Phosphodegrons	Phosphorylation-inducing Degradation Regions
PI	Propidium Iodide
PI3K	Phosphoinositide 3 Kinase
PIC	Pre-Initiation Complex
Pin1	Peptidylpropyl cis/trans isomerase 1
PKB	Protein Kinase B
Pol II	RNA Polymerase II
polyQ-HTT	PolyGlutamine expanded HTT

POU2F1	POU Class 2 Homeobox 1
PRC2	Polycomb Repressive Complex 2
PSM	Proteasome subunits
PTMs	Post-Translational Modifications
Q	Ubiquinone
qRT-PCR	Quantitative Real Time Polymerase Chain Reaction
RDs	Repression Domains
REST	Repressor Element-1 Silencing Transcription Factor
REST-FS	Truncated REST Protein
RILP/PRICKLE1	REST-Interacting LIM domain protein
RT-PCR	Reverse Transcription Polymerase Chain Reaction
SART3	Squamous cell Antigen Recognised by T-Cells 3
$SCF^{\beta\text{-}TrCP}$	Skp1-Cullin1-F-Box β-TrCP ubiquitin E3-ligase
SCG3	Secretogranin III
SCLC	Small Cell Lung Cancer
SCP1	Carboxyl-terminal domain Small Phosphatase 1
SDS-PAGE	SDS-PolyAcrylamide Gel Electrophoresis
SELEX	Systematic Evolution of Ligands by Exponential Enrichments
Ser/S	Serine
shRNA	Short Hairpin RNA
SILAC	Stable Isotope Labelling of Amino Acids in Cell Culture
SIN3A/B	SIN Transcription Regulator family member 3A/B
siRNA	Small Interfering RNA
SMARCA4/BRG1	SWI/SNF-related Matrix-Associated Actin-Dependent Regulator of Chromatin, subfamily A, member 4
SOD	Superoxide Dismutase 2
SOX5	SRY-related HMG box 5
SP1	Specificity Protein 1
SRRM4	Serine/Arginine Repetitive Matrix 4
SUMO	Small Ubiquitin-Like Modifier
SWI/SNF	Switch/Sucrose Non-Fermentable
TBP	TATA Binding Protein
TBS-T	Tris Buffered Saline-Tween-20
TCF	T-cell Factor
TEMED	Tetramethylethylenediamine
TFs	Transcription Factors
TGF-β	Transforming Growth Factor β
TOP2A	Topoisomerase II
TSS	Transcriptional Start Site

TβRI	TGF-β type I receptor
UAF1	USP1-Associated Factor
UBA	Ubiquitin Associated
UBL	Ubiquitin-Like
UCHs	Ubiquitin C-terminal Hydrolases
UIMs	Ubiquitin Interacting Motifs
UPS	Ubiquitin-Proteasome System
UQCRC	Ubiquinol-Cytochrome C Reductase
USP15	Ubiquitin Specific Peptidase 15
USP7	Ubiquitin Specific Peptidase 7
USPs	Ubiquitin Specific Peptidases
VCL	Vinculin
VEZF1	Vascular Endothelial ZF1
ΨM	Mitochondrial Protein Gradient
YY1	Ying-Yang 1
ZEB1	Zinc Finger E-box Binding Homeobox
ZF	Zinc Finger

CHAPTER 1: INTRODUCTION

1.1 Regulation of Transcription

1.1.1 Basal Gene Expression

Genes are transcribed by three core transcriptional complexes, the RNA polymerases, which convert DNA into all types of RNA. Importantly, RNA Polymerase II (Pol II) regulates the expression of messenger RNA (mRNA), which encodes proteins, as well as microRNA (miRNA) precursors and long non-coding RNA (lncRNA). In order to be transcribed, most genes contain a promoter sequence with a TATA box or TATA-like sequences. These provide interaction sites for the pre-initiation complex (PIC), a combination of polymerases and the general transcription factors (GTFs). GTFs are multi-subunit proteins which recognise the promoter to recruit, and assist in the positioning of Pol II and selection of the transcriptional start site (TSS). One GTF, TFIID, includes the TATA binding protein (TBP) subunit that recognises the promoter through interaction with the TATA box (Cormack and Struhl, 1992).

The selection of genes for expression is driven by diverse regulatory motifs, which act as binding sites for sequence-specific transcription factors. These can recruit transcriptional co-factors that remodel chromatin to allow or restrict access to the gene for transcription in spatially or temporally defined patterns.

1.1.2 Sequence-Specific Transcription Factors

The genes that are subject to regulation by individual transcription factors (TFs), are determined by the preference of each TF to interact with a specific DNA consensus sequence, known as a motif. The release of the human genome sequence and recent developments in computation analysis, in combination with improved methodologies such as chromatin immunoprecipitation sequencing (ChIP-Seq) and systematic evolution of ligands by exponential enrichments (SELEX), has dramatically increased our

knowledge of DNA binding proteins and TF motifs. It is now well documented that the expression of a gene can be regulated by a myriad of transcription factors, which are not limited by recruitment to TSS-adjacent motifs but can be recruited at distant *cis*-regulatory elements. Such distant TF-mediated regulation of gene expression can be implemented through interaction with the mediator complex, which binds to the C' terminal domain of Pol II and brings the TF into proximity with the basal transcriptional machinery (Allen and Taatjes, 2015).

The families of TFs are grouped by the sequence and structure of their DNA binding domains. The largest family of TFs are the C_2H_2 zinc finger proteins, which account for 3% of the genome (Klug, 2010). In addition to DNA binding, TFs can regulate PIC assembly and activity through the recruitment of co-factors and co-repressors, which provide additional biological functions, such as the ability to modify chromatin structure.

1.1.3 Transcriptional Co-Factors

1.1.3.1 Chromatin

Chromatin is composed of DNA and associated proteins, arranged in higher order structures of nucleosomes. A nucleosome consists of an octamer of histone proteins (H2A, H2B, H3 and H4) and 146 base pairs of DNA capped with a linker histone (H1). Histone post-translational modifications are complex and varied producing a 'histone code' (Jenuwein and Allis, 2001) with modifications including: acetylation, phosphorylation, methylation, ubiquitylation, sumoylation, deimination/citrullination, proline isomerization, ADP ribosylation, formylation, propinoylation and butyrylation. These modifications are predominantly localised on the tails of histones that protrude from the histone-DNA interface, and are primarily involved in the recruitment of non-histone proteins. The post-translational modification of histones and their ability to regulate DNA are associated with all manner of DNA-centric processes: transcription, replication, repair and condensation (Kouzarides, 2007). The recruitment of histone modifying enzymes by TFs is of specific

interest in understanding the nature of cell-specific gene expression. Here, those modifications that are associated with activation or repression of gene expression will be briefly discussed.

1.1.3.2 Transcriptional Regulation by Histone Modifications

Acetylation and methylation of histones and their involvement in the regulation of gene expression was proposed as early as 1964 (Allfrey et al., 1964). Recent decades have provided more detail about the molecular deposition ('writers'), removal ('erasers') and the effects post-translational modifications elicit through the recruitment of binding partners ('readers'). The acetylation of histones induces transcription with histone hypoacetylation around a gene, indicative of transcriptional repression (Jenuwein and Allis, 2001). Acetylation is deposited by histone acetylases (HATs) and removed by histone deacetylases (HDACs, class I and II).

The methylation of histones, performed by lysine methyltransferases, controls chromatin structure and protein interactions, and is associated with either activation or repression. For example, Histone 3 Lysine 4 mono-methylation (H3K4me1) activates expression whilst Histone 3 Lysine 9 tri-methylation (H3K9me3) is repressive. The reversal of methylation, by demethylases can counteract the positive or negative roles of methylation (Bannister and Kouzarides, 2005). For example, lysine specific demethylase 1 (LSD1 also known as KDM1A) specifically demethylates K9 to activate or K4 to repress transcription, the latter only in complex with REST co-repressor 1 (CoREST) (Chapter 1, Section 2.2.3) (Shi et al., 2004).

1.1.3.3 Transcriptional Regulation by ATP-Dependent Chromatin Remodelling

To access TF motifs, active remodelling of the chromatin may be required to reveal these sites. The Switch/Sucrose Non-Fermentable (SWI/SNF) remodelling complexes can be recruited by TFs, through interaction of their components such as SWI/SNF-related, matrix-associated,

actin-dependent regulator of chromatin, subfamily a, member 4 (SMARCA4/BRG1) and BRG1 associated factors (BAFs) (Spitz and Furlong, 2012).

1.2 The Repressor Element -1 Silencing Transcription Factor (REST)

1.2.1 Discovery of REST

Physiologically, the expression of sodium ion channels in neuronal cells, which contribute to their electrophysiological properties, was observed as a key behavioural change induced by differentiation in 1990 (Maue et al., 1990). Upstream of these sodium channel genes was a 21-base pair DNA sequence, now known as the Repressor Element-1 (RE-1) motif. Removal of this RE-1 motif resulted in increased sodium channel gene expression, indicating that it was the binding site for a transcriptional silencing factor.

REST, the protein responsible for RE-1 mediated gene repression was independently discovered in 1995 by two groups (Schoenherr and Anderson, 1995, Chong et al., 1995). Due to its perceived role, Schoenherr and Anderson named it the Neuron-Restrictive Silencing Factor (NRSF), whilst Chong *et. al* named the same protein REST. Following the identification of RE-1 motifs in additional genes not directly associated with a neuronal lineage differentiation (Otto et al., 2007, Johnson et al., 2007), the literal nomenclature Repressor Element-1 Silencing Transcription Factor (REST) became the official gene name. To date, more than 200 articles have been published about REST (PubMed, July 2017).

Prominent physiological roles of REST have been identified and, when the gene is ablated, this leads to embryonic lethality at day E11.5, after widespread apoptotic cell death at the onset of neurogenesis, as REST is important for neuronal differentiation (Chen et al., 1998, Ballas et al., 2005, Westbrook et al., 2008, Huang et al., 2011, Chong et al., 1995). The dysregulation of REST has functional roles in the pathology of neurological disorders and cancers (Lu et al., 2014, Coulson, 2005, Negrini et al., 2013,

Zhu et al., 2014, Westbrook et al., 2005). The physiological roles of REST will be discussed in more detail in Chapter 1, Section 4. To understand the mechanisms by which REST contributes to cell-specific functions first requires a greater understanding of the molecular biology of REST, and the complexity of the repression complexes and chromatin modifications that are targeted to RE-1 sites by REST.

1.2.2 REST Molecular Biology and Cellular Function

REST is a nuclear-localised glycoprotein consisting of a 120kDa protein, and post-translational modifications that can increase the apparent molecular weight by approximately 100kDa (Chapter 1, Section 3.4). REST is a multi-domain protein composed of a zinc finger (ZF) array that interacts with DNA, a nuclear localisation signal (NLS) and protein-interaction domains, including residue-rich regions and two repression domains (Figure 1). As a transcriptional repressor, the NLS, DNA-binding and repression domains are important for REST function. Less is known about the function of the residue-rich regions.

The major domains of REST, their functions, interacting proteins and roles in REST-mediated regulation of gene expression are discussed in more detail below. Here I focus on the description of the full-length isoform of REST known as REST1. Interestingly though, other REST isoforms have been described (Figure 1.1) that lack the canonical C' terminal exon, which encodes for several ZFs, the residue-rich regions and the C' terminal repression domain (Chapter 1, Section 3.3). These REST isoforms are capable of interacting with DNA and inducing repression, although with less efficiency than the full-length protein.

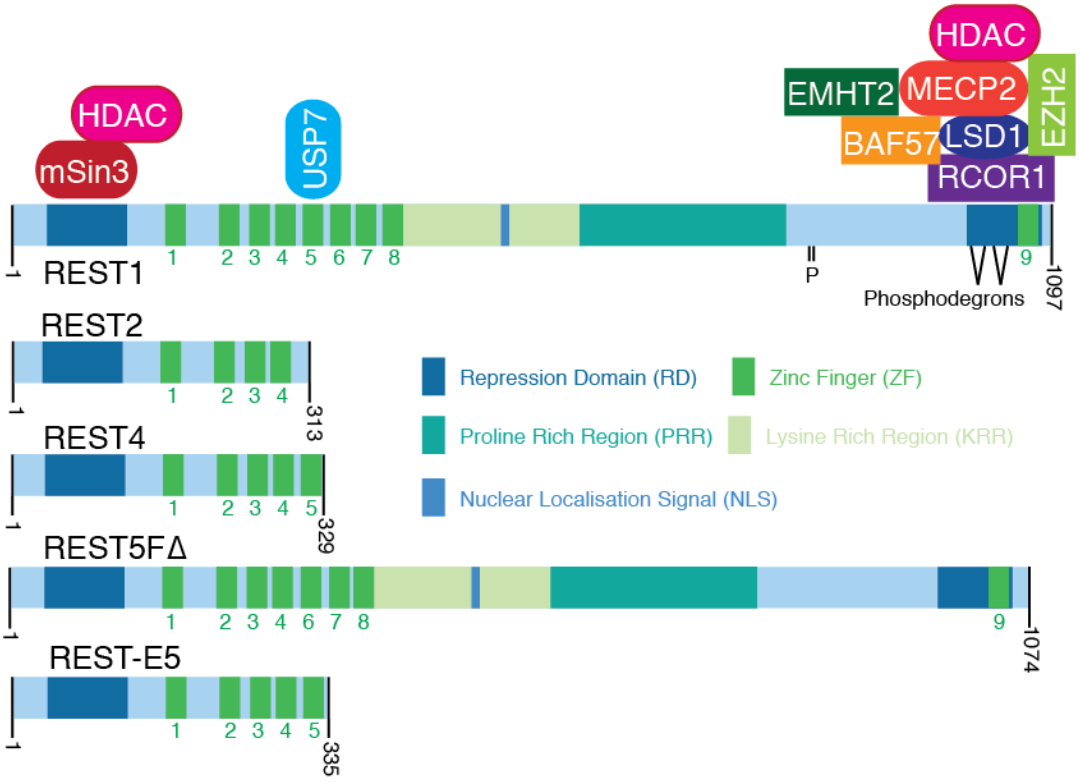

Figure 1.1 REST Protein Isoforms and Interactors
Full length REST protein, REST1 (Uniprot Q13127-1), is illustrated showing the domains, a selection of protein interactors and the major isoforms. Phosphorylation sites marked (P, phosphodegron) have been shown to contribute to REST stability. The truncated REST isoforms: REST2 (Uniprot Q13127-2), REST4 (Uniprot Q13127-3) and REST-E5 that lack the canonical REST C' terminal domains are generated from alternative splicing events. The REST isoform 4, retains the C' terminal, but REST5FΔ (Q13127-4) lacks ZF5 through exon skipping.

1.2.2.1 Zinc Fingers and DNA binding

REST protein contains nine ZFs and belongs to the large Kruppel transcription factor family (Vaquerizas et al., 2009). The Kruppel ZF forms a ββα fold in the presence of a Zn^{2+} ion (Frankel et al., 1987), which is tetrahedrally coordinated by two cysteine and two histidine residues (Wolfe et al., 2000). ZFs interact with DNA in tandem arrays, each making contact with three base pairs of DNA through the α helix (Pavletich and Pabo, 1991). This stoichiometry, means that the seven ZF array in REST interacts with 21-base pairs that form the canonical RE-1 motif. REST has seven ZFs (2-8) in close proximity, encoded across three exons, that are involved in this interaction. Interestingly, ZF5 encoded by exon 3 can be skipped during splicing (Chapter 1, Section 3.3). ZF1 is spaced further from the main ZF array, and is

presumably involved in interactions with non-canonical motifs, whilst ZF9 at the C-terminal is not thought to be involved in DNA binding.

The canonical RE-1 motif consists of two conserved regions of 9bp and 6bp that are separated by two non-conserved residues (Schoenherr et al., 1996, Johnson et al., 2012). Analyses of global chromatin occupancy revealed REST binding at non-canonical RE-1 motifs, where the non-conserved residues are either missing or extended by up to 9bp (Johnson et al., 2006, Otto et al., 2007). REST has been shown to interact with non-canonical RE-1 motifs or either of the two conserved sequences that constitute the canonical RE-1 (half-sites) (Johnson et al., 2007, Johnson et al., 2008, Bruce et al., 2009). Binding of REST to such non-canonical RE1 motifs was sufficient to induce repression of certain genes (Birney et al., 2007, Patel et al., 2007). Additionally, REST has been identified bound at regions of DNA that lack an RE-1, which may be artefacts as the mechanism of recruitment to these sites is unknown. Collation of identified RE-1 motifs from available chromatin occupancy screens suggest there are ~1000 sites for REST binding in the human genome (Johnson et al., 2012).

Recent global analyses of transcription factors, suggest that REST has a strong motif dependency relative to other transcription factors (Sherwood et al., 2014). REST, unlike other transcription factors of similar motif dependency, scores much lower on the chromatin opening index consistent with its transcriptionally repressive role.

1.2.2.2 Nuclear Localisation: NLS and ZFs

Effective regulation of gene expression requires localisation of REST to the nucleus to access DNA. Encoded within the lysine rich region of REST after the main ZF array is a putative NLS (512-522aa) (Grimes et al., 2000). Removal of this NLS results in some cytoplasmic REST redistribution, although mutation of these residues does not inhibit nuclear accumulation (Shimojo, 2006). These findings demonstrated that the putative NLS is not the

prominent driving force for REST nuclear localisation. This is further supported by the fact that truncated REST containing the ZFs 1-5 is capable of nuclear localisation, which appears to be predominantly mediated by ZF5 (Lee et al., 2000, Shimojo et al., 2001).

The factors regulating nuclear localisation of REST include nuclear protein REST-interacting Lin-11, Isl-1 and Mec-3 (LIM) domain protein (RILP, official gene name PRICKLE1) (Shimojo and Hersh, 2003, Shimojo and Hersh, 2006). RILP interacts with full length and truncated REST proteins, through ZFs 2-5. Interestingly, in neuronal cells REST interaction with Huntingtin (HTT) results in cytoplasmic sequestration of REST, but polyglutamine expanded HTT (polyQ-HTT) causes REST nuclear accumulation (Zuccato et al., 2003). Later studies of the REST nuclear trafficking complex demonstrated that this is an indirect interaction, mediated through HTT binding with dynactin $p150^{Glued}$ (DCNT1) that independently interacts with RILP (Shimojo, 2008). Huntingtin associated protein 1 (HAP1) also associates with the complex and prevents trafficking of REST to the nucleus (Shimojo, 2008). However in the presence of polyQ-HTT, HAP1 destabilised the complex releasing RILP and allowing nuclear trafficking of REST (Shimojo, 2008).

1.2.2.3 Repression Domains and Repression Complexes

To mediate repression, REST acts as a scaffold for large repression complexes via two repression domains (RDs) at its N' and C' terminus, called RD1 and RD2, respectively (Figure 1.1) (Tapia-Ramírez et al., 1997, Thiel et al., 1998, Leichter and Thiel, 1999). RD1 and RD2 function as independent domains and recruit co-repressors to modulate chromatin. Interestingly ZF9, a solitary ZF in the C' terminal, forms part of RD2.

Two major REST co-repressor complexes have been identified, scaffolded by SIN transcription regulator family member 3 A/B (SIN3A/B) (Grimes et al., 2000) and REST Corepressor 1 (CoREST or RCOR1), at RD1 and RD2 respectively. Both Sin3 and CoREST recruit histone deacetylase 1/2

(HDAC1/2) (Huang et al., 1999, Roopra et al., 2000, Andrés et al., 1999). In addition, CoREST also recruits euchromatic histone-lysine N-methyltransferase 2 [EHMT2, (H3K9me2)] and LSD1 (H3K4me/me2) and lysine specific demethylase 5C [KDM5C, (H3K4me2/me3)]. BRAF-HDAC complex protein 80 (BHC80, official gene name PHF21A) associates with CoREST and HDACs (Hakimi et al., 2002) and assists in the recognition of the H3K4 and LSD1 function (Lan et al., 2007). The methylated histones provided interaction sites for chromodomain Y-like (CDYL), which interacts with REST and assists in the recruitment of the histone methyltransferase EHMT2, which methylates H3K9 and H3K27 (Tachibana et al., 2001, Roopra et al., 2004, Mulligan et al., 2008).

Another CoREST partner, enhancer of zeste homolog 2 (EZH2) is both a methyl transferase (H3K9me, H3K27me) and a component of the polycomb repressive complex 2 (PRC2) (Ren and Kerppola, 2011, Dietrich et al., 2012). Interestingly, the recruitment of PRC2 can be mediated by the long intergenic non-coding RNA (lincRNA) HOTAIR, that interacts with the methyltransferase EZH2 and demethylase LSD1 (Tsai et al., 2010). However, a recent study demonstrated that the majority of PRC2 histone methylation was deposited independently of REST (McGann et al., 2014). CoREST can also interact with methyl-CpG binding protein 2 (MECP2) that assists with the recruitment of HDACs (Lunyak et al., 2002, Lorincz et al., 2001), and with BAF57 which recruits a SWI/SNF ATP-dependant chromatin remodelling complex (Battaglioli et al., 2002, Ooi et al., 2006).

In addition to chromatin modifying complexes, the extreme N'-terminal (1-44) and the C' terminal ZF9 also interact with the C' terminus of TBP, a constituent of the PIC (Murai et al., 2004). The proposed mechanism suggests REST could act as a barrier to transcription machinery. REST also inhibits the PIC, by recruitment of small RNA Pol II carboxyl-terminal domain phosphatase 1 (SCP1) (Yeo et al., 2005), which negatively regulates Pol II activity (Yeo et al., 2003).

The transition from REST repressed to actively transcribed genes, as proposed in reports of RE-1 enhancer capacity, can be achieved by REST displacement, degradation, dysfunction or perhaps REST-guided epigenetic regulation (Bessis et al., 1997, Kallunki et al., 1998, Seth and Majzoub, 2001, Kemp et al., 2003, Abramovitz et al., 2008, Perera et al., 2015). These data confirm that REST and its co-factors normally function to repress gene expression, although the activation of the genes may be permissible under the correct circumstances. Overall, RE-1 are negatively correlated with Pol II recruitment (Zheng et al., 2009) and associated with an increase in the repressive histone modifications H3K27me3 and H3K9me2, as well as a reduction in active expression marks H3K4ac, H4K8ac and H3K4me3, emphasising that REST generally is repressive.

The exact nature of the complexes that form around REST is dependent upon the cellular context (Greenway et al., 2007, Hohl and Thiel, 2005). The regulation of REST genes is dependent upon both the nature of the RE-1 motif (canonical, non-canonical, half-sites), the surrounding sequence context and TF motifs (Rockowitz et al., 2014), in addition to the combination of co-factors recruited (mSin3, CoREST, HOTAIR, TBP) that associate with REST and the repression complexes that are recruited. Thus, repression of REST target genes is mediated by both the RD1 and RD2 domains. Importantly, RD2 is capable of recruiting a large complex that modifies histone acetylation and methylation marks, as well as ATP-dependent remodelling complex. In some situations, the N' terminal RD1 domain alone is sufficient for repression, but REST isoforms that lack the RD2 (Chapter 1, Section 3.3) can only regulate a limited set of the REST genes.

1.3 Regulation of REST Expression and Activity

The *REST* gene is located on chromosome 4q12 (Cowan et al., 1996). REST expression is down regulated during neural differentiation (Chapter 1, Section 4.1.1) and dysregulated in disease (Chapter 1, Section 4.2) through a combination of transcriptional regulation (Chapter 1, Section 3.1), epigenetic

mechanisms (Chapter 1, Section 3.2), alternative splicing (Chapter 1, Section 3.3), and post-translational modifications (Chapter 1, Section 3.4).

1.3.1 Transcriptional Regulation of REST

Various studies have indicated transcription factor binding sites within the REST promoter that could contribute to REST expression, including POU class 2 homeobox 1 (POU2F1) , SRY-related HMG box 5 (SOX5), cAMP responsive element binding (CREB), CCAAT-enhance-binding protein (C/EBP), activator protein 1 (AP-1), specificity protein 1 (SP1), Yin-Yang 1 (YY1) and ETS-domain containing protein 1 (ELK1) (Jiang et al., 2008, Ravanpay et al., 2010). For example, the neurogenic differentiation (neuroD) family of transcription factors are expressed during neural differentiation and may precede the decrease in REST expression. The regulation of transcription factors downstream of NeuroD2, leads to an increase in ZF E-box binding homeobox (ZEB1), which represses REST mRNA and protein expression (Ravanpay et al., 2010). REST is also regulated by YY1, which binds to a conserved sequence in the REST promoter and promotes gene expression in a neuroblastoma cell line SH-SY5Y, which is consistent with reduced REST expression in partial knockout of YY1 in mouse embryonic fibroblasts (Affar et al., 2006, Jiang et al., 2008). As well, as these well-known transcription factors, huntingtin interacting protein 1 protein interactor (HIPPI), is reporter to bind to the REST promoter and induce expression of REST (Datta and Bhattacharyya, 2011).

REST transcription is responsive to several signalling pathways. The expression of REST can be modulated by mitogen-activated protein kinase (MAPK) - extracellular signal-regulated kinase (ERK) signalling (Formisano et al., 2015), which may occur via the TF ELK1, a well-known downstream target of MAPK-ERK signalling. The first link to epithelial growth factor (EGF) signalling reported that decreased ERK phosphorylation inhibited neuronal differentiation and correlated with an increase in REST binding to an RE-1 oligonucleotide probe (Tateno et al., 2006). More recently, both serum and

EGF stimulation were suggested to up-regulate expression of REST mRNA (Baiula et al., 2012). SP1 transcription factors also bind to the REST promoter (Ravache et al., 2010) and recent studies suggest ERK signalling may contribute to the dynamics of SP1 at the REST promoter (Formisano et al., 2015). REST expression may also be regulated by other signalling pathways. The expression of REST mRNA was induced following Wnt signalling (Willert et al., 2002). The overexpression of Wnt, and induction of canonical Wnt signalling via T-cell factor (TCF), result in increased REST expression in chick spinal cord (Nishihara et al., 2003).

The CREB transcription factor, involved in neuronal plasticity and long-term potentiation, also has a binding motif within the REST promoter. A mimetic of cAMP (SP-cyclic AMP) could further induce REST expression in H128 cells (Kreisler et al., 2010). In addition to promoting REST expression, CREB can positively regulate several miRNA genes that harbour RE-1 motifs and are involved in neuronal differentiation (Wu and Xie, 2006). Targets of these miRNAs include REST itself (Chapter 1, Section 3.2).

1.3.2 Epigenetic Regulation of REST

The expression of REST may be regulated by the interplay of epigenetic modifications, transcription factors, or post-transcriptional regulators (miRNAs). The factors that interact around the REST gene locus across multiple cell lines are mapped by the ENCODE project (Consortium et al., 2007). Interestingly, ChIP-Seq data (accessible from UCSC genome browser) around the REST locus has implicated REST-auto regulation through binding within its own promoter region. Indicative of an auto-regulatory negative feedback loop. Interestingly REST binding has been implicated in the generation and turnover of demethylation marks at low-methylation regions (Stadler et al., 2011, Feldmann et al., 2013). DNA methylation status might also modulate the activity of REST with increased methylation promoting binding to the RE-1 sequence of the pacemaker hyperpolarization-activated cyclic nucleotide-modulated potassium channel protein 2 (HCN2) (Zhang et

al., 2017). These data demonstrate that REST expression and activity is modulated by more than just transcriptional and post-translational modifications.

Expression of specific miRNAs can be regulated by REST, and in turn miRNA can post-transcriptionally regulate REST expression. One example of a REST regulated miRNA, is miRNA 9/9* (miR9/9*), both of which can be derived from three gene transcripts (miR9-1, miR9-2, miR9-3), of which miR9-1 and miR9-3 contain upstream RE-1 motifs (Packer et al., 2008). Interestingly, miR9 and miR9* were shown to target REST and CoREST, respectively. The expression of these miRNAs is downregulated during the pathogenesis of Huntington Disease, correlating with increased REST expression (Packer et al., 2008). In addition to miR9, miR-124 and miR-132 have been implicated in neuronal differentiation through regulation of REST or its co-factors (Wu and Xie, 2006, Klein et al., 2007). These examples demonstrate the interconnected nature of REST, its repressive complexes and miRNA regulation, where basal expression of REST can be modulated by the transcriptional environment.

1.3.3 Alternative Splicing of REST

REST, originally defined as a repressor of neuronal genes, was thought to be absent from neurons until it was discovered that C-terminally truncated isoform, REST4, was expressed in neuronal cells (Palm et al., 1998). It is now known that the *REST* gene can be expressed as multiple alternatively spliced transcripts including predicted protein-coding mRNAs (REST1, REST4, REST5FΔ, REST-E5) (Figure 1.1), although not all have been validated at a protein level. There are also examples of non-coding transcripts generated from the *REST* gene (Lee et al., 2015). These alternatively spliced REST mRNAs, both coding and non-coding, have been implicated in REST dysfunction in cancers, such as neuroblastoma, small cell lung cancer (SCLC) and breast carcinoma (Palm et al., 1999, Coulson et al., 2000, Wagoner et al., 2010, Lee et al., 2015), as discussed in more detail in Chapter 1, Section 4.

The functionality of REST can be dramatically altered through alternative splicing, most notably by encoding isoforms which lack the canonical C' terminal repression domain or lack ZF5 implicated in nuclear localisation of REST. These isoforms are generated through missed exon splicing (REST2), inclusion of a neuronal (N) exon (REST4) or an alternative exon (REST-E5). In contrast, REST5FΔ, is produced from skipping of ZF5 encoding exon.

In addition, REST mRNA may incorporate one of three alternative 5' non-coding exons (1A, 1B and 1C) (Palm et al., 1998, Palm et al., 1999, Chen and Miller, 2013). This suggests the use of three alternative gene promoters that may control REST expression in a context-dependent fashion. In most cases, REST mRNAs incorporate exon 1A, although mRNAs incorporating exon 1B have been reported in both neuronal cells and non-neuronal cells (Koenigsberger et al., 2000, Kojima et al., 2001). The expression of mRNA incorporating exon 1C is a rarer event, which occurs in less than 1% of REST transcripts (Koenigsberger et al., 2000).

Alternative splicing to generate the REST4 isoform has been attributed to the splicing factor serine/arginine repetitive matrix 4 (SRRM4) also known as neuronal-specific SR-related protein of 100kDa (nSR100) (Raj et al., 2011). SRRM4 has been implicated in the splicing of many neuronal-specific exons (Raj et al., 2014), including the N exon in the REST4 transcript. The elevated expression of REST4 in SCLC and neuroendocrine prostate cancer was subsequently shown to also be dependent upon SRRM4 (Zhang et al., 2015, Li et al., 2017). Interestingly, the expression of SRRM4 can be induced by MEK/ERK signalling (Shimojo et al., 2013), and is also regulated through an RE-1 motif forming a feedforward loop (Raj et al., 2011).

1.3.4 Post-Translational Regulation of REST

The diversity of the proteome is greatly increased by post-translational modifications (PTMs). A key purpose of PTMs is to trigger a new phase of protein function, which can be time-dependent. PTMs function in concert to

influence every aspect of protein function by inducing chemical changes that alter conformation, activity, interactions, localisation or stability of the protein. REST is known to be modified by three major classes of PTMs: glycosylation, phosphorylation and ubiquitylation. Whilst phosphorylation and ubiquitylation alter the stability of REST, glycosylation may alter DNA binding of REST.

1.3.4.1 Glycosylation

The expression of REST in *E. coli*, lacks glycosylation machinery (Baker et al., 2013) results in production of the predicted 120kDa REST protein (Carbonari, 2012). In mammalian cells, REST undergoes N-linked glycosylation during protein folding, and is post-translationally O-linked glycosylated at multiple sites, which results in the nascent 120kDa protein increasing in its apparent molecular weight on gel electrophoresis to ~220kDa (Pance et al., 2006, Kreisler et al., 2010, Lee et al., 2000). Glycosylation of REST is also evident for the truncated REST isoforms, through glycosylation sites located in the N' terminus (Lee et al., 2000). REST glycosylation is thought to modulate the REST-DNA interaction (Lee et al., 2000) although conclusive evidence for this remains to be determined (Carbonari, 2012).

1.3.4.2 Phosphorylation

The stability of REST is regulated by two adjacent phosphorylation-inducing degradation regions (phosphodegrons) close to the C-terminus (Figure 1.1). The crucial phosphodegron residues were identified as E1009 and S1013 (Guardavaccaro et al., 2008) and S1024, S1027 and S1030 (Westbrook et al., 2008). The phosphorylated Ser residues are targeted by the Skp1-Cullin1-F-Box (SCF) β-TrCP ubiquitin E3-ligase. Mutation of E1009 and S1013 alone was sufficient to inhibit $SCF^{\beta\text{-}TrCP}$ binding and degradation of REST (Guardavaccaro et al., 2008). Phosphorylation of these phosphodegrons is sufficient to induce REST ubiquitylation and degradation, although the kinase responsible was not initially identified. In more recent studies, mass spectrometry identified phosphorylation of REST at S1024, S1027, S1030 that was attributed to the activity of Casein Kinase I (CK1) and

Polo-like Kinase 1 (PLK1) (Kaneko et al., 2014, Karlin et al., 2014). Interestingly, mutation of S861 and S864 were shown to partly rescue degradation of REST, despite lying outside the known phosphodegrons (Nesti et al., 2014). This rescue was suggested to be through loss of interaction with peptidylpropyl cis/trans isomerase 1 (Pin1), that can enhance the binding of $SCF^{\beta\text{-}TrCP}$. Interestingly, phosphorylation of REST at S861 and S864 occurs downstream of EGF and MAPK signalling, which are the same residues dephosphorylated by SCP1 (Nesti et al., 2014). In total, Nesti and colleagues identified 14 phosphorylation sites on REST, although the function of additional phosphorylation was not ascribed. The effects of EGF signalling on REST protein stability and mRNA expression may suggest this pathway is a possible primer of the cyclical degradation and re-expression of REST.

Dual-specificity tyrosine phosphorylation regulated kinase 1A (DYRK1A) is found in complex with the ATP-dependent remodelling complex SWI/SNF (Lepagnol-Bestel et al., 2009), and has also been implicated in phosphorylation of REST. Overexpression of DYRK1A induced degradation of REST1, whilst frameshift mutant REST (lacking the C' terminus) was not markedly reduced by DYRK1A overexpression (Lu et al., 2011); if this is mediated directly through phosphorylation of REST the specific residue/s targeted by DYRK1A remain unknown. Interestingly, the same paper reports upregulation of DYRK1A mRNA, upon REST binding to the upstream RE-1 motif within the DYRK1A promoter (Lu et al., 2011); the activating nature of such an interaction appears to contradict the repressive function of REST. In the pathology of Down Syndrome, using a trisomy 21-model, *DYRK1A* (located on chromosome 21) is within the minimal trisomic region which correlates with reduced REST protein and gene expression (Canzonetta et al., 2008). The imbalance of DYRK1A disrupts the expression of REST mRNA in embryonic stem cells (ESC) leading to dysfunctional neurogenesis (Canzonetta et al., 2008). Together these papers suggest both indirect and direct mechanisms by which REST could be regulated DYRK1A.

1.3.4.3 REST Ubiquitylation

REST becomes acutely phosphorylated at the phosphodegrons described above during neural differentiation and cell division (Westbrook et al., 2008, Guardavaccaro et al., 2008). In each case, phosphorylation recruits the $SCF^{\beta\text{-}TrCP}$ E3 ligase to REST to trigger its degradation by the proteasome, although the specific lysine residue/s targeted by $SCF^{\beta\text{-}TrCP}$ for ubiquitylation are unknown. The acute degradation of REST at the onset of cell division is required for effective mitotic exit, with REST phosphodegron mutants causing aberrant anaphase and lagging chromosomes (Guardavaccaro et al., 2008). As well as cell cycle progression, the regulation of REST protein stability is also important for neuronal differentiation (Westbrook et al., 2008), with exogneous expression of REST phosphodegron mutants attenuating neuronal differentiaion. The degradation of nuclear REST is also promoted on transformation by the adenovirus early region 1A protein (E1A), mediated by upregulation of β-TrCP expression and phosphorylation of both phosphodegrons (Guan and Ricciardi, 2012).

Akin to phosphorylation, ubiquitylation is also reversible, with ubiquitin moieties removed by a family of deubiquitylase (DUB) enzymes (Chapter 1, Section 6). In the context of neuronal differentiation/pluripotency, REST is stabilised by the deubiquitylase ubiquitin specific protease 7 (USP7) (Huang et al., 2011). The gradual decrease of REST during differentiation is a result of a shift in turnover with decreasing USP7 and increasing $SCF^{\beta\text{-}TrCP}$ levels promoting REST degradation. The interaction of USP7 is dependent on an interaction motif and the presence of a serine residue (Ser, S) contained with ZF5 (Huang et al., 2011) suggesting certain REST isoforms may lack USP7 interaction. It is currently unknown whether this Ser residue is regulated by post-translational modification. In contrast, an unbiased DUB small interfering RNA (siRNA) library screen for REST expression in lung cancer cells, did not find a role for USP7, but instead identified ubiquitin specific protease 15 (USP15) as maintaining REST protein expression, specifically during the re-

expression of REST post-mitosis (Faronato et al., 2013) (Chapter 1, Section 6.2.4).

1.4 REST Physiology and Pathology

1.4.1 REST Physiology

REST was first identified as a repressor of neuron-specific genes, and as such, its activity restricts neurogenesis (Schoenherr and Anderson, 1995, Chong et al., 1995). REST is a critical protein, which when genetically ablated leads to embryonic lethality (Chen et al., 1998). To date many REST studies have focused on its role in embryonic and neural stem/progenitor cells (NSC/Ps) and during neuronal differentiation. REST is ubiquitously expressed in early mouse development (Chen et al., 1998, Grimes et al., 2000), where it functions in concert with other pluripotency factors to regulate gene expression. The role of REST was proposed to maintain the pluripotent state of ESCs (Singh et al., 2008), although others reported that loss of REST from ESCs did not affect their capacity to differentiate (Buckley et al., 2009, Jørgensen et al., 2009a). Later studies demonstrated that REST-deficient ESCs can become any of the three germ layers (Jørgensen et al., 2009b, Covey et al., 2012). The current consensus is that REST is not the master regulator of neuronal differentiation, but co-ordinates multiple tiers of neuronal development (Thiel et al., 2015). Here, I will briefly outline the role of REST during neuronal differentiation, its expression in adult tissues and involvement in the neuroendocrine phenotype.

1.4.1.1 Neuronal Differentiation

Orderly expression of genes occurs during development, which is regulated at various stages of neurogenesis by REST (Ballas et al., 2005). In the ESCs, REST restricts neuronal differentiation through the chromatin modifying actions of its co-factors, including, but not limited to, SCP1 and CoREST (Yeo et al., 2005, Abrajano et al., 2009). Physiologically, homozygous deletion of REST causes notable growth defects around the time of neural crest development, although without apparent defects in the neural

tube, with embryos dying prior to the completion of the nervous system (Chen et al., 1998). The cause of REST-null embryonic lethality is unknown, and a conditional knockout of REST within the neural tube suggested that it was dispensable for functional brain development (Aoki et al., 2012). Recently, however, conditional knockout of REST expression, generated by genetic trapping, demonstrated reduced brain mass (Nechiporuk et al., 2016). These data demonstrate that REST plays an important role in the later stages of neurogenesis.

As discussed in Chapter 1, Section 3.4, during the differentiation from ESCs to NSC/Ps, REST is targeted for ubiquitin-mediated degradation by the E3 ligase $SCF^{\beta\text{-}TrCP}$ (Westbrook et al., 2008) that can be opposed by ubiquitin specific peptidase 7 (USP7) (Huang et al., 2011). This degradation of REST is specific and expression of its co-factors persists into mature neurons (Ballas et al., 2005). In mature neurons, REST is displaced from RE-1 sites, transcriptionally repressed, and REST levels cannot be rescued by proteasome inhibition (Ballas et al., 2005). The expression of REST is regulated by transcriptional, epigenetic, alternative splicing and post-translational mechanisms (Chapter 1, Section 3). Importantly, the co-ordinated regulation of expression may be under the control of miRNAs (Chapter 1, Section 3.2). To further understand the nature of REST-mediated regulation during neurogenesis, current research continues to focus on the contribution of REST co-factors to the epigenetic status around REST-target genes (McGann et al., 2014) and the validation of novel regulators of the REST complex (Volvert et al., 2014).

1.4.1.2 Adult Tissue

In mature neurons, loss of REST releases membrane channel and transporter genes from REST repression, such as the type II voltage-dependent Na+ channel (Chong et al., 1995) that ensures membrane excitability and the K^+/Cl^- co-transporter (KCC2) (Yeo et al., 2009) which alters the response of neurons to agonists and forms part of a developmental switch.

Importantly though, the expression of REST is not ablated from neurons of the hippocampus, pons/medulla and midbrain (Chong et al., 1995, Palm et al., 1998). Temporary loss of REST allows for a compositional change to synaptic receptors such as the glutamatergic receptors that results in modified synaptic transmission (Rodenas-Ruano et al., 2012). Together, these studies demonstrate that the function of REST extends beyond the embryonic lethal effects to modulate neuronal cellular behaviour in adult tissues.

Non-neuronal cells maintain high levels of REST expression, primarily restricting neuron-specific genes, yet REST can also regulate the expression of non-neuronal genes. The extent of REST regulation has been assessed using microarray analysis, polymerase chain reaction and chromatin-immunoprecipitations techniques. Microarray analysis of non-neuronal cells following conditional ablation of REST demonstrates upregulation of only a subset of REST target genes at embryonic day 13.5 (Aoki et al., 2012). Likewise, only 54 genes were demonstrated to be upregulated, following siRNA knockdown of REST, in the non-neuronal human embryonic kidney cells (HEK 293) (Liu et al., 2009). These data demonstrate that only a subset of REST-target genes are transcribed in non-neuronal cells, which is dependent upon the cellular context.

1.4.1.3 Neuroendocrine Phenotype

Neurotransmitters are required for synaptic transmission, but signalling to distant cells and organs requires the endocrine system, which releases peptide hormones into the bloodstream. Neuroendocrine cells are stimulus-induced secretory cells that require the expression of neuropeptide and specialised exocytosis machinery for their function. REST has been shown to regulate the expression of some of these components (Bruce et al., 2006, D'Alessandro et al., 2008, D'Alessandro et al., 2009, Moss et al., 2009). At a cellular level, REST overexpression was also shown to reduce the number and size of secretory dense-core vesicles in the phenochromoytoma cell line (PC12) (Bruce et al. 2006; D'Alessandro et al. 2008). In addition to this, REST

mediated repression is also thought to reduce the capacity of cells to sense changes in resting membrane potential. REST expression is therefore low in neuroendocrine cells to enable sensing of stimuli and regulate secretion.

The role of REST in such secretory behaviour is interesting as loss of REST expression has also been associated with differentiation of non-neuronal endocrine cells of the pancreas (Atouf et al., 1997, Martin et al., 2008, Martin et al., 2012). This differentiation is important as loss of REST-mediated regulation can underpin a neuroendocrine phenotype, promoting autocrine/paracrine signalling that may stimulate growth (Chapter 1, Section 4.2.2).

1.4.2 REST Pathology

As the expression of REST is controlled during neuronal differentiation, it is unsurprising that defects in its function are strongly associated with neurological disorders during development or aging. As well as the role of REST in maintaining NSC/P self-renewal (Covey et al., 2012), loss of REST can also cause neuronal pathfinding errors (Paquette et al., 2000) and inhibit the acquisition of excitability (Ballas et al., 2001). Persistent REST expression was also shown to causes defects in the migration of NSC/Ps to their final location in the brain (Mandel et al., 2011). REST-mediated regulation of gene expression demonstrates a broad spectrum of effects on cellular processes including excitability, cellular migration, proliferation as well as the neuroendocrine phenotype (Chapter 1, Section 4.1.3).

As our interests lie with non-neuronal cells and the loss of REST in cancer, I will only briefly summarise the roles of REST in some neurological pathologies (Chapter 1, Section 4.2.1). For further detail of REST involvement in neurological disease and psychiatric disorders, I refer the reader to a recent review (Baldelli and Meldolesi, 2015). I will describe in more detail here the context-dependent roles of REST as either a tumour suppressor or oncogene in cancers (Chapter 1, Section 4.2.2).

1.4.2.1 Adult Neurons

REST has been associated with aging and Alzheimer's disease. REST expression increases with age in the prefrontal cortex and hippocampal neurons, which is proposed to be enacted through the regulation of the Wnt/β-catenin signalling pathway (Lu et al., 2014). In this context, the expression of REST is neuroprotective and negatively correlates with pro-apoptotic gene expression and reduced sensitivity to oxidative stress (Lu et al., 2014). In Alzheimer's, however, the expression of REST is either lost or, REST is sequestered in cytoplasmic punctate, in which it can be degraded along with misfolded proteins (Lu et al., 2014). Another age-related disease, Parkinson's, involves degeneration of dopaminergic neurons and is accompanied by reduced expression of brain derived neurotrophic factor (BDNF) (Mogi et al., 1999). BDNF is an RE-1 restricted gene and can be downregulated through increased activity of REST (Timmusk et al., 1999). Interestingly, the expression of REST is also upregulated in neuronal cells after ischemic insult, which is followed by cell death (Calderone et al., 2003). In this case, the activation of CK1 stimulates REST degradation by $SCF^{\beta\text{-}TrCP}$ leading to reduced cell death (Kaneko et al., 2014). These studies provide evidence that induced REST expression may contribute to pathogenesis of a variety of neurological diseases.

1.4.2.2 REST in Cancer: Oncogene or Tumour Suppressor

The clearest indication of REST dysfunction in non-neuronal cells is in cancers, such as breast, lung, and prostate, that can exhibit a neuroendocrine phenotype (Coulson et al., 1999a, Neumann et al., 2004, Tawadros et al., 2005). In general, REST dysfunction modulates the transcriptome of cancer cells, including both mRNA and non-coding RNAs (ncRNA), ultimately leading to physiological changes in cellular behaviour. Depending on the initial context of REST expression, REST protein has been reported as either oncogenic or tumour suppressive (Coulson, 2005, Negrini et al., 2013). This dichotomy of REST function in general can be summarised as such: REST acts as a tumour

suppressor in cells that normally express REST, whilst REST re-expression in cells normally lacking REST is oncogenic. Here, I will focus on the mechanisms and consequences of REST dysfunction in cancers.

1.4.2.2.1 Genetic Causes of REST Dysfunction

Loss-of-function induced by single nucleotide polymorphisms is a common feature of prominent tumour suppressors. Recently, inactivating mutations of REST within the DNA binding domain, have been implicated in the development of the childhood kidney cancer Wilms Tumour 6 (Mahamdallie et al., 2015). The mutations within the DNA binding domain compromise REST transcriptional function and are likely to affect expression of a broad range of target genes. The effects of REST dysfunction on the development of this cancer remain unknown.

A frameshift mutation that produces a truncated REST protein (REST-FS), was identified in a colorectal adenocarcinoma cell line (Westbrook et al., 2005). Despite REST1 being tumour suppressive in this context, REST-FS increased cells capacity to form anchorage independent colonies. REST-FS was shown to increase the phosphorylation of protein kinase B (PKB) downstream of phosphoinositide 3 kinase (PI3K) (Westbrook et al., 2005). Westbrook and colleagues postulated that REST-repressed BDNF, which activates the neurotrophic receptor tyrosine kinase 2 (NTRK2), may be induced by loss of REST resulting in suppression of anoikis via PI3K-dependent pathways (Douma et al., 2004). Further analysis showed this truncated variant lost the requisite phosphodegron and was unresponsive to $SCF^{\beta\text{-}TrCP}$ mediated degradation, which can lead to genomic instability through incomplete separation of sister chromatids during mitotic division (Guardavaccaro et al., 2008). As such, the oncogenic expression of truncated REST promotes cancerous invasion by increasing cells' capacity to overcome anchorage-dependency and can contribute to a loss of genomic integrity, ultimately leading to further mutational change.

The expression of REST in cancer can also be modulated by copy number changes in the gene. A loss of REST copy number was reported by Westbrook and colleagues, who demonstrated that 14/42 colorectal cancers contained deletions encompassing the REST gene (Westbrook et al., 2005). In addition, the 4q12 chromosome region that harbours the REST gene, is amplified in non-small cell lung cancer (Ramos et al., 2009), medulloblastoma (Northcott et al., 2009) and glioblastoma (Schròck et al., 1994) although not specifically associated with REST. The amplification of 4q12 in medulloblastoma could promote increased expression of REST, which in this cellular context is oncogenic (Lawinger et al., 2000, Fuller et al., 2005, Su et al., 2006). Mechanistically, REST expression is thought to repress the deubiquitylase USP37, which normally stabilises p27, a cyclin-dependent kinase inhibitor, that in turn inhibits proliferation (Das et al., 2013). As a result of increased REST expression, the medulloblastomas increased proliferation (Das et al., 2013).

1.4.2.2.2 Dysfunctional Alternative Splicing of REST

As described in Chapter 1, Section 3.3, alternative splicing of REST can produce coding and non-coding RNA variants that are associated with cancer (Chen and Miller, 2013). Loss of full-length REST function, through alternative splicing can lead to aberrant expression of neuropeptides such as secretogranin III (Moss et al., 2009) and preprotachykinin-A in breast cancers (Reddy et al., 2009) that can be used as potential biomarkers for neuroendocrine cancers.

The best characterised alternatively spliced isoform is REST4, which has been associated with neuroblastoma, breast cancer, SCLC and prostate cancers (Palm et al., 1999, Coulson et al., 2000, Wagoner et al., 2010, Zhang et al., 2015). The status of REST in breast cancers could be used as a prognostic indicator (Wagoner et al., 2010). REST4 expression, together with downregulation of full length REST1 gives license to inappropriate expression of neuropeptides, receptors and secretory pathways that allow for autocrine or

paracrine signalling and may convey a growth advantage (Coulson et al., 1999a, Coulson et al., 2000, Gurrola-Diaz et al., 2003, Moss et al., 2009). In prostate cancer, REST expression was shown to regulate Islet-Brain1/c-Jun amino-terminal kinase Interacting Protein-1 (IB1/JIP-1), a scaffold component of the mitogen-activated kinase pathway (Tawadros et al., 2005). The expression IB1/JIP-1 correlated with the prostate neuroendocrine marker synaptophysin and decreased REST expression (Tawadros et al., 2005).

1.4.2.2.3 Post-Transcriptional Regulation of REST

Other proposed mechanisms for loss of REST in prostate cancers are either by the actions of hypoxia-induced miRNA (Liang et al., 2014) or interlukin-6 induced downregulation of USP7, allowing for unopposed degradation of REST (Zhu et al., 2014). The loss of REST in androgen-sensitive prostate cancer cells promoted the expression of autophagy related genes, which are proposed to provide a survival benefit (Chang et al., 2014). As well as licensing expression of neuropeptides, prolonged knockdown of REST in pancreatic cancers was shown to promote the expression of cell adhesion molecules such as CD44 (Chang et al., 2017). The extent to which REST regulates cellular adhesion in response to loss of expression is not fully understood. The epigenetic changes that are regulated by REST, and REST-regulated RNAs are being investigated in a variety of cancers (Dobson et al., 2017, Coulson, Unpublished). However, given the role of REST in regulating both ncRNA and mRNA the effects of these transcript changes in determining protein expression remain unclear, so that cellular pathways influenced by loss of REST repression in cancer require further exploration.

1.5 Ubiquitylation: A Versatile Post-Translational Modification

Ubiquitylation is a reversible post-translational modification that can be written, read and erased, in a manner analogous to phosphorylation. However, the ubiquitin code is far more complex than phosphorylation. Ubiquitin is conjugated to a myriad of proteins, and the dynamics of ubiquitylation regulate a variety of signalling pathways and networks (Komander and Rape, 2012).

1.5.1 Discovery of Ubiquitin

Ubiquitin, a small protein of 76 amino acids and approximately 8.5kDa, was first isolated from bovine thymus in 1975 (Goldstein et al., 1975). Ubiquitin is ubiquitously expressed in cells and accounts for ~0.4% of total cellular protein in the form of either solitary units or polyubiquitin chains (Kaiser et al., 2011). Ubiquitous and abundant expression of a protein suggests it has integral and essential cellular functions. The first indication for the function of ubiquitin was the discovery in 1977 that ubiquitin was covalently attached to the histone H2A protein (Goldknopf and Busch, 1977, Hunt and Dayhoff, 1977). These studies were the first indication that ubiquitin functions as a protein-based PTM. The addition of ubiquitin was shown to be a key factor in ATP-dependent proteolytic degradation in 1980 (Hershko et al., 1980, Ciechanover et al., 1980, Wilkinson et al., 1980).

1.5.2 The Ubiquitylation Machinery: Writing the Ubiquitin Code

The addition of ubiquitin is dependent upon a cascade of enzymatic reactions mediated by E1, E2 and E3 enzymes. The E1 activating enzymes conjugate with and activate ubiquitin in an ATP-dependent manner. The E1 enzymes then transfer the activated ubiquitin to an E2-conjugating enzyme. The E3 ligating enzyme, interacts with both the protein substrate and the E2, facilitates the transfer of the ubiquitin moiety from the E2 to the target protein. Subsequent ubiquitylation can generate polyubiquitin chains.

1.5.3 Diversity of the Ubiquitin Code

The post-translational addition of ubiquitin occurs via the covalent linkage of the C' terminal glycine residue to a lysine residue within a substrate, or indeed within ubiquitin itself. Monomeric ubiquitin contains seven lysine residues (K6, K11, K27, K29, K33, K48 and K63) that are known sites of polyubiquitylation. These seven lysine residues allow ubiquitin chains to be extended in different ways to generate a plethora of signals (Swatek and Komander, 2016, Akutsu et al., 2016). The extent of ubiquitylation is complex and can result in different outcomes for the substrate depending on the type

and number of ubiquitylation events, as summarised in Table 1.1. Whilst the ubiquitin modification of substrates occurs primarily through an isopeptide linkage to a lysine residue, it has been suggested that serine, threonine and cysteine residues may also be potential ubiquitylation target sites (McDowell and Philpott, 2013).

Table 1.1 Ubiquitin Chain Linkages and Functions

Ubiquitylation	Description	Functions
Mono-ubiquitylation	A single ubiquitin bound to the substrate.	Involved in membrane trafficking, regulation of protein function and transcriptional regulation. Additional mono-ubiquitylation may allow for integration of multiple regulatory events (Nakagawa and Nakayama, 2015).
Multi-mono-ubiquitylation	Multiple single ubiquitin bound to different residues of the substrate.	
Homotypic poly-ubiquitylation	A chain of ubiquitin covalently attached via particular lysine residues, emanating from a single site on the substrate	K48 and K11 linked chains, primarily involved in targeting proteins to the 26S proteasome (Bremm and Komander, 2011). K63 linked chains involved in protein sorting and DNA repair (Lauwers et al., 2009, Hoege et al., 2002). K63 and N' terminal linked ubiquitin regulate NF-kB signalling (Gerlach et al., 2011, Xu et al., 2009a). The roles of K6, K27, K29, K33 chain linkages are emerging (Yau and Rape, 2016, Akutsu et al., 2016).
Heterotypic poly-ubiquitylation	A chain of ubiquitin covalently attached using a variety of lysine residues, which emanate from a single site in the substrate. Chains may be branched, so that a single ubiquitin is modified on more than one K.	Heterotypic / branched ubiquitin changes enhance recognition and degradation of proteins (Meyer and Rape, 2014). The extent of roles that atypical ubiquitin chains perform remains to be determined and may have protein-specific effects.
Hybrid Chains	A chain of ubiquitin that is complemented with the inclusion of other ubiquitin-like proteins.	Hybrid SUMO and Ubiquitin chains regulate IKKB protein degradation (Emmerich et al., 2013).

1.5.4 Reading the Ubiquitin Code

Ubiquitin modified proteins are recognised by specific interacting proteins, often bearing ubiquitin interacting motifs (UIMs) or ubiquitin associated (UBA) domains that recognise specific ubiquitin moieties. Polyubiquitin chains, depending on the chain linkage, produce linear or branched topologies that are recognised by different ubiquitin binding motifs, perhaps with different affinities (Meyer and Rape, 2014). The ubiquitin chain binding specificity of ubiquitin interacting proteins is therefore fundamental to divergent polyubiquitin chain functions.

1.6 Deubiquitylation and Deubiquitylases

The deubiquitylases (DUBs) are a family of 96 isopeptidases that may cleave the isopeptide bond of ubiquitin linkages to provide mechanistic reversion of ubiquitylation. The excision of ubiquitin from chains, or directly from a protein substrate, modifies the signalling outcome of the PTM. The reversible processes of ubiquitylation and deubiquitylation are important for dynamic signalling, as demonstrated by the opposition of ubiquitin-mediated protein degradation by DUBs. In addition to these functions, DUBs are responsible for the generation of ubiquitin monomers from precursor proteins which, together with their role in recycling ubiquitin, maintains the free ubiquitin pool. The DUBs, their activity, regulation, substrates and cellular roles have been extensively reviewed in recent years (Komander et al., 2009, Komander, 2010, Clague et al., 2012, Clague et al., 2013, Heideker and Wertz, 2015). Here I will summarise some key points, before focusing on one DUB, ubiquitin specific peptidase 15 (USP15), which I investigate in this thesis.

1.6.1 Deubiquitylases: Erasing the Ubiquitin Code

The 96 DUBs fall into six sub-families based upon the structure and activity of their catalytic domains. The majority of DUBs are thiol proteases divided into five families: the ubiquitin specific peptidases (USPs) (56 members), ovarian tumour proteases (OTUs) (16 members), ubiquitin C-terminal hydrolases (UCHs) (four members), Machado-Josephin domains

(Josephins) (four members) and the recently discovered motif interacting with ubiquitin-containing novel DUB (MINDY) family (four members) (Abdul Rehman et al., 2016). The remaining 12 DUBs are metalloproteases that form the JAB1/MPN/MOV34 (JAMM) family.

Ubiquitylation and deubiquitylation have been implicated in a vast array of cellular activities, including the degradation of proteins via the ubiquitin-proteasome system (UPS), the organisation of cellular structures (endosomes and trafficking) and timing of multiprotein complex activity (cell cycle progression). The extent of DUB-mediated regulation in diverse signalling pathways have been reviewed more extensively in the following publications (Reyes-Turcu et al., 2009, Hammond-Martel et al., 2012, Heideker and Wertz, 2015, Clague et al., 2012). Cancer associated signalling regulated by DUBs, either through regulating oncogenes or tumour suppressors are discussed in these articles (Sacco et al., 2010, Pinto-Fernandez and Kessler, 2016). The gradual assignment of DUB functions has depended on identifying: (1) the protein substrates from which ubiquitin is cleaved, (2) cellular localisation and recruitment, (3) specificity for ubiquitin chain length or linkage, and (4) regulation of catalytic activity.

Deubiquitylases carry an array of non-catalytic domains (Clague et al., 2013), which are often involved in regulating their substrate specificity. Highly similar deubiquitylases such as USP4, USP11 and USP15 may share common substrates or have distinctive roles in regulating different pathways (Chapter 1, Section 6.2). One systematic approach for the identification of DUB substrates, based on mass spectrometry for high confidence protein interactions, associated homologous DUBs with common functions (Sowa et al., 2009). Importantly though, the transient nature of DUB-substrate interactions makes it difficult to assign DUB function by interaction. DUBs are often found in complex with accessory proteins or with E3-ligases, that may or may not be direct deubiquitylation targets themselves, but can help recruit a DUB to ubiquitylated substrate proteins (Ventii and Wilkinson, 2008, Heideker

and Wertz, 2015). It is thought that this mechanism can allow DUBs to utilise the repertoire of substrates selected for by the complex whilst providing a localised enhancement of DUB activity. For instance, the DUB ataxin-3 (ATXN3) associates with the E3 ligase, C-terminus of the heat shock cognate (Hsc) 70-interacting protein (CHIP), which promotes ATXN3 monoubiquitylation and its catalytic activity (Todi et al., 2009, Todi et al., 2010, Durcan and Fon, 2013).

The subcellular localisation of DUBs provide an insight into the cellular systems they regulate, exemplified by USP21 association with microtubules and centrosomes (Urbé et al., 2012). As well as subcellular location, DUBs are regulated by spatiotemporal mechanisms which are likely stimulated by phosphorylation. An example of a DUB that requires tight control of its activity is USP44, which was shown to be a regulator of the anaphase-promoting complex (APC), that restricts ubiquitin-mediated degradation of spindle checkpoint complexes (Stegmeier et al., 2007). Spatiotemporal regulation can also be seen with the recruitment of USP15, a predominantly cytoplasmic DUB, to sites of DNA damage (Nishi et al., 2014).

The specificity and activity of DUBs towards ubiquitin chain linkages are currently under intense scrutiny, with the goal of systematically reading the ubiquitin code (Ritorto et al., 2014, Crowe et al., 2016). One technique for determining ubiquitin chain architecture that has been developed named UbiCRest, utilizes parallel ubiquitin restriction reactions based upon the specificity of a panel of DUBs (Hospenthal et al., 2015). Such DUB-based tools should help improve the accuracy of our description of polyubiquitin chains and their function.

Interestingly, the catalytic activity of DUBs can be regulated in many ways, as recently reviewed (Sahtoe and Sixma, 2015). For example, regulation by allosteric co-factors is exemplified by USP1 and USP1-associated factor (UAF1) (Cohn et al., 2007). The activity of a DUB can also

be regulated intrinsically, which will be discussed later in relation to the USP15 homolog USP4 (Chapter 1, Section 6.2.1). Importantly, these structural and mechanistic insights can highlight signalling pathways, upstream regulators and even DUB interfaces that could be targeted to limit specific roles of DUBs.

Our understanding of DUB activity and cellular function is derived from structural insights, interactions, post-translational modifications and verified substrates. Here, I will overview the current understanding for one DUB, USP15, which has been implicated in the regulation of REST.

1.6.2 Ubiquitin Specific Peptidase 15 (USP15)

1.6.2.1 Domain Structure and Regulation of USP15

USP15 is a cysteine DUB that is a member of the USP family (Baker et al., 1999). The UCH domain carries the catalytic triad (Cys, His, Arg), with the Cys separated from the His and Arg, by a single ubiquitin-like (UBL) domain (Ye et al., 2009) and four zinc co-ordinating cysteine residues (Hetfeld et al., 2005) (Figure 1.2). Similar to its two most closely related DUBs, USP4 (57% identity) and USP11 (40% identity), the N-terminal of USP15 comprises a domain present in USPs (DUSP) and an UBL domain that form the major non-catalytic part of the protein (Elliott et al., 2011). Structural analysis of the USP15 DUSP-UBL improved our understanding of the residues and interfaces likely to be involved in protein-protein interactions (Elliott et al., 2011, Harper et al., 2011). USP15 also contains putative nuclear localisation and export signals (Park et al., 2000, Soboleva et al., 2005).

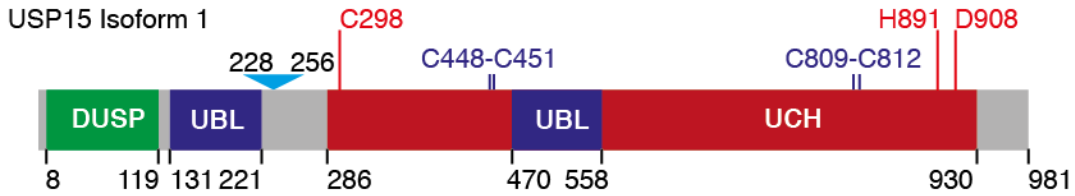

Figure 1.2 USP15 Protein Isoform 1 and Domains
USP15 isoform 1 (Q9Y4E8-1) contains isoform specific residues, through the inclusion of an alternatively spliced exon encoding amino acids 228-256 (blue) that is absent from USP15 isoform 2 (Q9Y4E8-2). The Ubiquitin C terminal hydrolase (UCH) domain is separated by a ubiquitin-like domain (UBL) insertion that separates the catalytic triad (red). The N' terminal domain present in ubiquitin-specific peptidase (DUSP) and UBL are involved in substrate recognition. The zinc co-ordination residues (purple).

Human USP15 has four potential isoforms (Table 1.2) (Faronato et al., 2011) generated by alternative splicing, the longest of which is USP15 isoform 1. The USP15 isoform 1 transcript retains a single exon that is absent in USP15 isoform 2. This alternative exon encodes 29 amino acids that are inserted between the DUSP-UBL and UCH domains (Figure 1.2). The predicted USP15 isoform 3 retains a different alternative exon resulting in a small insert within the DUSP-UBL domain. USP15 isoform 4 is truncated prior to the catalytic triad of USP15, making it catalytically inactive. USP15 isoforms 1 and 2 appear to be the major endogenous isoforms (Angelats et al., 2003). The literature often fails to discriminate between these isoforms when describing experiments using exogenous USP15, but in general earlier references relate to USP15 isoform 2, with more recent papers relating to USP15 isoform 1. Recently, it was reported that these two major isoforms of USP15 have some differential substrate preference suggesting divergent functions (Kotani et al., 2017). Our data have also demonstrated that these isoforms have differential effects in supporting accurate separation of sister chromatids at anaphase (Fielding et al., manuscript in preparation).

Table 1.2 USP15 Protein Isoforms

Protein Isoform	Uniprot	Size (AA)	Mw (kDa)
USP15 isoform 1	Q9Y4E8-1	981	112
USP15 isoform 2	Q9Y4E8-2	952	109
USP15 isoform 3	Q9Y4E8-3	956	109
USP15 isoform 4	Q9Y4E8-4	235	27

Human USP15, is expressed in most tissues, with the highest levels in testes; similar to its mouse and rat orthologs, human USP15 is least abundant in brain, lung and kidney (Park et al., 2000, Angelats et al., 2003). At a cellular level, USP15 is a relatively abundant DUB that is estimated to be present at ~$3.5x10^4$ copies per cell (Clague et al., 2013, Schwanhäusser et al., 2011). USP15 has a predominantly cytoplasmic localisation, despite internal nuclear import and export sequences, and in contrast to its homologs USP4 (cytoplasmic and nuclear) and USP11 (mainly nuclear) (Urbé et al., 2012). However, USP15 is also found associated with specific cellular organelles, including the outer membrane of the mitochondria (Cornelissen et al., 2014) and polysomes (Faronato et al., 2013). In addition, USP15 can translocate into the nucleus, localising at sites of DNA damage upon laser micro-irradiation (Nishi et al., 2014).

USP15 is a promiscuous DUB, which appears to exhibit catalytic activity towards all ubiquitin chain linkages, although more recently it has been suggested that USP15 prefers branched ubiquitin chains (McGouran et al., 2013, Ritorto et al., 2014, Crowe et al., 2016). Interestingly, the zinc co-ordinating amino acids are thought to play a role in the ability of USP15 to select for polyubiquitin chains (Hetfeld et al., 2005). For the USP15 homolog USP4, the DUSP-UBL domain is involved in dissociation of ubiquitin and catalytic turnover (Clerici et al., 2014). Comparison of USP15 and USP4 suggested similar catalysis, although the effects of the DUSP-UBL domain on USP15 catalytic efficiency does not appear to be as potent as in USP4. To date, no external factors (PTMs or cofactors) have been verified that regulate USP15 catalytic activity or linkage specificity.

Interestingly, several lines of evidence suggest USP15 may be regulated by phosphorylation. USP15 phosphorylation *in vitro* was first demonstrated for the constitutive photomorphogenesis 9 (COP9) signalosome (CSN) associated casein kinase II (CK2). The modified residues were not shown, but phosphorylation was predominantly within, but not completely

limited to the C' terminus of USP15 (Hetfeld et al., 2005). USP15 could also be a substrate for the ataxia-telangiectasia mutated (ATM) and ATM- and Rad3-Related (ATR)-checkpoint kinases (Mu et al., 2007), which if not involved in regulating catalytic activity might act as a trigger for USP15 co-localisation with sites of DNA damage (Nishi et al., 2014). The laboratory has also shown that USP15 isoform 1 becomes phosphorylated during mitosis at S229, although the functional consequences of this remain to be determined (Faronato et al., 2013, Fielding et al., manuscript in preparation).

1.6.2.2 Cellular Roles of USP15

Given the ubiquitous expression of USP15 and its promiscuous activity towards ubiquitin chain linkages, it is unsurprising that USP15 has multifaceted cellular roles. Specific roles may depend on different USP15 isoforms or PTMs, its interacting partners, or cellular location. A proposed conserved function of USP15, inferred from substrate interactions shared with the DUBs USP4 and USP39, is in processing of mRNA (Sowa et al., 2009). USP15 interacts with squamous cell carcinoma antigen recognised by T-cells 3 (SART3) via its DUSP-UBL domain (Long et al., 2014, Timani et al., 2014, Zhang et al., 2016). The functional roles of USP15-SART3 are to mediate deubiquitylation of histone H2B ubiquitylation and/or regulate the recycling of the spliceosome, as shown for USP4 (Song et al., 2010). The DUSP-UBL of USP15 is implicated in its interaction with the E3-ligase BRCA1-associated protein (BRAP), which also bound the DUSP-UBL of USP4, although only knockdown of USP15 was sufficient to promote BRAP degradation (Hayes et al., 2012). In this study, depletion of USP15 reduced phosphorylation of dual specificity mitogen activated protein kinase kinase (MEK) and subsequent phosphorylation of ERK in response to stimulus.

USP15 is known to associate with the CSN, a conserved multi-protein complex found in all eukaryotes. The activity of the CSN deconjugates the ubiquitin-like neural precursor cell expressed developmentally down-regulated gene 8 (NEDD8), supressing activation of the cullin-RING ligase (CRL) family

of ubiquitin E3 ligases (Wei et al., 2008, Kumar et al., 1992, Liakopoulos et al., 1998). The CSN has been shown to regulate the expression of the RING-box protein Rbx1 (Hetfeld et al., 2005), the adenomatous polyposis coli tumour suppressor (Huang et al., 2009c), and the NF-kb inhibitor IkBa (Schweitzer et al., 2007). USP15, through its association with CSN, is implicated in the regulation of these cellular signalling pathways.

As eluded to earlier, USP15 is predominantly cytoplasmic with the intrinsic capacity to shuttle in and out of the nucleus. USP15 has been found at a variety of cellular locations where it is implicated in a vast array of cellular roles including: plasma membrane (regulation of receptors), mitochondria (mitophagy), polysomes (stability of newly synthesised protein), and nucleus (DNA damage). Despite these diverse cellular roles for USP15, knockout mice with a homozygous USP15 deletion, are viable and demonstrate no overt phenotype, which was proposed to be due to some functional redundancy with the homologous DUB USP4 (Vlasschaert et al., 2015). The lack of an overt phenotype would appear to demonstrate that related DUBs may act collectively to protect the cell from catastrophe.

1.6.2.3 USP15 Association with Cancer

Genetic amplification of USP15 has been observed in ~2% of glioblastoma and breast cancer (Eichhorn et al., 2012). Amplification of USP15 conferred poor prognosis in glioblastoma, which was attributed to hyper activation of transforming growth factor β (TGF-β) signalling, through stabilisation of the TGF-β type I receptor (TβRI) by countering the E3 ligase (SMURF2). USP15 was also shown to deconjugate monoubiquitin and activate SMADs downstream of TGF-β and bone morphogenetic protein (BMP) signalling (Inui et al., 2011). Interestingly, the homologous USP4 has also been associated with deubiquitylation of TβRI only in response to TGF-β (Zhang et al., 2012).

As well as TGF-β, a number of key cancer associated signalling pathways have been shown to be regulated by USP15. For example, USP15 has been implicated in stabilising mouse double minute 2 homolog (MDM2), with USP15 short hairpin RNA (shRNA) expressing xenografts demonstrating reduced tumour growth (Zou et al., 2014). USP15 involvement in cancer extends to roles in promotion of migration, drug resistance and viral oncoprotein expression. For example, knockdown of USP15 reduces hepatocyte growth factor (HGF)-dependent scattering of cancer cells (Buus et al., 2009), demonstrating that loss of function impairs cell migration. Another study proposed that reduced expression of USP15 in response to Paclitaxel treatment encouraged drug resistance through the down regulation of an apoptotic pathway. USP15 was shown to stabilise pro-caspase 3, which upon cleavage produces potent pro-apoptotic signalling, a reduction in USP15 therefore reduces apoptosis (Xu et al., 2009b). USP15 has also been implicated in cervical cancer through an oncogenic role of USP15 in promoting stabilisation of the human papilloma virus type 16 (HPV16) E6 oncoprotein (Vos et al., 2009). Importantly E6, together with the E6 associated protein (E6AP) promotes the degradation of p53 (Scheffner et al., 1990, Scheffner et al., 1993). Thus, USP15 stabilisation of the E6 oncoprotein supresses p53 mediated apoptosis of cancer cells.

1.6.2.4 USP15 Role in the Reversible Ubiquitylation of REST

REST is periodically degraded during the cell cycle (Chapter 1, Section 3.4.3, Figure 1.3). Importantly, $SCF^{\beta\text{-}TrCP}$ induced degradation is also used to supress REST during neuronal differentiation. Following these discoveries, it was of interest to identify any deubiquitylases that could regulate REST protein expression during either the cell cycle or neurogenesis. One DUB, USP7, was identified as a positive regulator of REST stability during neurogenesis through the countering of $SCF^{\beta\text{-}TrCP}$ mediated degradation (Huang et al., 2011). Interestingly, although USP7 can deubiquitylate REST, it was not identified from an unbiased siRNA screen for regulating DUBs that regulate endogenous levels of REST, in the non-neuroendocrine A549 lung cancer cell line (Faronato et al., 2013). This screen highlighted four DUBs whose depletion

was associated with a reduction in REST protein abundance: USP15, USP47, USP49 and USP52, however only USP15 was validated by deconvolution of the siRNA pool. Further characterisation showed USP15 involvement in the re-expression of REST, following mitotic exit, through regulation of newly synthesised REST protein in early G1 (Faronato et al., 2013). This mechanism by which USP15 regulates REST re-expression is distinct from the role of USP7 in opposing $SCF^{\beta\text{-}TrCP}$ ubiquitylation in neural stem cells (Huang et al., 2011).

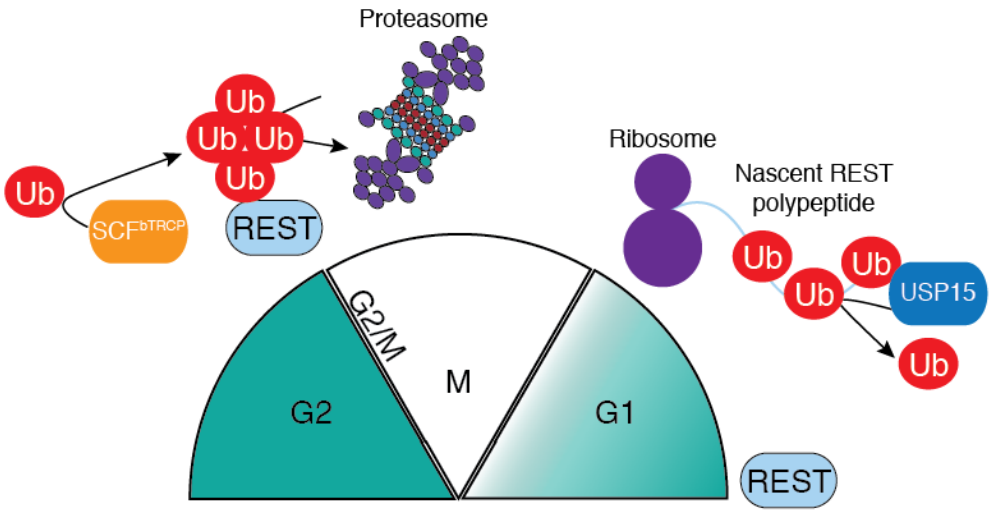

Figure 1.3 Cell Cycle Dependent Ubiquitylation and Deubiquitylation of REST
Cell cycle regulation of REST expression controlled by the E3 ligase $SCF^{\beta\text{-}TrCP}$ at the G2/M checkpoint. The re-expression of REST is supported by the deubiquitylation of the nascent REST polypeptide by USP15.

The co-translational ubiquitylation of newly synthesized REST is presumably regulated by the pool of REST demonstrated to be associated with polysomes (Faronato et al., 2013). Co-translational ubiquitylation acts as a quality control mechanism to degrade misfolded proteins (Smith et al., 2011) and occurs on 12-15% of nascent polypeptides (Duttler et al., 2013, Wang et al., 2013). The post-translational ubiquitylation of transcription factors is a common mechanism that allows for dynamic control of their levels and activity. Transcription factors such as p53 are rapidly degraded by a ubiquitin-dependent mechanism when not required. The consequences of USP15-mediated REST regulation on cellular processes remains to be determined.

1.7 Project Aims

The broad aim of this thesis was to investigate the expression and relationship of REST and USP15 in lung cancer cells. Specifically, I set out to (1) quantify REST and USP15 splicing/expression in thoracic cancers and explore any dynamic changes during the cell cycle, (2) use quantitative proteomic analysis to delineate the cellular response to loss of USP15 and/or REST1 function.

1.7.1 Chapter 3

The expression and splicing of REST has previously been addressed in lung cancers, with expression of the REST4 isoform identified as a SCLC phenomenon (Coulson et al., 2000, Gurrola-Diaz et al., 2003, Moss et al., 2009). In this chapter, my first aim was to increase the scope of these investigations by expanding the cell panel to include carcinoid and mesothelioma cell lines and to use quantitative reverse transcription polymerase chain reaction (RT-PCR). In tandem, I aimed to investigate the expression of specific DUBs and the splicing factor SRRM4 that are known to regulate REST, to determine correlative expression patterns.

During the cell cycle, REST is acutely degraded at the onset of mitosis by the E3 ligase $SCF^{\beta\text{-}TrCP}$, which is required to allow for effective mitotic division (Guardavaccaro et al., 2008). As cells exit mitosis, re-expression of REST protein is regulated through the stabilising role of USP15 on the nascent polypeptide in early G1 (Faronato et al., 2013). REST1 protein re-expression in G1 is crucial for effective repression of a broad range of transcripts. The expression of other REST isoforms during the cell cycle were unknown. Therefore, my second aim was to profile the expression of REST isoforms, and the known regulators of REST expression and splicing through the cell cycle.

1.7.2 Chapter 4

REST is known to repress expression of a myriad of mRNA and non-coding RNAs. In lung cancer cells the loss of REST-mediated repression is thought to contribute to the neuroendocrine phenotype. Previous studies of REST-dependent expression in lung cancer have focused solely on mRNA transcript expression following REST knockdown (Coulson, data unpublished). Limitations of such studies are that proteins do not always reflect mRNA levels (Maier et al., 2009) and that protein level changes can be a consequence of miRNAs regulated by REST. Here, I investigate the consequences of loss of REST expression in lung cancer using siRNA knockdown and a proteomic approach, to provide a more accurate picture of the protein expression changes that influence cell physiology. In parallel I also investigated the USP15 dependent proteome, using siRNA knockdown. Importantly these studies can be analysed independently to identify protein targets of REST or USP15 dependent proteins and maybe combined to address the importance of USP15 regulation on REST dependent proteins, through comparison of proteome datasets.

1.7.3 Chapter 5

Proteome analysis of USP15 depleted lung cancer cells revealed a co-ordinated response in mitochondrial proteins. USP15 has previously been associated with the mitochondria through a role in mitophagy (Cornelissen et al., 2014), however this preliminary data suggested that USP15 may play a more fundamental role in the function of the mitochondria in energy production. In Chapter 5, I aimed to validated and investigate USP15-mediated regulation of mitochondrial proteins that are involved in the electron transport chain.

CHAPTER 2: MATERIALS AND METHODS

2.1 Cell Biology

2.1.1 Reagents

All routine cell culture reagents, including Foetal Bovine Serum (FBS), 10x 0.5% Trypsin-EDTA (15400-054), high glucose 4.1 g/L Dulbecco's Modified Eagle Medium (DMEM) containing 2% GlutaMAX (31966-21), Media 199 (31153-026) and Roswell Park Memorial Institute (RPMI) media (61870-010) were purchased from Gibco, Invitrogen (Life Technologies, UK). General cell culture plastic-ware and chemicals were obtained from Corning Inc. (NY, USA) and Sigma Aldrich (Poole, UK) respectively. FBS was heat-inactivated at 56^{o}C for 25-30 mins before use in cell culture. Synchronisation of cells required Thymidine (T1895) and Nocodazole (M1404) purchased from Sigma. Cell cycle flow cytometry; Propidium iodide (P4864) and RNase A (R613) were purchased from Sigma. FACScalibur reagents including FACsflow and FACsRinse were purchased from BD Biosciences (New Jersey, USA). Cellular bioenergetics assays were performed using a Seahorse XF^{e}96 Metabolic Analyser, with reagents for the Seahorse XF Cell Mito Stress Test (103015-100) [containing Oligomycin, MA, Antimycin A and Rotenone], together with; XF Calibrant Solution (100840-000), XF Base Medium (102353-100) and XFe96 Cell Culture Microplates (101085-04) purchased from Seahorse Bioscience, Massachusetts, USA. Collagen (C3867), L-Glutamine (G7513), D-Glucose (G5400) and Sodium Pyruvate (S8636) were purchased from Sigma Aldrich.

2.1.2 Routine Cell Culture

Descriptions of all cell lines used in this project and their specific culture conditions are listed in Table 2.1. Cell lines were routinely verified as mycoplasma free and were cultured for limited passage numbers in a humidified incubator at 37°C and 5% CO_2.

A549 cells, which were used most extensively, were passaged once they reached 80-90% confluence, typically using a 1:5 split ratio for two days growth or a 1:7.5 split ratio for three days growth, and were used for experiments between passages two and 20. A549 and most adherent cell lines were grown in 10 cm dishes unless otherwise stated, and were passaged using a standard protocol. Media was aspirated and cells were washed with warm 1x Phosphate-Buffered Saline (PBS), once aspirated 1x trypsin was added for 30 secs before being aspirated and the plate incubated for a maximum of five mins at 37^{o}C. Dishes were then gently tapped to release cells from the plastic, these were resuspended in 10 mL of complete media and seeded at the appropriate densities (Table 2.1). One exception to this was the loosely adherent U2020 cell line, for which media was gently removed, and cells washed off in 1x PBS and collected in a sterilin, before centrifugation at 300 x relative centrifugal force (rcf) for two mins to collect the cells. PBS was aspirated and cells were re-suspended in complete media. The suspension aggregate cell lines were routinely grown in T75 or T175 flasks in 25 mL or 50 mL of media respectively. To passage these lines, the cells were allowed to settle into a corner of the upright flasks for five mins at room temperature, the majority of the media was then gently aspirated and the cells were disaggregated in the residual media by tituration, before being split at the appropriate ratios into complete media in new flasks.

To freeze cell line stocks, cells were collected by trypsinisation or aggregate sedimentation and resuspended in freezing media (Media, 20% FBS, 10% DMSO) in cryogenic vials (BC163, Corning). Vials of cells were frozen slowly to -80^{o}C overnight in a Nalgene Mr Frosty (C1562, Sigma) then transferred into long term liquid nitrogen storage. When required cells were rapidly thawed at 37^{o}C and initially grown with media in T25 flasks to establish fresh cultures.

Table 2.1 Cell Lines

Cell Line	Origin	Cell Type (subtype)	Sex	Adherence	Media	Recommended Split Ratio	References
A549	ECACC	NSCLC (alveolar cell)	M	Adherent	DMEM/10%FBS/0.1 mM NEAA	1:5 -1:7.5	(Giard et al., 1973)
BEAS-2B	Stuart Marshall-Clarke	SV40 transformed human bronchial epithelium	?	Adherent	RPMI/10% FBS	1:2 - 1:4	(Reddel et al., 1988)
COR-L23	Penella Woll	NSCLC (Large cell)	M	Adherent	RPMI/10% FBS	1:5	(Walls and Twentyman, 1985, Coulson et al., 1999b)
COR-L47	CRUK	SCLC (classical)	M	Suspension aggregate	RPMI/10% FBS	1:3 - 1:4	(Baillie-Johnson et al., 1985)
COR-L88	CRUK	SCLC (classical/morphological variant)	M	Suspension aggregate/ partially adherent	RPMI/10% FBS	1:3 - 1:4	(Walls and Twentyman, 1985)
GLC-19	Penella Woll	SCLC (classical)	F	Suspension aggregate	RPMI/10% FBS	1:3 - 1:4	(Coulson et al., 1999b)
Lu-165	Penella Woll	SCLC (classical)	M	Suspension aggregate	RPMI/10% FBS	1:2 – 1:4	(Terasaki et al., 1994)
MeT5a C2	ATCC	Mesothelioma (Clone 2)	?	Adherent	Media 199/10%FBS	1:2.5	(Lechner et al., 1985)
MRC5	CRUK	Normal lung fibroblasts	M	Adherent	DMEM 10% FBS	1:2 - 1:4	(Jacobs et al., 1970)
MRC5VA	CRUK	SV40 transformed normal lung fibroblasts	M	Adherent	DMEM 10% FBS	1:2 – 1:4	(Huschtscha and Holliday, 1983)
MSTO-211H	ATCC	Mesothelioma (sarcomatoid) (Clone 5)	M	Adherent	RPMI/10%FBS	1:3	(Bepler et al., 1988)
NCI-H2052	ATCC	Mesothelioma (biphasic)	M	Adherent	RPMI/10%FBS	1:3	(Gazdar and Minna, 1996)

NCI-H2170	CRUK	NSCLC (Squamous)	M	Adherent	RPMI/10% FBS	1:2	(Gazdar and Minna, 1996)
NCI-H322	CRUK	NSCLC (broncheoalveolar)	M	Adherent	RPMI/10% FBS or DMEM/10%FCS	1:3	(Gazdar and Minna, 1996)
NCI-H345	Youqiang Ke	SCLC (classical)	M	Suspension aggregate	RPMI/10% FBS	1:3-1:4	(Gazdar and Minna, 1996)
NCI-H460	Penella Woll	NSCLC (Large cell)	M	Adherent	RPMI/10% FBS	1:8	(Gazdar and Minna, 1996, Coulson et al., 1999b)
NCI-H647	CRUK	NSCLC (adeno-/squamous mixed)	M	Adherent	RPMI/10% FBS	1:5	(Gazdar and Minna, 1996)
NCI-H69	Penella Woll	SCLC (classical)	M	Suspension aggregate	RPMI/10% FBS	1:4 - 1:6	(Coulson et al., 1999b)
NCI-H727	CRUK	Carcinoid	F	Adherent	RPMI/10% FBS	1:3	(Gazdar and Minna, 1996)
SV40-HBE	W Franklin	SV40 transformed human bronchial epithelium	?	Adherent	DMEM 10% FBS	1:2- 1:4	(Coulson et al., 1999b)
U2020	Pamela Rabbitts	SCLC (morphological variant)	?	Very loosely adherent	RPMI/10% FBS	1:4 - 1:6	(Heppell-Parton et al., 1999)
WI38-VA	CRUK	SV40 transformed embryonic lung fibroblast	F	Adherent	DMEM 4.5g/L glucose/10% FBS	1:2 – 1:4	(Ponten et al., 1963)
UPS15+/+ and USP15-/- MEF	Klaus-Peter Knobeloch	Mouse embryonic fibroblast and USP15 knockout mouse embryonic fibroblast	?	Adherent	DMEM/10% FCS/ Pen Strep/ ß-Mercaptoethanol	1:3	(Torre et al., 2017)

Origins: European Collection of Cell Cultures (ECACC), Cancer Research UK (CRUK), American Tissue Culture Collection (ATCC). Cell Type: Non-Small Cell Lung Cancer (NSCLC), Small Cell Lung Cancer (SCLC). Sex: Male (M), Female (F) and unknown (?). NEAA: MEM non-essential amino acids

2.1.3 Stable Isotope Labelling with Amino Acids in Cell Culture (SILAC)

A549 cells were grown for seven passages in SILAC-labelling media, to allow for complete incorporation of isotopic amino acids. Labelling media was made using DMEM without lysine or arginine (Dundee Cell Products, Dundee, UK), 10% dialyzed foetal bovine serum (dFBS) (Dundee Cell Products or LabTech (Uckfield, UK)) and supplemented with 84 mg/L of Arginine, 126 mg/L of Lysine and 200 mg/L of Proline amino acids (Table 2.2). To supress the interconversion of Arginine to Proline, I supplied cells with Arginine at the concentration as standard DMEM, and excess Proline. The conversion of arginine to proline would cause an increase in the mass of proline-containing peptides, which hinders the accurate identification of peptides. Labelling was calculated to be >95% before experiments were performed.

Table 2.2 SILAC Amino Acids

Condition	Amino Acid	Catalogue number and Supplier
Light	Proline 0	P-5607 (Sigma)
	Lysine 0	L-8662 (Sigma)
	Arginine 0	A-8094 (Sigma)
Medium	Proline 0	P-5607 (Sigma)
	Lysine 4	616192-SPEC (CK Gas), DLM-2640-1 (Sigma)
	Arginine 6	643440-SPEC (CK Gas), CLM-2265-H-1 (Sigma)
Heavy	Proline 0	P-5607 (Sigma)
	Lysine 8	608041-SPEC (CK Gas), CNLM-291-H-1 (Sigma)
	Arginine 10	608033-SPEC (CK Gas), CNLM-539-H-1 (Sigma)

2.1.4 Cell Synchronisation

A549 cells were synchronised to enrich for specific cell cycle phases, as illustrated in Figure 2.1. Timings were based on previous synchronisation protocols (Faronato et al., 2013). Cells were seeded at 1x 10^6 cells /10 cm dish to obtain asynchronous cell populations and for double thymidine synchronisation, or at 1.5x 10^6 cells/10 cm dish for thymidine/nocodazole synchronisation. For thymdine/nocodazole synchronisation, two replicate dishes were seeded to allow for ~50% loss of cells during mitotic shake-off.

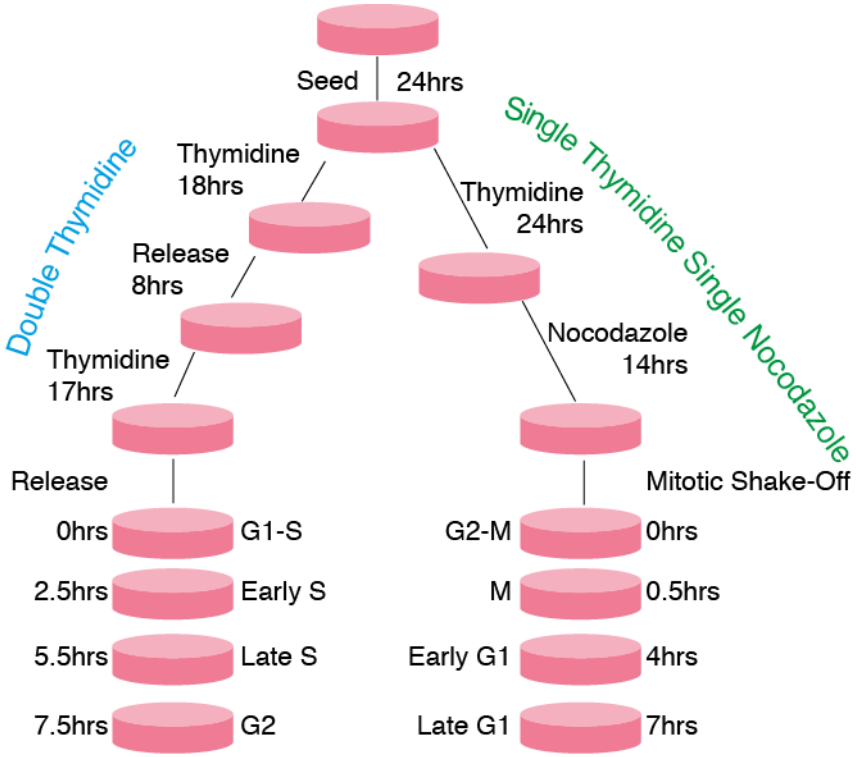

Figure 2.1. Cell Cycle Synchronisation Regime
A549 cells were seeded 24 hrs, prior to synchronisation with double thymidine (left) to generate an enriched population of cells in G1-S, Early S, Late S or G2, or with thymidine/nocodazole (right) to generate cells in G2-M, M, Early G1 and Late G1.

Double thymidine treated cells were incubated for 18 hrs with 2 mM thymidine, then released for eight hrs into fresh media, before a second incubation with thymidine for 17 hrs. Cells were washed once with warm 1x PBS between treatments, before release into the next condition. Following release from the second thymidine block cells were incubated for 0, 2.5, 5.5 or 7.5 hrs to generate an enriched population of cells in G1-S, Early S, Late S and G2 respectively. Thymidine/nocodazole treated cells were incubated for 24 hrs with thymidine followed by release into nocodazole (10 ng/mL) for 14 hrs, before mitotic shake-off. Cells were incubated for 0, 0.5, 4 and 7 hrs to generate cells in G2-M, M, Early G1 and Late G1.

Double thymidine synchronised cell populations (G1-S, Early S, Late S and G2) were harvested by gently aspirating the media, then scraped into PBS using a rubber cell scraper, collected in a sterilin and centrifuged at 300 x rcf for two mins. The supernatant was aspirated, the cells resuspended in PBS, and collected by centrifugation. The PBS was aspirated, and the tube briefly

vortexed to dislodge the pellet before processing for subsequent analyses. For mitotic shake off, the media was collected into a 25 mL steriln. Cells were manually dislodged, collected in PBS and added to the steriln, then centrifuged at 300 x rcf for two mins, the supernatant aspirated, and the cells resuspended in complete media. Cells from two dishes were pooled to re-seed for each condition (M, Early G1 and Late G1). For the G2-M enriched population, mitotic shake-offs from two dishes were resuspended in PBS, pooled and collected by centrifugation. The remaining PBS was aspirated, and the tube was briefly vortexed to dislodge the pellet prior to processing for subsequent analyses.

To validate enrichment of the desired cell cycle phase, samples prepared in this manner were processed for subsequent analysis by flow cytometry (Chapter 2, Section 1.6), RNA extraction (Chapter 2, Section 2.2) for qRT-PCR (Chapter 2, Section 2.3) or protein extraction (Chapter 2, Section 3.2) for western blotting (Chapter 2, Section 3.3).

2.1.5 siRNA Knockdown

$5x10^4$ cells were plated per well of a six-well plate (Costar). 24 hrs after seeding, cells were transfected with 50 nM of siRNA oligonucleotides (Table 2.3), with Oligofectamine and OptiMEM (Invitrogen) in 1 mL serum free media. The cells were incubated for four hrs before the addition of FBS to a final concentration of 10%. The following day the media was replaced with fresh complete media. Cells for six-day knockdown were split 48 hrs after transfection and seeded at 1.5 $x10^5$ cells/6 cm with the transfection protocol repeated at 24 hrs later. After three days or six days protein lysates or RNA were extracted from the cells.

Table 2.3 Details of siRNA oligonucleotides

siRNA Name	Pools	Sequence / Product Code	Provider
siCon1		UAG CGA CUA AAC ACA UCA A (D-001210-01-05)	Dharmacon – siGenome
siCon2		(D-001210-02-20)	Dharmacon – siGenome
siNT1		UGG UUU ACA UGU CGA CUA A (D-001810-01)	Dharmacon – On Target Plus
siREST1		CAA CGA AUC UAC CCA UAU UUU (FARM-000005)	Dharmacon – siGenome
siREST5		CAU CCU ACU UGU CCU AAU AUU (FARM-000003)	Dharmacon – siGenome
siUSP15-1	**siUSP15-Pool**	GAA GAA GGC UCA CCA AGU G (D-006066-1)	Dharmacon – siGenome
siUSP15-2		GAA CGC ACC UUG GAA GUU U (D-006066-2)	Dharmacon – siGenome
siUSP15-17		CAG AUA AGG UGG UUG CCG A (D-006066-17)	Dharmacon – siGenome
siUSP15-iso1	**siUSP15-isoPool**	ACA ACA UGA ACA ACA GAA AUU (COUJA000007)	Dharmacon – Custom -siGenome
siUSP15-iso2		CUU UCU ACU CCU AAU GUG AUU (COUJA000009)	Dharmacon – Custom siGenome

2.1.6 Flow Cytometric Analysis of Cell Cycle

Propidium Iodide (PI) is a nucleic acid intercalating agent commonly used in cell cycle analysis. The incorporation of PI labels the DNA of permeabilised cells which, together with the cell shape and size can discriminate between cells in the G0/G1, S and G2/M phases of the cell cycle. Cells were synchronised and harvested as described above (Chapter 2, Section 1.4) with centrifugation at 4^{o}C. Following aspiration of the final PBS wash, a further 1 mL of ice-cold PBS was added. The cells were gently resuspended and fixed with 3 mL of ice-cold molecular grade 100% ethanol. Samples were placed on ice and processed in batches. Samples were centrifuged at 1x10^{3} x rcf for 10 mins, resuspended in 1.4 mL of PBS and transferred to microcentrifuge tubes for further centrifugation a 1x10^{3} x rcf for 10 mins. The PBS was aspirated and the cells washed by resuspending in 1 mL PBS for a further centrifugation step. PBS was aspirated and the cells were resuspended in 400 µL PI (50 µg/mL) and 4 µL of RNase A (1 mg/mL), protected from light and incubated for 30 mins at 37^{o}C. Following this, 360 µL of PBS was added, and samples transferred to FACS tubes (Eppendorf) for

analysis. Samples could be stored for up to one week at 4^{o}C in the dark before flow cytometry.

Analysis was performed using a FACScalibur flow cytometer (BD Biosciences), in accordance with departmental tutelage (Stewart Marshall-Clarke, University of Liverpool). The instructions for optimisation of the flow cytometer for PI cell cycle analysis can be found at the following web address: https://research.missouri.edu/cic/files/Cell%20Cycle%20Basics.pdf correct as of 07/09/2016. The instrument parameters were initially set using unstained fixed cells. The distribution of cells was optimised to centre the cells in forward and side scatter parameters (FSC and SSC, repectively). The unlabelled cells were used to set a base fluorescence reading (FL2) adjusting parameters to centre a peak of cells between 10^0 and 10^1. On analysis of a fluorescently-labelled sample, the FL2 peak shifts to the right. The separation in the FL2 channel, allows for separation of cell size and staining, with G2 and M cells having twice as much DNA than G1/G0 cells, as it is replicated during S phase. Asynchronous cells labelled with PI generates a 'horse-saddle' distribution (peak, trough, peak). Single cells were isolated through gating the FSC and SSC to exclude aggregates and cell debris. Data were collected with the requirement that 10,000 gated events were recorded for each sample. Data was imported into WIN-DMI 2.9 software, and the single cell region was plotted and kept consistent through all samples. The percentage of cells in each cell cycle phase was determined using markers to define the boundaries between G0/G1, S and G2-M.

2.1.7 Measuring Cellular Bioenergetics

A549 cells were transfected with siRNA for six days as previously described (Chapter 2, Section 1.5) prior to performing a mitochondrial stress test using a Seahorse XF^{e}96 Metabolic Analyser. 48 hrs prior to analysis a XFe96 Cell Culture Microplate was coated with collagen and 24 hrs later cells were seeded. For initial optimisation, a range of cell densities ($1x10^3$ to $4x10^4$) were seeded to determine that which produced a tight monolayer of cells. The

cells were viewed under a microscope and protein lysates taken to assess the protein content. Subsequent experiments used $3x10^4$ cells/well.

The Seahorse injection cartridge was hydrated overnight, by submerging the sensors in 200 µL/well of calibrant in the utility plate, which were stored in a humidified 37°C incubator. On the day of the Mitochondrial Stress Test, XF basal medium was supplemented with sodium pyruvate (1 mM), D-Glucose (4.5 g/L) and L-Glutamine (2 mM), to generate the assay medium, which was calibrated to a pH of 7.4 $\pm$ 0.05 and incubated at 37°C. At the start of the assay, the cell culture plate was removed from the CO_2 incubator and the time recorded. The media was gently removed and the plate washed twice with 100 µL of assay media. All the media was gently removed and exactly 175 µL of assay media added to each well. The cells were checked using a microscope to ensure they had not been dissociated by washing. The cell plate was incubated in a non-CO_2 incubator for at least 1 hr before starting the assay. A series of Oligomycin (0.75 µM, 1 µM, 1.25 µM, 1.5 µM), FCCP (0.75 µM, 0.25 µM), FCCP injection 2 (0.25 µM), Antimycin A (1 µM) + Rotenone (1 µM) solutions were prepared in assay medium. Inhibitors (25 µL) are injected sequentially into wells, to obtain the desired final concentrations at each stage of the protocol. 25 µL of the stress test solutions at appropriate concentrations were added to ports of the Seahorse XF cartridge, before calibration in the metabolic analyser. Once calibrated, the utility plate is removed and replaced with the microplate containing cells in assay medium. Three readings, each separated by ~seven mins, were taken before the initial injection to establish a basal reading, with three readings after each subsequent injection. For optimisation experiments, Oligomycin was followed by two separate injections of FCCP and finally Rotenone + Antimycin A. Under optimal conditions a single in injection of FCCP (1 µM) was used. Once the assay was completed, protein lysates were collected using a cold lysis procedure. Cells were washed three times with ice-cold 1x PBS before 10 mins incubation in ice-cold NP40 buffer (50mM Tris, 150mM NaCl, 1% NP40, pH

7.4, 30 µL/well). 10 µL was collected and used in a BCA assay (Chapter 2, Section 3.2), using standards prepared in NP40 buffer.

Analysis of data was performed using Seahorse Wave Software (v2.2.0) downloaded from the Seahorse Biosciences website, as well as MitoStress Test Report Generator Excel Spreadsheet v2. The Wave data visualisation software allows discrimination between non-responsive and responsive samples. The MitoStress Test Report details response profiles associate with key bioenergetics phenotypes such as oxidative phosphorylation and glycolysis. The protein concentration from each well, were used to normalise data in the MitoStress Test Report Generator to account for differences in cell density due to seeding or growth of cells.

2.2 Molecular Biology

2.2.1 Reagents

RNA extraction was performed on an RNAse free worktop, RNAzap (R2020, Sigma) using ethyl-alcohol molecular grade (E7023, Sigma), RNeasy Kit (74106), RNase-free DNase (79254) and Qiashredder (79656) purchased from Qiagen (Manchester, UK). Reaction mix reagents for reverse transcription or quantitative real-time polymerase chain reaction (qRT-PCR) were obtained from Promega (Madison, USA) or BioRad (California, USA), respectively unless otherwise stated. Primers were purchased form Eurofins MWG Operon (Ebersberg, Germany) with nuclease free H_2O (W4502) purchased from Sigma. qPCR-specific white walled plates were also purchased Bio-Rad, USA. For gel electrophoresis, samples were combind with 5x DNA loading buffer (BIO-37045, Bioline, London, UK) and run in parallel with Hyperladder (BIO-33057, Bioline). Ethidium bromide (43992U, VWR, Lutterworth, UK)) containing agarose (50005, Lonza, Basel, Switzerland) gels were electrophoresised using horizontal agarose gel electrophoresis cassettes and combs (CSSU1214, Thermo Scientific, Massachusetts, USA). General palsticware, including pipette tips and microcentrifuge tubes were purchased from Starlabs (Milton Keynes, UK), unless otherwise stated.

2.2.2 RNA Extraction

RNA was extracted and handled in a dedicated RNAse-free area, taking all standard precautions to maintain RNA integrity. Total RNA was prepared from cells using an RNeasy Mini Kit, in accordance with manufacturers instructions. Briefly, media was aspirated from the cells and directly lysed in 700 µL of RLT buffer (containing 10 µL β-mercaptoethanol/ 1 mL lysis buffer). If required, the lysate was divided into two, with 350 µL each loaded onto two Qiashredder columns and centrifuged as per the manufactors instructions. The flow-through was retained and mixed with an equal volume of 70% ethanol before applying onto RNeasy Mini Spin Columns. An on column DNAse treatment was always performed following the intial washes, according to the manufacturers instructions. The RNA samples were eluted in 10 µL of ddH_2O and, where samples had been processed in two halves, the samples pooled together prior to the quality control steps. Once eluted, RNA samples were kept on ice during processing then immediately stored at -80^{o}C.

The concentration of RNA and purity of the samples was determined using a NanoDrop Spectrophotometer (Thermo Scientific), as per manufactures instructions. Briefly, the concentration of RNA was determined using the Beer-Lambert equation [c = (A*ε)/b)]. For RNA, ε (wavelength-dependent extinction coefficient) is 40ng-cm/µL. The absorbance (A) is detected and the pathlength (b) is controlled by the Nanodrop, with 1 µL of sample applied to the spectrophotometer. Protein contamination of RNA samples is assessed using the A260/280 ratio, with a value of ~2.0 being accepted as pure for RNA. The absorbance at 230 nm can indicate the presence of contaminants such as phenols. An A260/230 ratio of 1.8-2.2 is also considered pure for nucleic acids. The integrity of the RNA was determined by 1.2% agarose gel electrophoresis (Chapter 2, Section 2.4). Gels were visually assessed for evidence of low molecular weight degradation products, the relative intensity of the 18S and 28S ribosomal RNAs, and a lack of genomic DNA contamination.

2.2.3 Reverse Transcription Polymerase Chain Reaction (RT-PCR)

Reactions for cDNA preparation and PCR analysis were prepared in a clean PCR hood using dedicated equipment and sterile filtered pipette tips. All sample and reagent tubes, with the exception of enzymes, were briefly vortexed and pulse-spun before opening.

2.2.3.1 Reverse Transcription

cDNA was generated from 1 µg of RNA, unless otherwise stated. For each sample, 1 µg of RNA was made up to a final volume of 10 µL with the addition of nuclease free water (Sigma). 1 µL of Oligo dT was added to the cDNA and placed in the thermocycler (Hybaid Px2, Thermo Scientific) at 70^{o}C for five mins; samples were then quickly snap-cooled on ice, which reduces template secondary structure to improve cDNA yield for long mRNAs and GC-rich regions. A reaction Master Mix was prepared, consisting of 4 µL 5x reverse transcription buffer (250 mM Tris-HCl, pH 8.3, 250 mM KCl, 20 mM $MgCl_2$, 50 mM DTT), 2 µL PCR Nucleotide mix, 0.5 µL RNAsin and 1.5 µL Nuclease free ddH_2O per sample. 8 µL of the master mix was added to each sample and the tubes were returned to the thermocycler for incubation at 37^{o}C for five mins, before the addition of 1 µL of RevertAid H-minus M-MuLV reverse transcriptase (200 U/µL, EP0451, Thermo Scientific). The samples were incubated at 42^{o}C for 1 hr followed by 70^{o}C for 10 mins, before being snap cooled on ice. The cDNA was then diluted with 80 µL of ddH_2O, mixed by vortexing, briefly centrifuged and stored at -20^{o}C. In tandem with the production of cDNA, control reactions were processed in the same way with only the omission of the reverse transcriptase, to produce RT- negative controls.

2.2.3.2 Endpoint RT-PCR

Endpoint PCR was used to validate specificity and to determine the optimal working conditions for the RT-PCR primer pairs (Table 3). The majority of primers were designed for quantitative Real-Time PCR (qRT-PCR), generating products between 100 and 200 bp. Primers were designed with the

assistance of BLAST (NCBI) (Altschul et al., 1990), UCSC Genome Browser and BLAT (Kent et al., 2002, Kent, 2002) and additionally NetPrimer (http://www.premierbiosoft.com/netprimer/) (PREMIER Biosoft, Palo Alto, California, USA). BLAST allows for a confirmation of primer specificity to a single gene target, UCSC genome browser help provide detail of isoforms that will be amplified as well as providing the product sizes for a pair of primers from transcript or the whole genome assembly. NetPrimer software allows for the calculation of primer properties including GC content and secondary structures. The primers were designed to adhere as close as possible to primer design guidelines (PREMIER Biosoft).

Table 2.4. PCR Primers

Primers	Pairing	Sequence 5' -> 3'	Product size cDNA	Product size gDNA
Actin	ACTBFnew9-06 ACTBRnew9-06	CACCTTCTACAATGAGCTGCGTGTG ATAGCACAGCCTGGATAGCAACGTAC	159bp	599bp
USP15-All	USP15-all-for USP15-all-rev	ATGTTGTAACTCGAAGATTTAGC GCTGTCTGGTTTATTCAGTGG	152bp	-
USP15iso1	USP15mwgFOR USP15iso2REV	CAGACAGCACCATTCAGGATGC AAAATTGGATGCACCTGGGGAC	125bp	-
USP15iso2	USP15mwgFOR USP15iso1REV	CAGACAGCACCATTCAGGATGC GAGTTTTTCACATTAGGAGTAG	115bp	-
REST1	3NRSFfor WTrev	GCATGTTAGAACTCATACAGG GCTTCTCATCTGAATGAGTAC	113bp	8343bp
REST4	3NRSFfor nNRSFrev	GCATGTTAGAACTCATACAGG ATCACACTCTAGTAAATATTACC	146bp	16559bp
REST-E5	3NRSFfor REST-E5-qPCR	GCATGTTAGAACTCATACAGG CCCTGTGCATATCACCTC	141bp	55176bp
USP7	HAUSPfor HAUSPrev	ACTTTGAGCCACAGCCCGGTAATA GCCTTGAACACACCAGCTTGGAAA	149bp	-
SRRM4	SRRM4for SRRM4rev	AGACTTGACACCACCACCTTCCTC TGACCTGCGTCGCTTGTGTTTC	148bp	2720bp
SCG3	SCG3for SCG3Rev	GATCCAGATGGTCTTCATCAAC CTGATTCTCAGTCCAGCTTGTG	267bp	1083bp
Cyclin B1	CCNB1- CCREG CCNB1 R	GCTCTTCTCGGCGTGCTGC CCTGCCATGTTGATCTTCG	190bp	814bp
Cyclin E1	CCNE1for CCNE1rev	CCTTATGGTATACTTGCTGCT CCACTGATACCCTGAAACC	81bp	-

The primers used to detect each transcript, the pairings used and corresponding sequence. The size of the product expected to be amplified from cDNA is shown, together with predicted size of amplicon from genomic DNA.

For endpoint PCR, master mixes were prepared so that each 30 µL reaction would contain: 1.5 µL forward and 1.5 µL reverse primers (final concentration 300 nM per primer), 10 µL ddH_2O, 15 µL HotStar Taq Plus

Mastermix (Qiagen), to which 2 µL of cDNA template would be added. In tandem, control reactions were set up using 2 µL of RT- template (produced during cDNA synthesis) and H_20 instead of cDNA. These negative controls demonstrated that the amplification product was derived from the template cDNA and was not attributable to genomic DNA or other contamination of the reaction mix. Endpoint PCR programs followed a standard thermo cycling profile: Step 1: 95°C for two mins; Step 2: 95°C for 30 secs, 60°C (annealing), followed by 72°C for 30 secs; Step 3: 72°C for 10 mins. The annealing temperature is variable and was optimised for primer pairs using gradient PCR settings, although primers were design to work at 60°C. Step 2 was repeated 40 times with the exception of actin, a highly abundant transcript (27 cycles). Amplified products were assessed by agarose gel electrophoresis (Chapter 2, Section 2.4).

2.2.3.3 Quantitative Real-Time PCR (qRT-PCR)

Primers that had been validated in end-point PCR were used for quantitative determination of transcript expression. qPCR plate layouts were designed for optimal annealing of primers and product amplification, and included negative controls to ensure specific product formation with three technical replicates for each sample. Master mixes were prepared for 10 µL PCR reaction volumes, containing 0.15 µL of Forward and 0.15 µL Reverse Primers (final concentration 300 nM / primer) (Table 2.4), 5 µL of 2x SYBR iTaq Master Mix (172-5121) and 0.7 µL ddH_20 (Sigma) per sample, with 8 µL aliquoted into the appropriate wells of the qPCR plate. cDNA and RT- samples (Chapter 2, Section 2.3.2) were further diluted 1:4 with ddH_20. Using a fresh pipette tip for each sample, 2 µL of cDNA, RT- template or ddH_2O was added to the appropriate wells). qRT-PCR analysis was performed on a BioRad CFXConnect instrument using a 2-step protocol (Step 1 95°C for three mins. Step 2 95°C for 10 secs, 60°C for 30 secs, repeat 39 times) followed by melt curve analysis (95°C for 10 secs, then 65°C with temperature rises by 0.5°C every five secs), unless otherwise stated.

The melt curves were analysed for primer dimers or secondary products, any samples where the Cq (threshold cycle) values were influenced by primer dimer formation were omitted from the analysis. The Cq value was taken from the intersection of the amplification curve and an instrument/experiment defined threshold. A comparative Cq method ($2^{-\Delta\Delta Cq}$) was used to determine the relative difference in mRNA expression (Schmittgen and Livak, 2008). The ΔCq is defined as the average Cq of three technical replicates for the gene of interest subtracted from the average Cq of three technical replicates for the housekeeping gene, actin. The ΔΔCq is the ΔCq(sample)-ΔCq(control). One exception was for the analysis of USP15 isoform expression, in which the isoform $2^{-\Delta Cq}$ of the sample was made relative to the USP15-all $2^{-\Delta Cq}$ of the corresponding sample. Expression values for the lung cancer panel represent one biological replicate of extracted RNA, and are derived from the three technical replicates where possible.

2.2.4 Agarose Gel Electrophoresis

Electrophoresis grade agarose was added at 1.2% (w/v) for RNA or 2% for PCR products to 100 mL 0.5x TBE (45 mM Tris-borate, 1mM EDTA). The agarose was dissolved in a microwave (~90 secs). This was allowed to cool slightly before the addition of ethidium bromide to a final concentration of 0.5 µg/mL. The solution was gently mixed, and poured into horizontal agarose gel electrophoresis cassettes and left to set (~30-60 min). 5x DNA loading buffer was added to DNA or RNA samples to generate 1x concentration. The agarose gel cassette was filled with 0.5x TBE buffer. The samples were loaded and the gels electrophoresed at 140 V for 1 hr (RNA gels), or 120 V for one hr (DNA gels). DNA bands were visualized using the GeneFlash UV transilluminator (Syngene, Cambridge, UK).

2.3 Protein Biochemistry

2.3.1 Reagents

ProtoGel Acrylamide (EC-890), Resolving (EC-892) and stacking (EC-893) buffers were purchased from National Diagnostics (Atlanta, USA). Ammonium persulphate (APS, A3678), Tween-20 (P9416), and Ponceau S solution (P7170) were obtained from Sigma. Tetramethylethylenediamine (TEMED, 303853V), BioTrace NT nitrocellulose membrane (0.2 µm pore size, 732-3032) and Rainbow marker (RPN800E) were purchased from VWR. Perfect protein ladder (69079-3) was obtained from Merck Biosciences (Darmstadt, Germany). Marvel skimmed milk powder was obtained from Premier Brands (St Albans, UK). NuPage 4-12% gradient gels (NP0321) were run with 1x MES buffer [[50 mM 2-(*N*-morpholino)ethanesulfonic acid (MES), 50 mM Tris Base, 0.1 % SDS, 1 mM EDTA, pH 7.3], NP0002] or 1x MOPS buffer [[50 mM 3-(*N*-morpholino)propanesulfonic acid (MOPS), 50 mM Tris Base, 0.1 % SDS, 1 mM EDTA, pH 7.7], NP0001] purchased from Invitrogen. Reagents for liquid chromatography-tandem mass spectrometry (LC/MS): Acetonitrile (ACN, 20060.320), Mass spec grad water (23595.328) and formic acid (20318297) were purchased from VWR, with Ammonium bicarbonate (Ambic, A1641) and Iodoacetamide (I1149) purchased from Sigma. Additional reagents included Dithothreitol (DTT, MB1015, Melford, Ipswich, UK)), LoBind centrifuge tubes (022431081, Eppendorf, Hamburg, Germany) and Trypsin Gold (V5280) purchased from Promega.

2.3.2 Protein Extraction and Sample Preparation

Cells were rinsed twice with PBS before “hot lysis”. PBS was aspirated and denaturing protein lysis was performed by addition of hot (110^{o}C) Laemmli buffer (50 mM Tris, pH 6.8, 2% SDS, 10% glycerol) to the cell culture plate on a dry heat block at 110^{o}C. 150 µL of Laemmli buffer was used per well of a 6-well plate; 900 µL was used for lysis of cells in 10 cm dishes. Cells were scraped with a rubber policeman and the lysate collected into preheated screw-capped eppendorf tubes and incubated at 110^{o}C for 10 mins, vortexing every two mins to ensure thorough mixing and lysis. 16 µL of each sample was

put aside for Bicinchoninic Acid (BCA) assay (23225, Thermo Scientific), the remaning samples were diluted with 10x sample buffer (1M DTT, 1% Bromophenol Blue) and stored at -20^{o}C. Protein lysates were kept on ice whilst the BCA assay was performed or stored immediately at -20^{o}C. Bovine Serum Albumin (BSA) protein standards were dissolved in a one in five dilution of the same batch of lysis buffer used for protein extraction, in order to reduce the concentration of SDS. Protein samples were diluted one in five prior to the assay. The BCA assay was prepared according to the manufacturer's instructions using equal volumes of each sample and incubated at 37^{o}C for 30 mins, before the absorbance at 560 nm was measured using a Glomax-Multi Detection System (Promega). The concentration of the samples was calculated from the BSA standard curve accounting for the five-fold dilution of the samples.

2.3.3 SDS-PolyAcrylamide Gel Electrophoresis (SDS-PAGE)

SDS-PAGE gels were poured by hand using Bio-Rad Mini Gels and ProtoGel reagents (National Diagnostics). The desired thickness and acrylamide concentration of the resolving gels, was normally 0.75 mm and 8% unless otherwise stated. 15 mL of 8% resolving gel contains 5.3 mL ProtoGel, 5.2 mL Resolving Buffer, 9.2 mL ddH_2O, 150 µL 10% APS and 15 µL TEMED. In general, 0.75 mm thick gels were preferred for transfer of high molecular weight proteins, such as REST. Resolving gels were poured and overlaid with water. Once set, a stacking gel (1.3 mL ProtoGel, 2.5 mL Stacking Buffer, 6.1 mL ddH_2O, 50 µL of 10% APS and 10 µL TEMED) was poured on top and a well-forming comb inserted. Once set the, gels were assembled in a Bio-Rad Mini-Protean® 3 system tank with 1x running buffer diluted from 5x stock (15.15 g Tris, 72 g glycine, 5 g SDS in 1 L water). For separation of low molecular weight proteins 4-12% gradient gels were run with 1x MES buffer at 200 V for 35 mins as per manufactures instructions. Protein samples were thawed on ice, vortexed and briefly spun before incubation at 95^{o}C for five mins, to denature the proteins immediately prior to loading. Equal volumes of samples were loaded on the gel, flanked by lanes loaded with 5 µL of the

molecular weight markers and electrophoresed for 1 hr at 200 V until the dye front had just run out of the gel.

2.3.4 Immunoblotting

During SDS-PAGE, fresh transfer buffer (25 mM tris-glycine, 20% Methanol) was prepared. Whatman paper and nitrocellulose (VWR) were cut to size, and together with scotch brite pads were pre-soaked in transfer buffer. Following SDS-PAGE, the stacking gel was removed and transfer apparatus assembled. Proteins were transferred onto nitrocellulose (pore size 0.2 µm) at 24V for 90 mins using a Genie Blotter (41017, Idea Scientific, Minneapolis, USA). The efficient and even transfer of proteins to the nitrocellulose was determined using Ponceau-S staining. Membranes were then blocked using the optimal conditions, as determined by the primary antibody (Table 2.5). In general, blots were blocked for 1hr at room temperature using 5% non-fat milk (Marvel) in Tris-Buffered Saline (20 mM Tris base, 137 mM NaCl, pH 7.6) containing 0.1% Tween-20 (TBS-T). Primary antibodies were diluted in the appropriate blocking buffer and incubated with rocking, either overnight at 4^{o}C, or for one hr at room temperature. The membranes were then washed three times for 10 mins in TBS-T, with the exception of the REST antibody, which was washed two times for 10 mins in ddH_2O. Complementary fluorescent-secondary antibodies (Table 2.6), under the same blocking conditions, were incubated for one hr at room temperature whilst protected from light. The membrane was washed three times for 10 mins with TBS-T and then a final ddH_2O wash prior to imaging. When REST antibodies were used, TBS-T washes were replaced with ddH_2O. Blots were scanned and quantified using the LI-COR Odyssey and Image Studio Software (LI-COR, Nebraska, USA). Images processed in Adobe Photoshop and Illustrator CS6 (Adobe Systems Inc, San Jose, California, USA).

Table 2.5. Primary Antibodies

Target Protein	Species	Source (Cat #)	Blocking Buffer	Dilution and incubation (time and temperature)
ACTB	Mouse	Abcam (Ab6276)	Marvel 5% TBS-T	1:10000 1hr RT
CCNB1	Mouse	Millipore (05-373)	Marvel 5% TBS-T	1:2000 O/N 4°C
CCNE1	Mouse	Cell Signalling (4129)	Marvel 5% TBS-T	1:1000 O/N 4°C
REST	Rabbit	Millipore (07-579)	3% Marvel TBS	1:2000 O/N 4°C
USP7	Rabbit	Abcam (ab4080)	Marvel 5% TBS-T	1: 2000 O/N 4°C
USP15	Mouse	Abnova (H00009958-M01)	Marvel 5% TBS-T	1: 1000 O/N 4°C
NDFUB6	Mouse	Abcam (ab110244)	Marvel 5% TBS-T	1: 1000 O/N 4°C
NDUFB4	Rabbit	Abcam (ab192243)	Marvel 5% TBS-T	1: 1000 O/N 4°C
EGFR	Rabbit	Cell Signalling (D38B1)	Marvel 5% TBS-T	1: 1000 O/N 4°C
VCL	Mouse	Sigma (V9131)	Marvel 5% TBS-T	1: 1000 O/N 4°C
ITGA2	Rabbit	Abcam (ab133557)	Marvel 5% TBS-T	1: 1000 O/N 4°C
ITGB1	Rabbit	Abcam (Ab52971)	Marvel 5% TBS-T	1: 1000 O/N 4°C

Room temperature (RT), Overnight (O/N), Tris-buffered saline (TBS). Companies; Abcam (Cambridge, UK), Millipore (Massachusetts, USA). Abnova (Taipei City, Taiwan). Cell Signalling Technologies, Inc. (Massachusetts, USA).

Table 2.6. Secondary Fluorescent Antibodies

Catalogue Number	Antibody	Dilution
926-32213	IRDye 800CW Donkey anti-Rabbit	1:15000
926-32212	IRDye 800CW Donkey anti-Mouse	1:15000
926-68023	IRDye 680LT Donkey anti-Rabbit	1:20000
926-68020	IRDye 680LT Donkey anti-Mouse	1:20000

Antibodies purchased from LI-COR.2.3.5 Liquid Chromatography-Tandem Mass Spectrometry (LC-MS/MS)

2.3.5 Liquid Chromatography-Tandem Mass Spectrometry (LC-MS/MMS)

2.3.5.1 1D PAGE and Sample Preparation

SILAC-labelled A549 cells (Chapter 2, Section 1.3) were transfected with siRNAs (Chapter 2, Section 1.5) so that proteins from siCon1, siUSP15-Pool and siREST5 depleted cells were labelled with light, medium, heavy amino acids, respectively (Figure 4.1). Proteins were extracted by hot lysis and protein concentrations determined by BCA assay (Chapter 2, Section 3.3). Equal amounts of protein (33.3 µg/condition) were combined, loaded and run on a 4-12% Gradient Gel at 200 V for 50 mins in 1x MOPS buffer. The gel was fixed by incubating in fixing solution (10% acetic acid, 50% methanol, 40% mass spectrometry grade H_2O) for 10 mins at room temperature. The gel was placed in a 15 cm dish and the sample lane divided into 50 slices, using sterile scalpels, with each slice being sub-divided into ~1 x 1 mm pieces and transferred to a 1.5 mL LoBind Eppendorf. The pieces of gel were dehydrated using 100 µL of Acetonitrile (ACN), incubated in a thermoshaker for five mins at 900 rpm at room temperature. The supernatant was then discarded and the gel pieces dried using the rotational vacuum concentrator (RVC) 2-25, with cooling trap CT 02-50 (CHRIST, Osterode am Harz, Germany) at 37^{o}C for five mins. The RVC reduces the boiling point, which allows for evaporation and drying of peptide samples at lower temperatures.

The cysteine residues of the proteins within the gel pieces were then reduced in 10 mM DTT in 100 mM Ambic, within incubation in a thermo-shaker for one hr at 56^{o}C and 900 rpm. The samples were allowed to cool for five mins, before the supernatant was discarded. The cysteine residues were then alkylated, to prevent cysteine disulphife bond formation reoccurring, by incubation with 50 mM iodoacetamide in 100 mM ambic, whilst protected from light for 30 mins at room temperature and 900 rpm. The supernatant was again discarded and the samples washed in 100 mM ambic for 15 mins, at 900 rpm. The supernatant was discarded and the samples were washed with 20 mM ambic/20% ACN for 15 mins, at 900 rpm. The samples were then dehydrated

again with 100% ACN for five mins at 900 rpm and returned to the RVC for five mins.

In-gel digestion of proteins was performed with the addition of Trypsin Gold diluted in reaction buffer (40 mM ambic, 9% ACN). Each gel slice receiving ~50 ng of trypsin, additional reaction buffer was added after 30 mins if required to cover the gel pieces. The samples were left to incubate for at least 16 hrs at 37^{o}C. The gel pieces were then incubated with an equal volume of 100% ACN at 30^{o}C for 30 mins, 900 rpm. The supernatant, containing the peptides, was transferred to a new LoBind tube. 1% formic acid was added to the gel pieces, and incubated for 20 mins, 900 rpm. The supernatant was transferred to a new LoBind tube containing the corresponding peptides. The formic acid wash was repeated and the supernatant transferred. 150 µL ACN was added to dehydrate the gel pieces, for 10 mins, 900 rpm. The supernatant was transferred to the LoBind tube and dried in the RVC, after which samples were stored at -20^{o}C.

2.3.5.2 Liquid Chromatography (LC) and Tandem Mass Spectrometry (MS/MS)

For liquid chromatography, samples from 2.3.5.1 were resuspended in 25 µL 1% formic acid, and centrifuged at 1.3 x10^{4} g for 10 mins, with 20 µL being transferred to a glass vial. In brief, the samples were separated using reverse phase liquid chromatography, to increase the separation of peptides. 4 µL of sample was injected and run on an 80 min ACN gradient (low to high) in the NanoAcuity UPLC system (Waters Corporation, Massachusetts, USA). The column is connected to an electrospray ionization LTQ OrbiTrap XL (Thermo Scientific). The mass spectrometer identifies the mass/charge of a peptide, which can be used to determine the amino acid composition. The mass spectrometer then selects peptides, which are broken into fragments by collision-induced dissociation. This allows for the sequence of the amino acids to be determined.

2.3.5.3 Protein Assignments

Mass spectrometry .RAW files were analysed using MaxQuant (Cox and Mann, 2008, Cox et al., 2011) v.1.3.0.5 downloaded from: www.coxdocs.org, together with the International Protein Index (IPI) (Kersey et al., 2004) database (v.3.77). Despite the discontinuation of IPI database (Griss et al., 2011), it was continually used by the laboratory during the time in which proteomic experiments and analysis were performed. MaxQuant analysis identifies the peptides from the chromatography, and together with the MS/MS analysis determines the amino acid composition of the peptide. Multiple unique "razor" peptides are required to determine a protein identity and add confidence to the difference in peptide scores. These scores are made into ratios by placing these scores relative to another condition (i.e. the control). The gene name associated with each protein was extracted from the database using an excel formula, in some instances this was unsuccessful in returning a gene name. Following shortlisting of proteins, any without a gene name were assigned manually using the IPI.

2.4 Bioinformatics and Statistics

2.4.1 Statistical Analysis

Routine data calculations and visualisations were performed in Microsoft Excel and proteomic supplementary table was saved in excel format. Detailed statistical analyses were calculated using specialised statistics packages. Analysis of variance (ANOVA) were performed using GraphPad Prism version 6.00 for Mac (https://www.graphpad.com, GraphPad Software, Inc. La Jolla, California, USA). For the proteomics dataset statistical analysis was performed using a Significance B statistical test embedded within the Perseus program (Tyanova et al., 2016) (www.coxdocs.org), which determines if specific protein changes are significantly different from the majority of protein differences within the dataset, whilst also accounting for the intensity.

2.4.2 Gene Ontology and Pathway Analysis

Gene Ontology (GO) analysis was performed using the online tool DAVID Bioinformatics Database (Huang et al., 2009a, Huang et al., 2009b), and was limited to either Biological Process and Molecular Function or Cellular Compartment annotations. Shortlists of proteins that exhibited >1.5-fold change in response to either USP15 or REST knockdown were analysed. Lists of proteins were inputted using the official gene name. Over represented terms within the shortlists were compared to a human background (threshold count = 2; EASE score = 1). Terms with a p-value of <0.01 in at least one condition were isolated, with redundant terms (those containing an almost identical selection of proteins) manually removed to provide an overview of gene ontology results. The P value of these terms were transformed into a heatmap using MeV (version. 4_8_10.2; www.tm4.org/mev) (Saeed et al., 2006) (Figure 4.6). The manually ascribed 'redundant terms' and the proteins therein, were combined with a similar specific term into a general category for later analysis to ensure that no unique proteins were overlooked (Figure 4.7-8). Cellular pathway mapping was performed by overlaying proteomic data upon publically available cellular pathways (http://wikipathways.org) (Kelder et al., 2012, Kutmon et al., 2016) using Pathvisio v.3.2 (https://www.pathvisio.org) (van Iersel et al., 2008, Kutmon et al., 2015).

CHAPTER 3: REST AND USP15 EXPRESSION IN THORACIC CANCERS AND THROUGH THE CELL CYCLE

3.1 REST and USP15 Expression

3.1.1 Thoracic Cancers

Lung cancer occurs within the airways and is predominantly associated with tobacco exposure, it is estimated to be the most common cancer worldwide (Ferlay et al., 2015, Torre et al., 2015). There were 46,403 new lung cancer cases diagnosed and 35,895 fatalities in the UK in 2014 (Cancer Research UK, https://www.cancerresearchuk.org/). Lung cancers are primarily classified by their cellular morphology and phenotype. They are broadly divided into small cell lung cancer (SCLC) and non-small cell lung cancers (NSCLC). Of these NSCLC are the most common, representing around 80% to 85% of cases, whilst SCLC account for the remainder and are the most aggressive. NSCLCs are further sub-divided into the major types of adenocarcinoma, squamous cell carcinoma and large cell carcinoma, which each have different histology and aetiology. SCLC has a neuroendocrine (NE) phenotype, in common with large cell neuroendocrine carcinoma and the more benign carcinoid tumours. NE cancers express and secrete neuropeptides and hormones that may sustain their growth through autocrine and paracrine mechanisms.

In contrast to lung cancer, malignant pleural mesothelioma occurs in the mesothelial lining of the thoracic cavity. It is a relatively rare cancer, as it is almost exclusively associated with asbestos exposure. Only around 2000 new mesothelioma cases are diagnosed in the UK each year, but it accounts for a similar number of fatalities annually (Cancer Research UK, https://www.cancerresearchuk.org/). Mesothelioma are histologically classified as epithelioid, sarcomatoid or biphasic, and do not exhibit a NE phenotype.

Reduced expression and alternative splicing of REST has been linked to NE breast, prostate and lung cancers. Previously, the expression of REST variants has been reported for a small panel of lung cancer cell lines (Coulson et al., 2000, Kreisler et al., 2010). Here, I expand the cell panel to include additional thoracic cancers and examine co-expression of REST with known regulators of REST expression.

3.1.2 Cell Cycle

The cell cycle is a process that results in the division of a cell into two daughter cells. The process of division occurs through phases, gap phase one (G1), DNA synthesis (S), gap phase two (G2) and mitosis (M). The mitotic phase is only brief taking ~30 mins, and consists of condensation of the chromatin, alignment and attachment to kinetochores and separation of sister chromatids that ends with the process of cytokinesis and cellular division. The transition through G1/S and G2/M phases provide important checkpoints and act as temporal sensors that regulate unidirectional progression through the cell cycle. The transition to the next phase of the cell cycle is controlled by the actions of cyclin dependent kinases that are regulated by phase specific cyclins. During cellular division, cyclin dependent kinases regulate the activity of many proteins including ubiquitin E3 ligases, notably APC and SCF. The $SCF^{\beta\text{-}TrCP}$ ligase regulates the degradation of proteins at the G2/M checkpoint, including REST and its displacement from the Mad2 RE-1 site allows for optimal expression (Guardavaccaro et al., 2008). The expression of Mad2 restricts cell cycle progression, at the spindle assembly checkpoint, until microtubule attachments to kinetochores by inhibition of APC. During anaphase, chromatin condenses and displaces many transcription factors, that once ejected from the DNA are targeted for degradation. Lack of REST degradation can promote DNA damage through modulation of the spindle assembly checkpoint (Guardavaccaro et al., 2008). Following mitotic exit, transcription factors that are important to maintaining cellular identity are re-expressed and maintained through the opposing actions of synthesis and degradation. The re-expression of REST during G1 is stabilised co-

translationally by USP15 (Faronato et al., 2013). In this context, REST is a tumour suppressor, which when dysregulated reduces genome integrity. Dysfunctional REST expression should therefore promote prolonged transcription of RE-1 regulated genes. Here, I will assess the mRNA and protein levels of REST variants through the cell cycle and examine co-expression with known REST regulators.

3.2 Results

3.2.1 The Differential Expression of REST Splice Variants in Lung Cancer Cell Lines

The repertoire of REST splice variants has recently been increased to include many ncRNAs and REST-E5, a protein coding mRNA that contains a novel C' terminal exon (Chen and Miller, 2013). The expression of the REST-E5 transcript, only found in humans, can theoretically produce a truncated REST4-like protein (Chen and Miller, 2013). A simplified schematic of the REST gene structure is presented in Figure 3.1A. The REST gene has a non-coding first exon, with alternative transcriptional start sites (Chen and Miller, 2013). The corresponding REST protein regions and domains are shown beneath their coding exons.

To investigate the differential expression of REST isoform transcripts, I selected PCR primers that could selectively amplify the REST1, REST4 and REST-E5 protein coding transcripts (Figure 3.1B). The reverse primers were designed to anneal within exons or at exon boundaries, the position of which are illustrated on the schematic of the REST gene (Figure 3.1A), and in combination with a common forward primer could amplify a specific sized product for the desired transcript (Figure 3.1B). To demonstrate primer specificity, I amplified REST isoforms using endpoint RT- PCR on cDNA templates generated from RNA extracts of one NSCLC cell line, A549, and one SCLC cell line, Lu-165. The PCR products were separated by agarose gel electrophoresis and visualised by ultraviolet fluorescence of the DNA intercalating agent ethidium bromide (Figure 3.1C, D).

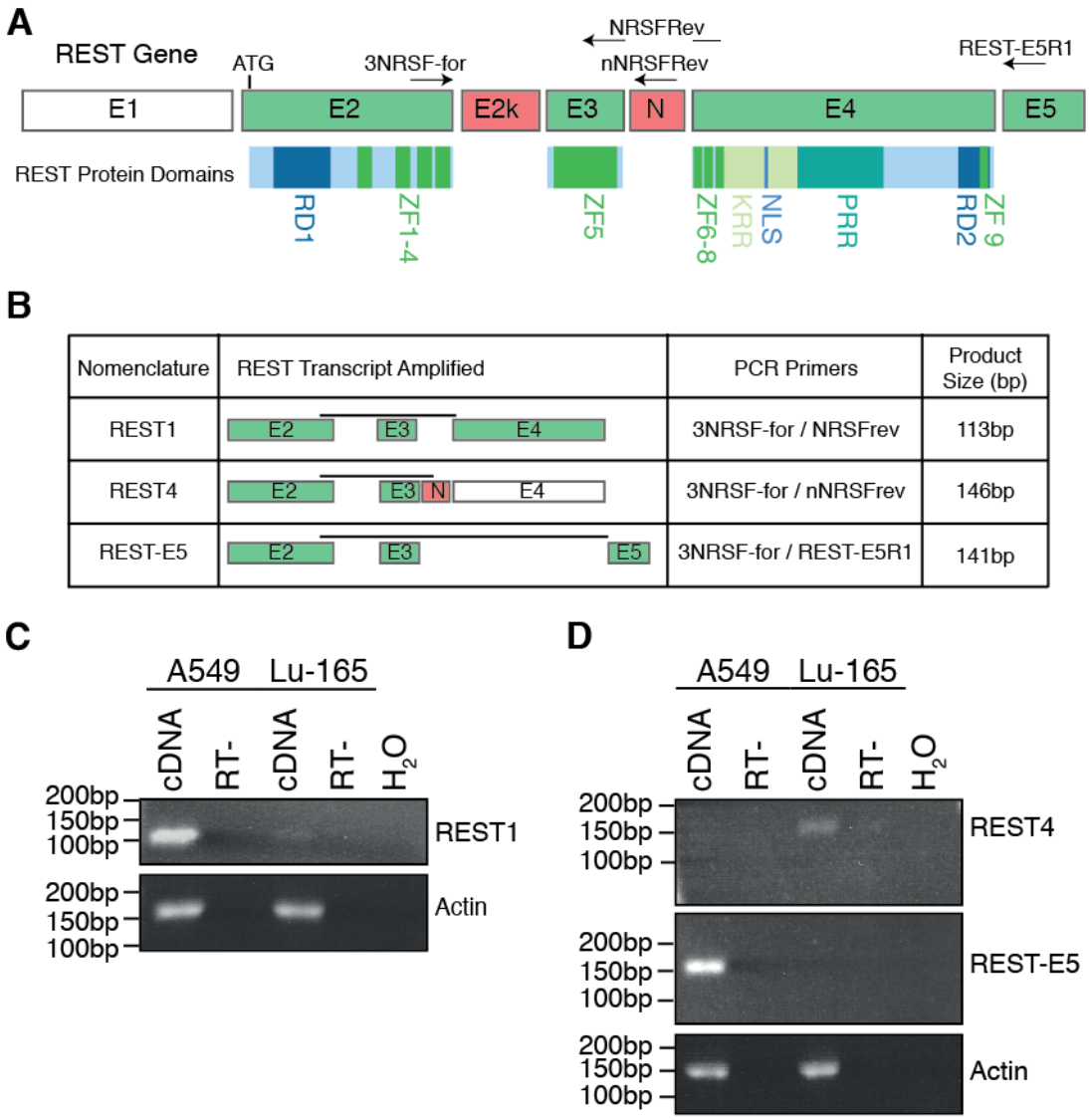

Figure 3.1. Validation of PCR Primers for REST Splice Variants
(A) Schematic of the REST gene and corresponding protein domains encoded by exons, with the position of PCR primers mapped to the REST gene. Inclusion of the orange exons into the REST transcript result in translational termination. The translation start ATG codon is in exon 2. The REST protein coding regions include Repression Domains (RD1-2), Zinc Fingers (ZF1-9), Lysine rich region (KRR), Proline rich region (PRR) and Nuclear localisation signal (NLS). **(B)** Table of PCR products and the corresponding transcripts from which they are amplified. **(C,D)** The expression of REST isoforms was determined by endpoint PCR (40 cycles) using cDNA templates generated from the NSCLC cell line, A549, and the SCLC cell line, Lu-165. Expression of actin (28 cycles PCR), was used as a positive control for the presence of cDNA. RT- negative control consists of the reverse transcription reaction mix, in which reverse transcriptase enzyme was omitted. H_2O negative control consists of PCR reaction reagents with water instead of cDNA. PCR products were separated by 2% agarose gel electrophoresis.

Each primer pairing amplified a single product of the expected size in base pairs (bp) from the cDNA, which was absent in the RT- and H_2O controls. The REST1 isoform transcript was expressed only in A549 cDNA (Figure 3.1C). The REST4 encoding transcript was expressed in Lu-165, in accordance with previous studies of REST expression (Coulson et al., 2000). Notably, I was also able to detect REST-E5 transcript in A549 cells (Figure 3.1D) in agreement with expression of the E5 exon in these cells (Chen and Miller, 2013).

To determine the expression levels of REST isoforms in a panel of thoracic cell lines I used quantitative reverse transcription PCR (qRT-PCR), in which the intercalation of SYBR green was measured after each cycle of amplification (Figure 3.2). The cDNA templates were reverse transcribed from RNA extracted from a large collection of cell lines, that represent different thoracic cancer types, including SCLC, carcinoid, NSCLC and mesothelioma. In addition to these cancer cells I generated cDNA from SV40-transformed normal lung cell lines representing epithelial cells (SV40-HBE, BEAS-2B), fibroblasts (MRC5-VA, W138-VA) and mesothelial (Met5a) cells. The expression of the different REST splice variants was determined by qRT-PCR, with data normalised to the endogenous housekeeping gene actin, and shown relative to expression in the SV40-HBE cells. REST1 transcript was expressed in the normal lung, NSCLC and mesothelioma cell lines, although it was dramatically reduced in both SCLC and carcinoid cell lines (Figure 3.2A). In contrast, REST4 was expressed in SCLC and carcinoid cells, but substantially lower in normal, NSCLC and mesothelioma cell lines (Figure 3.2B). Therefore, expression of REST1 and REST4 transcripts demonstrates a mutually exclusive relationship. The REST-E5 transcript was expressed in lung cancer cells irrespective of cell type (Figure 3.2C). Whilst REST-E5 was expressed in all cell types, its expression was variable.

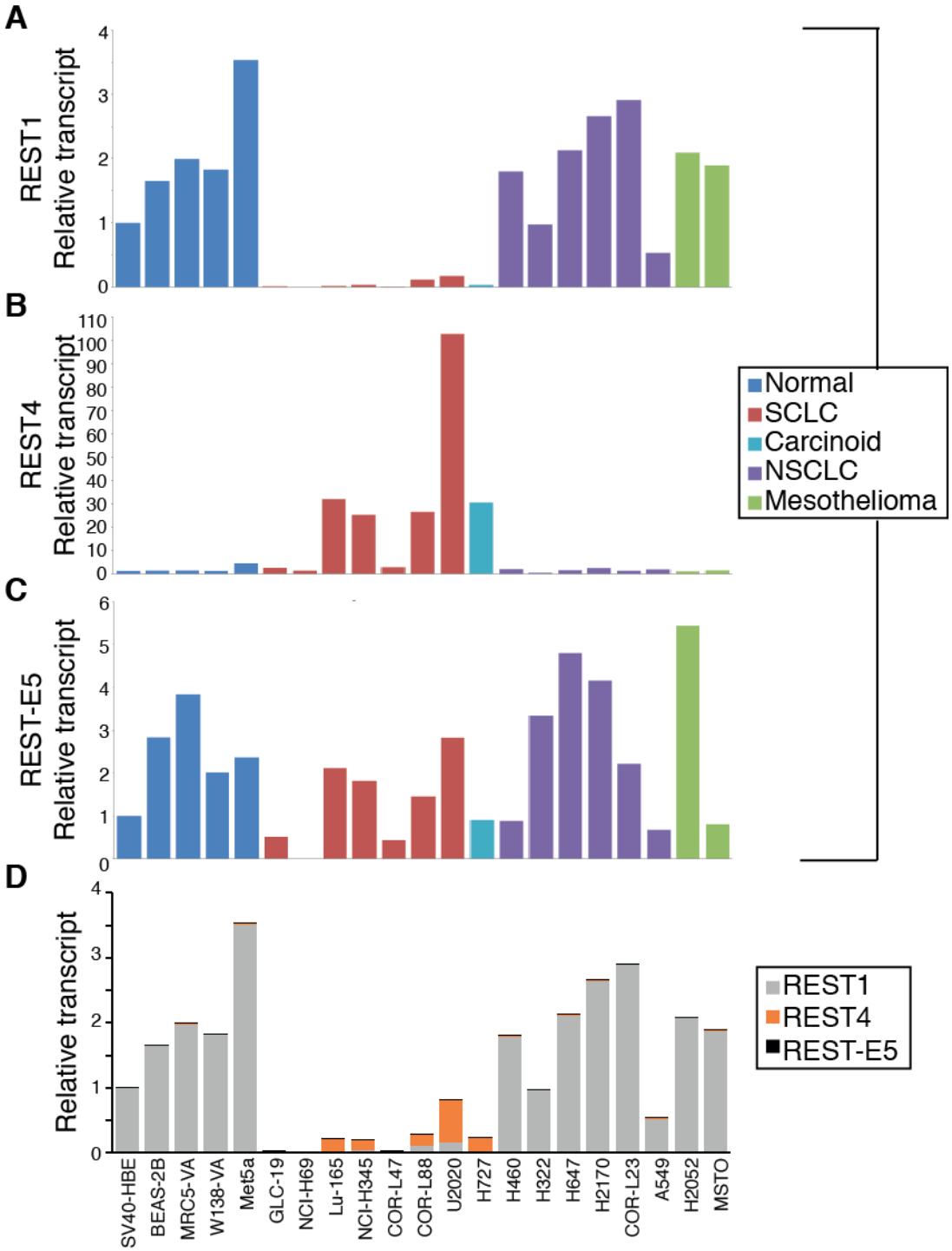

Figure 3.2. REST Splice Variant Expression in a Lung Cell Line Panel
qRT-PCR analysis of REST isoforms: **(A)** REST1, **(B)** REST4 and **(C)** REST-E5 across the cell panel. The cell lines are colour coded based upon phenotype; Normal (blue), Small Cell Lung Cancers (SCLC, red), Carcinoid (teal), Non-Small Cell Lung Cancers (NSCLC, purple), and Mesothelioma (green). **(D)** qRT-PCR analysis of the contribution of REST isoforms to overall REST expression. qRT-PCR data represent triplicate analysis of cDNA derived from n=1 RNA extracts, with transcript expression normalised to actin and expressed relative to SV40-HBE.

The proportion of REST isoforms contribution to overall REST expression, calculated by the addition of mean ΔCq values of REST isoforms, demonstrate that REST1 is the primary isoform in normal and non-NE cells, with REST4 and REST-E5 expressed at low levels (Figure 3.2D). In NE cells, the alternative splicing of REST4 predominates, although is not commensurate with the levels of REST expression found in the normal cells. These data agree with the understanding that loss of REST1 expression is required for relief of REST-mediated repression. Despite the almost ubiquitous expression of REST-E5 in the cell panel, the expression of REST-E5 does not make a large contribution to the overall levels of REST isoform expression.

To compare expression profiles of REST isoforms I decided to group lung cells based on the phenotypic differences. Here, I have divided the cell lines into those expressing NE markers, that is SCLC and carcinoid, and those that are non-neuroendocrine (non-NE), that is NSCLC and mesothelioma. There was a distinct difference between these groups in expression of the REST isoforms (Figure 3.3). The full length REST1 transcript was significantly decreased in NE cells (Figure 3.3A), whilst REST4 was significantly increased relative to non-NE cells (Figure 3.3B). In contrast, the REST-E5 variant was not differential expressed between NE and non-NE cells (Figure 3.3C).

The relation between REST splice variants in individual cell lines are illustrated as scatter plots in Figure 3.3D-F. Interestingly, the expression of REST1 and REST4 variants correlate when analysed in a context specific manner. NE cells, which have a dramatic reduction in the amount of REST (Figure 3.2D), demonstrate a positive correlation with REST1 (Figure 3.3D). In Non-NE and normal cells, in which the levels of REST are higher (Figure 3.2D), there is a positive correlation of REST4 (Figure 3.3D). Interestingly a similar positive correlation with REST1 are seen with the expression of the REST-E5 variant. RESTE5 and REST4 demonstrate a similar positive trend in NE cells (Figure 3.3F).

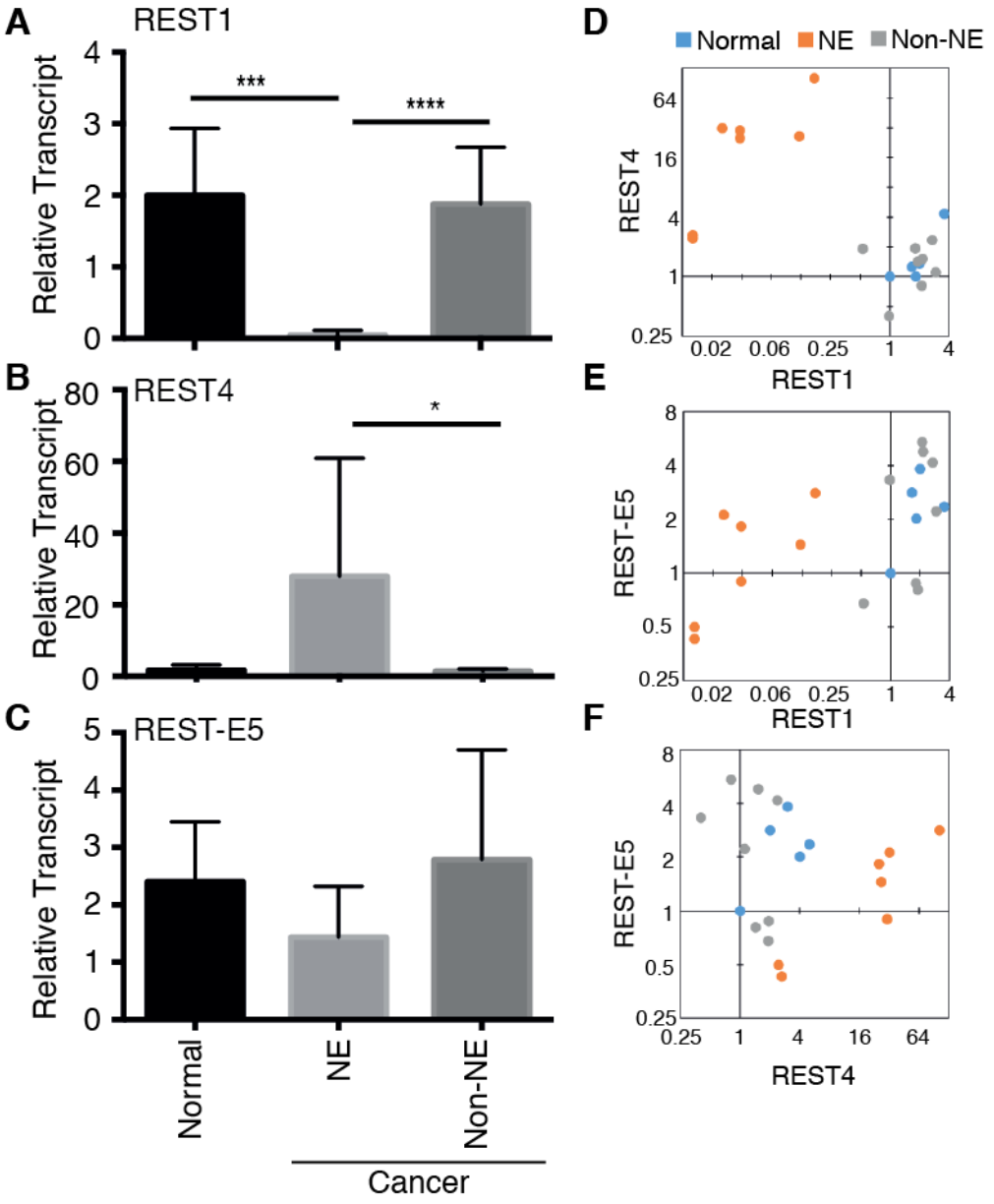

Figure 3.3. Comparison of REST Splice Variant Expression between Neuroendocrine and Non-Neuroendocrine Cells

The transcript expression of REST isoforms: **(A)** REST1, **(B)** REST4 and **(C)** REST-E5 were grouped into three cell types; Normal (n=5), Neuroendocrine (NE, n=8) and Non-Neuroendocrine (Non-NE, n=8). Data are plotted as the mean, error bars represent standard deviation. Statistical significance was tested using an ordinary one-way ANOVA with Tukey's post hoc test. * $P \leq 0.05$, *** $P \leq 0.001$, **** $P \leq 0.0001$. Scatter plots of REST isoform expression in individual cell lines: **(D)** REST4 vs REST1, **(E)** REST1 vs REST-E5, **(F)** REST4 vs REST-E5. The data points are coloured coded by lung grouping; Normal (blue), NE (orange) and Non-NE (grey).

In summary, as previously described the expression of REST and REST4 are differentially expressed in lung cancer phenotypes. In this analysis, I demonstrate that REST1 and REST4 splice variants can be positively correlated in individual cell lines (Figure 3.3D), whilst having a tendency for mutual exclusivity (Figure 3.2D, Figure 3.3A-B). This relationship of REST isoforms together with a decrease in REST levels separates NE cells from other lung cell lines. Here, I have: (1) expanded the comparative quantitative analysis of REST1 and REST4 isoforms to a larger panel of lung cancers and mesothelioma cell lines and confirmed NE association of REST4. (2) Included new analysis of the REST-E5 transcript, which demonstrated variable expression in lung cancer cell lines, yet had no association with lung/thoracic cancer cell types. (3) Demonstrated that REST1 is the predominant isoform in normal and non-NE cell lines. (4) Splicing resulting in REST4 is dramatically increased in NE cells, although these variants are not commensurate with the levels of REST1 in normal cells. (5) The expression of REST-E5 variants may appear to correlate with REST1 or REST4, although it should be noted that these differences aren't apparent without normalisation to SV40-HBE, which indicate that such correlations are artefacts.

3.2.2 Expression of REST-Regulators in Lung Cancer Cell Lines

The functional output of REST is dependent upon a range of regulators, that can modulate REST splicing and protein stability (Figure 3.4A). These regulators have been shown to act at different points in the cycle of REST expression (Chapter 1, Section 3.3-3.4). Briefly, the splicing of the REST4 transcript is regulated by SRRM4 during and post transcription (Raj et al., 2011, Shimojo et al., 2013). The E3-ligase $SCF^{\beta\text{-}TrCP}$ mediates ubiquitylation and degradation of REST during mitosis (Guardavaccaro et al., 2008). The re-expression of REST is supported by the co-translational deubiquitylation by USP15 (Faronato et al., 2013), whilst USP7 opposes degradation in the context of neuronal differentiation (Huang et al., 2011). Together these layers of regulation control expression of REST in the cell. These regulators produce different types of changes to REST either by inclusion of exons or through

changes in post-translational modifications (REST intermediates, Figure 3.4A). The presence of full length REST has the potential to repress many transcripts in proximity to the RE-1 sequence. Loss of REST-mediated repression either through degradation or alternative exon splicing will result in transcriptional changes that may determine the cellular proteome.

To investigate the regulators and outputs of REST, I performed endpoint RT-PCR on cDNA derived from A549 and Lu-165 cell lines to demonstrate that PCR primer pairs amplify a specific product (Figure 3.4B). The deubiquitylases USP15 and USP7 generated specific products expressed in both cell lines. USP15 isoforms 1 and 2 were investigated using the isoform specific primer parings (USP15-iso1 and USP15-iso2), and demonstrate expression of the two isoforms in both cell lines. In accordance with previous studies (Raj et al., 2011, Shimojo et al., 2013), the splicing factor, SRRM4, and REST-regulated transcript, SCG3, are expressed in Lu-165 cDNA, a SCLC cell line (Figure 3.4B). These PCR amplicons will be quantified in the lung cell panel using qRT-PCR (Figure 3.5, Figure 3.7). The cell cycle markers Cyclin B1 and Cyclin E1, used in later experiments (Figure 3.11), also produced a specific product in both cell lines (Figure 3.4B).

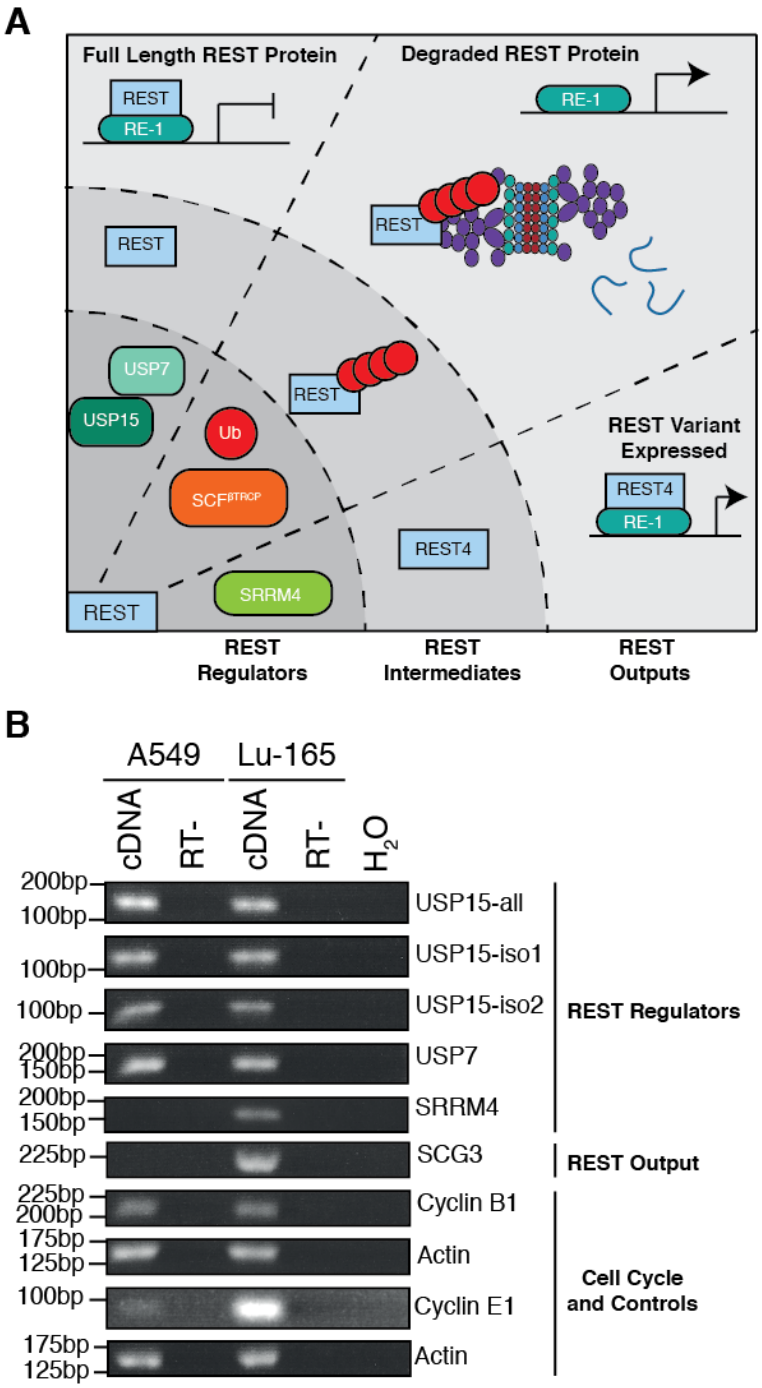

Figure 3.4. Validation of PCR Primers for REST Regulators and Dependent Transcript

(A) The expression of REST repressed transcripts is dependent upon a range of REST regulators, which can modulate REST splicing (SRRM4) and protein stability ($SCF^{\beta\text{-}TrCP}$, USP7 and USP15). **(B)** Endpoint RT- PCR using cDNA derived from A549, NSCLC cells, and Lu-165, SCLC cells, demonstrates the specificity of primer pairs for amplification of REST regulators (USP7, USP15 and SRRM4), REST output (SCG3) and cell cycle markers (Cyclin B1 and Cyclin E1). USP15-all primer pairs, amplified USP15 transcripts irrespective of exon splicing. The USP15 isoform specific transcripts were amplified using USP15-iso1 and USP15-iso2 primer pairs. The amplification of the housekeeping actin transcript acts as a positive control for cDNA.

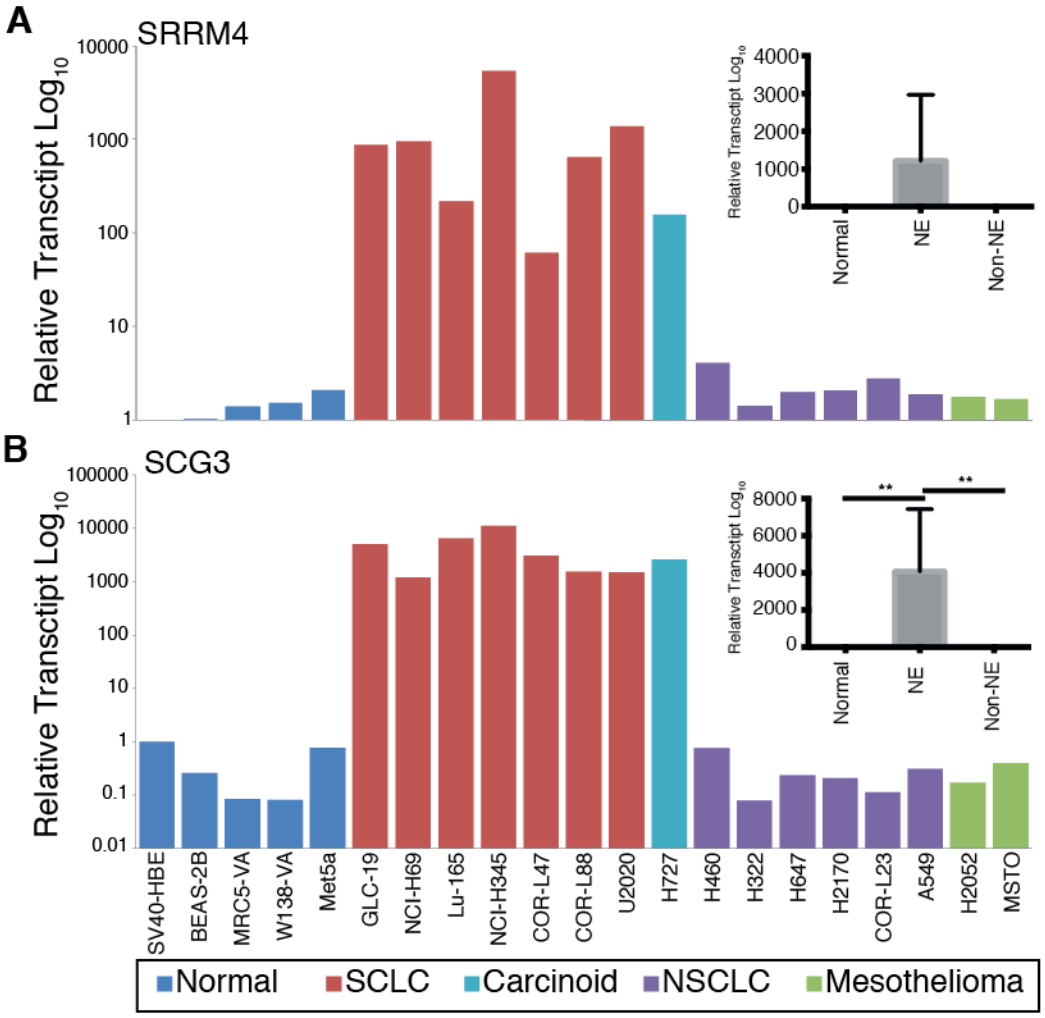

Figure 3.5. REST Splicing Factor and REST-Dependent Transcript Expression in Thoracic Cells

The expression of **(A)** SRRM4 and **(B)** SCG3 were determined across the thoracic cell panel, colour coded based upon phenotype; Normal (blue), Small Cell Lung Cancers (SCLC, red), Carcinoid (teal), Non-Small Cell Lung Cancers (NSCLC, purple), and Mesothelioma (green). qRT-PCR data represent cDNA derived from n=1 RNA extracts from lung cells, with expression of transcripts normalised to actin and expressed relative to SV40-HBE cell line. Insert graphs compare expression between cell groups; Normal (n=5), Neuroendocrine (NE, n=8) and Non-Neuroendocrine (Non-NE, n=8). Data presented as mean with standard deviation error bars, statistical significance calculated using an ordinary one-way ANOVA with Tukey's post hoc test, ** $P \leq 0.01$.

SRRM4 was highly expressed in SCLC and carcinoid cell lines, and as such was increased in NE cells (Figure 3.5A). Similarly, the expression of the SCG3 transcript, which acts as a direct readout for loss of REST-mediated repression, was significantly increased in NE cells (Figure 3.5B). As described above, the NE cells can be separated from other lung cancers based upon the differential expression of REST isoforms: low REST1 and high REST4 (Figure 3.6A). The presence of SRRM4 was associated with decreased REST1 and increased REST4 (Figure 3.6C-D). These data agree with a model where SRRM4-mediated splicing results in REST4. SCG3 demonstrates a similar relationship with the REST isoforms as SRRM4 (Figure 3.6E-F), and supports the idea that expression of REST4 results in loss of REST1-mediated repression. As such, the expression of SCG3 is positively associated with expression of SRRM4 (Figure 3.6B). In contrast, the expression of the REST-E5 transcript does not correlate with either SRRM4 or SCG3 (Figure 3.6G-H). These data suggest that neither the splicing of REST-E5 nor the transcriptional output dependent upon REST-E5 are equivalent to that of REST4.

3.2.3 USP15 Expression and Relationship with REST in Thoracic Cell Lines

This was the first investigation into the expression of USP15 in thoracic cancer cell lines. I was particularly interested in the expression of USP15, which was shown to regulate REST expression (Faronato et al., 2013). Novel data arising from our laboratory implicated differential regulation of USP15 isoforms 1 and 2 (Fielding et al., manuscript in preparation). Thus, I set out to quantify the expression of total USP15 and the USP15 isoforms using qRT-PCR in the thoracic cell line panel and to ask whether USP15 isoforms (together or individually) correlated with REST expression.

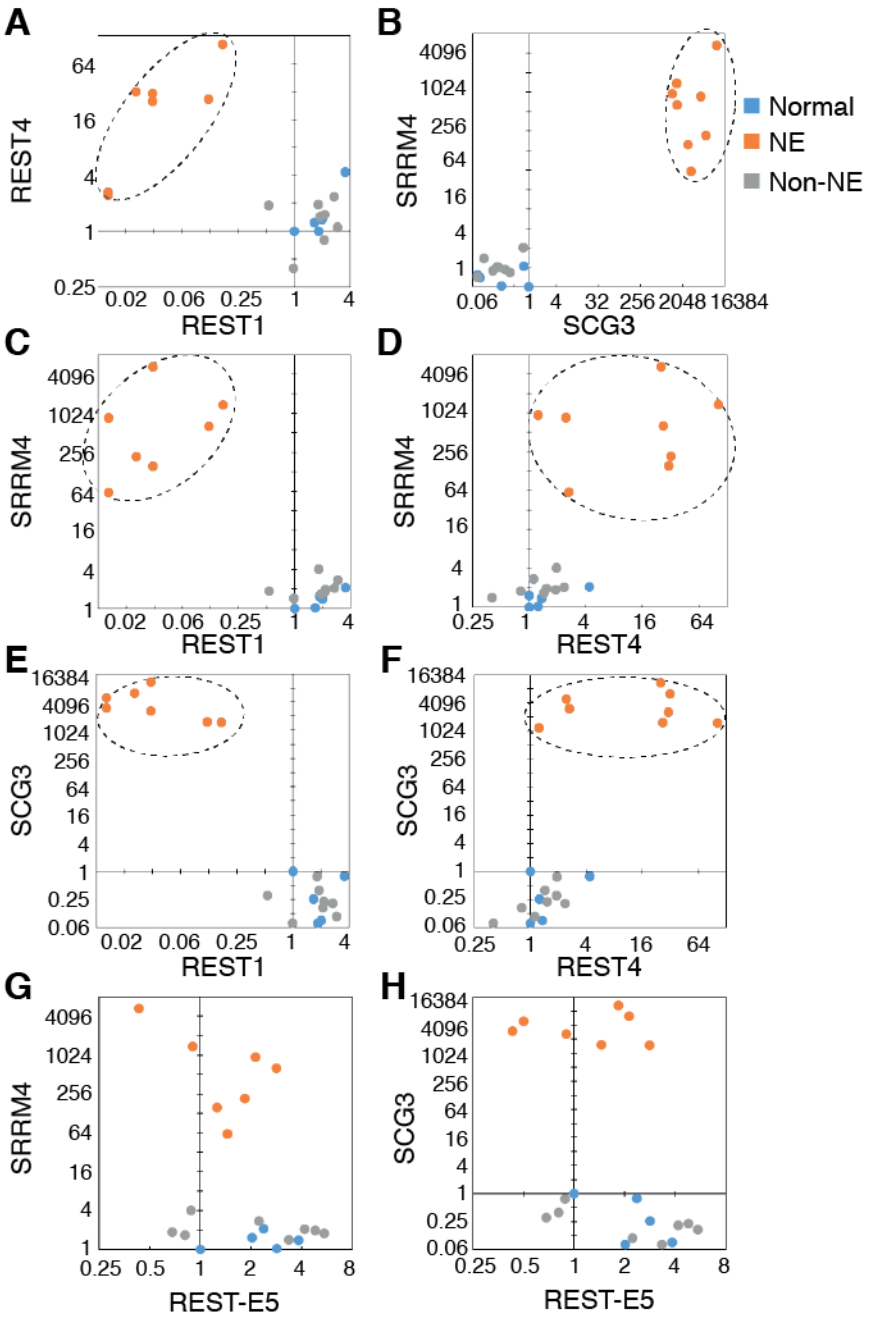

Figure 3.6. Comparison of REST Transcripts with SRRM4 and SCG3
REST isoforms were compared to REST splicing factor, SRRM4 and REST-dependent transcript SCG3. The data points are coloured coded by lung grouping; Normal (blue), NE (orange) and Non-NE (grey). **(A)** The expression of REST1 and REST4 are mutually exclusive and demonstrate clear separation of NE cells from other cell types. **(B)** The expression of SRRM4 and SCG3 are both markedly increased in NE cells. **(C)** SRRM4 and REST1 are mutually exclusive. **(D)** SRRM4 expression is markedly increased in NE cells, similar to the REST4 splice variant. **(E)** SCG3 is markedly increased in the neuroendocrine cells. **(F)** SCG3 expression is markedly increased in NE cells, and is co-expressed with REST4. REST-E5 transcript does not appear to favour co-expression or exclusivity with either **(G)** SRRM4 nor **(H)** SCG3. qRT-PCR data from Figures 3.2 and 3.5.

The expression of all USP15 isoforms (USP15-All) demonstrates that USP15 was ubiquitously, but variably expressed across the thoracic cell line panel (Figure 3.7A). To investigate the contribution of USP15 isoforms to USP15 expression, I calculated the expression of USP15 isoforms 1 and 2 (normalised to sample reference gene actin) and made relative the levels of USP15-All (Figure 3.7B). The difference between USP15-All and the combination of USP15 isoforms 1 and 2, I define here as USP15 isoforms x (Figure 3.7B). USP15-All primer pairs can amplify alternative USP15 isoforms, although the discrepancy in part may be due to variation in primer efficiency (100 $\pm$ 5%). USP15 isoforms 1 and 2 on average account for 40% and 36% of total USP15 expression, respectively, which together make them the predominant USP15 isoforms (Figure 3.7B). Total USP15 expression and the levels of USP15-isoform 2 are not differentially regulated between NE and non-NE cells (Figure 3.7C,E), USP15-isoform 1 was significantly increased in NE cell lines compared to normal cells (Figure 3.7D). In addition, I notice that the balance of USP15 isoform expression (USP15-isoform 1:USP-isoform 2) favours isoform 1 in NSCLCs including the carcinoid H727, in comparison to normal cells or SCLCs (Fielding et al., manuscript in preparation). Here, I focus on the impacts of increased USP15 isoform levels. As such I decided to correlate the expression of USP15-isoforms to each other, SRRM4 and REST splice variants. USP15 isoforms 1 and 2 demonstrate a positive correlation and do not tend to be mutually exclusive (Figure 3.8A). Both USP15 isoforms are expressed in normal and non-NE cells, with low SRRM4, suggesting that isoform expression is independent of SRRM4 (Figure 3.8B-C). In NE cells, there is a trend for SRRM4 to decrease with increasing USP15 isoform 1 expression (Figure 3.8B). In relation to REST expression, REST1 demonstrate a tendency to increase with USP15 isoforms in most non-NE and normal cells (Figure 3.8D-E). In NE cells despite the increase in the expression of USP15 isoforms levels of REST1 decrease (Figure 3.8D-E). These results may suggest that in these cells USP15 is unable to support the expression of REST during transcription. In relation to REST4, the USP15 isoforms in general do not demonstrate a clear correlation, although in the context of NE cells, which

predominantly express REST4 (Figure 3.2D), there appears to be a slight tendency to decrease with increased USP15 isoforms (Figure 3.8F-G). The REST-E5 transcript, expressed at low levels in all cell types (Figure 3.2D), does not appear to correlate with the expression of USP15 isoforms (Figure 3.8H-I). These data represent the first attempt to specifically address the relationship between USP15 and REST isoforms.

In summary, these data confirm that the alternative splicing factor SRRM4 correlates to the expression of the REST4 transcript in thoracic cancer cell lines (Figure 3.6D). SRRM4 and REST4, also correlate with an increase in the expression of the REST-repressed SCG3 (Figure 3.6F). In contrast, based on expression patterns, the REST-E5 isoform does not appear to be regulated by the same splicing factor as REST4 (Figure 3.6G) nor relate to increased SCG3 expression (Figure 3.6H). These data may suggest that REST-E5 is subject to SRRM4-independent regulation, so that in this case of exon 4 skipping a different splicing factor is involved. In relation to REST-regulated transcripts, these data suggest REST-E5 also has a different mechanism of action, or influences the expression of REST-repressed transcripts other than SCG3. In relation to USP15, the total expression of USP15 does not appear to be significantly different between lung cancer phenotypes (Figure 3.7A,C). The expression of USP15-isoform 1, however, was significantly increased in NE cells (Figure 3.7D), and this provides the first evidence of differential expression of USP15 isoforms in cancer. These data would suggest that USP15 and REST are both subject to alternative splicing in the NE cell lines, although this data does not suggest that the splicing of USP15 isoforms was related to the expression of SRRM4 (Figure 3.8B-C).

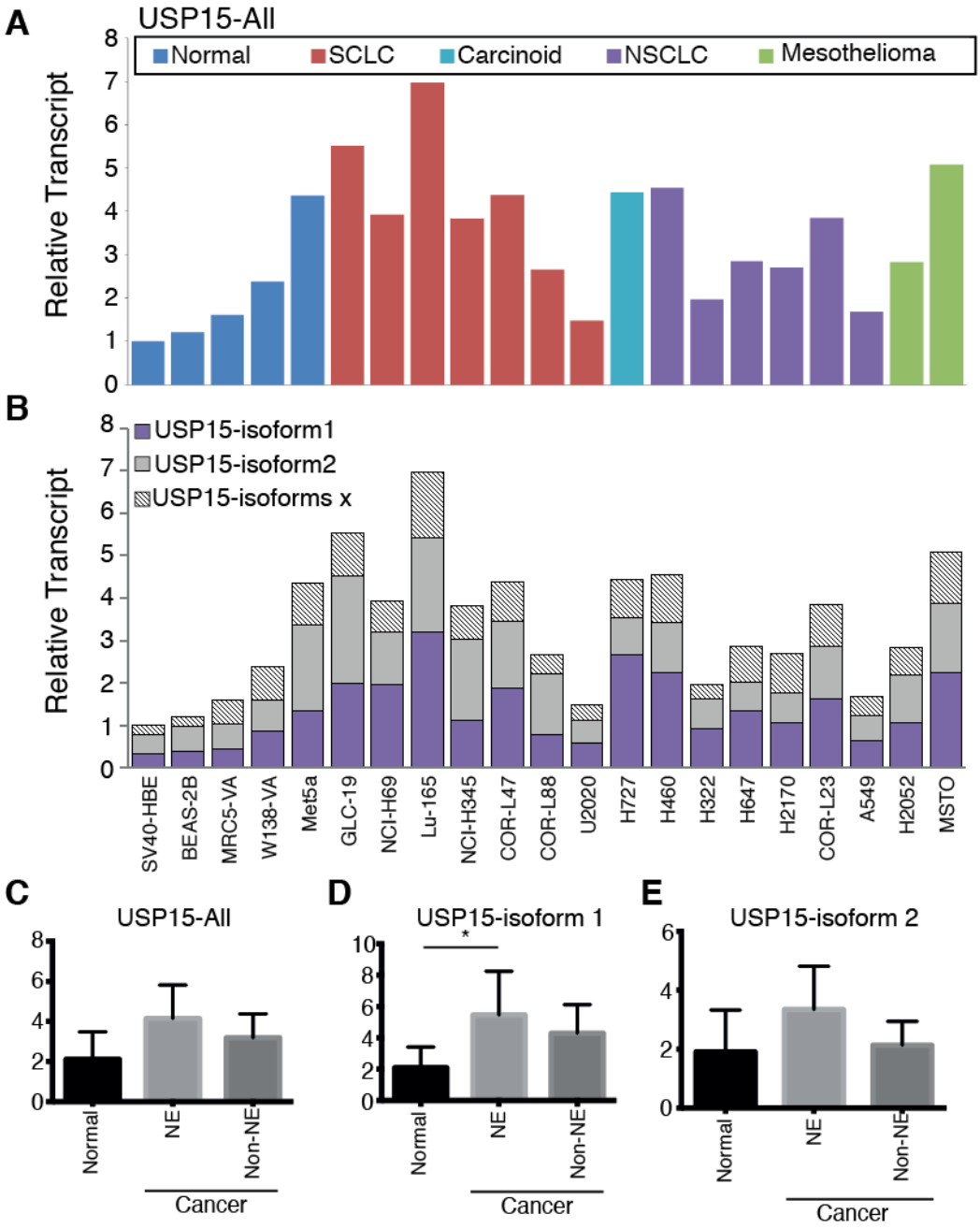

Figure 3.7. USP15 Transcript and Splice Variants in a Thoracic Cell Panel
(A) USP15 transcript (USP15-All) expression in the lung cell panel. **(B)** Expression of USP15-isoform 1 (purple) and USP15-isoform 2 (grey) transcripts made relative to total USP15 expression. USP15-isoforms x represent the discrepancy between USP15-All and the combination of isoforms 1 and 2. As previously, lung cells were grouped into cell types; Normal (n=5), Neuroendocrine (NE, n=8) and Non-Neuroendocrine (Non-NE, n=8), and the expression compared between groups, **(C)** USP15-All, **(D)** USP15-isoform 1 and **(E)** USP15-isoform 2. Statistical significance was calculated using an ordinary one-way ANOVA, 95% confidence, with Tukey's post hoc test. * $P \leq 0.05$. qRT-PCR data represent cDNA derived from n=1 RNA extracts of lung cells, with transcript expression normalised to the housekeeping gene actin and expressed relative to SV40-HBE cells.

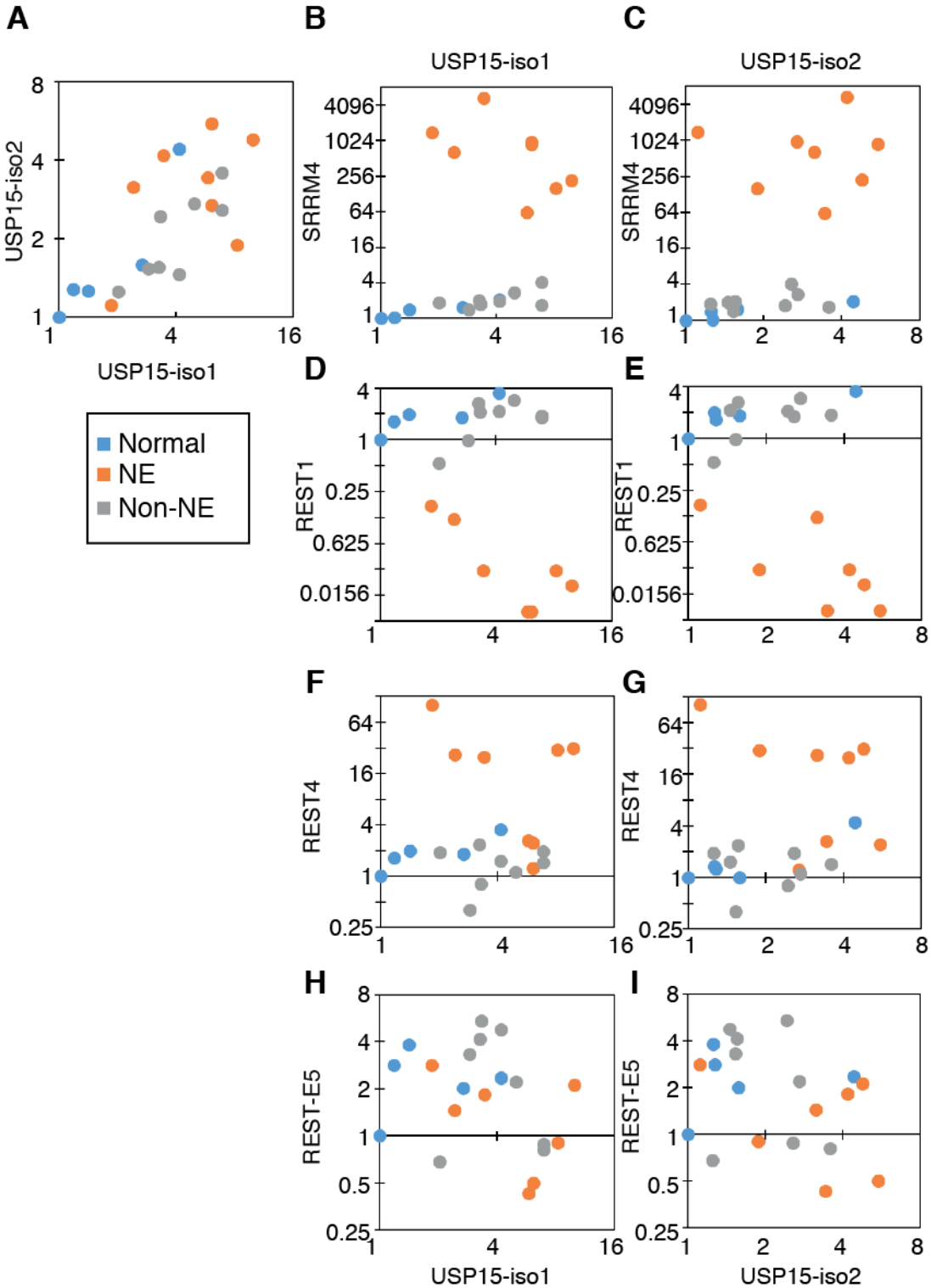

Figure 3.8. USP15 Isoforms Expression Comparisons with REST Variants
USP15 isoforms 1 and 2 transcript expression from thoracic cells were plotted against **(A)** each other, **(B-C)** SRRM4 and REST splice variants: **(D-E)** REST1, **(F-G)** REST4 and **(H-I)** REST-E5. The data points are coloured coded by lung grouping; Normal (blue), NE (orange) and Non-NE (grey). qRT-PCR data from Figures 3.2, 3.5 and 3.7

3.2.4 Cell Cycle Profiles of REST and REST-Regulators

REST1 encoded protein (henceforth referred to as REST) undergoes acute mitotic degradation and recovers post-mitosis with re-expression of REST, which is in-part regulated by the deubiquitylase USP15 (Faronato et al., 2013). Here, experiments were designed to collect mRNA and protein extracts for correlative investigation of the isoforms of REST, USP15, and other regulators of REST during the cell cycle.

Firstly, I set out to synchronise a lung cancer cell line to enrich specific cell cycle phases. Cell cycle synchronisation methodology (Chapter 2, Section 1.4) used a combination of thymidine and nocodazole blocks. Phase enrichment was validated by western blotting for cell cycle markers, Cyclin B1 and Cyclin E1, and by DNA-staining flow cytometry. A549 cells, a non-small cell lung cancer that express REST1, but not REST4 mRNA and protein, were chosen for the study. Synchronous A549 protein lysates, extracted at multiple time points following thymidine and nocodazole block regimes to represent different phases of the cell cycle, were immunoblotted for the cell cycle markers Cyclin B1 and Cyclin E1 (Figure 3.9A). The asynchronous protein lysate, containing cells at various stages of the cell cycle, expressed lower levels of both Cyclin E1 and Cyclin B1. Cyclin B1 and E1, showed dynamic expression profiles, as expected for cells enriched in the appropriate phases. Cyclin E1 peaks during S phase and decreases during G2 until absence at the onset of mitosis. Conversely, Cyclin B1 increases through S and G2 until peaking during mitosis, followed by acute degradation at mitotic exit.

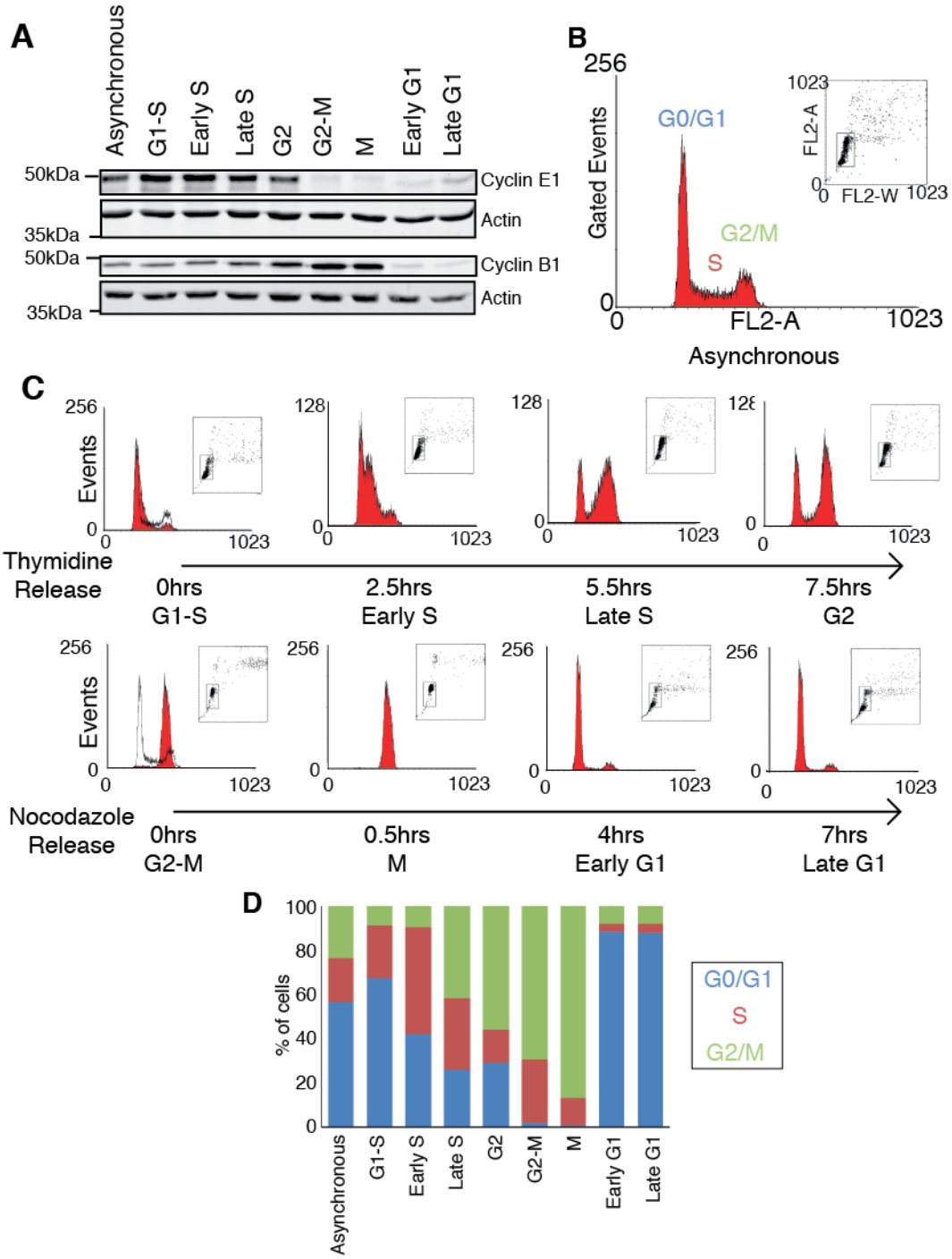

Figure 3.9. Cell Cycle Synchronisation of A549 cells
(A) Western blotting of A549 protein lysates extracted at intervals after release from thymidine or nocadozole block, that represent different cell cycle stages. Cell cycle markers: Cyclin E1, peaks during S phase and Cyclin B1 peaks during mitosis. **(B)** Flow cytometry analysis of asynchronous A549 cells demonstrate three distinct phases of the cell cycle (G0/G1, S and G2/M). All FL2-A histograms are generated from gated selection of 10,000 single cells (events, insert). **(C)** FL2-A histograms of single cells at time intervals following release from thymidine or nocodazole block, with an asynchronous sample overlaid on the initial release time point. **(D)** Bar chart represents the percentage of cells in each phase (G0/G1, S and G2/M) as calculated from histograms at each time point.

Propidium iodide, an intercalating agent, allows for the discrimination of cells based on DNA content, which doubles on DNA replication during S phase. This characteristic together with the size of the cell, which increases in size to accommodate the additional protein and DNA required prior to mitotic division, allows for the separation of cells into three distinct phases G1/G0, S and G2/M. However, DNA-staining flow cytometry is unable to differentiate between quiescent G0 cells and those in G1, due to equal size and DNA content. The light scatter profile of the DNA-stained cells and the time taken to pass between the laser and detectors, are used to identify single cells (events) and exclude aggregated cells or cellular debris (Figure 3.9B insert). An asynchronous population of A549 cells was used to demonstrate the range and abundance of cells in each phase. 10,000 single cells (gated events) were recorded, and a histogram plot of the area of fluorescence (FL2-A) allows for the separation into three distinct phases (Figure 3.9B). The number of cells in each phase was determined by counting the number of cells within boundary markers.

An overlay of the asynchronous histogram profile serves as a baseline to demonstrate that cell synchronisation protocols enrich the population for cells in the appropriate cell cycle phase. Flow cytometry analysis of cells, following release from thymidine or nocodazole block, clearly demonstrates progression through the cell cycle phases (Figure 3.9C). Cells blocked with thymidine accumulate in G1 with a depletion of cells in S and G2-M, when compared to the overlay of the asynchronous cell phase distribution. Following release from thymidine, most cells progress through S phase, by 7.5 hours the majority of cells are in the G2/M phase. Cells blocked in nocodazole are enriched in the G2/M phase of the cell cycle, compared to the asynchronous overlay. Following mitotic shake off, cells progress through mitosis and enter G1 (Figure 3.9C). Taken together with western blotting for cyclins, these flow cytometry data demonstrate an effective enrichment of cells in the appropriate cell cycle phases.

3.2.4.1 Protein Expression Profiles of REST and USP15

Next, I used these same synchronisation protocols to assess the expression of REST and proteins that regulate REST during the cell cycle. Due to availability and efficacy of antibodies, I focused on the REST1 encoded protein and USP15. Their expression at different phases of the cell cycle, was determined by western blot using lysates from synchronised A549 cells (Figure 3.10A). USP15 and REST levels in asynchronous cells were used as a control, to which expression at other cell cycle phases were normalised. Validation of cell cycle progression was confirmed by Cyclin B1 expression, which increases through the cell cycle and peaks during mitosis (Figure 3.10A). USP15 expression showed a marked induction at the onset of mitosis. In A549 cells, REST is present predominantly as the mature protein, with post-translational modification by O-linked glycosylation, causing it to migrate with an apparent Mw of 220kDa. The newly synthesised REST protein of 120kDa is also visible. Both these forms of REST decrease at the onset of mitosis (Figure 3.10B), in agreement with previous publications (Guardavaccaro et al., 2008, Faronato et al., 2013). Due to potential differential roles of USP15 isoforms (Fielding et al., manuscript in preparation), I wanted to determine whether specific isoforms increased protein expression of USP15 at mitosis. However, due to similar molecular weights of USP15 isoform 1 (USP15iso1, 112kDa) and USP15 isoform 2 (USP15iso2, 109kDa) and a lack of USP15-isoform specific antibodies, I was unable to do this by western blotting. I therefore decided to perform qRT-PCR analysis.

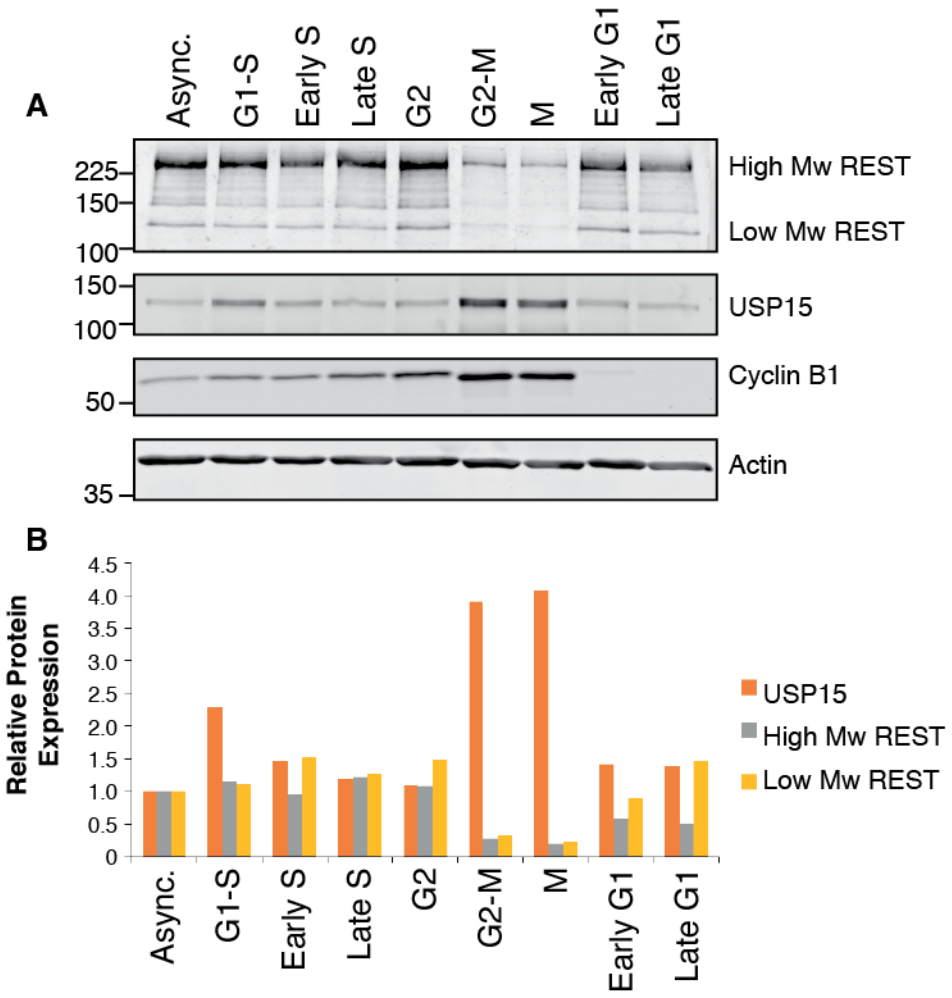

Figure 3.10. REST and USP15 Protein Expression Throughout the Cell Cycle
(A) Immunoblotting for REST1 protein, USP15, Cyclin B1 and Actin in A549 cells at different stages of the cell cycle. **(B)** Protein expression of USP15 and REST (High Mw, glycosylated and Low Mw) proteins, were normalised to loading control actin and made relative to asynchronous levels, calculated from n=2 biological replicates.

3.2.4.2 qRT-PCR Analysis of Deubiquitylase Regulators of REST

The deubiquitylation of REST by USP15 is important for post-mitotic re-expression of REST (Faronato et al., 2013). USP7 (HAUSP), unlike USP15, has previously been implicated in antagonising the $SCF^{\beta\text{-}TrCP}$-mediated ubiquitylation and degradation of REST (Huang et al., 2011). Despite the notable increase of USP15 protein during mitosis (Figure 3.10), qRT-PCR analysis of all USP15 isoforms demonstrated no significant change through the cell cycle phase (Figure 3.11A). USP15 isoform 1 and isoform 2 transcripts (Figure 3.11B-C) also did not demonstrate phase specific changes in expression. The increase in USP15 protein levels at mitosis, is therefore likely

due to protein stability which were previously shown to increase 2-fold during G_2 (Faronato et al., 2013). Similarly, to USP15, USP7 transcript expression does not change in through the cell cycle (Figure 3.11D). These data suggest the two deubiquitylases previously reported to regulate REST, do not undergo cell cycle phase specific changes in RNA expression or splicing.

In summary, I confirmed that REST exhibits a cyclical expression profile and that the total USP15 protein levels increase and peak at mitosis as previously described (Faronato et al., 2013). Here, for the first time, I investigated the contribution of USP15 splice variants to this mitotic increase in USP15 expression. qRT-PCR analysis of USP15 isoform transcript expression suggested no difference in expression through the cell cycle (Fielding et al., manuscript in preparation). In addition, USP7 also known to regulate REST (Huang et al., 2011), was not differentially transcribed through the cell cycle.

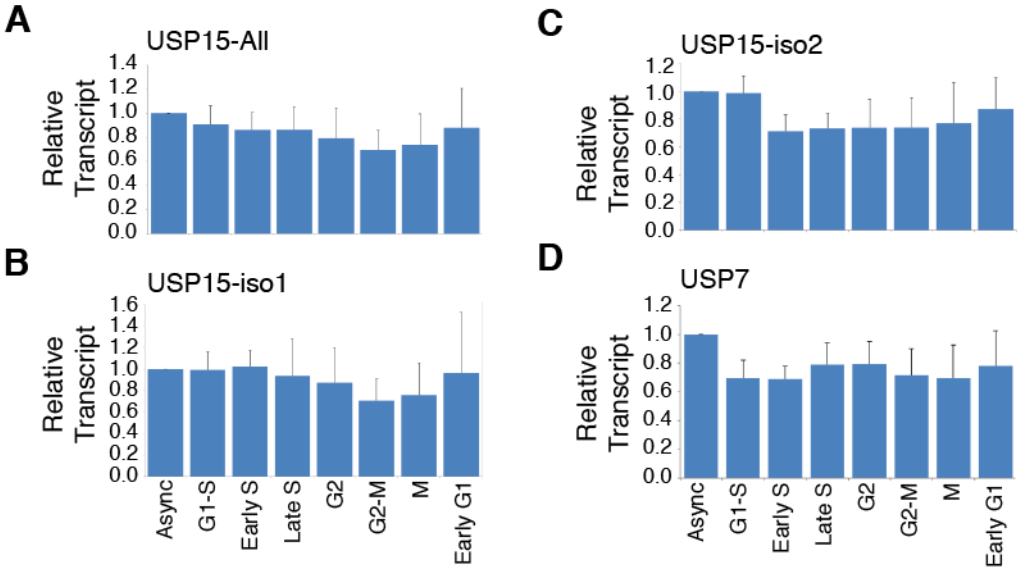

Figure 3.11. qRT-PCR Analysis of REST Regulators Through the Cell Cycle
Relative transcript expression of REST regulators **(A)** USP15-All**, (B)** USP15-iso1, **(C)** USP15-iso2 and **(D)** USP7, was determined through the cell cycle. Transcript expression was normalised to the housekeeping gene actin and made relative to asynchronous samples. qRT-PCR cDNA derived from synchronous and asynchronous RNA extracts of A549 cells, error bars show standard deviation, n=3 biological replicates.

3.2.5 Differential Expression of REST Isoforms Through the Cell Cycle

During the analysis of REST and the REST regulators, I investigated differential expression of REST transcripts through the cell cycle. qRT-PCR analysis of transcript expression was performed on cDNA produced from asynchronous and synchronous A549 cells. REST1 expression remained relatively consistent throughout the cell cycle (Figure 3.12A). REST4 in contrast, demonstrated a statistically significant increase in expression by approximately eight-fold during mitosis (Figure 3.12B). The expression of REST4 was then significantly reduced following mitotic exit in early G1. The data are supported by the transcriptional expression of cell cycle markers, Cyclin E1 and B1 levels (Figure 3.12C-D). Cyclin E1 transcript peak at G1-S phase, decrease through S phase and remain low during mitosis. Cyclin B1 transcript levels increase from late S phase through G2 and peak during mitosis.

This is the first example of differential splicing of REST through the cell cycle. The splicing of REST4 was known to be regulated by the splicing factor SRRM4 (Raj et al., 2011, Shimojo et al., 2013). Thus, I attempted to assess the expression of SRRM4 through the cell cycle in A549 cells. However, SRRM4 is expressed at very low levels in asynchronous A549 cells (Figure 3.5). I therefore attempted to precisely optimise the annealing temperature of the SRRM4 primers using gradient PCR (Figure 3.13A) to obtain accurate quantitation. qRT-PCR amplification of SRRM4 from NCI-H69 SCLC cDNA, a positive control for SRRM4 expression, resulted in detectable product amplification after approximately 26 cycles across the range of annealing temperatures (Figure 3.13B). Melt curve analysis of these PCR products demonstrated a change in fluorescence caused by dissociation of SYBR green from a distinct product (Figure 3.13C). H69 RT- samples, in which the same RNA extracted from NCI-H69 cells underwent cDNA conversion without the reverse transcription enzyme, demonstrate amplification of a non-specific product with high Cq values >35 cycles (Figure 13.3B). The melt curve analysis of these H69 RT- samples showed dissociation of SYBR at lower temperatures

(Figure 3.13D), indicate these represent primer dimers, rather than the cDNA amplicon. RNA extracted from asynchronous A549 cells was reverse transcribed, and primer product formation tested by gradient PCR. qRT-PCR analysis of A549 cDNA samples produced high Cq values (Figure 3.13B), which like the H69 and A549 RT- samples appear to be due to non-specific annealing of the primers (Figure 3.13D-F). I concluded that the expression of SRRM4 transcript was below the limit of detection as data are indistinguishable from the non-template controls.

To assess if the cyclical peak of REST4 at G2-M, was mimicked by SRRM4 I performed qRT-PCR, under optimal conditions (64^{o}C annealing, ½ primer concentration), on three biological replicates of synchronised A549 cDNA samples (Figure 3.13G). The expression of SRRM4 in these conditions was again not distinguishable from the RT- A549 samples or those in which cDNA was replaced with H_2O. These data demonstrate that SRRM4 was not expressed or at least at very low levels in A549 cells, and does not increase in expression at mitosis.

In conclusion, I show for the first time that expression of REST4 peaks during mitosis in non-neuroendocrine A549 cells, however the expression of the splicing factor that favours REST4 product SRRM4 was (1) beyond the limits of detection in A549 cells and (2) does not demonstrate a detectable cell cycle specific increase that could coincide with REST4 expression.

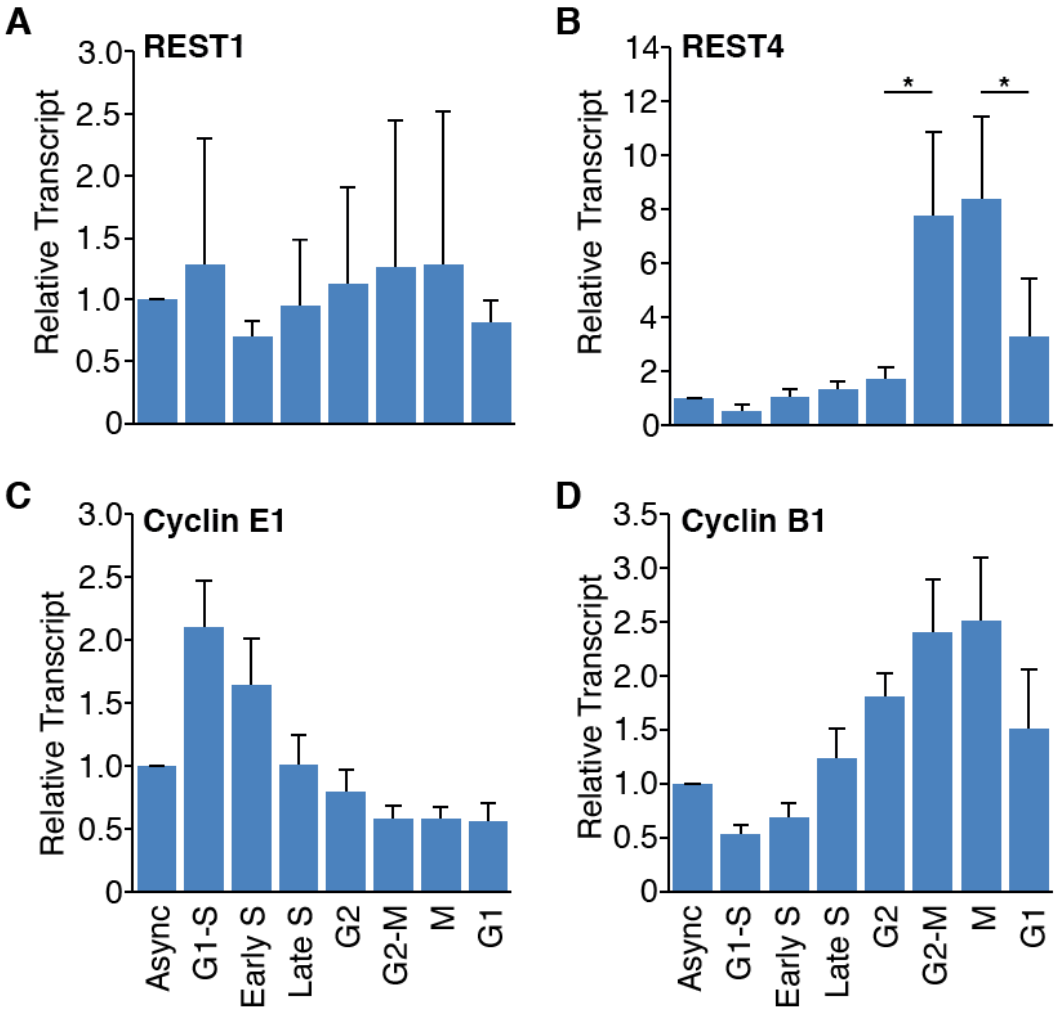

Figure 3.12. Increased REST4 Splicing During Mitosis
Relative transcript expression of **(A)** REST1, (**B)** REST4, **(C)** Cyclin E1 and **(D)** Cyclin B1 through the cell cycle. The expression of transcripts was normalised to actin and made relative to asynchronous cells. Data presented are the mean expression with standard deviation error bars, statistical significance was calculated using an ordinary one-way ANOVA with Tukey's post hoc test, * $P \leq 0.05$. qRT-PCR cDNA derived from synchronous and asynchronous RNA extracts of A549 cells, n=3 biological replicates.

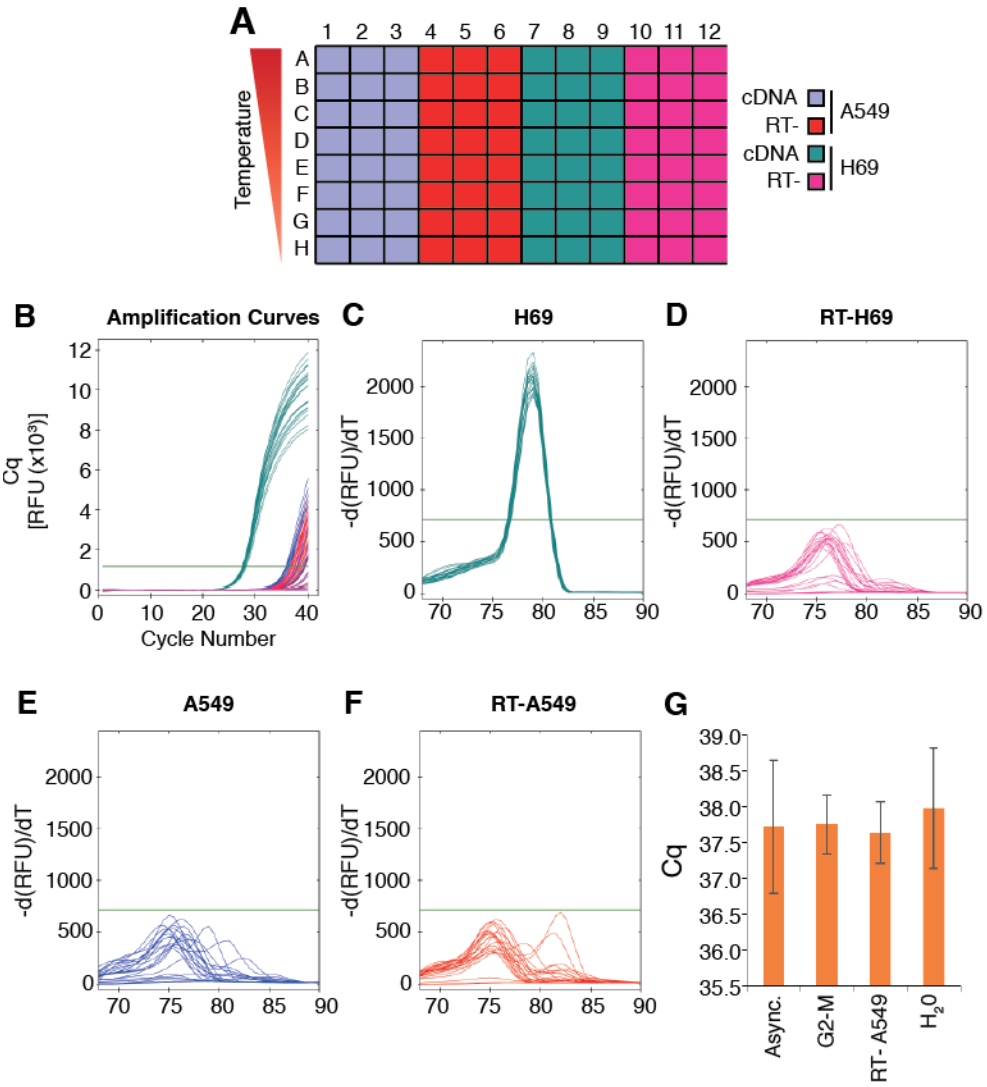

Figure 3.13. SRRM4 Primer Optimisation for A549 Cell Cycle Expression
(A) Gradient PCR design of providing optimal SRRM4 primer conditions, with H69 cDNA used as a positive control for SRRM4 expression. **(B)** qRT-PCR amplification curves of derived from gradient PCR. Post qRT-PCR melt curve analysis of; **(C)** H69 cDNA, **(D)** RT-H69, **(E)** A549 cDNA and **(F)** RT- A549. **(G)** qRT-PCR expression of SRRM4, under optimal conditions, was performed with cDNA derived from asynchronous and G2-M synchronised RNA extracts with negative controls, asynchronous RT-A549 and H_2O.

3.3 Discussion

The aims of this chapter were to investigate the isoform and total expression of REST, its DUB regulator USP15, and their correlation to thoracic cancer cell types and cell cycle expression. Here, I demonstrate that REST and USP15 isoforms are differentially expressed in the NE cell type from this thoracic cell panel (Figures 3.3 & 3.7). The novel REST protein coding isoform REST-E5, however, was not associated with the NE-cell type or differentially expressed in this subset of thoracic cancers. Interestingly, the expression of USP15 increased in cancers and isoform 1 was significantly increased in the NE cell lines (Figure 3.7). The correlations of USP15 isoform 1 and the splicing factor SRRM4 demonstrate that any preferential isoform splicing programme of USP15 is unlikely associated with its expression (Figure 3.8).

The expression of REST and its regulators demonstrate no significant fluctuations through the cell cycle. Interestingly, the REST4 transcript was markedly increased in the nocodazole-treated G2-M and M phases (Figure 3.12). These data demonstrate that alternative splicing of REST4 may occur prior to mitosis. This would suggest that the conditions required for REST-dependent differentiation are primed at mitosis and that the decision to re-express REST1 occurs during G1.

3.3.1 Expression of REST and USP15 in Thoracic Cancers

Here, I have performed qRT-PCR to provide a quantitative assessment of REST splice variant expression. The data from this cell panel recapitulates the previous reports of a REST isoform switch from REST1 to REST4 that occurs in NE cells (Coulson et al., 2000, Gurrola-Diaz et al., 2003, Moss et al., 2009). Importantly, my data now demonstrate that mesothelioma cells express REST1 but not REST4.

In addition to the differential expression of REST4 in lung cancer and other NE cancers, it was previously reported that exon skipping was prominent and that the REST-E5 variant was differentially expressed in breast cancers

compared to adjacent normal tissue (Chen and Miller, 2013). Included in the analysis of REST transcripts, Chen and Miller identified a novel protein-coding transcript formed by inclusion of a novel C' terminal exon. Here, I investigated the differential expression of this transcript, REST-E5, in lung cancer cell lines for the first time. qRT-PCR analysis demonstrated low level expression of REST-E5, however unlike REST4, the levels of REST-E5 did not correlate with NE phenotype.

The NE expression of SRRM4 and REST4, concurs with previous reports of SRRM4 mediated splicing of REST4 (Raj et al., 2011, Shimojo et al., 2013). As a positive control the expression of REST4 allows for upregulation of the model RE-1 restricted gene, SCG3 (Moss et al., 2009). The mesothelioma cell lines, a cancer primarily associated with asbestos exposure, does not express NE markers SRRM4, REST4 or SCG3. This suggests that there is not a correlative link between this asbestos-induced cancer and the development of a NE cell type. Unlike REST4, the abundance of the REST-E5 transcript is not associated with the increased expression of SRRM4 in NE cells. This would suggest that alternative splicing, that favours REST4 or REST-E5, are driven by alternative mechanisms. One major difference between these two splice variants is that REST4 is generated by internal inclusion of a cassette exon, whist REST-E5 is generated by use of an alternative final exon that is mutually exclusive with the canonical C' terminal (Chen and Miller, 2013). In line with these findings, the primary function of SRRM4 is to perform neuronal specific splicing of cassette exons (Calarco et al., 2009).

For the first time, I investigate the expression of the REST regulating DUB USP15 and its isoforms in lung cancer cell lines. These data demonstrate an increase in expression of USP15 in lung cancer cell lines relative to the normal bronchial cell lines. In general, the expression of USP15 isoforms 1 and 2 mRNA are equivalent across most cell types, although my data imply that USP15 isoform 1 could be preferentially upregulated in NE cells lines

(Figure 3.7). This differential expression is of interest, as a recent paper has suggested that the isoforms demonstrate preferential interactions (Kotani et al., 2017). The bias in splice variant expression could imply a subtle difference in USP15 substrates or activity in NE cells. The splicing of USP15 isoforms 1 and 2 has been associated with polymerase pausing and the expression of vascular endothelial zinc finger 1 (VEZF1), which binds to the gene (Gowher et al., 2012). As USP15 isoform 1 is increased in NE cells, this might suggest an increase in the expression of factors that promote polymerase stalling which potentially contributes to exon inclusion of multiple genes and ultimately promote cancer-specific differential splicing.

3.3.2 REST Expression During the Cell Cycle

The periodic expression of REST1 through the cell cycle has been well documented (Guardavaccaro et al., 2008, Faronato et al., 2013). In early G1 nascent REST is expressed and rapidly acquires post-translational modifications. REST expression accumulates through S and G2, binding to newly replicated DNA, before undergoing acute degradation at the onset of mitosis. The data generated in this thesis recapitulate this cyclical expression pattern (Figure 3.10). To date, it is unknown how the PTMs of REST regulate its structure or ability to interact with DNA, only that phosphorylation and subsequent ubiquitylation of REST ultimately leads to its displacement from the DNA by degradation. The lack of an established transient or reversible PTM-controlled displacement from DNA, suggest that regulation of gene expression is likely regulated by the activity of its co-repressors. The measurement of REST DNA binding displacement and co-repressor activity are not accurately quantifiable with whole lysate biochemical analysis of multiple cells.

Here, I explore for the first time the expression of REST4 during the cell cycle. Whilst I was unable to clearly visualise REST4 protein using antibodies, the expression of the REST4 splice variant was notably upregulated during the G2 and M phases of the cell cycle (Figure 3.12). This increase in REST4

expression occurs at the time when full length REST1 protein is degraded. A lack of REST1 degradation was shown to cause defective mitotic sister chromatid separation, resulting in a loss of genome instability (Guardavaccaro et al., 2008). At mitosis, it has been reported that splicing factors can be phosphorylated and this alters their activities (Gui et al., 1994, Dominguez et al., 2016). A mitotic increase in expression or PTM-dependent regulation of splicing factors are potential mechanisms for the demonstrated increase in REST4. In the A549 cell line, however, I was unable to identify any expression of SRRM4 mRNA, even at mitosis (Figure 3.12). These data suggest that mitotic upregulation of REST4 is not mediated by SRRM4. The increase in mitotic splicing of many mRNAs has previously been reported, the purpose of such regulation is currently known. One presumes that splicing is required to reset the cell to a state that would prepare it for asymmetric division for senescence or replication and/or differentiation depending on stimulus.

Although, I have not validated whether REST4 mRNA produces REST4 protein, if this were the case it is tempting to speculate that REST4 may act as a pioneer factor (Zaret, 2014). Pioneer factors, are transcription factors with a strong affinity for DNA and serve as bookmarks for gene expression and chromatin modification. As a pioneer factor, REST4 could function to mark chromatin to ensure repression of RNAs (mRNA, miRNA, ncRNA). The marking of RE-1 target sequences both during and post- mitosis could be required to induce or supresses REST-dependent stages of neuronal differentiation. Thus, the expression of REST1 or REST4 protein post-mitosis may act as a marker for a differentiation decision, with REST1 expression displacing any mitotic REST4-bound RE-1 motifs. As well as regulating gene expression, expression of REST in replicating cells may also be critical to limit DNA damage that occurs during S phase (Nechiporuk et al., 2016), whilst its degradation is required for effective chromosome segregation during mitosis (Guardavaccaro et al., 2008). These would suggest that master transcription factors, including REST, could be vital for ensuring genome integrity at multiple phases of the cell cycle.

CHAPTER 4: REST AND USP15-DEPENDENT PROTEOMES

4.1 The REST and USP15-Dependent Proteomes

4.1.1 Proteomic Analysis

The differential expression of proteins underpins the biological activities and capabilities of cells. The proteins expressed by a cell are known as a proteome. As the proteome, transcribed from ~20,300 genes, can be modified to produce a greater diversity of proteins, it is crucial to determine the identity of proteins to understand their roles in cellular behaviour. To identify proteins without sequence information required proteins to be described by distinct yet variable characteristics (size, isoelectric point and expression pattern). The accurate identification, was greatly improved with the development of mass spectrometry (MS) and tandem mass spectrometry (MS/MS) for its ability to provide sequence data of protein isoforms and locate post-translationally modified residues.

Tandem mass spectrometry (MS/MS) can characterise unidentified proteins by analysis of cleaved peptide fragments. The assembly of these fragments determines the peptide sequence, that is used to predict the protein identity when compared to a library of peptide fragments. A bottom-up proteomics approach, samples all peptides supplied and is the most effective method for identifying novel proteins in the absence of a physiological assay. Importantly, the amount of a given protein can be inferred from the relative quantification of peptides.

The cellular changes that are implemented in response to the loss of a protein or activity should provide a dependence proteome. In this chapter, I will attempt to define the contribution of REST or USP15 to the cellular proteome. Proteins that change in response to either USP15 or REST knockdown could demonstrate novel roles in cellular pathways not previously described. These data will be used to steer later experiments to test the robustness of the cellular pathway.

4.1.2 A REST-Dependent Proteome

As loss of REST expression is associated with the neuroendocrine phenotype, of which indicative markers can be used as prognostic indicators, I decided to ascertain the contribution of REST to the cellular proteome following siRNA mediated knockdown. Due to the nature of REST as a transcription factor, little emphasis has been placed on the consequences of REST depletion on the proteome. Most studies focus on the interaction of REST with RE-1 sequences (ChIP-seq) or the transcriptional changes caused by REST (microarray and RNAseq) (Johnson et al., 2006, Johnson et al., 2008, Johnson et al., 2009, Johnson et al., 2012, Coulson, Unpublished, Rockowitz et al., 2014). Although REST-dependent transcript expression has been confirmed using siRNA in lung cancer cells (Moss et al., 2009) and other cell types, little evidence exists that REST depletion greatly influences protein levels and signalling pathways in non-neuronal or non-neuroendocrine cells. This is perhaps in part due to the limitations of transcriptional analysis, which does not reflect the interplay of REST-regulated miRNAs on mRNAs. It is suggested that miRNAs might contribute to the general discrepancy between mRNA and protein expression (Maier et al., 2009). Although transcriptome analysis is the logical option for studying the outcome of REST depletion, a proteomic approach is required to provide a REST-dependent protein signature.

4.1.3 The USP15-Dependent Proteome

Unlike REST, USP15 can regulate ubiquitin-dependent degradation it can have a direct effect on protein levels. USP15 is known to regulate ubiquitination associated with the CSN, and importantly the activity of E3 ligases that regulate protein degradation. Previously, the substrates of USP15, and its involvement in cellular pathways, has been inferred through interaction studies (Hayes et al., 2012). However, deubiquitylated substrates may be missed due to the transient nature of the interaction or dependency upon proteins that bind to interacting partners of USP15 at specific locations or

times. Here, I will attempt to address the functional roles of USP15 using siRNA depletion coupled with an unbiased proteomic approach.

4.1.4 A USP15-REST Axis

Here, I use a stable isotope-labelling of amino acids in cell culture (SILAC) proteomics approach that allows for a comparison of USP15 and REST-dependent proteomes. I hypothesise that as USP15 depleted cells indirectly reduce REST accumulation, the concurrent protein changes between USP15 and REST knockdown could demonstrate a USP15-REST axis that is important during the re-establishment of REST expression in G1.

4.2 Results

4.2.1 Experimental Design for Proteome Analysis

In order to establish proteins that are responsive to the loss of USP15 or REST, and to compare these conditions, I decided to use a relative quantification approach, known as stable isotope labelling of amino acids in cell culture (SILAC)(Ong et al., 2002). SILAC requires cells to be grown in specific media that allows incorporation of different isotopic amino acids in different experimental conditions. The stable isotopes impart defined mass increases on the amino acids of +4 Da or +8 Da for medium or heavy arginine and +6 Da or +10 Da for medium or heavy lysine. Trypsin is used to digest proteins into peptides as it cleaves C-terminal to an arginine or lysine. This means that all peptides will contain an amino acid that allows relative quantitation between conditions that can be discriminated from each other, based on the isotopic differences in the mass of the peptides identified, by using mass spectrometry (MS). The SILAC-MS workflow I employed is based on previous whole proteome analysis performed in our laboratory (Malec et al., 2015, Hernandez-Valladares and Prior, 2015, Hernandez-Valladares et al., 2014). The workflow and experimental conditions are summarised in Figure 4.1A.

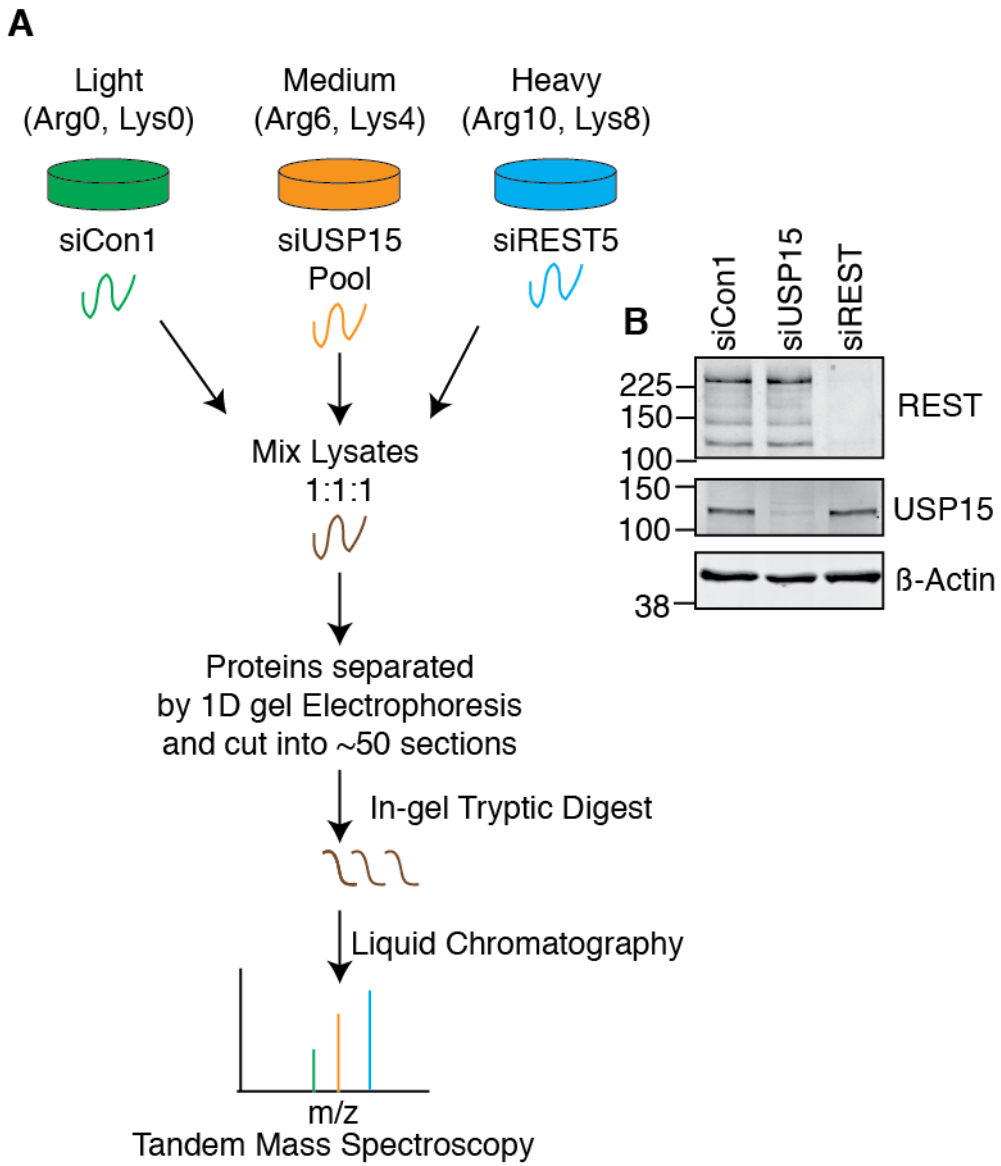

Figure 4.1. SILAC Experiment Configuration

(A) A549 cells were labelled with Light, Medium or Heavy amino acids so that proteins originated from each sample could be distinguished by tandem mass spectrometry (mass/charge = m/z). The lysates were collected and an equal amount of protein from each sample mixed to produce a combined sample that was separated by gel electrophoresis into ~50 sections for in-gel tryptic digest. The peptides produced were released from the gel and resuspended in 1% formic acid in preparation for liquid chromatography, using the NanoAcquity UPLC, and subsequent tandem mass spectrometry, using the LQT Orbitrap XL. **(B)** A representative immunoblot showing knockdown of USP15 and REST in lysates prior to mixing, for one of the 3 biological replicates that was analysed.

A549 cells were labelled with heavy, medium, or light amino acids over the course of several passages (Chapter 2, Section 1.3), enabling a triplex experimental configuration. REST or USP15 were depleted for 6-days with siRNA (Chapter 2, Section 1.5) in the heavy or medium labelled cells, respectively. The cells labelled with light amino acids were transfected with a non-targeting siRNA, siCon1, as a control condition to which protein expression in the siREST or siUSP15 treated samples would be normalised. Independent knockdown experiments were performed to generate three independent experiments for analysis (numbered 1, 2 and 3). The six-day knockdown protocol resulted in a robust decrease of REST (81% ± 0.13) or USP15 protein levels (98% ± 0.03)(Figure 4.1B).

For MS analysis (Chapter 2, Section 3.5), equal amounts of protein lysates from the three conditions within an experiment were combined into a single sample to minimise differences in sample processing. Proteins were first separated by size, using one dimensional SDS-PAGE and the gel divided into 50 sections prior to tryptic digest, to reduce complexity and allow for greater coverage of the proteome. Each sample was run through a reverse phase liquid chromatography column, allowing separation by retention time on the column, a parameter that varies according to hydrophobicity of peptides. The sample was then subject to electrospray ionisation (ESI) and detected using an LTQ OrbiTrap XL mass spectrometer. The top six peptides, i.e. those with the highest intensity, were continuously selected by the quadrupole for collision induced dissociation (CID). The LC-MS analysis was performed twice, generating technical replicates for each of the three experiments (replicates A and B). The sequence of the peptide was then inferred from the fragments produced by CID.

4.2.2 Protein Sampling and Reproducibility of Protein Identification

Data from LC-MS were processed using MaxQuant (Chapter 2, Section 3.5.3)(Cox and Mann, 2008)) in three different ways: (1) separate analysis of each technical replicate from each experiment (1A, 1B, 2A, 2B, 3A, 3B), (2)

combined analysis of the technical replicates for a given experiment (1AB, 2AB, 3AB), and (3) collective analysis of all technical replicates for all three experiments (ALL).

To ensure that the data collected were reliable and comprehensive, I compared the proteins identified by separate MaxQuant analysis of the technical replicates within each experiment (Figure 4.2A). The independent experiments identified between 924 and 1820 proteins, with each sequential experiment increasing the number of peptides identified. On average 68% of proteins were identified in both technical replicates, suggesting that inclusion of both LC-MS runs will increase the proteome coverage achieved for the experiments.

Technical replicates were combined into a single MaxQuant analysis for each experiment (1AB, 2AB and 3AB). The overlap in proteins identified between the independent experiments was then compared (Figure 4.2B). In total, 2077 proteins were identified. Around 37% of proteins were only identified in one experiment however, 63% were identified in at least two experiments and 34% were identified in all three experiments. Data from this method of MaxQuant analysis is used in subsequent figures to illustrate the reproducibility of global and specific protein expression changes for the independent experiments.

Finally, data from all the individual experiments and technical replicates were subject to a single collective MaxQuant analysis. The protein list generated by this 'ALL' analysis was compared with the 2077 proteins amalgamated from analysis of the individual experiments (1AB+2AB+3AB) (Figure 4.2C). The ALL analysis identified 1915 proteins, and shares 98% of these with the amalgamated list of 2077 proteins. The ALL analysis provides a single numerical value that will be used as the basis of subsequent gene ontology analysis.

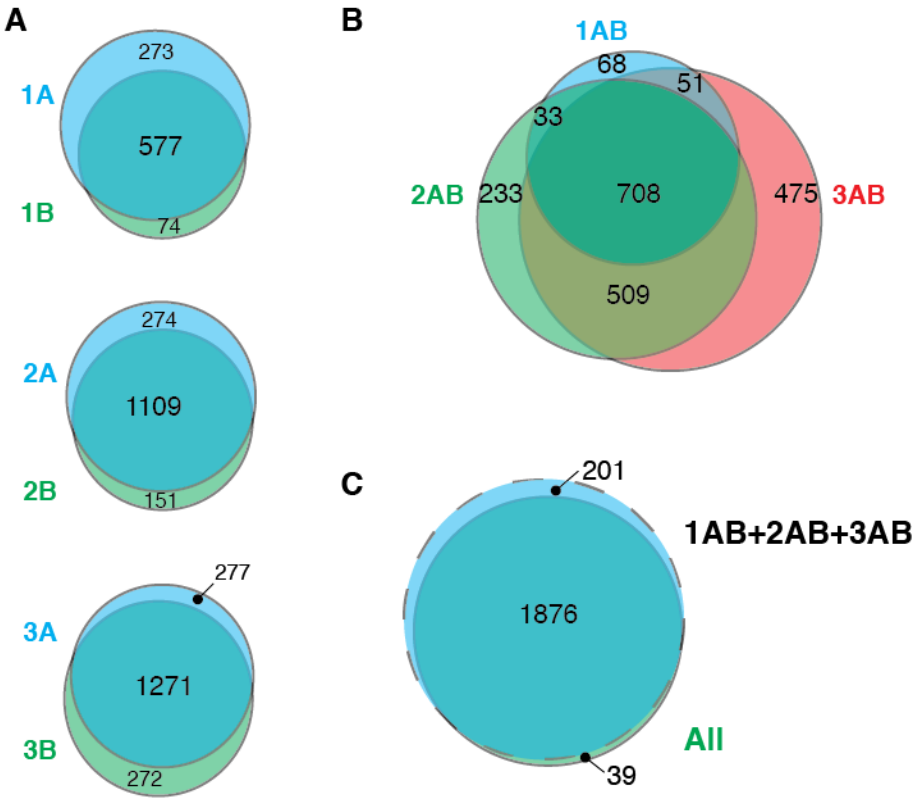

Figure 4.2. Peptide Sampling and Reproducibility of Protein Identification
Proteomic peptides were sampled using the LQT Orbitrap XL mass spectrometer and proteins identified by MaxQuant analysis. **(A)** Proteins identified from technical replicates (A and B) were compared within biological experiments (1-3). **(B)** Technical replicates (AB) were compared between biological replicates. **(C)** A combined MaxQuant analysis of all biological and technical replicate datasets (ALL) was performed and compared to the collection of proteins identified from the analysis of biological replicates (1AB+2AB+3AB).

All the unique identifiers from the MaxQuant analyses were extracted and compiled into one table. The normalised protein ratio, calculated as described in (Cox and Mann, 2008), were $Log_{(2)}$ transformed. Intensities were $Log_{(10)}$ transformed for the corresponding proteins for each of the individual experiments and technical replicates (Supplementary Table 1). I used an inclusive method for shortlisting the protein changes to ensure that all protein systems affected by the knockdown were represented. Included in the shortlist were any proteins that exhibited ≥1.5-fold change, either increasing or decreasing for the targeting siRNAs (siUSP15-Pool, siREST5), relative to non-targeting control siRNA (siCon1). These responsive proteins were used for

gene ontology analysis (Chapter 4, Section 2.4). In addition to the arbitrary 1.5-fold threshold, I also applied a Significance B statistical test (Chapter 2, Section 4.1). Unlike other statistical tests that assume a normal distribution of protein ratios Significance B accounts for the intensity of the protein, which means that proteins that may exhibit a proportionally large increase may be included despite the protein occurring at a low abundance (Cox and Mann, 2008).

The expression of proteins was compared between independent experiments to determine the reproducibility and reliability of data. The comparison of Log_{10} protein intensities (Figure 4.3A) demonstrated a clear positive correlation between data points from each experiment. Comparison of the siUSP15/Control protein ratios (Figure 4.3B) provided an insight into the similarities and differences in response to USP15 depletion between experiments. No apparent correlation of protein changes is seen when accounting for all data points, however, prominent protein changes are broadly similar between experiments. The correlation coefficients suggest that independent experiments 1 and 3 were more similar to each other than 1 and 2 or 2 and 3. The siREST/Control ratio comparisons (Figure 4.3C) also support the notion that replicates 1 and 3 were most similar. Western blotting for REST in the independent experiments demonstrated similar knockdown efficiency in experiments 2 and 3 (~80%), whilst 1 exhibited the most effective knockdown (~98%). USP15 knockdown was effectively knocked down in experiments 1 and 3 (~99%), with 2 (~95%).

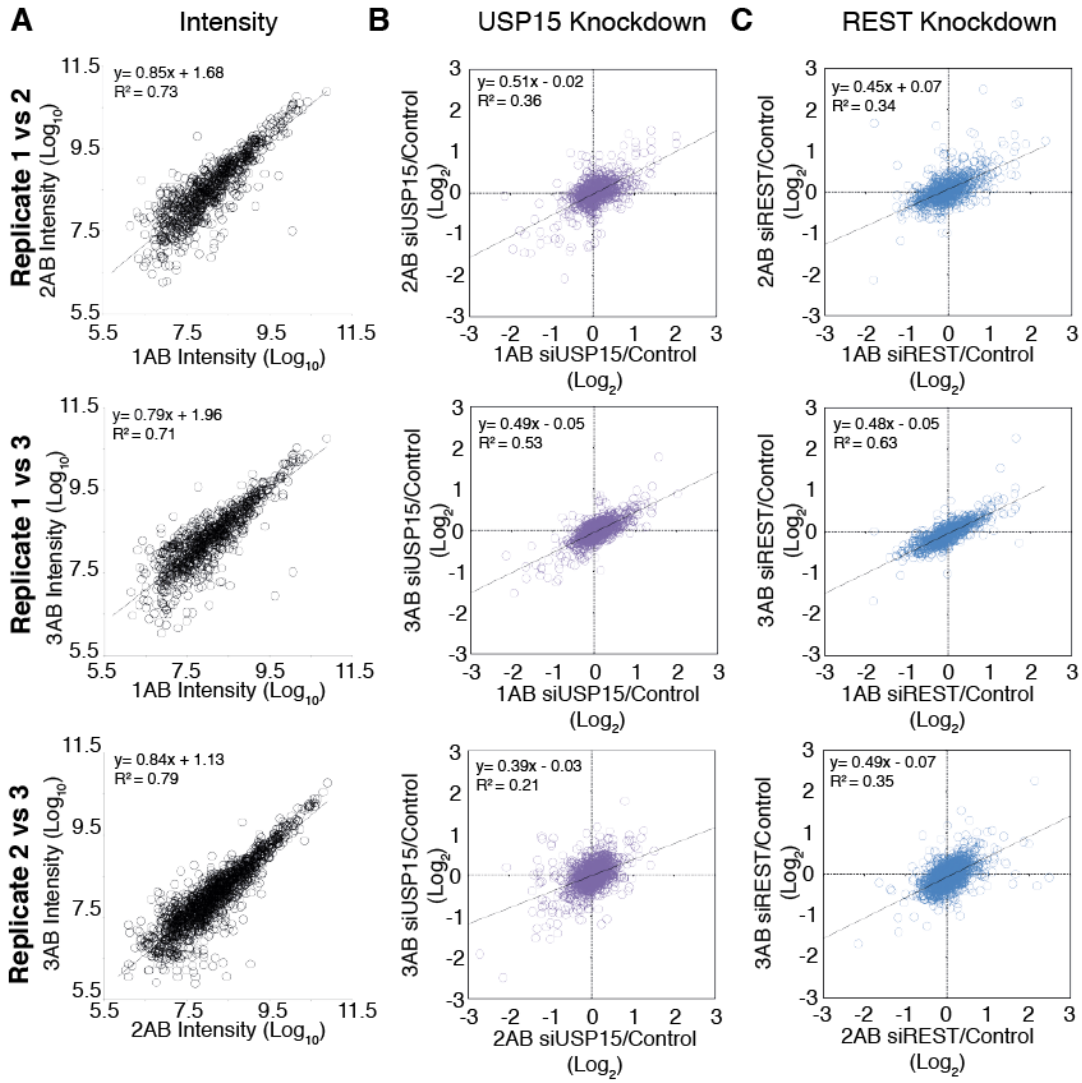

Figure 4.3. Comparison of Protein Responses between Independent Experiments

(A) Proteins detected from biological replicates (1AB, 2AB and 3AB) were correlated against each other based on Intensity. **(B)** Cross-correlation of protein levels changes of siUSP15 treated cells/Control. **(C)** Cross-correlation of protein level changes of siREST5 treated cells/Control.

4.2.3 The USP15 and REST Responsive Proteomes

An arbitrary 1.5-fold change in protein levels in ALL analysis was used to designate proteins that were responsive to the knockdown of USP15 or REST (Figure 4.4A and 4.4B), with proteins that met this criterion forming the basis of future analyses. Overall, 8.2% (156/1915) of proteins were responsive to USP15 knockdown and 7.1% (135/1915) of proteins responsive to REST knockdown. The relative protein expression in siUSP15-treated or siREST-treated cells, compared to Control (siCon1-treated) cells, are presented as a scatter plots (Figure 4.4C and 4.4D). Responsive proteins are highlighted, based on ≥1.5-fold change and/or Significance B analysis. To assess the consistency of protein changes in response to USP15 or REST knockdown I cross-correlated the protein ratios from independent experiments (Figure 4.4E-F). Data demonstrate a clear positive correlation with very few proteins showing a reciprocal change between experiments.

To investigate any potential USP15-REST axis I compared the 234 proteins that were responsive to either USP15 or REST knockdown (Figure 4.5A). 99 of the 234 (42%) were responsive only to USP15 knockdown, whilst 78 (33%) were responsive only to REST knockdown. Interestingly however, almost a quarter of these proteins (57/234) were responsive to both siUSP15 and siREST. Of these 57 proteins (Figure 4.5B), 32 proteins (56%) increased and 21 proteins (37%) decreased in expression in response to either siRNA. Strikingly, only four proteins demonstrated a reciprocal relationship between USP15 and REST knockdown. Expression ratios for proteins that are responsive to either USP15 or REST depletion are plotted in Figure 4.5C, with those responsive to both plotted in Figure 4.5D. The proteins responsive to siUSP15 and siREST have a correlation of 0.77, despite the inclusion of proteins that were not significant, as determined by Significance B. This small group of proteins represents the most promising assembly of downstream targets dependent upon USP15-mediated regulation of REST. The validation of some of these protein changes will be investigated in later figures.

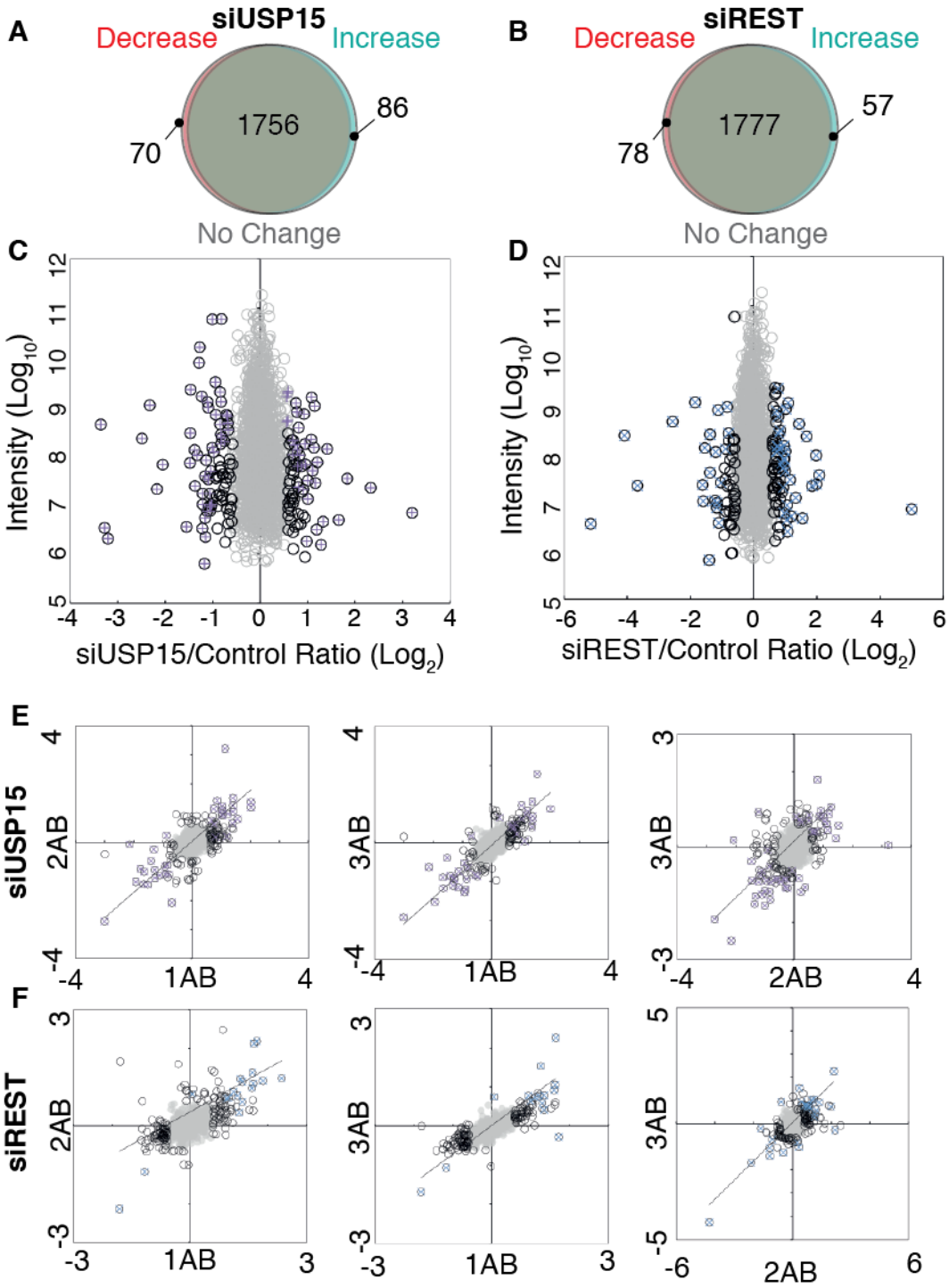

Figure 4.4. Distribution of Responsive and Significant Proteins
The response of proteins to siRNA knockdown are summarised in Venn diagrams, **(A)** siUSP15 and **(B)** siREST. Responsive proteins are those that exhibited > 1.5 fold-change, with 156 proteins responsive to siUSP15 and 135 responsive to siREST. Scatter plots of protein changes relative to **(C)** siUSP15 or **(D)** siREST knockdown, with responsive proteins (black circles) used to generate lists of proteins that will be used in later analysis. Proteins that were statistically significant as determined by having a P value of < 0.5 as determined by Significance B (Perseus), are highlighted; + siUSP15, x siREST significant. The protein ratios were compared between experiments in response to either **(E)** siUSP15 or **(F)** siREST.

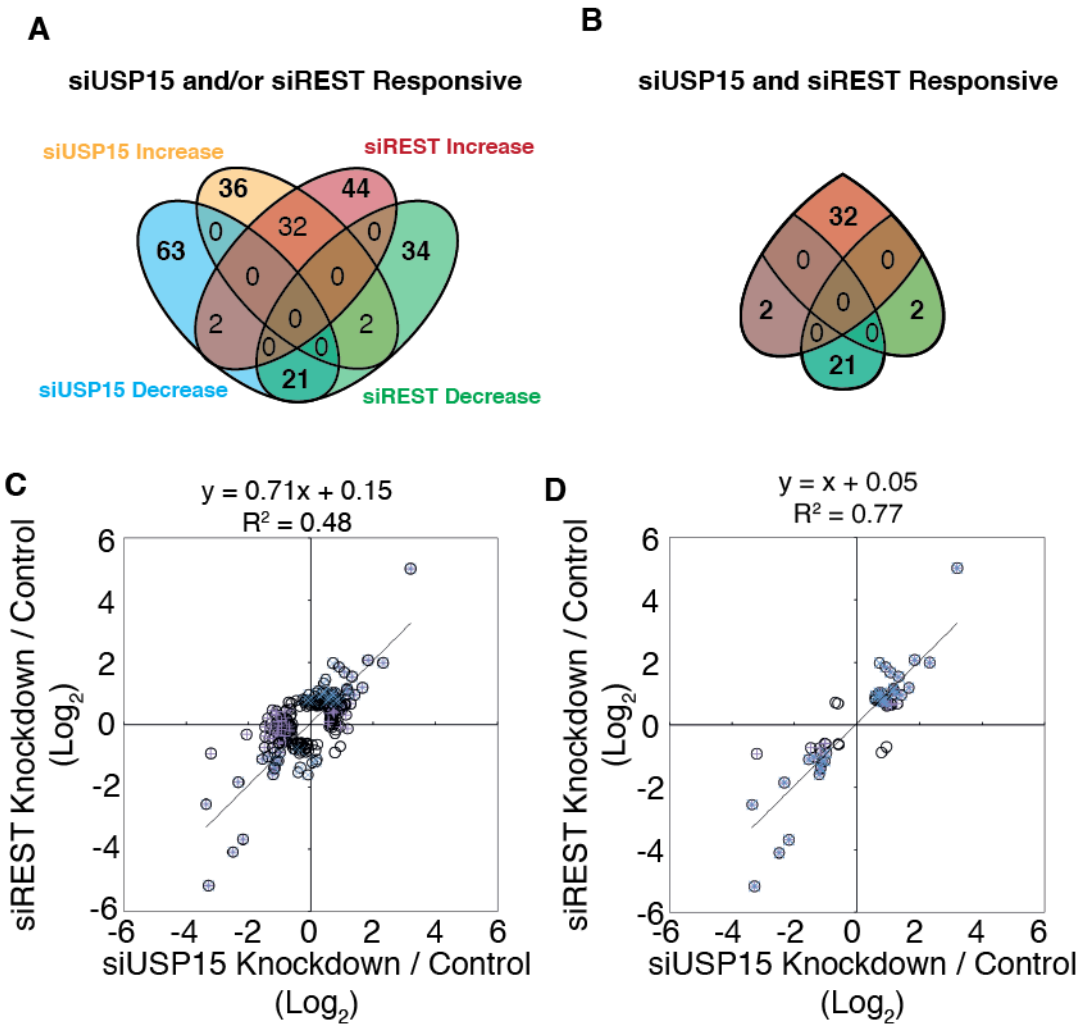

Figure 4.5 Cross Correlation of siUSP15 and siREST Responsive Proteins
(A) Proteins that exhibited a >1.5-fold change in response to siUSP15 or siREST, **(B)** those responsive to both siUSP15 and siREST. 234 proteins were responsive to either siUSP15 or siREST. These proteins were separated into lists based upon the direction of protein change. 57 proteins were common to both siUSP15 and siREST with 53 sharing the direction of protein change **(C)**. Only 4 proteins demonstrated opposing protein levels, resulting in a strong correlation of data between siUSP15 and siREST protein change **(D).** Proteins that were significant as determined by Significance B are highlighted as such; + siUSP15, x siREST significant.

4.2.4 Cellular Functions of USP15 and REST-Responsive Proteins

The responsive proteins were used to investigate biological systems that may be dysregulated by USP15 or REST knockdown, through gene ontology analysis using DAVID (Chapter 2, Section 4.2). Lists of responsive proteins were separated based on the condition and directionality of response, e.g. siUSP15 responsive and ≥1.5-fold positive change (siUSP15 Increase). Gene ontology terms that were significantly enriched ($P < 0.01$) in response to either USP15 or REST knockdown, were selected and shortlisted to remove similar terms. To provide a broad overview of the localisation of responsive proteins, I initially performed analysis restricted to cellular compartment GO terms; the statistical significance for enriched terms is presented as a heatmap (Figure 4.6A). I also performed a similar analysis that combined molecular function and biological process GO terms (Figure 4.6B). These data demonstrated that the proteins responding to USP15 or REST depletion share some GO terms, whilst both groups are also enriched for unique terms.

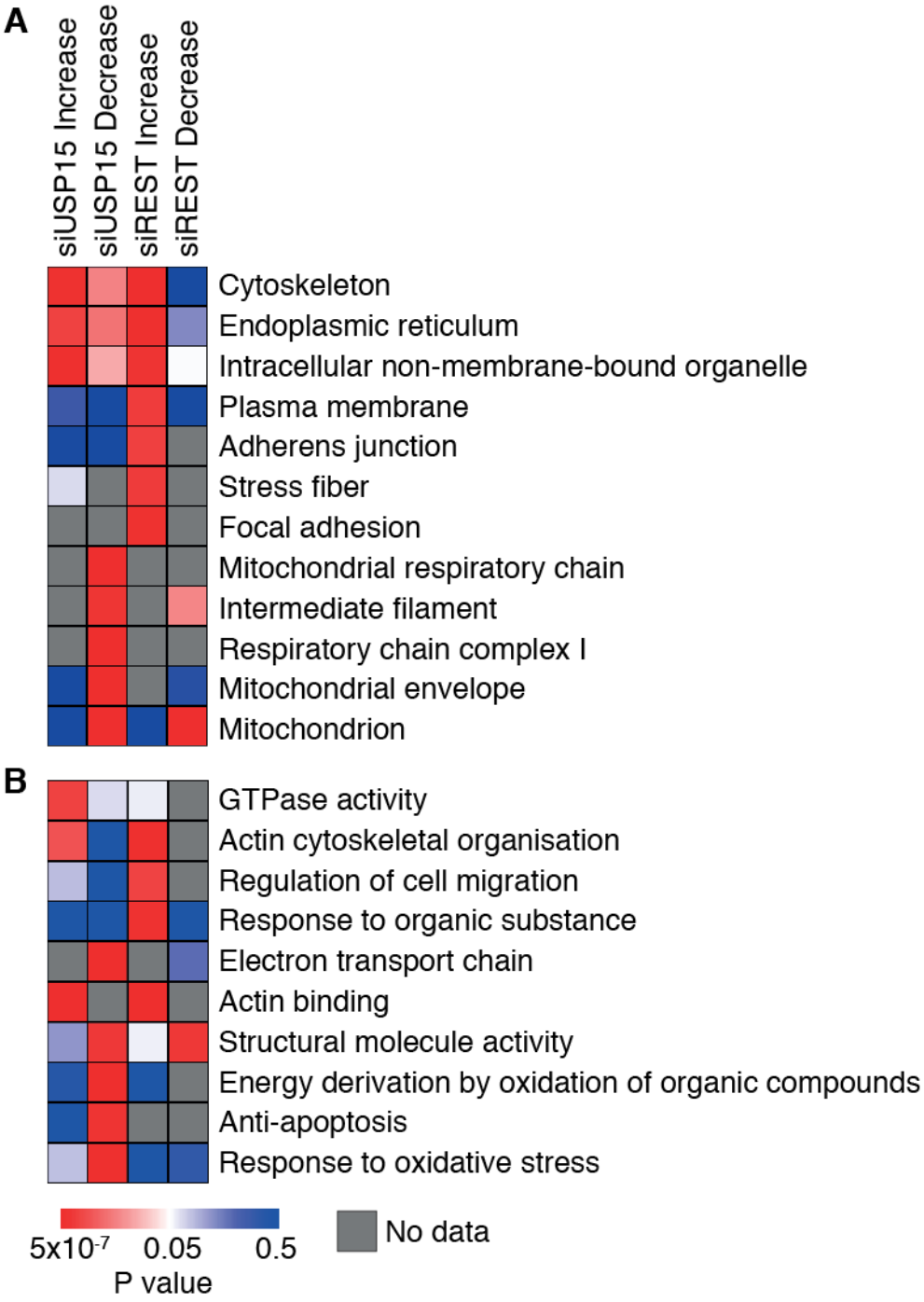

Figure 4.6. Gene Ontology Analysis of siUSP15 or siREST Responsive Proteins
Heatmaps of gene ontology term relating to **(A)** cellular compartments or **(B)** biological processes and molecular function, were derived from a list of responsive proteins (exhibited >1.5-fold change) following either siUSP15 or siREST knockdown. A shortlist of gene ontology terms is presented due to multiple redundant gene ontology terms.

The enriched cellular compartment terms were manually collated with closely related terms to generate a broad overview of proteins that share the similar cellular location. This collation of terms generated three distinct categories known simply as ‘Plasma membrane’, ‘Endoplasmic Reticulum’ and ‘Mitochondria’. Scatter plots of these cellular compartment categories are presented in Figure 4.7(A-F).

The broad ‘Plasma Membrane’ category, includes related terms including; plasma membrane, adherens junctions and cell cortex. The ‘Plasma Membrane’ consists of 53 proteins of which, 20 decrease and 21 increase in response to USP15 knockdown (Figure 4.7A). REST depletion results in increased expression of 24 proteins, whilst only six proteins decrease (Figure 4.7B). These data graphically demonstrate the enrichment of the plasma membrane term for siREST increasing proteins (Figure 4.6A).

The endoplasmic reticulum category presented is that of a unique GO term. This GO term was significantly enriched in response to both USP15 and REST knockdown (Figure 4.6A). This proteomic study identified 33 proteins from this terms that were responsive to either USP15 or REST. 14 of 33 proteins increased in response to REST depletion. USP15 knockdown, however, resulted an almost equal increase and decrease of responsive proteins.

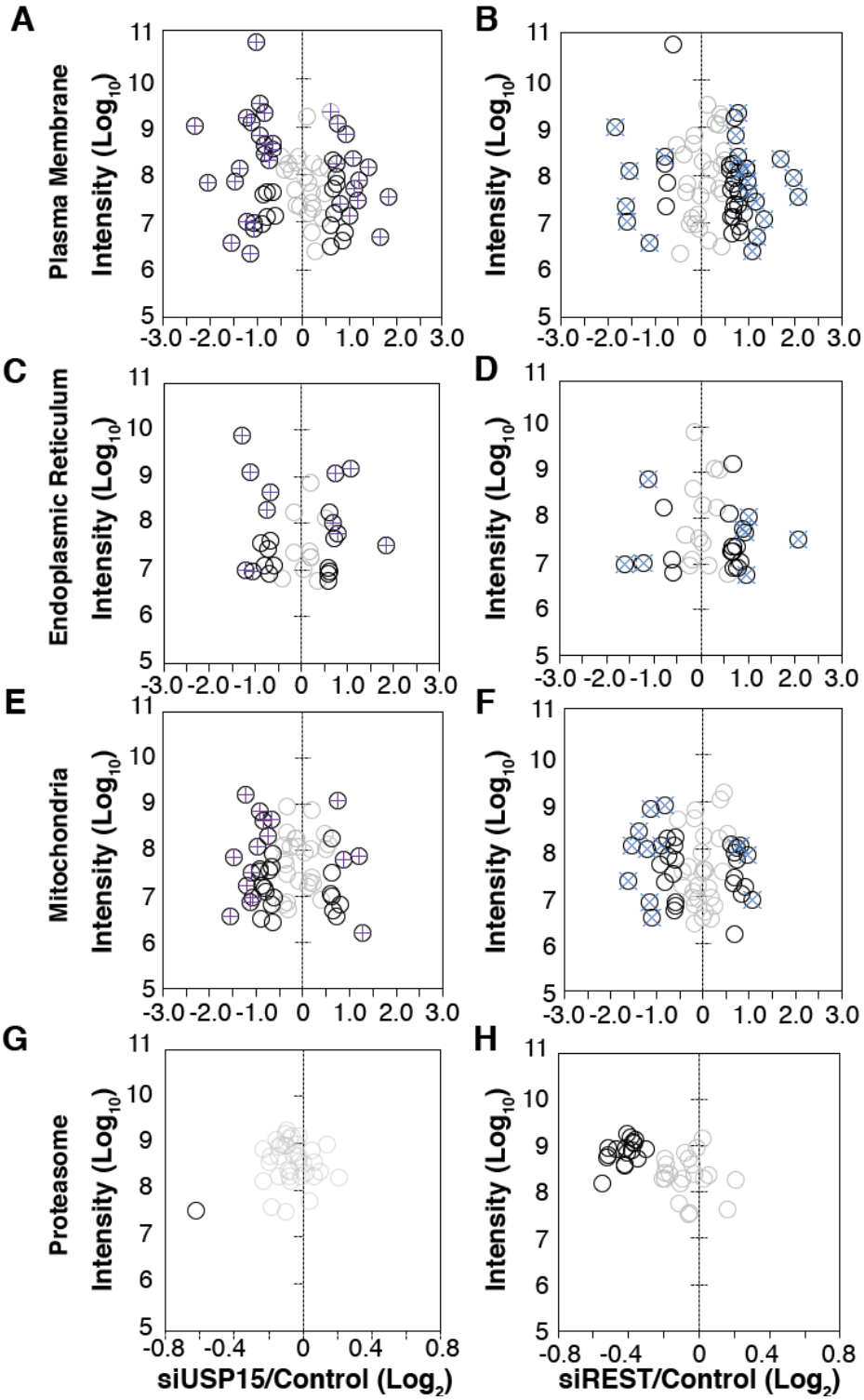

Figure 4.7. Cellular Components Categories
Cellular compartment gene ontology terms were collated into three broad categories; **(A-B)** Plasma membrane, **(C-D)** Endoplasmic Reticulum and **(E-F)** Mitochondria. The response of these proteins to **(A,C,E)** siUSP15 or **(B,D,F)** siREST knockdown are presented as scatter plots, with unresponsive proteins (hollow grey circles) and 1.5 fold-change responsive proteins (hollow black circles). **(G-H)** Proteasome proteins are plotted in response to either siUSP15 or siREST, with a 1.2 fold-change threshold for responsive changes (hollow black circles). Proteins that were significant as determined by Significance B are highlighted as such; + siUSP15, x siREST significant.

The ‘Mitochondria’ collated term includes GO terms such as; mitochondrion, mitochondrial envelope and mitochondrial respiratory chain. The ‘Mitochondria’ category consists of 60 proteins responsive to either USP15 or REST knockdown (Figure 4.7E). Of the 35 proteins responsive to siUSP15, 24 decreased in expression. USP15 depletion resulted in protein changes in particular from the respiratory chain (Figure 4.6A). In this collated term, REST depletion also resulted in a decreased expression of 20 proteins (Figure 4.7F). These data demonstrate that both USP15 and REST knockdown influence mitochondrial proteins.

Relaxation of the threshold to 1.2-fold change highlighted several proteasome proteins that decreased in response to REST knockdown (Figure 4.7G-H). Despite the relatively small changes in expression level, it was striking that 18 proteasome subunits decreased in a co-ordinated way. I decided to investigate the response of all 39 proteasome subunit proteins identified by MS in each of the experiments. A general trend for decreased expression following REST knockdown was evident (Figure 4.8A). PSMA1,2,3,4, PSMB1,2,3,5,7, PSMC6, PSMD6, PSME3 all decreased by more than 1.5-fold in at least one independent experiment. A schematic showing arrangements of these proteasome subunits within the proteasome is presented in Figure 4.9B, in which the proteins are coloured based upon the expression ratios determined by ALL analysis. The majority of proteasome proteins that decreased in response to REST knockdown are the alpha and beta subunits that form the 20S proteasome core. Other prominent changes include PSMC6, PSMD6 and PSME3.

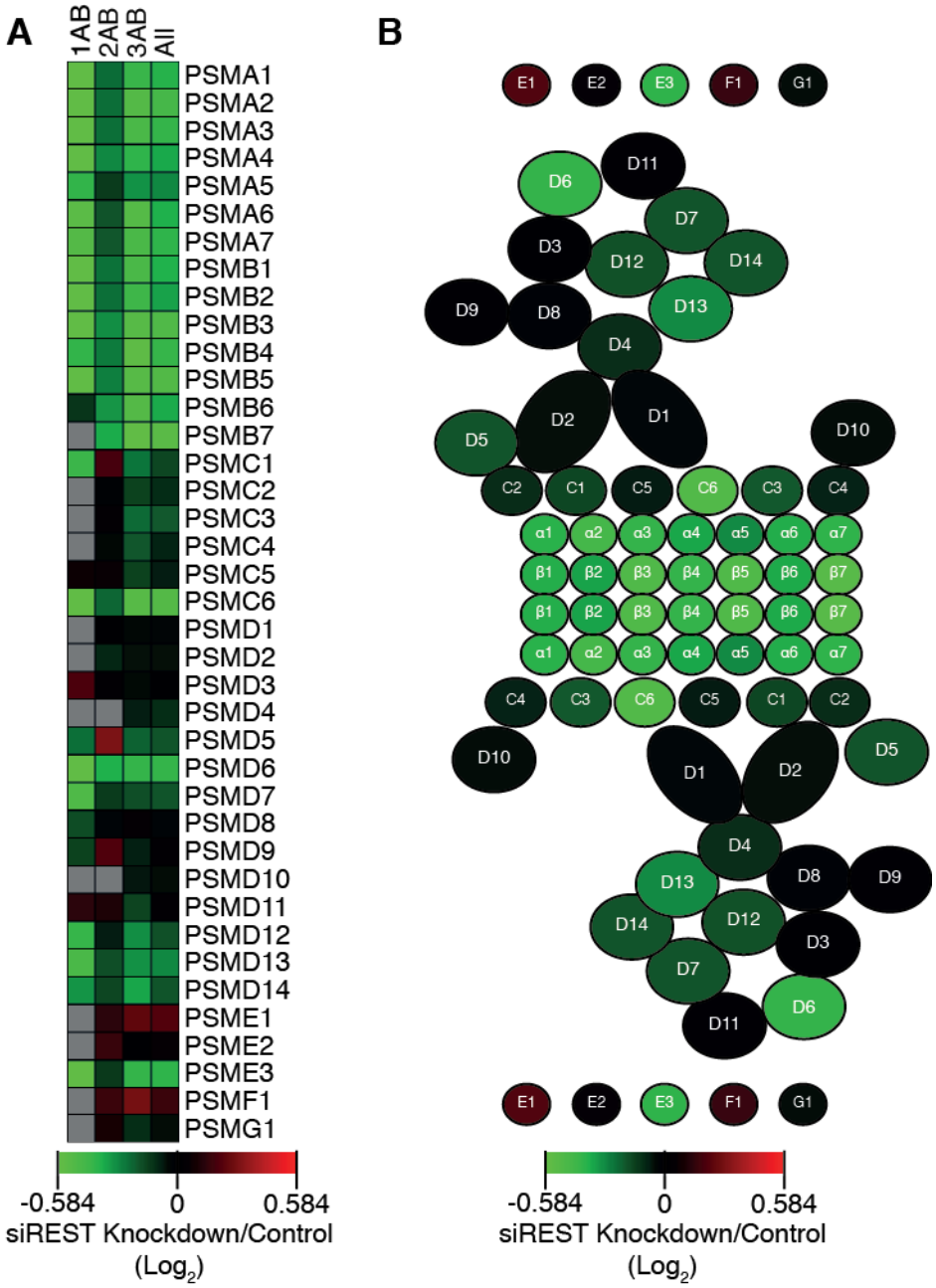

Figure 4.8 Proteasome Protein Response to siREST Knockdown
(A) Heatmap of proteasome subunit protein levels across biological replicates (1AB, 2AB, 3AB) and the combined analysis (ALL) data. **(B)** The response of proteasome subunits is presented as a proteasome schematic image.

The molecular function and biological process gene ontology terms that were enriched ($P < 0.01$) to generate a category of proteins with shared attributes. This collation of alike terms generated four broad categories of proteins, which I have simply called ‘Actin’, ‘GTPase’, ‘Energy’ and ‘Apoptosis’. The assembly of these categories selects proteins that were responsive to either USP15 or REST. The response of these categories of proteins to USP15 or REST knockdown are presented as scatter plots in Figure 4.9.

The ‘Actin’ category includes GO terms including actin cytoskeleton organisation, actin binding, cell migration and cell adhesion terms. The ‘Actin’ category consists of 51 proteins (Figure 4.9A-B), of which 40 proteins increase in response to either USP15 or REST knockdown. USP15 knockdown results in 29 responsive protein changes of which 20 increase (Figure 4.9A). REST depletion, however, leads to 40 responsive protein changes of which the majority (33/40) increase. Further investigation into proteins and specific gene ontology terms enriched within the ‘Actin’ category are explored in Chapter 4, Section 2.5.

The ‘GTPase’ category consists of terms including; GTPase activity, small GTPase mediated signal transduction and regulation of small GTPase mediated signal transduction. The ‘GTPase’ category consists of 17 proteins, and despite GTPase activity enriched in the siUSP15 Increase cohort (Figure 4.6B), I observe a mixed picture of seven protein increases and six decreases in response to USP15 depletion (Figure 4.9C). REST depletion results in four protein increases and two protein decreases (Figure 4.9D). One protein, RAB3B, is significantly increased in response to both siUSP15 knockdown and siREST knockdown.

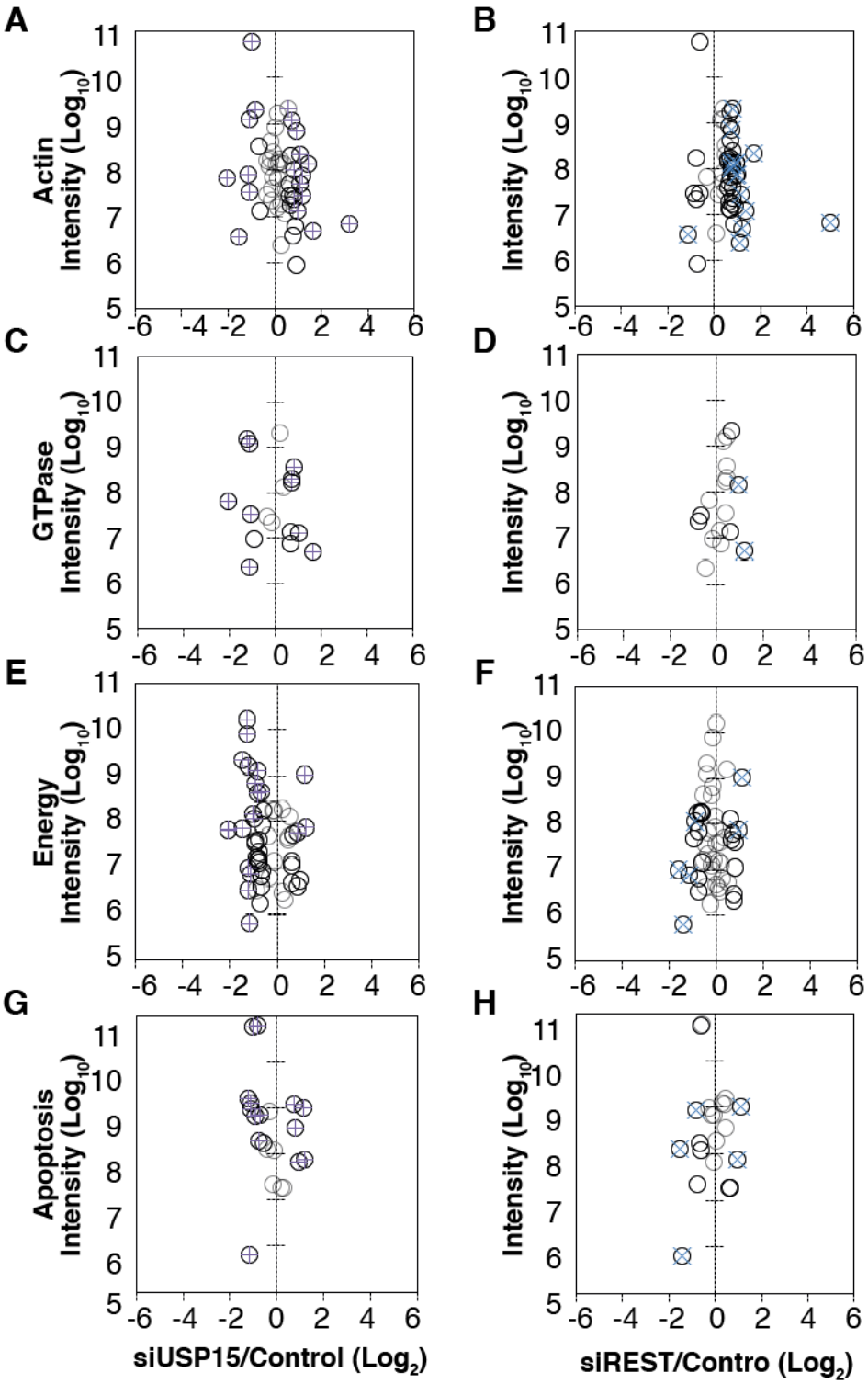

Figure 4.9. Molecular Function and Biological Process GO Categories
Molecular function and biological process gene ontology terms were collated, and together with non-significant terms of similar definition into 4 broad categories; **(A-B)** Actin associated, **(C-D)** GTPase, **(E-F)** Energy and **(G-H)** Apoptosis. The response of these proteins to **(A,C,E,G)** siUSP15 or **(B,D,F,H)** siREST knockdown are presented as scatter plots. Unresponsive proteins (hollow grey circles), responsive proteins (hollow black circles) and those that were significant as determined by Significance B are highlighted as such; + siUSP15, x siREST significant.

The ‘Energy’ category proteins are collated from terms including energy derived by oxidation of organic compounds, electron transport chain and ATP metabolic process. The ‘Energy’ category consists of 51 proteins of which 31 decrease in response to USP15 depletion (Figure 4.9E). The number and significance of the responsive proteins suggest that USP15 may have an important role in the regulation of energy status in the cell. These GO evidence suggest that USP15 depletion affects proteins localised to the mitochondria (Figure 4.6A) in particular those involved in energy production (Figure 4.6B). Further analysis and investigation into mitochondrial role of USP15 are explored in Chapter 5.

The ‘Apoptosis’ category includes gene ontology terms; regulation of apoptosis, cell death and regulation of anti-apoptosis, the latter was shortlisted as a response GO term of proteins decreasing following siUSP15 (Figure 4.6A). USP15 depletion led to a responsive change in 15 out of 21 ‘Apoptotic’ proteins (Figure 4.9G).

4.2.5 Identification and Validation of Responsive Proteins

I decided to plot a subset of proteins against the broad categories in Figure 4.9. I chose the ‘Actin’ category (Figure 4.9A), being one of the most responsive terms, to plot specific gene ontology terms that included Actin Binding (Figure 4.10A-B), Cell Migration (Figure 4.10C-D) and Cell Adhesions (Figure 4.10E-F).

The actin binding gene ontology term was enriched amongst proteins that were upregulated in response to both siUSP15 and siREST (Figure 4.6A). Amongst the responsive proteins, Vinculin (VCL) and Epidermal Growth Factor Receptor (EGFR) are both significantly increased in USP15 and REST knockdown (Figure 4.10).

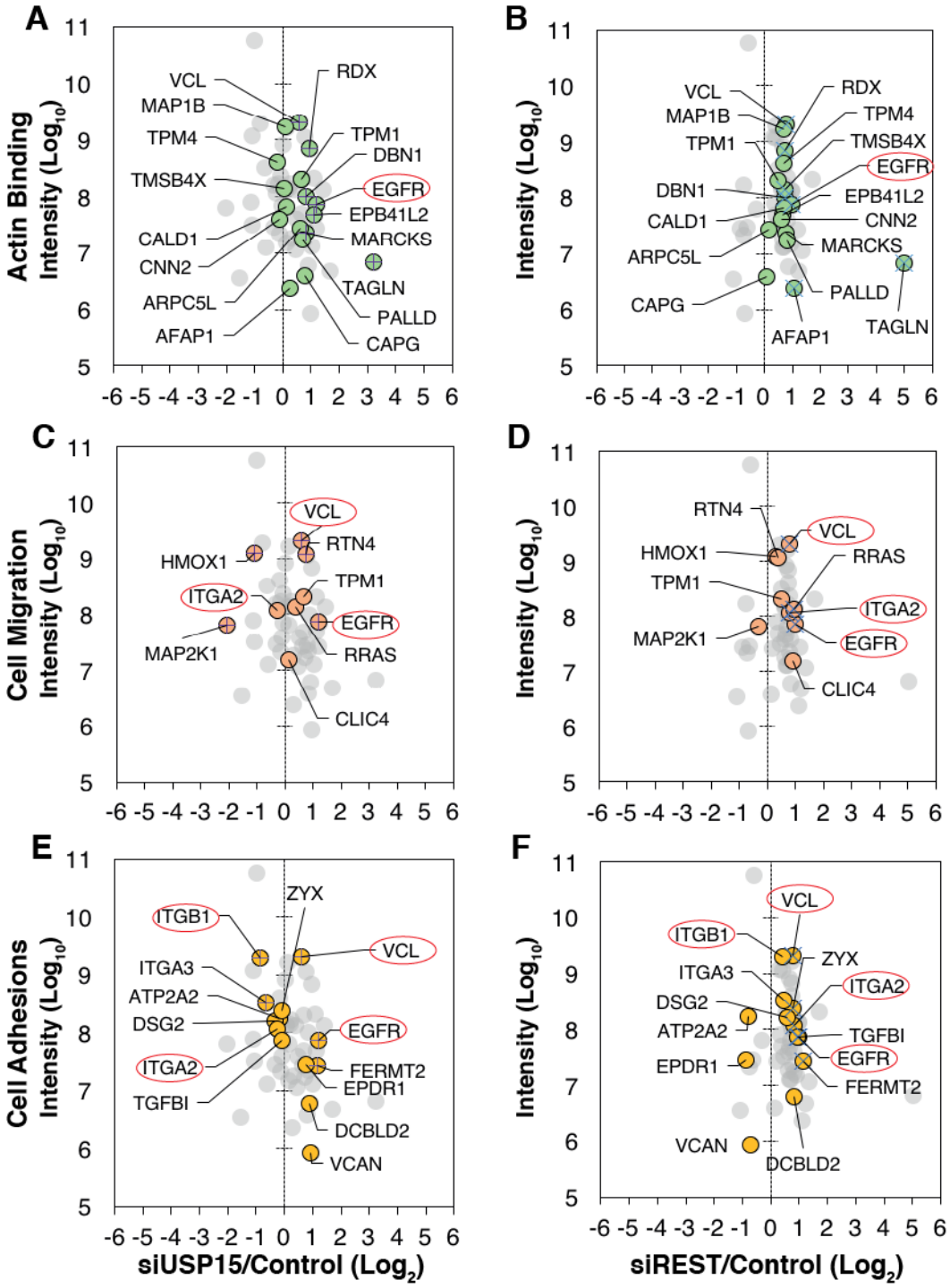

Figure 4.10. Significant Actin-Associated Terms Respond Differently to siUSP15 and siREST

Specific actin terms were significantly enriched in response to either siUSP15 or siREST including; **(A-B)** actin binding term (GO:0003779), **(C-D)** regulation of cell migration term (GO:0030334) and **(E-F)** cell adhesion (GO:0007155). Proteins within the gene ontology terms are distinguished by coloured circles (Actin Binding, Green; Cell Migration, Orange; Cell Adhesion, Yellow) from a background of 'Actin' proteins (grey). Plotted here are the protein expression response to **(A,C,E)** siUSP15 or **(B,D,F)** siREST knockdown. Four proteins are highlighted by red circles that showed a significant response to either USP15 or REST knockdown.

The cell migration term was enriched amongst proteins that were upregulated in response to siREST (Figure 4.6A), as such I was interested in proteins that were specifically increased in response to siREST knockdown. From these proteins, I selected Integrin α2 (ITGA2) that could be a REST-specific protein change.

The cell adhesion protein gene ontology term was not significantly enriched ($P > 0.01$), although it was included in the 'Actin' category. This GO term included one additional integrin protein and I was intrigued by the expression of Integrin β1 (ITGB1), which decreased significantly in response to USP15 knockdown. Thus, EGFR, ITGA2, ITGB1 and VCL, were chosen for further validation. These proteins were identified by MaxQuant in each of the three independent experiments (Figure 4.11A-B), shared the same directional change in each experiment.

Using the protein lysates from the SILAC experiments I again demonstrated the knockdown of USP15 and REST (Figure 4.11C) and evaluated the expression of the selected proteins by immunoblot (Figure 4.11D-E). ITGB1 was significantly reduced in response to siUSP15 as determined by MS (Figure 4.11A). Although ITGB1 reduced in experiment 1 (Figure 4.11D), no significant decrease was observed across the three independent experiments (Figure 4.11F). Interestingly, ITGB1, only moderately increased in response to siREST knockdown by MS (Figure 4.11B), shared a significant increase in expression as deduced by immunoblotting (Figure 4.11D,F).

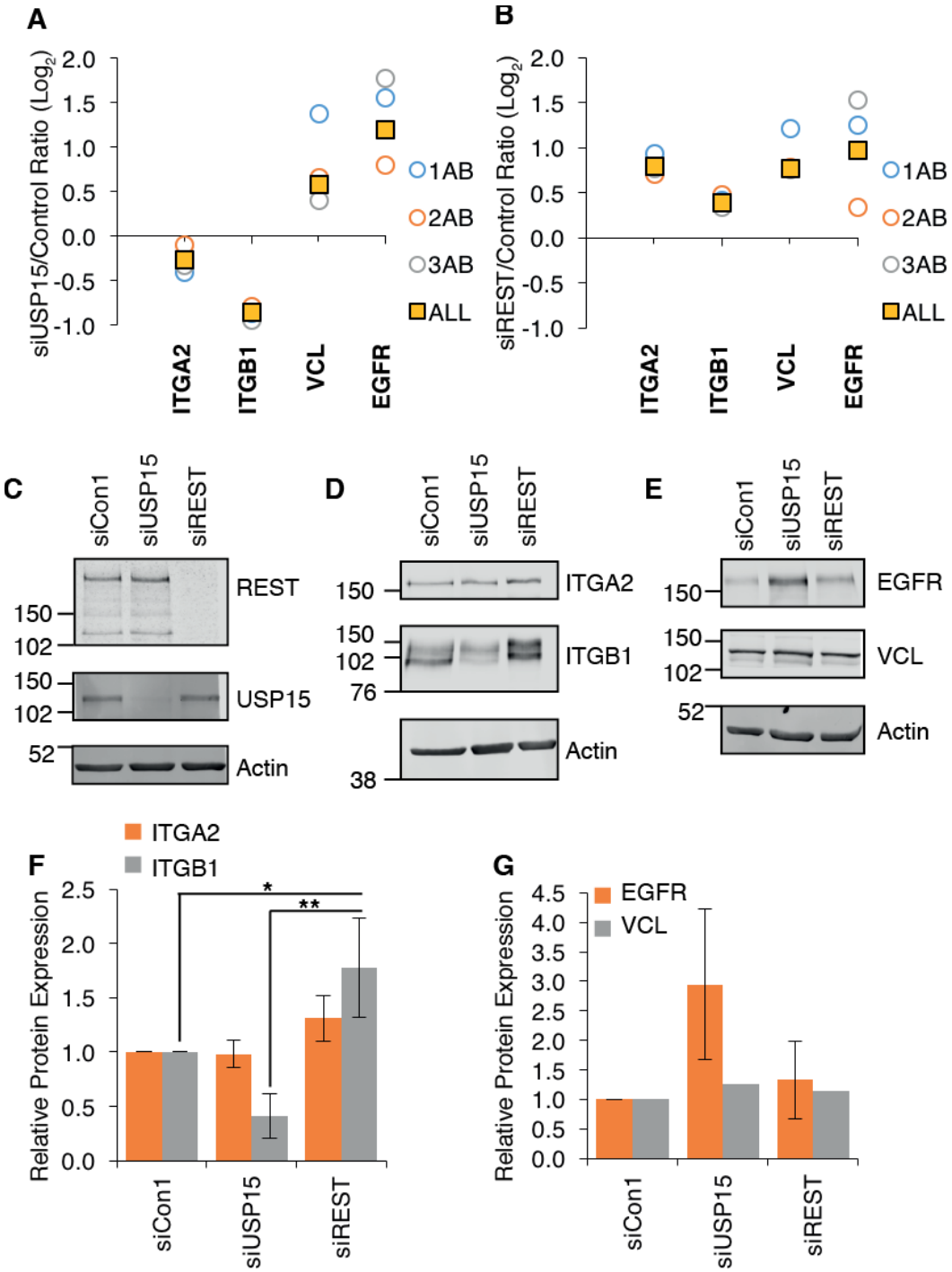

Figure 4.11. Validation of Selected Actin-Related Proteins Response to siUSP15 and siREST

(A-B) The siUSP15 and siREST ratio of ITGA2, ITGB1, VCL and EGFR, from independent proteomic replicates and the ALL analysis. Proteomic sample lysates were immunoblotted for **(C)** REST and USP15, **(D)** ITGB1 and ITGA2 and **(E)** EGFR and VCL. **(F-G)** Bar chart quantification of ITGB1, ITGA2, EGFR and VCL. Data represent n=3 replicates, expect VCL immunoblot n=2, Error bars = standard deviation; Statistics one-way ANOVA * $P < 0.05$ with Tukey's correction for multiple tests.

ITGA2 was significantly increased in response to siREST (Figure 4.10, Figure 4.11B). In experiment 1, ITGA2 was shown to increase by western blot (Figure 4.11D). ITGA2 demonstrated an overall trend to increase across independent replicates in response to REST depletion, although this was not significant (Figure 4.11F). In contrast, ITGA2 was not responsive to USP15 depletion by MS (Figure 4.10, 4.11A) and this was confirmed by western blotting (Figure 4.11F).

EGFR and VCL were both significantly upregulated in response to either USP15 or REST depletion as determined by MS (Figure 4.11A-B). EGFR was increased in response to USP15 depletion although not significantly, due to experimental variability (Figure 4.11G). The expression of VCL did not appear to change in response to either USP15 or REST depletion (Figure 4.11E, G).

4.2.5.1 The Response of EGFR and VCL to USP15 Depletion

I decided to test the expression of these proteins in unlabelled A549 cells, using alternative targeting and control siRNAs (Figures 4.12-13), to account for potential off target effects of siRNAs. EGFR was one of the most prominent increases in response to USP15 pool knockdown. I decided to reduce USP15 expression, using siRNAs that target different sequences, using a series of siRNAs including siUSP15-2, siUSP15-17 and siUSP15-Pool. siCon1 and siNT1 treated cells express similar levels of EGFR, however, siCon2 treatment may appear to induce expression of EGFR (Figure 4.12A). USP15-targetting siRNAs, alone of pooled, reduce USP15 protein levels (Figure 4.12A). The increase expression of EGFR in siUSP15-Pool treated cells relative to siCon1 reconfirms MS findings. Individual USP15 targeting siRNAs, siUSP15-2 and siUSP15-17, both increase EGFR expression relative to siCon1, with siUSP15-17 exhibiting a > four-fold increase of EGFR (Figure 4.12B).

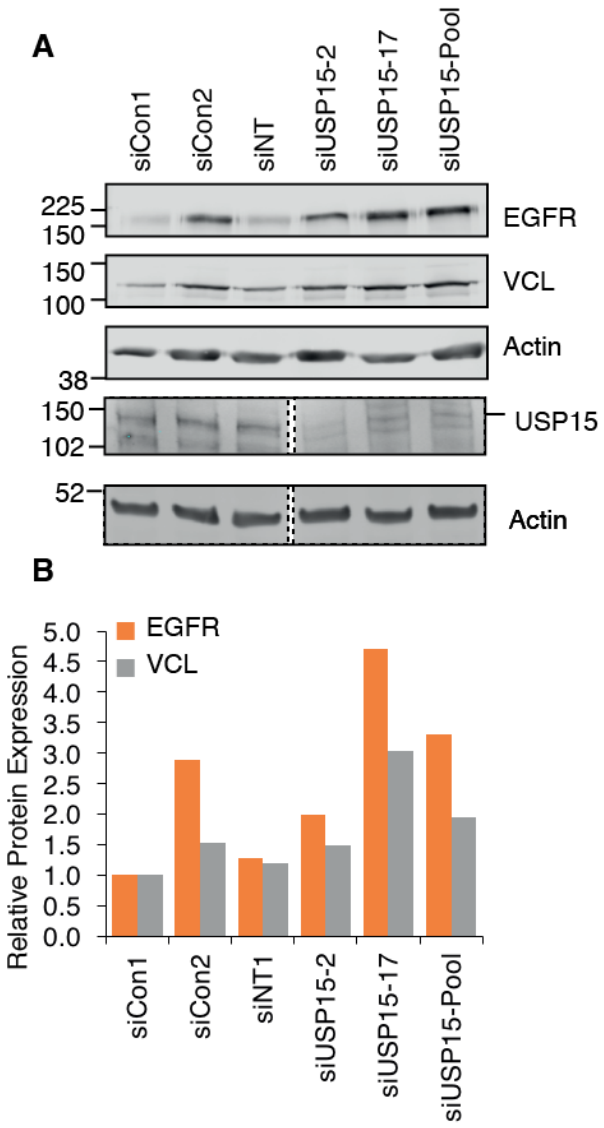

Figure 4.12. Response of EGFR and VCL in an Independent USP15 Knockdown **(A)** EGFR and VCL protein expression was examined using a series of control and USP15 siRNAs. **(B)** Bar chart quantification of EGFR and VCL relative to siCon1 (n=1).

In addition to EGFR expression I immunoblotted for VCL, which previously increased relative to siCon1-treated cells as determined by MS (Figure 4.11B), whilst it did not appear to change by western blotting (Figure 4.11G). This independent experiment demonstrated that siUSP15-Pool induces ~two-fold increase in VCL expression relative to siCon1 and siNT1. siUSP15-17 appears to have the greatest effect on both EGFR or VCL.

4.2.5.2 The Response of Integrins to REST Depletion

I decided to validate the Integrin protein response to REST depletion by using two REST-targeting siRNAs. siREST5, used in proteomic experiments, and siREST1 effectively deplete REST protein levels (Figure 4.13A). Interestingly, siCon2-treated cells have reduced the expression of both ITGB1 and ITGA2. Relative to siCon2-treated cells REST targeting siRNAs exhibit a ~1.5 fold increase in ITGB1 expression. Protein changes relative to siCon1, demonstrate that ITGB1 is slightly increased in response to either siREST1 or siREST5, which corroborate the slight increase seen in proteomic samples (Figure 4.11B). Interestingly the lower molecular weight ITGB1 appears to demonstrate a greater increase than the higher molecular weight.

The expression of ITGA2 was decreased in response to either REST targeting siRNAs relative to siCon1-treated cells (Figure 4.13A-B), with siREST1 inducing the greatest decrease. Relative to siCon2-treated cells, which have reduced expression of ITGA2, the decrease of ITGA2 induced by siREST5 is less apparent. These data support the evidence from previous experiments that ITGA2 is responsive to REST knockdown, however, ITGB1 is the more robust and reliable protein change. Interestingly, ITGB1 increases whilst ITGA2 decreases in response to REST depletion.

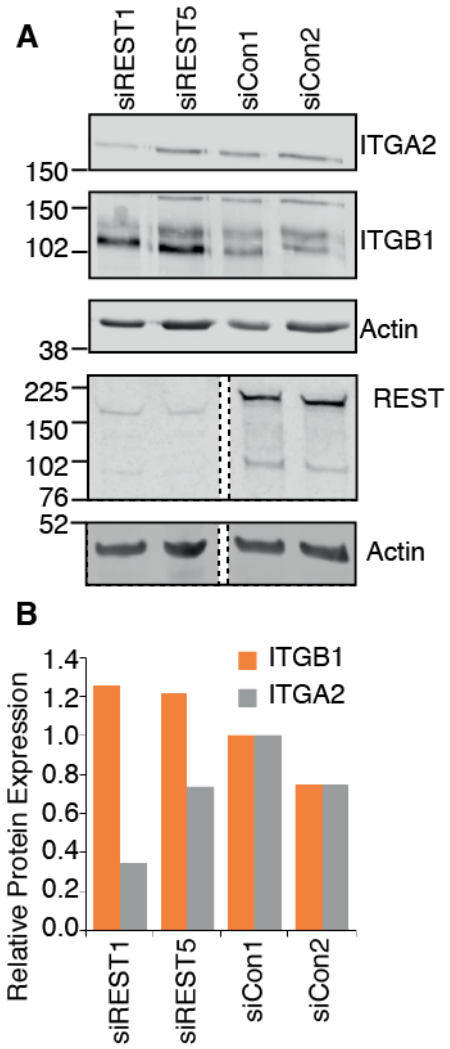

Figure 4.13. Response of ITGA2 and ITGB1 in an Independent REST Knockdown

(A) ITGA2 and ITGB1 protein expression was examined using a series of control and REST siRNAs. **(B)** Bar chart quantification of ITGA2 and ITGB1 relative to siCon1 (n=1).

4.3 Discussion

The purpose of this investigation was to determine the proteins and pathways that are regulated by either REST or USP15 and those that respond concordant with a USP15-REST axis. Here, I identified 1915 proteins from three biological and two technical replicates of whole proteome analysis following siRNA knockdown of either REST or USP15. Of these, 234 were responsive to either knockdown and the involvement of these proteins was investigated using gene ontology analysis. I demonstrated that REST and USP15 share 57 responsive proteins, the majority of which (53/57) respond concordantly. Of these protein changes, gene ontology analysis demonstrates that ~25% were actin-cytoskeletal proteins (14/57). I validated a selection of protein changes by western blotting. Importantly, striking changes were identified in mitochondrial and energy proteins in response to USP15 knockdown, which are investigated in Chapter 5.

4.3.1 Proteomic Analysis

The proteome, transcribed from ~20,300 genes, can be modulated to produce a 'proteoform' that greatly increases the diversity of proteins (Smith and Kelleher, 2013). Despite the ability of MS/MS to identify proteins, the depth of coverage is dependent upon technique, protocol, resolution and accuracy. The SILAC-MS workflow I employed is based on previous whole proteome analysis performed in our laboratory (Malec et al., 2015, Hernandez-Valladares and Prior, 2015, Hernandez-Valladares et al., 2014). The whole proteome approach accounts for isoform-specific peptides, although post-translation modifications and site-specific features are not included, which require additional stages of sample processing. As such, these data generated are limited to basal expression. Others studying A549 cells generate a range of ~700 to ~5000 proteins depending on methodology and equipment (Dave et al., 2014, Korrodi-Gregório et al., 2016). The resolution and accuracy of peptides is defined by the instrument and analysis, with the top six identified peptides being used for MS/MS analysis. As the identification of peptides is highly dependent upon their intensity, this method is biased towards highly

abundant proteins. These inherent limitations of the experiments should be considered when investigating the biological roles of protein dependent proteomes.

In addition to the technique, the type of experiment using siRNA knockdown also has the potential to influence outcomes. These cellular changes are dependent upon unforeseen effects on gene expression. Here, I used the siCon1 oligonucleotide, which has been used extensively and as such some of these off-target effects are now known. Primarily amongst these effects is a down-regulation of EGFR mRNA by ~50% (product information, Table 2.3). The proteomic quantification is made relative to that of control siRNA, with any off-target effects of the control siRNA likely to be reflected in both siUSP15 and siREST conditions. This should be noted whilst investigating USP15 and REST dependent changes.

Of the proteins identified 234 were responsive to either UPS15 or REST knockdown and analysed further. A conservative approach would have limited the number of analysed proteins to those that were statistically significant. I used a more inclusive method, based upon a >1.5-fold average threshold, which although arbitrary, contains a broader portfolio of proteins. This threshold is more inclusive than a conventional two-fold threshold and was used in collaboration with statistical analysis to identify proteins of interest after GO analysis. This inclusive approach was taken to promote enrichment of modulated pathways, which could then be investigated further. These responsive proteins were then investigated using gene ontology analysis tools. The most highly enriched GO terms identified proteins that were associated with the actin cytoskeleton. These proteins are generally highly abundant and are preferentially identified by MS due to peptide sampling bias, which might introduce a level of bias for enrichment towards actin related GO-terms, although the response of proteins to treatment is not influenced by this bias. The number of proteins, significance and shared response to both USP15 and

REST knockdown, as well as the novelty of these data was worth investigating further.

4.3.2 REST 'omics'

The contribution of REST to cellular behaviour has been interrogated using multiple approaches to investigate its function. The regulation enacted by REST has been assessed by RE-1 genome mapping, repressive epigenetic marks around RE-1 proximal genes, REST-DNA binding and transcriptional response (Chapter 1, Section 2.2). RE-1 genome mapping predictions were originally used to describe the variety of genes that could be regulated by REST, and although useful were shown to be context dependent. Repressive epigenetic marks (including H3K27me3 and H3K9me2) around RE-1/REST proximal genes are indicative of REST-dependent recruitment of co-repressors and chromatin modifiers. The interaction of REST with cis-acting RE-1 sites on a genome-wide scale is known as a 'cistrome'. The cistrome of REST has been performed in a variety of cell types, including A549 cells (Rockowitz et al., 2014), the same cell type used here. Unlike previously discussed methods, cistromes place REST at the RE-1 sites in this specific context. Here, I will briefly compare some of the major similarities and differences between the cistrome and proteomics which were both performed in A549 cells. Rockowitz et al. demonstrated that REST interacts with >3000 gene products 7% were shared in non-neuronal cells, which includes differentiation promoting genes. The REST cistrome in A549 cells includes NE markers and REST-regulated genes TUBB3, SCG3 and SRRM4. In this data, TUBB3 increased at a protein level, SCG3 is upregulated transcriptionally. Similar to RE-1 motif and REST-dependent transcript gene ontology analyses, the REST cistrome of A549 cells preferentially interacts at genes involved in neuronal systems (Rockowitz et al., 2014). The difference between the transcript derived terms and protein derived terms identified by omics studies, is perhaps due to REST targeted miRNAs that may regulate co-ordinated neuronal gene translation (Chapter 1, Section 3.2), which is likely to contribute to the discrepancy between transcript and protein levels. In addition, REST

also regulates secreted proteins which are not apparent in these data without further analysis of collected cell media fractions for analysis.

The data presented here are novel, as for the first time, I have investigated the net effects of REST transcript changes by quantifying the proteomic response to its depletion. Importantly, REST knockdown efficiency and the increased expression of TUBB3, demonstrate there has been a significant reduction in REST levels and that REST-regulated genes have been translated and transcribed. The REST-dependent proteome following six-day knockdown can demonstrate some protein signatures of REST de-repression, although these are not as pronounced as cistrome or transcriptome analysis.

4.3.3 GO Analysis of USP15 or REST-Dependent Proteomes

The responsive proteins generated by both USP15 and REST knockdown was interpreted using gene ontology analysis (Figure 4.6). The terms generated by this analysis demonstrated distinct and shared pathway enrichments for REST and USP15 knockdown. Unlike GO terms generated from cistrome or transcriptome analysis, a proteomic approach to pathway analysis should be interpreted with greater caution due to the interplay of signalling within the cell. This is the first attempt to interpret the contribution of a DUB to cellular function, based solely upon the response of proteins following its depletion. The knowledge of previous studies will be discussed when these are either in agreement or oppose the proteomic response generated.

The loss of USP15 or REST expression leads to the dysregulation of many proteins. Mechanistically, loss of REST and USP15 differ, based upon the major biological activity of the protein, with REST acting transcriptionally and USP15 classically acting post-translationally. USP15 is located in the cytoplasm and nucleus, whilst REST is exclusively nuclear. Interestingly both USP15 and REST depletion demonstrated changes in mitochondrial proteins,

which will be discussed in greater detail in Chapter 5. In addition to this, subcellular organelle proteins from the plasma membrane and endoplasmic reticulum were responsive to either UPS15 or REST knockdown. Amongst the plasma membrane group were mitogen signalling and actin-cytoskeletal proteins, that will be discussed later. Although not amongst the proteins identified here, a recent report has implicated a role for USP15 in the regulation of ER-associated E3 ligase RNF26, involved in the architecture of endosomal positioning. RNF26 recruits and ubiquitylates SQSTM1, which is subsequently deubiquitylated by USP15. Notably, SQSTM1 was downregulated in response to USP15 knockdown. The function of USP15-mediated deubiquitylation of SQSTM1 allows for vesicle release to the cell periphery (Jongsma et al., 2016).

4.3.3.1 REST and the Proteasome

The proteasome is a multi-subunit complex which regulates ATP-dependent degradation of proteins. The downregulation of proteasome subunits is counterintuitive to a loss of REST-mediated repression of mRNA, although 12 proteasome subunits were part of the A549 REST cistrome (Rockowitz et al., 2014). The transcriptional regulation of the proteasome subunits are regulated by anti-oxidant response elements (ARE), which are target binding sites for transcription factors Nrf1 and Nrf2. Nrf1 and subsequently proteasome subunits are regulated by USP15 (Fukagai et al., 2016), although no notable change in proteasome subunits were found in response to USP15 knockdown. Interestingly Nrf1 (NFE2L1) was also amongst the REST cistrome in A549 cells (Rockowitz et al., 2014). The decrease in proteasome subunits identified here may imply an interplay of REST and Nrf1 responsive genes.

4.3.3.2 REST and/or USP15 Responsive Proteins

Apoptosis-associated proteins that were responsive to either REST and USP15 included a marked upregulation of EGFR, which was investigated by western blotting in relation to actin-cytoskeletal proteins. Studies have suggested a potential role for REST in suppression of apoptosis or anoikis (Lu

et al., 2014, Westbrook et al., 2005, Baiula et al., 2012). In this context, the signalling pathway appears to be enriched for USP15-responsive proteins. USP15 has also been associated with apoptosis mediated by stabilisation of caspase-3 (Xu et al., 2009b). Amongst the downregulated proteins included SQSTM1, superoxide dismutase 2 (SOD2), pro-apoptotic BAX. USP15 has previously been associated with the regulation of Nrf2-Keap1 (Villeneuve et al., 2013). Although involved in apoptosis these proteins do not appear to form a cogent pathway for modulation.

REST has previously been associated with GTPases due to their role in the regulation of neurosecretion. In particular, RAB3B significantly upregulated by both knockdown of USP15 and REST, is involved in synaptic vesicle (SV) exocytosis (Binotti et al., 2016). It should be noted that RAB3B, was also identified in the REST cistrome of A549 cells (Rockowitz et al., 2014). Interestingly, amongst these RAB27B, which is also proposed to have a role in the recycling of SVs was significantly downregulated by USP15, but not by REST. This would appear to demonstrate that although USP15 and REST may share a pro-secretory role, REST alone promotes recycling. Although not followed up with further studies, these primary data would appear to suggest a novel role for REST and USP15 functions in the promotion of neuroendocrine cell exocytosis.

4.3.4 REST and USP15-Dependent Actin Cytoskeletal Proteins

From the data I identified integrins, extracellular matrix binding proteins, that co-ordinate with receptors to regulate mitogen signalling as well as regulating the cellular death programme of anoikis (Gilmore, 2005). The regulation of these proteins was interesting due to previous association of loss of tumour suppressive REST in anchorage-independent growth and evasion of anoikis (Westbrook et al., 2005).

REST regulation of integrins, as determined from the cistrome, implicates regulation of alpha and beta integrins (A3, A9, B1, B5, B8)

(Rockowitz et al., 2014). The increase in ITGB1 which was noted here, again is counter intuitive to REST-mediated repression of mRNA. These data would appear to suggest that the characterisation of REST regulated transcripts by interaction at the gene is not sufficient to determine the extent of protein expression. The capacity of REST to regulate primary signalling molecules is perhaps overlooked and contribute to signalling, that together with co-ordinated changes of apoptotic associated proteins allows cells to overcome anoikis.

4.3.5 The USP15-Dependent Proteome

The role of USP15 in regulating REST re-expression was presumed to encourage dysregulation of REST responsive genes. As a target of USP15-mediated regulation under basal conditions, REST was proposed to act as a positive control of a classical knockdown (Faronato et al., 2013), however, it was not detected by MS. The loss of USP15, unlike REST is not expected to demonstrate a clear characteristic, due to its involvement in a myriad of signalling pathways. Notably, the most prominent protein changes following USP15 knockdown were associated with the mitochondria and will be explored in further detail in Chapter 5.

USP15 regulation of actin-cytoskeletal proteins can be inferred from changes in mitogen signalling (Buus et al., 2009, Faronato et al., 2013, Hayes et al., 2012, Eichhorn et al., 2012, Herhaus et al., 2014), although a demonstration of direct deubiquitylation by USP15 has not previously been described. Importantly the regulation of protein function by USP15 is not limited to post-translational degradation, with co-translational regulation of protein expression and regulation of the ubiquitin code. Here, I chose to investigate the expression of EGFR and VCL proteins following USP15 depletion as a means of identifying novel proteins and pathways that it regulates. Although, the actin-cytoskeletal changes that appeared promising from the proteomic analysis were not conclusive in later western blotting.

Parallel to this proteomics approach USP15 was identified in a cellular phenotype assay, and proteomic data was investigated to isolate potential proteins of interest. The USP15-mediated regulation of one such protein has since been recapitulated by members of the laboratory and forms the molecular basis that contribute to cellular behaviour (Fielding et al., manuscript in preparation). This success demonstrates the capacity of this technique in investigating the regulation of a protein without prior knowledge of the protein target in question. USP15 roles in mitochondrial function explored in Chapter 5.

CHAPTER 5: THE USP15-MEDIATED REGULATION OF MITOCHONDRIAL PROTEINS

5.1 The USP15-Mediated Regulation of Mitochondrial Proteins

5.1.1 The Mitochondria

The mitochondria, a double membraned organelle that is inherited maternally, contains mitochondrial DNA (mtDNA). Many of these mitochondrial encoded genes are dedicated to the production of energy from aerobic respiration via the oxidative phosphorylation. The mitochondria also act as a subcellular store of Calcium (Ca^{2+}), produce reactive oxygen species and release cytochrome c (Cyt c) during apoptosis (Garrido et al., 2006). The dysfunction of the mitochondria has also been associated with a variety of pathologies including cancer (Giampazolias and Tait, 2016, Zong et al., 2016).

The mitochondrion acts as a cellular powerhouse, in which adenosine diphosphate (ADP) is converted into adenosine triphosphate (ATP) through the addition of a phosphate group. ATP acts as the energy currency of the cell, which allows the cell to perform unfavourable chemical reactions. Aerobic respiration generating ATP from glucose, a common source of stored chemical energy, requires cytoplasmic and mitochondrial reactions of glycolysis and the Krebs cycle, respectively. These processes generate reduced forms of nicotinamide adenine dinucleotide (NADH), which are subsequently oxidised to release electrons that power the electron transport chain (ETC). The ETC is the site of oxidative phosphorylation.

5.1.2 The Electron Transport Chain Complexes

The ETC consists of five multi-subunit complexes that function to generate the mitochondrial membrane potential (Figure 5.2). Complex I, is a composite of nuclear and mitochondrial encoded proteins. At Complex I, NADH is oxidised transferring protons to the prosthetic group reducing Flavin mononucleotide (FMN) to $FMNH_2$. The electrons are transferred through the complex by Iron – Sulphur (Fe-S) clusters, whilst four protons transverse the

membrane, leading to the reduction of ubiquinone (Q) to ubiquinol (QH_2) within the membrane. Complex II, is an alternative site of entry into the electron transport chain in which succinate is reduced to fumarate and oxidises Q, although to a lesser extent than Complex I. Complex III oxidises ubiquinol and reduces the heme containing protein Cyt c allowing for the transfer of protons across the membrane. At Complex IV, protons are removed from Cyt c and transferred to oxygen (O_2) to produce water (H_2O). The cumulative effect of these four complexes is the removal of protons from the mitochondrial matrix, which generates the gradient required to power Complex V. Complex V, F_oF_1 ATP synthase, consist of a channel (F_o) which rotates with the down-gradient flow of protons, and powers ATP synthase (F_1) catalysing the addition of a phosphate to ADP to produce ATP.

5.1.3 Mitochondrial Protein Regulation

The expression of mRNA encoding mitochondrial proteins are regulated by transcription factors, both mitochondrial-specific and nuclear factors that localise to the mitochondria (Szczepanek et al., 2012, Bestwick and Shadel, 2013). In addition to mitochondrial proteins, nuclear encoded proteins are regulated by shared pathways that allows for a co-ordinated response. Nuclear encoded proteins classically contain an N' terminal mitochondrial target sequence (MTS). This pro-sequence allows the protein to be transported through the outer mitochondrial membrane transporter (TOMM).

The roles of deubiquitylases in the regulation of the mitochondria have focused primarily around the regulation of inducing apoptosis and mitophagy. Interestingly, USP15 is known to associate with the mitochondria at the TOMM complex (Cornelissen et al., 2014). The function of USP15 has been proposed to regulate mitophagy, a feature that is thought to be regulated by other deubiquitylases (Durcan and Fon, 2015, Liang et al., 2015). In this chapter, I would like to address the findings from the proteomic analysis that implicates a role of USP15 in the routine role of regulating expression of proteins and ultimately energy production capacity of the mitochondria.

5.2 Response of Mitochondrial Proteins and Processes to USP15 and/or REST Depletion

Mitochondrial proteins were significantly enriched as determined by GO analysis of responsive proteins to siUSP15 or siREST knockdown (Chapter 4, Figure 4.6A). I identified 60 proteins in the 'Mitochondria' category responsive to either USP15 or REST knockdown (Figure 4.7E). This 'Mitochondria' collated category includes GO terms such as mitochondrion, mitochondrial envelope and mitochondrial respiratory chain. The response of proteins, within the specific mitochondrion GO term (GO:0005739), following either USP15 or REST depletion are plotted against the background of the broader 'Mitochondria' category (Figure 5.1). Interestingly, of the proteins associated with the mitochondrion term only ATP6 is encoded by the mitochondrial DNA. In total, I identified 39 proteins from the specific mitochondrion GO term by mass spectrometry. 20/39 (51%) decreased in response to USP15 depletion. Interestingly, the expression of 11 (28%) proteins were significantly changed by USP15 depletion, nine (23%) of which were decreased. Five (13%) mitochondrion proteins increased in response to USP15 depletion, of which two (5%) were significant. The response of mitochondrion proteins to REST depletion resulted in a total of 19 (48%) protein changes, 15 (38%) of which decreased, with eight (20%) of these being significant.

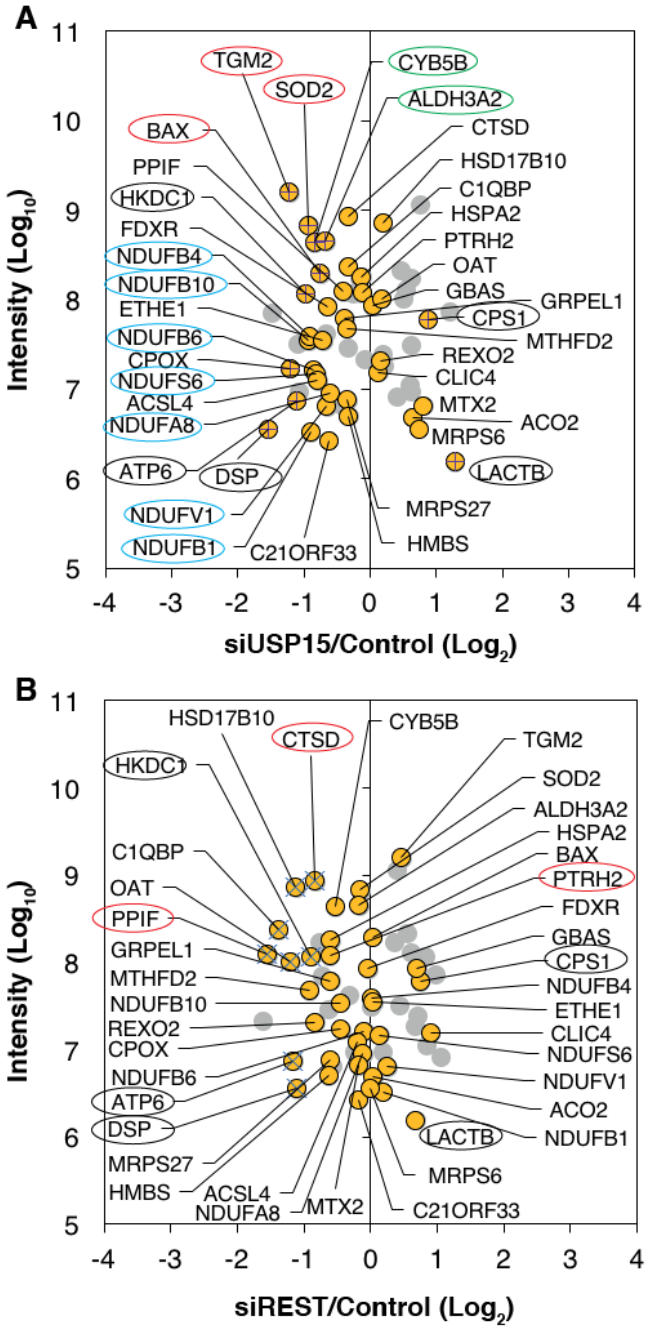

Figure 5.1. The Mitochondrion Protein Response to siRNA knockdown
The expression of mitochondrion proteins (yellow circles) derived from the GO term (GO:0005739) following knockdown of either (A) siUSP15 or (B) siREST. The scatter plot of mitochondrion proteins, Log(2) Ratio vs Log(10) Intensity, was created from 'ALL' analysis. Significant proteins, as determined by Significance B are highlighted as; + siUSP15, x siREST. Background data points are of the 'Mitochondria' group of proteins (grey circles, Figure 4.7). Common changes (black circles), Apoptosis-related proteins (red circles), NDUF family of proteins (blue circles), Energy-related proteins not involved in electron transport chain (green circles).

Five proteins were responsive to USP15 and REST depletion (Figure 5.1, black circles). ATP6, DSP and HKDC1 significantly decreased in both conditions. CPS1 and LACTB were increased in response to REST depletion and significantly so upon USP15 depletion. Upon further research into the biology of desmoplakin (DSP), and hexokinase domain-containing protein 1 (HKDC1) both have little evidence to support a mitochondrial association. ATP6, a mitochondrial encoded subunit of the electron transport chain, will be discussed later in the context of electron transport chain complexes (Chapter 5, Section 2.3). CPS1, Carbamoyl-Phosphate Synthase 1 localises the mitochondria and encodes a protein involved in the urea cycle (Uniprot, http://www.uniprot.org/uniprot/P31327). LACTB, lactamase beta is a filament forming protein that is abundant within the mitochondrial intermembrane space (Polianskyte et al., 2009). It was suggested that LACTB may influence sub-mitochondrial structure. These data demonstrate that both USP15 and REST knockdown influence the abundance of certain mitochondrial proteins in the same way. This may indicate shared regulation or that these were an off-target of siCon1-treated cell line.

I noticed that several of these proteins belong to the NADH:ubiquinone oxidoreductase (NDUF) family (Figure 5.1, blue circles) and are functionally related. As such, I decided to subgroup these proteins based on similar or related function by comparing them to the biological process and molecular function GO term analysis (Chapter 4). Interestingly, the mitochondrion term includes 19 proteins that are also shared with the 'Energy' category of proteins, as well as six proteins previously associated with the 'Apoptosis' category. I decided to investigate the specific proteins within these terms and their relationship between these proteins and the response to REST or USP15 depletion.

5.2.1 Identifying Biological Processes of Mitochondrion-based siREST Responsive Proteins

In the collated 'Mitochondrial' category REST depletion resulted in a decreased expression of 20 proteins (Figure 4.7F), of which 15 belong to the specific mitochondrion GO term (Figure 5.1B). REST depletion resulted in fewer protein changes than USP15 depletion and identified only five REST responsive 'energy'-related proteins. These five 'energy'-related proteins were: ATP6, CPS1, HKDC1, HSPA2 and MTHFD2. Of these five proteins CPS1 increased in response to REST depletion, whilst the other four proteins decreased (Figure 5.1B). Of these five proteins, only HSPA2 and MTHFD2 were responsive only to REST depletion, neither of which were significant. HSPA2 was associated with the energy category due to the inclusion of an ATP binding term. Whilst, MTHFD2 has oxidoreductase activity, which could transfer electrons to NAD or NADP. These few protein changes do not demonstrate a co-ordinated protein change within a biological process. In order to ascribe processes, I attempted gene ontology of mitochondrion protein responsive to REST depletion. This analysis suggested roles for REST regulation of ATP biosynthesis, response to amino acid or zinc and cellular response to Ca^{2+} ions. These processes however, are identified by only two proteins and are greatly influenced by the presence of a single protein, for example, ATP biosynthesis annotation is dependent upon ATP6. Response to amino acid or zinc mediated by HMBS and CPS1, with cellular response to Ca^{2+} ions mediated by PPIF and CLIC4. Together these data do not provide strong evidence for REST in the regulation of mitochondrial energy production.

REST depletion did not have a significant enrichment of protein associated with apoptosis (Chapter 4). Gene ontology comparison of the siUSP15 or siREST responsive mitochondrion proteins with the apoptotic category, identified six proteins (Figure 5.1, red circles). Of these six proteins, PPIF, CTSD and PTRH2 were responsive to REST depletion. Interestingly all three proteins decreased upon REST knockdown with PPIF and CTSD significantly decreased (Figure 5.1B). These protein changes may suggest

that downstream signalling of REST has a role at the mitochondria that is distinctively different from that of USP15.

5.2.2 Identifying Biological Processes of Mitochondrion-based siUSP15 Responsive Proteins

Of the 19 mitochondrion proteins I identified that are involved in 'Energy', 17 were responsive to USP15 depletion. USP15 depletion resulted in the decrease of 15 mitochondrion-targeted energy proteins. The majority of siUSP15 responsive mitochondrion-targeted proteins involved in energy were involved in the Electron Transport Chain (ETC), which will be discussed in more detail in Chapter 5, Section 2.3.

Two mitochondrion-energy proteins increased in response to USP15 depletion, ACO2 and CPS1, of which only CPS1 was significantly increased (Figure 5.1A). Excluding electron transport chain proteins, I also identified fatty aldehyde dehydrogenase (ALDH3A2) and Cytochrome b5 type B (CYB5B) as significantly decreased in response to USP15 depletion (Figure 5.1A, green circles). These two proteins, are associated with the oxidation-reduction process. ALDH3A2 is involved in the generation of NADH from the metabolism of fatty acids (Uniprot, http://www.uniprot.org/uniprot/P51648). CYB5B is an electron transporter within a complex involved in lipid metabolism (Neve et al., 2012) and N-reductive drug metabolism (Jakobs et al., 2014). These proteins were significantly changed in response to USP15 depletion and provide the first evidence of USP15-mediated regulation of metabolism.

Of the six mitochondrion-apoptotic proteins identified, three were siUSP15 responsive proteins: BAX, SOD2 and TGM2, with all three significantly decreased upon USP15 depletion (Figure 5.1A, red circles). Interestingly, SOD2 and TGM2 were also associated with energy terms. SOD2 and TGM2 were amongst the most prominent USP15 depletion responsive proteins decreasing by 1.9-fold and 2.3-fold, respectively (Supplementary Table 1). Further investigation and validation of USP15-mediated regulation of

these proteins will be required to demonstrate a novel role for USP15 in regulating the sensitivity of apoptotic signalling.

5.2.3. The Electron Transport Chain Response to USP15 Depletion

5.2.3.1 ETC Complex I Proteins are Selectively Reduced by siUSP15

The most prominent group of proteins identified from cell compartment GO analysis (Figure 4.6A) also belong to the ETC GO term. The effect on the electron transport chain proteins was most marked in response to USP15 depletion. To visualise and summarise the effects of USP15 depletion I decided to map these protein expression changes to the cellular pathway using Pathvisio (Chapter 2, Section 4.2). The ETC process, is enacted by mitochondrial membrane bound protein complexes (Figure 5.2A). The release of H^+ protons, from NADH or succinate sources, are utilised to form the mitochondrial proton gradient (ΨM) for ATP synthase, resulting in ATP production. Proteomic data (Chapter 4) was overlaid upon publically available cellular pathway maps, that provide an overview of the components within the protein complexes and the protein level changes in response to USP15 depletion (Figure 5.2B).

The protein changes in response to USP15 depletion are not represented equally across the ETC complexes. Proteomic analysis identified 16 Complex I subunits all of which were nuclear encoded proteins. Interestingly, these proteins demonstrate a concordant decrease with siUSP15 (Figure 5.2B). These Complex I subunits will be discussed in greater detail in Chapter 5, Section 3.2. In contrast, USP15 depletion does not result in differential expression of Complex II subunit proteins (Figure 5.2B). Together Complex I and II are the primary protein complexes that supply electrons to the ETC. The data would appear to indicate that Complex I is selectively influenced by USP15 depletion.

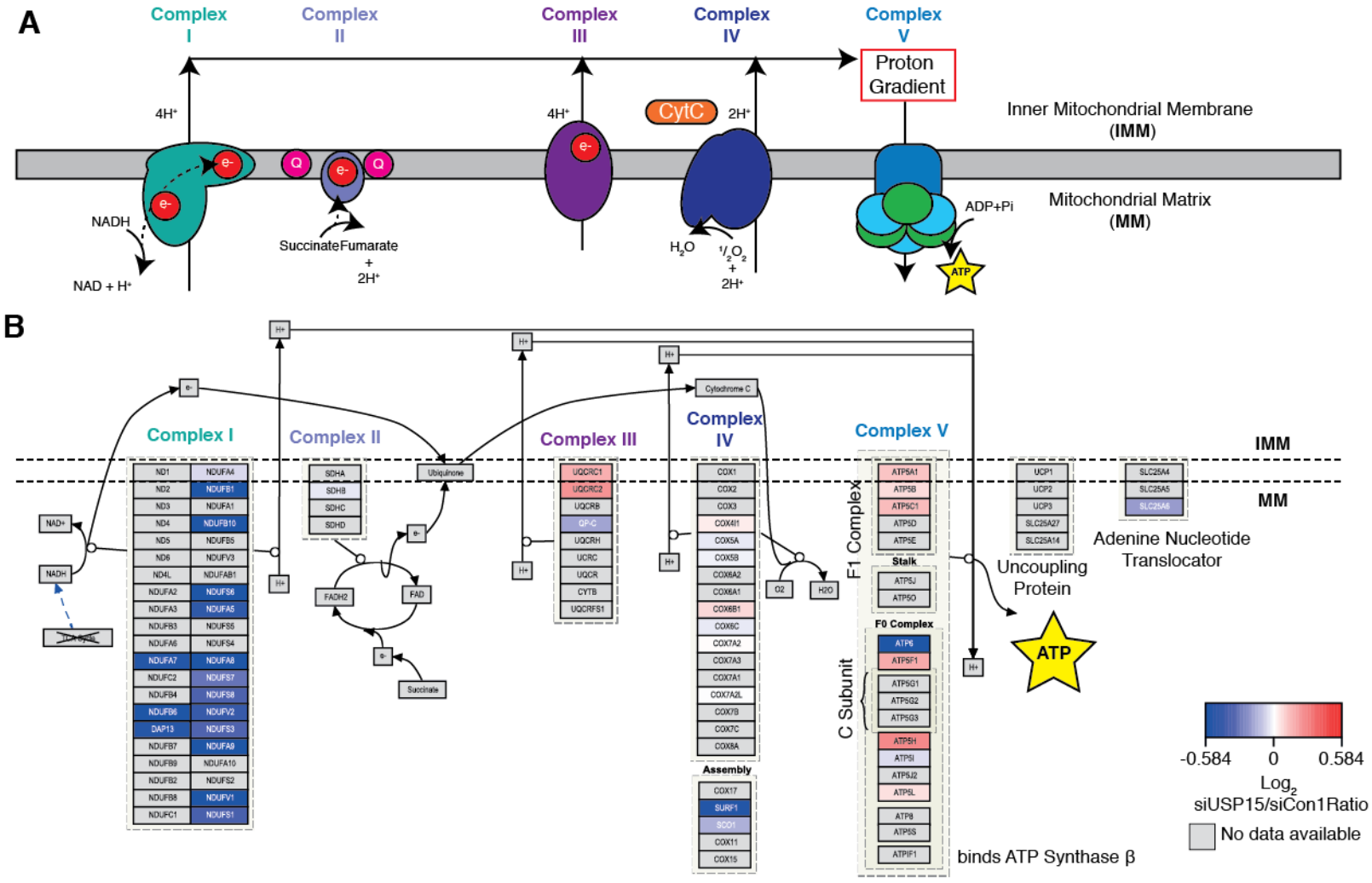

Figure 5.2. The Electron Transport Chain (ETC)

Figure Legend Overleaf

Figure 5.2. The Electron Transport Chain (ETC)
(A) The ETC is the site of oxidative phosphorylation resulting in the generation of ATP, which is driven by a proton gradient between the Inner Mitochondrial Membrane (IMM) and the mitochondrial matrix. A series of protein complexes are embedded in the membrane, with Complex I, II, III and IV involved in the generation of the proton gradient, when utilised by Complex V induces phosphorylation. **(B)** Overlaid upon the ETC pathway are the Log(2) M/L Ratio derived from the 'ALL' analysis (n=3). The colour scale for the pathway is based upon the 1.5-fold threshold as in previous experiments.

In addition, USP15 depletion increased expression of UQCRC1 and UQCRC2 (Figure 5.2B), core subunits of the Ubiquinol-Cytochrome C Reductase (Complex III), which utilises Ubiquinol, the electron dense form of Ubiquinone (Q), generated by either Complex I or Complex II. Conversely, the QP-C core subunit of Complex III decreased slightly. The proteins of Complex III do not demonstrate a concurrent change in response to USP15 depletion. USP15 depletion does not result in dramatic changes to the subunits of Complex IV (Figure 5.2B). Although SURF1, a nuclear encoded gene involved in the assembly of Complex IV was decreased in one technical replicate and did not surpass the 1.5-fold change threshold. Overall, I did not detect many proteins from Complex IV, and those identified demonstrated no clear directional change.

Lastly, USP15 depletion effects the ATP synthase Complex V (Figure 5.2B), which consists of two multi-subunit Complexes F0 and F1 that form the proton channel and catalytic core respectively. One of the most prominent changes within Complex V is that of ATP Synthase 6 (ATP6), a mitochondrial encoded protein, which decreased significantly in response to either USP15 or REST depletion (Figure 5.1). Conversely, I identified a slight increase in ATP5 subunits A1, B and C1 within the catalytic F1 Complex in response to USP15 depletion (Figure 5.2B). ATP5H and ATP5F1 subunits of the F0 Complex increase in response to USP15 depletion. These data demonstrate USP15 depletion has contrary changes on subunits of the ATP synthase. Additionally, USP15 depletion also results in a slight decrease in the SLC25A6 subunit of the adenine nucleotide translocator, involved in the exchange of cytoplasmic ADP for mitochondrial ATP.

These data suggest a novel and testable role for USP15 at the mitochondria. The decrease in Complex I subunit proteins are indicative of a novel role for USP15 in their co-ordinated regulation. I decided to select Complex I proteins for further study and investigate the impact of USP15 depletion upon the ETC process and subsequent energy generation.

5.2.3.1 Validation of siUSP15 Effect on Complex I Protein Expression

Mitochondrial Complex I is composed of mitochondrial and nuclear encoded proteins, which produce a membrane domain and a hydrophilic arm that extends into the mitochondrial matrix. The proteomic study did not identify any mitochondrial encoded Complex I proteins. The expression of the nuclear encoded mitochondrial Complex I proteins, the NADH:ubiquinone oxidoreductase subunits, from independent proteomic experiments were collated and compared in a heatmap (Figure 5.3A). Of the NDUF subunits identified, nine out of 18 were detected in at least two experiments. Most NDUF subunits are part of the hydrophilic arm of Complex I, including the core subunits NDUFS3 and NDUFS7. These core subunits, together with NDUFA9, which interacts with NDUFS7 and is involved in the NADH binding, were decreased in the ALL analysis (Figure 5.3A). These subunits tended to decrease in response to USP15 depletion in each biological experiment in which they were detected.

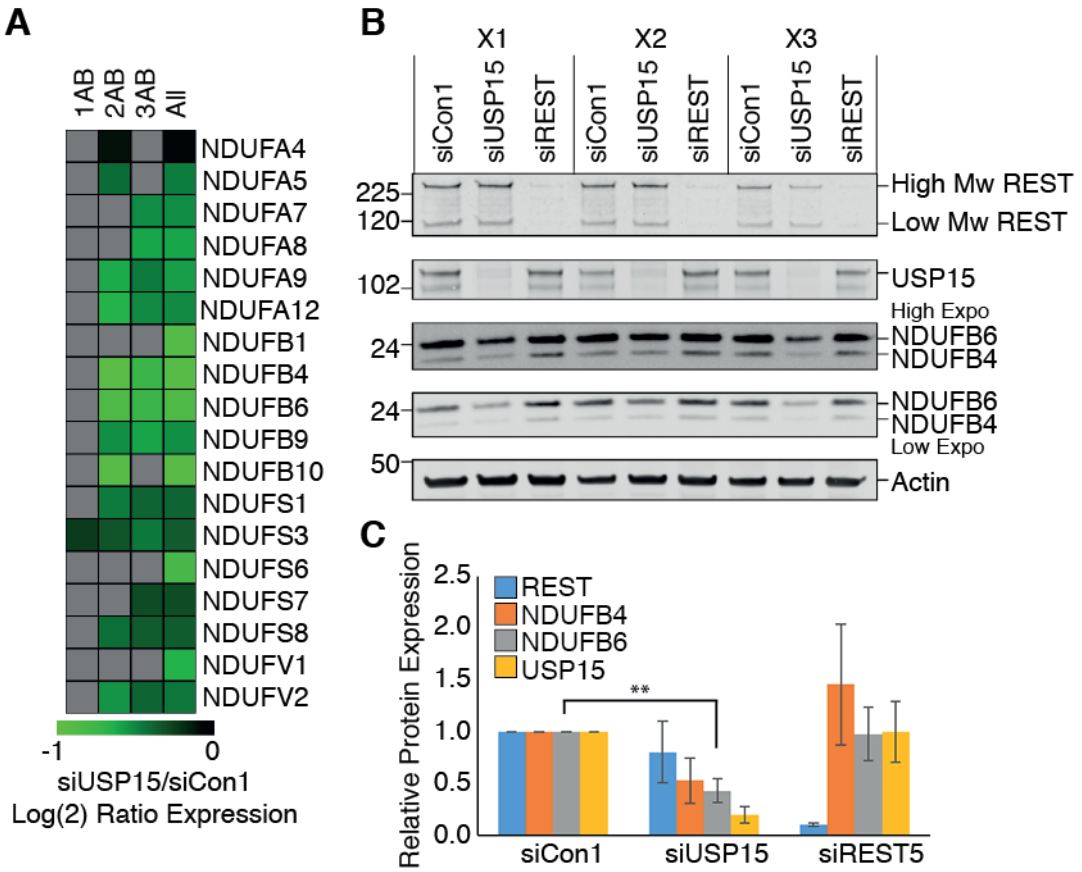

Figure 5.3. Validation of NDUF Protein Changes
(A) NDUF proteins were identified across biological (numbers) and technical (letters) replicates and 'All' analysis from mass spectrometry. **(B)** Western blotting of three biological replicates of siRNA knockdown with siCon1, siUSP15-Pool and siREST5. siUSP15-Pool and siREST5 treatments show a clear knockdown of their specific target. siUSP15-Pool also have an effect on the protein levels of NDUFB6 and NUDFB4 proteins. **(C)** siUSP15-Pool causes approximately a 50% reduction in both NDUFB4 and NDUFB6 protein, whilst siREST5 has no effect. Quantification of western blot (n=3), statistical significance was calculated using an ordinary one-way ANOVA, 95% confidence, with Tukey's post hoc test. * $P \leq 0.05$, ** $P \leq 0.01$.

The expression of NDUFB4 and NDUFB6, two of the most consistent and prominent responsive siUSP15 proteins, were selected for further validation. The expression of NDUFB4 and NDUFB6 proteins in the three SILAC-MS experiments was validated by western blotting (Figure 5.3B) and quantified (Figure 5.3C). The expression of NDUFB6 was significantly decreased in response to USP15 depletion. NDUFB4 expression also decreased in each case, although this did not reach statistical significance on quantification. Western blotting indicates that NDUFB4 expression did not decrease in experiment two, to the same extent as experiments one and three

(Figure 5.3B). Thus, based on an antibody method of detection expression of NDUFB6 decreases following knockdown with the siUSP15-Pool siRNA.

To demonstrate that this was an on-target effect, I performed western blotting for NDUFB4 and NDUFB6 in response to a series of control and targeting siRNAs (Figure 5.4A). USP15 and REST targeting siRNAs demonstrated a decrease in their respective target proteins (Figure 5.4B). Quantification of NDUFB6 expression was again significantly decreased in response to siUSP15-Pool (Figure 5.4C), which replicated the response seen in the SILAC samples (Figure 5.3). Both NDUFB4 and NDUFB6 protein levels were markedly decreased by siUSP15-2, however, siUSP15-1 and siUSP15-17 did not cause a significant decrease in NDUF protein levels (Figure 5.4C). siUSP15-1 clearly causes a decrease in USP15 protein levels, whilst siUSP15-17 was less efficient on average across three biological replicates (Figure 5.4B). In order to ensure that the response of the NDUF proteins were not an off-target effect of siUSP15-2, alternative siRNAs were also tested. I used two siRNAs that specifically target each of the USP15 isoforms, which when mixed as a pool (siUSP15-isoPool), should effectively reduce USP15 protein levels. The siUSP15-2 again resulted in a marked decrease of NDUFB6 and NDUFB4 proteins (Figure 5.5). siUSP15-isoPool markedly reduced of USP15 levels and phenocopied the effect of siUSP15-2 by decreasing NDUFB4 and NDUFB6 protein levels. In A549 cells, USP15 isoforms 1 and 2 were expressed at equal levels, as determined by qRT-PCR analysis (Chapter 3), however, western blotting demonstrates that isoform 1 is the major isoform. Knockdown of USP15 isoform 1 alone caused ~70% decrease in USP15 expression, resulting in a smaller but discernible decrease in NDUFB6. In contrast, knockdown of USP15 isoform 2 alone did not decrease USP15 expression and has no discernible effect on NDUF protein levels (Figure 5.5B). To assess the reduction the effects of USP15 on NDUF protein levels in an siRNA independent method, I performed western blotting of cell lysates from mouse embryonic fibroblast (MEF) cells with or without USP15 expression (Figure 5.5C). A549 treated with siUSP15-2 and siUSP15-pool were run as positive

control for NDUF protein decrease. As expected the expression of NDUFB4 and NDUFB6 were decreased upon siRNA knockdown of USP15 (Figure 5.5D). The expression of USP15 is lost from $USP15^{-/-}$ MEF cells, and results in a 60% reduction in NDUFB4 and 35% reduction in NDUFB6 relative to $USP15^{+/+}$ cells (Figure 5.5D). Protein expression of USP15 appear lower in $MEF^{+/+}$ than A549, whist NDUFB4 and NDUFB6 appear higher in both $MEF^{+/+}$ and $MEF^{-/-}$ cells relative to A549 (Figure 5.5C). It should be noted that these lysates are from different species and thus USP15 and NDUF antibodies may have a different affinity to the target proteins, as such it would be inappropriate to compare between cell lines. In either cell line, however, loss of USP15 does result in a decrease in NDUF protein levels (Figure 5.5D). Together, these data demonstrate that the decrease in NDUF protein expression is not an off-target effect of siUSP15-2, that was part of the pool used in the proteomic analysis. These data implicate Complex I protein changes, and as such the ETC, as a novel USP15 regulated physiological system (Figure 5.2).

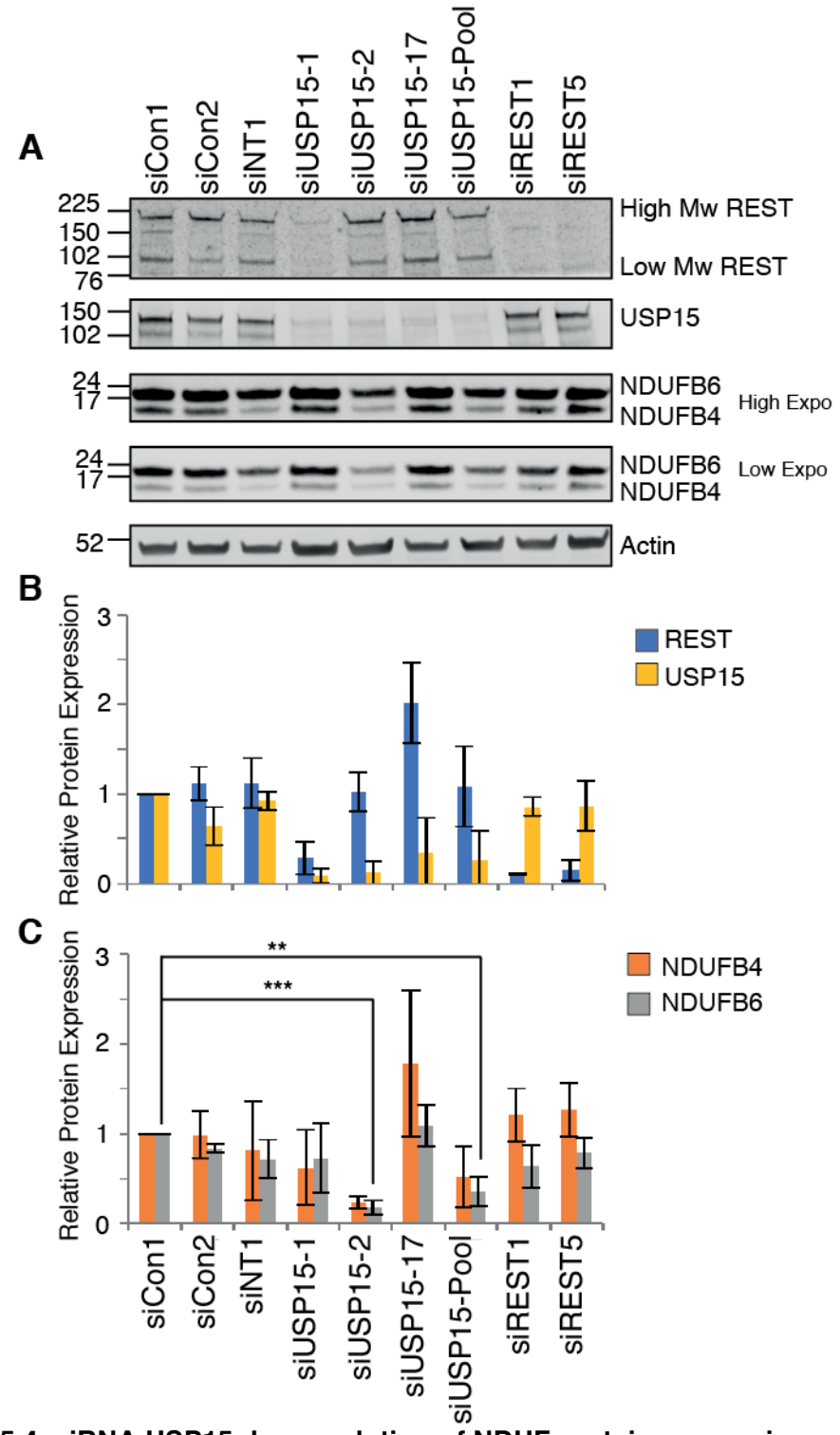

Figure 5.4. siRNA USP15 deconvolution of NDUF protein expression
(A) A representative western blot from three biological replicates of A549 cells treated with a selection of control, USP15 and REST siRNAs. **(B)** Quantification demonstrates USP15 and REST proteins are specifically targeted by desired siRNAs. **(C)** The expression of NDUFB4 and B6 proteins is responsive to the siUSP15-Pool and siUSP15-2 siRNAs. Statistical significance was calculated using an ordinary one-way ANOVA, 95% confidence, with Tukey's post hoc test. * $P \leq 0.05$, ** $P \leq 0.01$, *** $P \leq 0.001$.

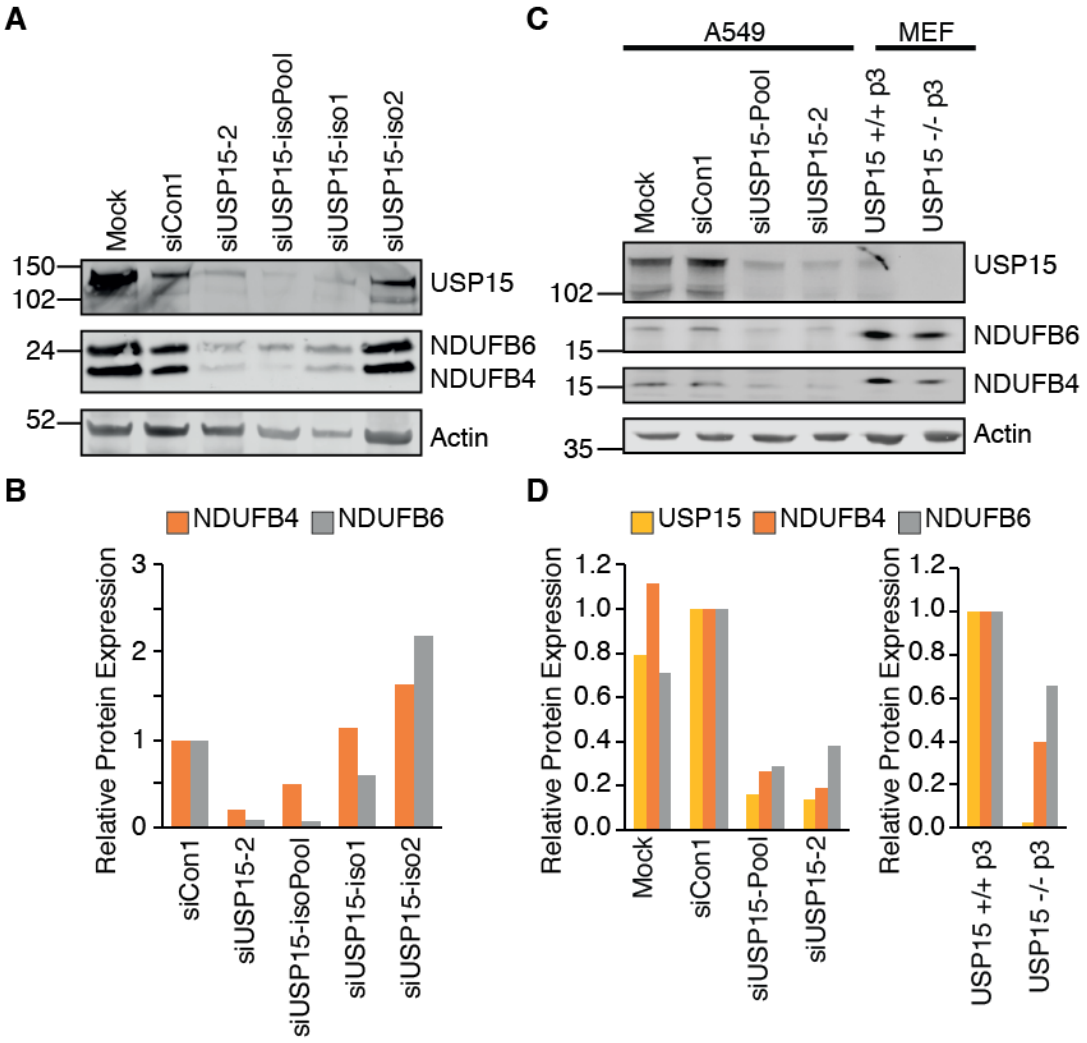

Figure 5.5. Validation of NDUF knockdown using isoform specific siRNA
(A) Western blot of A549 cells treated with control or USP15-targeting siRNAs, including isoform specific siRNAs pooled (siUSP15-isoPool) or separate (iso1, iso2). **(B)** Quantification of NDUFB4 and NDUFB6 proteins normalised to actin, made relative to siCon1. **(C)** NDUF expression in MEF cells **(D)** Quantification recapitulates reduced NDUF expression with siRNA, and NDUF reduction in long term USP15$^{-/-}$ cell line.

USP15 depletion may result in a reduced amount of Complex I. Based on NDUF protein expression data I hypothesised that functionally, this may lead to a decrease in the amount of Ubiquinol, the electron dense form of Ubiquinone (Q), generated from Complex I. I therefore predicted that this reduced flow of electrons would negatively impact upon the transfer of protons and thus the proton gradient (ΨM), causing a decrease in ATP generation. In order to investigate the effect of USP15 on the ETC, I decided to challenge cells with mitochondrial stressors using a commercially available cell-based test.

5.2.3.2. Bioenergetic Assessment of Cells in Response to USP15 Knockdown

The bioenergetics of cells can be investigated using the Seahorse Biosciences XF system, an in-well schematic diagram is presented in Figure 5.6A. The system produces measurements of the oxygen consumption rate (OCR) and extracellular acidification rate (ECAR), calculated from changes in the fluorescence from the oxygen and proton sensitive fluorophores, respectively. The 96-well plate cell assay allows for multiple biological conditions and technical replicates. For assays, cells are plated at a suitable density to ensure a confluent monolayer of cells, and are then treated via four drug ports with specific timed injections of Oligomycin A, FCCP, Rotenone and Antimycin A. These compounds result in the inhibition of mitochondrial complexes and uncoupling of the ETC (Figure 5.6B). The effects of these compounds on the OCR, can be used to calculate parameters of the ETC (Figure 5.6C). Firstly, the addition of Oligomycin A (Complex V inhibitor), inhibits the down-gradient movement of protons across the membrane and thus reduces the consumption rate from the basal respiration level (Figure 5.6C). The difference between the OCR pre- and post-Oligomycin can be used to calculate a value that reflects the ATP production of the mitochondria. Secondly, the addition of FCCP causes proton permeability of the inner mitochondrial membrane allowing for the movement of protons across the gradient ΨM. This induces the generation of ATP and results in a dramatic increase in consumption of oxygen (Figure 5.6C). The addition of Antimycin A and Rotenone, which inhibit Complex III and I respectively, reduce transport of protons across the membrane and terminate the supply of protons for ETC produced ATP. The difference between pre- and post-Antimycin A and Rotenone OCR provides a value that reflects the maximal respiration of the mitochondria (Figure 5.6C).

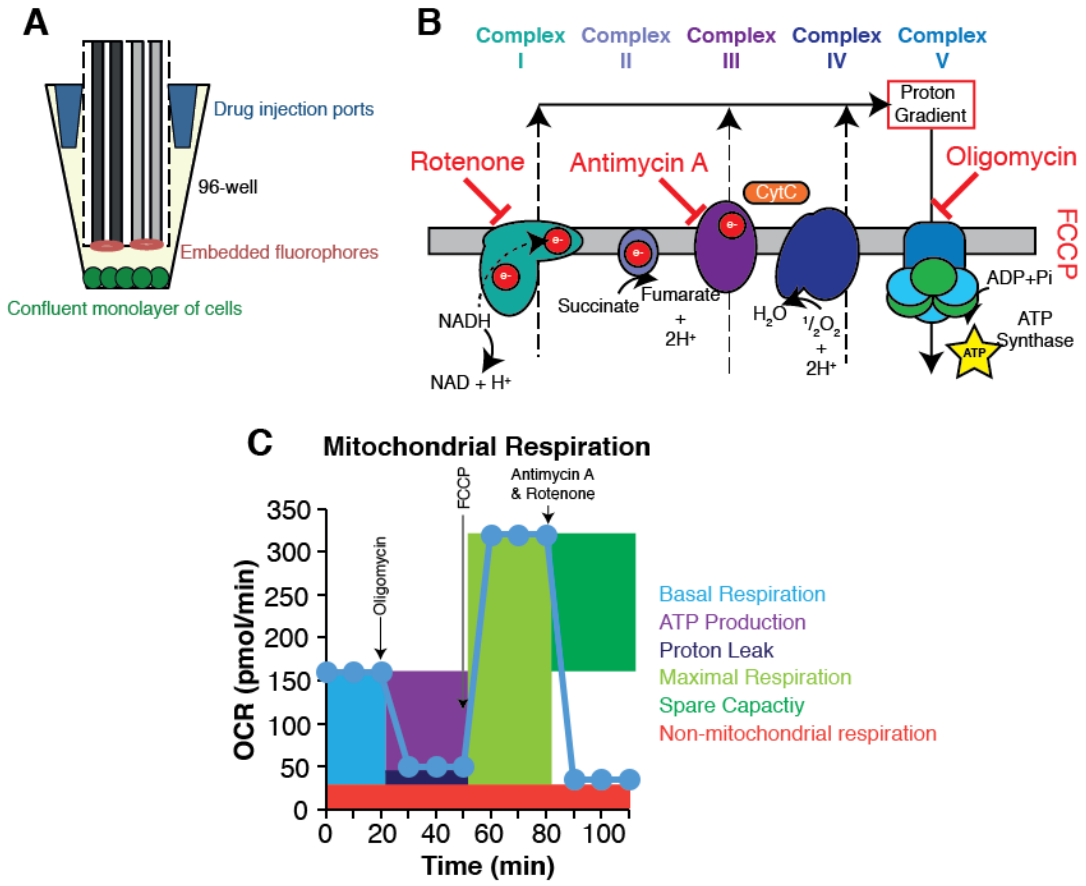

Figure 5.6. Seahorse System and the Mitochondrial Stress Test
(A) Cells are grown as a confluent monolayer for effective measurement of oxygen consumption rate and extracellular acidification. A sensor plate that contains the drug injection ports and fluorophores sits within the wells of the 96-well plate. **(B)** Inhibition of the electron transport chain using; Oligomycin, FCCP, Antimycin A and Rotenone, modifies the oxygen consumption rate (OCR). The OCR is measured by oxygen-sensitive fluorophores, and recorded in response to the addition of mitochondrial stressors. **(C)** An example line plot of OCR changes in response to inhibitors. These measurements can be used to calculate features of electron transport chain activity such as ATP production.

Optimisation of the mitochondrial stress test required the selection of the most appropriate cell density and the drug concentrations required for this density of cells. I began by establishing an optimal cell plating density for A549 cells. Cells were seeded as if for a Seahorse assay, but lysates were extracted and the protein concentration analysed (Figure 5.7A). Together with visual observation of the cells (Figure 5.7B), I was able to reliably plate a confluent monolayer of cells. I then used a selection of cell densities and subjected the monolayers to a range of drug concentrations (Figure 5.7C). The change in the oxygen consumption rate (OCR) was used to validate effective drug inhibition of the ETC complexes and also to determine the minimal drug

concentration required to induce sustained change in OCR. I selected 30 x 10^3 cells/well as the most appropriate cell seeding density. At this density the first injection A, 1.25μM of Oligomycin was required to produce a sustained decrease in OCR. At the second injection B, neither 0.25 μM or 0.75μM were capable of sustained increase in the OCR. At the third injection C, an additional 0.25μM of FCCP was added. This maximal concentration of 1μM of FCCP was determined to be the most effective for sustaining increased OCR. At the final injection D, a standard concentration of 1μM of Rotenone and Antimycin A was used to ensure effective termination of mitochondrial respiration.

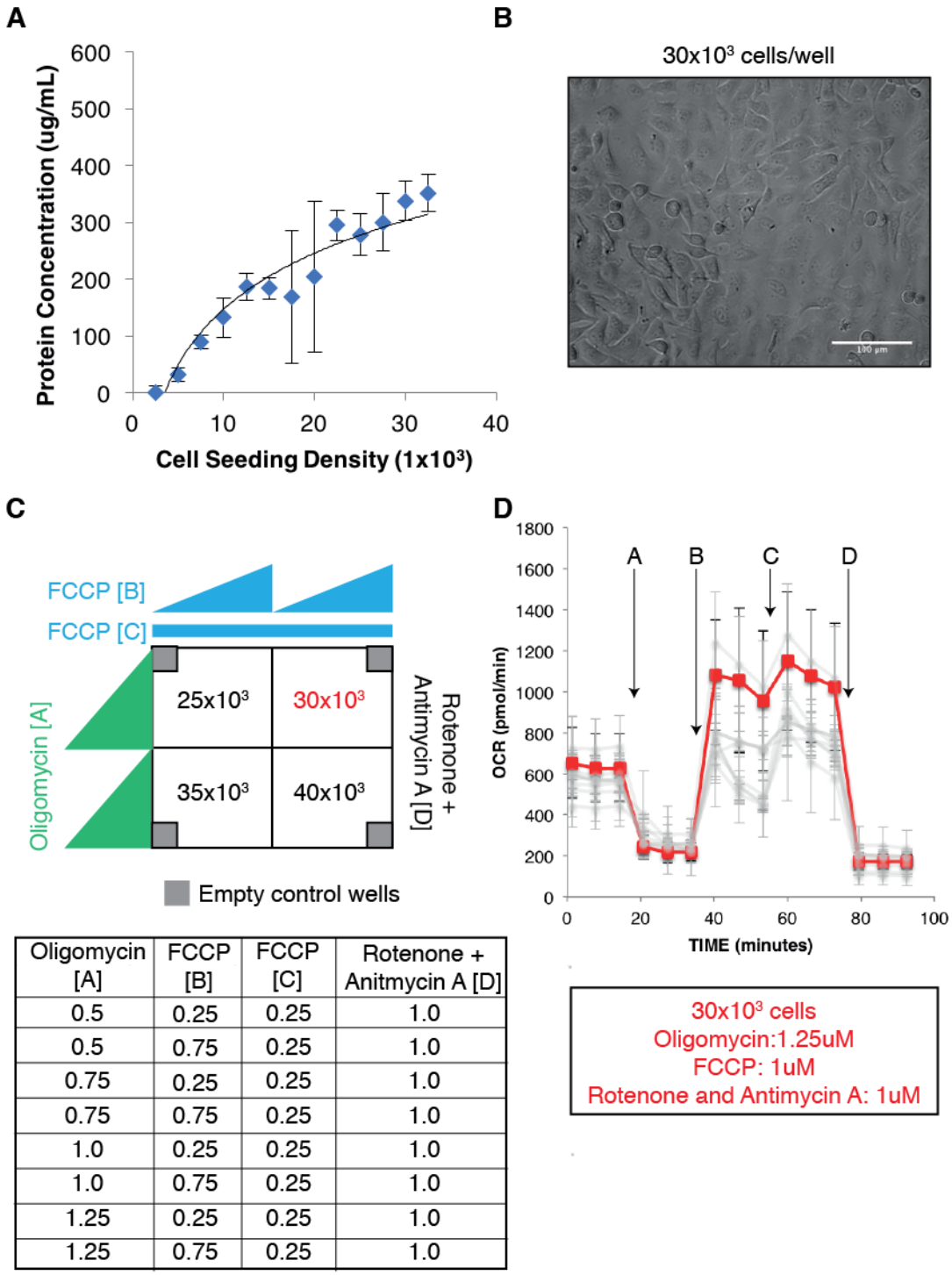

Oligomycin [A]	FCCP [B]	FCCP [C]	Rotenone + Anitmycin A [D]
0.5	0.25	0.25	1.0
0.5	0.75	0.25	1.0
0.75	0.25	0.25	1.0
0.75	0.75	0.25	1.0
1.0	0.25	0.25	1.0
1.0	0.75	0.25	1.0
1.25	0.25	0.25	1.0
1.25	0.75	0.25	1.0

Figure 5.7. Seahorse Optimisation

(A) A series of A549 seeding densities were plated and extracted after 24 hours from a XF96 well plate. The protein concentration was used to help to determine an optimal range for the MitoStress Test. **(B)** Bright field image of A549 cells 24 hours after seeding at 30x10^3 cells/well. **(C)** A mitochondrial stress regime of Oligomycin, Rotenone, Antimycin and FCCP was performed using different drug concentrations, under optimal seeding conditions. **(D)** The oxygen consumption rate profile of A549 cells in response to drug concentrations was used to identify the minimal concentration required to generate sustained effect on the OCR.

Upon USP15 depletion, and subsequent reduced expression of key NDUF proteins I predict this will cause a reduction in mitochondrial respiration, which would manifest as a decrease in oxygen consumption and perhaps a basal increase in the rate of glycolysis in the cells. The OCR and ECAR response was determined for A549 cells treated with control or targeting siRNAs, siCon1, siUSP15-Pool or siREST5. Untransfected A549 cells, of the same passage, were included to demonstrate that prior to siRNA treatment, cells respond to drug injections as expected. The cells were seeded 24 hours before the experiment in standard media, with all cells derived from a single dish and divided into the corresponding 96-well plate.

Initially the OCR and ECAR (Figure 5.8A and 5.8C), were calculated independently of the protein concentration, and were therefore 'unnormalised'. The siCon1 non-targeting siRNA did not cause any significant deviation relative to the OCR or ECAR of untreated A549 cells. Neither siRNA knockdown of USP15 nor REST caused a significant deviation from the OCR or ECAR profile. These unnormalised data assume that the number of cells remains consistent between experimental conditions. To ensure that the data were not influenced by siRNA induced differences in cell number at the time of the assay, I normalised OCR and ECAR (Figure 5.8B and D), using the protein concentration from each well as determined at the end of the analysis by BCA assay. The normalised data recapitulates the result for unnormalised values, with no significant difference of the OCR and ECAR profiles in response to either USP15 or REST depletion. These data demonstrate that the OCR and therefore ATP production were not significantly affected under normal media conditions (high glucose, 4mg/mL), following USP15 depletion. These data suggest that the effects of USP15 depletion on the ETC are subtler than expected and have no direct effect on ATP production in high glucose conditions.

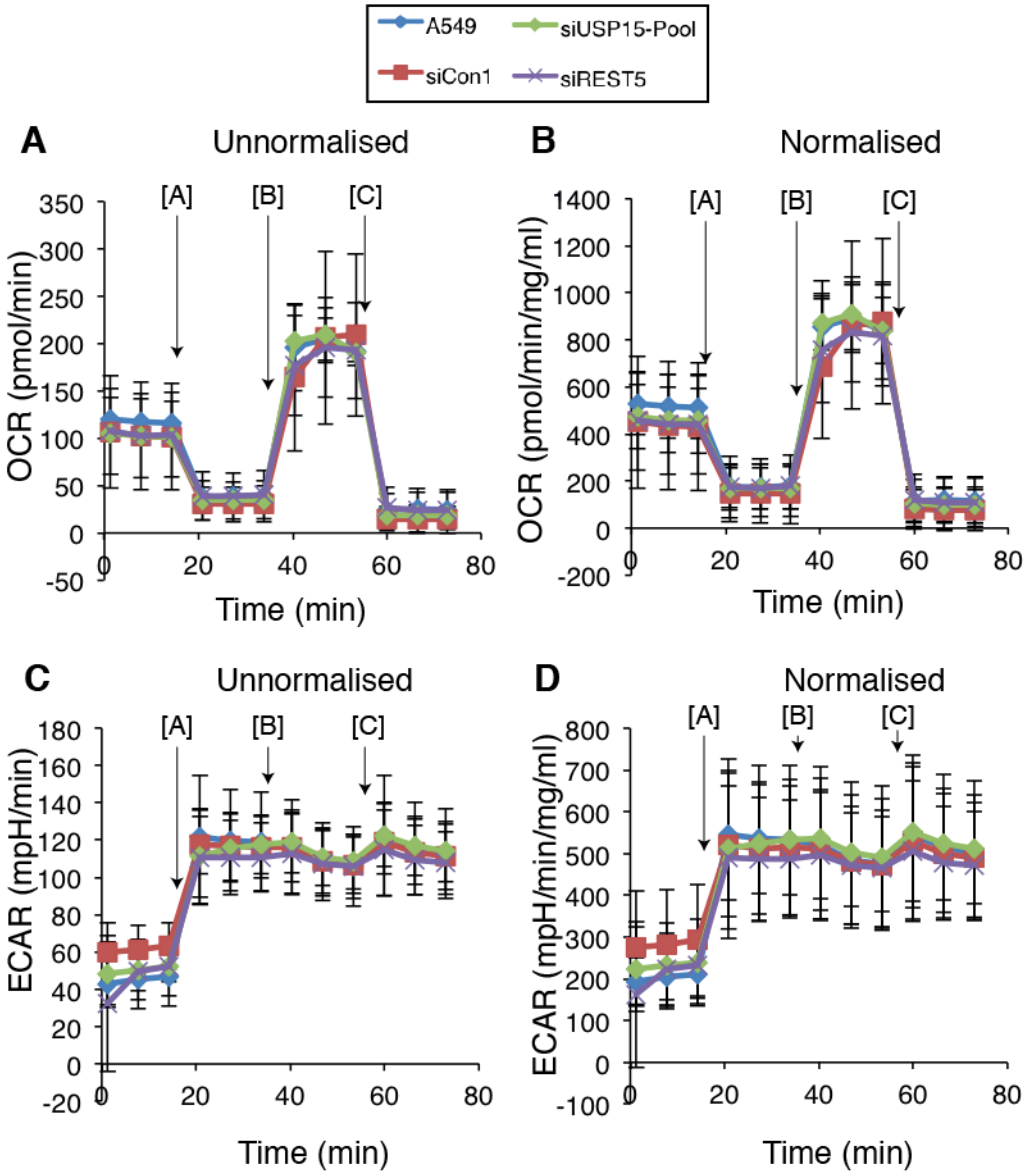

Figure 5.8. siRNA knockdown effects on Mitochondrial Stress Test
The knockdown of siUSP15 or siREST5 does not appear to have an effect on either **(A-B)** the oxygen consumption rate (OCR) or **(C-D)** the extracellular acidification rate (ECAR) of the A549 following siRNA treatments. Data points are by colour A549, siCon1, siUSP15-Pool and siREST5. Data represent the average of **(A,C)** unnormalised or **(B,D)** normalised values from (n=3) biological replicates. Error bars are standard deviations of the mean values from biological replicates.

In conclusion, I began to expand the diversity of USP15 regulated proteins and processes (Figure 5.1-5.2), with emphasis on the mitochondrial proteins subject to USP15-dependent regulation. I demonstrated that the NDUF family of nuclear encoded mitochondrial Complex I proteins are affected at the protein levels by loss of USP15 expression using siRNA and knockout cell lines (Figure 5.3-5.5). I optimised and attempted to address the

physiological consequences of these protein changes by performing an *in vitro* electron transport chain study (Figure 5.6-5.8). Although USP15 depletion was unable to detectibly alter mitochondrial respiration under normal conditions, I presume that compensatory mechanisms must be at work to sustain cells.

5.3 Discussion

Proteomic analysis revealed mitochondrial protein changes in response to REST and USP15 knockdown. Of these the nuclear-encoded NDUF proteins that constitute the mitochondrial matrix orientated arm of Complex I, were specifically and concertedly downregulated by depletion of USP15 (Figure 5.2). NDUFB4 and NDUFB6, which were consistently downregulated in replicate proteomic analyses were chosen as surrogates for Complex I. NDUFB6 was significantly downregulated as confirmed by multiple siRNAs targeting USP15 (Figure 5.4). Although NDUFB4 was not significantly decreased by siRNA deconvolution of the original USP15 siRNA pool, an independent pool of siRNAs targeting both USP15 isoforms, and siRNA-independent analysis of USP15$^{-/-}$ MEF cells, recapitulated the downregulation of NDUF proteins (Figure 5.5C). I hypothesised that the loss of USP15-dependent regulation of the NDUF proteins of Complex I could dysregulate the ETC. My preliminary data, however, did not appear to demonstrate a significant dysfunction in the activity of complexes within the ETC (Figure 5.8).

5.3.1 Complex I Dysfunction and NDUF Proteins

The data generated by proteomic analysis led to the hypothesis that ubiquitylation, and the DUBs USP15, are potential regulators of the ETC. The dysfunction of ETC has been associated with a variety of pathologies (Alston et al., 2017). Here, I will outline data relating to the expression of NDUF proteins and their association or contribution to pathologies. The activity of Complex I, due to the oxidoreducates capacity of its subunits influences the ratio of NAD/NADH (Zhu et al., 2016). Interestingly the expression of NDUF proteins, and their influence on the ETC, the NAD/NADH ratio and the activity of the sirtuin HDACs are of interest to the study of aging. A specific reduction

in the expression of NDUF proteins was shown to be a characteristic of long-lived mice (Miwa et al., 2014). The mechanism and specific role of ubiquitin-dependent regulation of these proteins is however is limited.

At a molecular level, an RNA interference screen of mitochondrial proteins in cells which alter ATP levels demonstrated different responses depending upon the type of fuel (Lanning et al., 2014). These data suggest that the influence of Complex I on the generation of ATP levels is more crucial when cells are provided with pyruvate of glutamine. The downregulation of NDUF proteins by USP15 in cells supplied with these fuels, rather than high glucose, might demonstrate a more notable difference in the generation of ATP. Currently, the downregulation of NDUF proteins does not appear to support reports that NDUFB6 was proposed to directly modulate the function of Complex I (Loublier et al., 2011).

Interestingly, the downregulation of NDUFB6 gene locus, 9p24.1-p13.3 has been implicated as an indicator of clear cell renal carcinoma (CCRC) survival (Narimatsu et al., 2015). In a cell line model, the downregulation of NDUFB6 by siRNA did not alter migration, but did result in increased cellular proliferation. The proposed regulation of NDUFB6 protein levels by USP15 would suggest that USP15 inhibition could modulate cellular proliferation in a CCRC cell line. To date these experiments have not been performed. The consequences of USP15-mediated regulation of cellular proliferation would add to the multiple mechanisms through which USP15 behaves as a tumour suppressor in this context.

The data generated in this chapter demonstrate that despite reduced levels of NDUF proteins, no noticeable dysfunction in the ETC was observed. These data appear to challenge the hypothesis that USP15-dependent regulation is important for the ETC or mitochondrial function. Discrepancy between the proposed hypothesis and the data could potentially be accounted for by: (1) the concentration of NDUF proteins not being limiting or limited

demand (2) compensatory actions of other related DUBs in the absence of USP15 or (3) that ubiquitylation-dependent regulation is not required under basal conditions. Further experiments should be performed to test the contribution of ubiquitin-dependent regulation before discarding the proposition.

The full complement of Complex I requires enough nuclear-encoded proteins to contribute to the assembled complex. The partial downregulation of NDUF proteins, may not be sufficient to inhibit complex formation and function. The reduction in NDUF levels following USP15 depletion does not affect complex function and presumably does not limit complex assembly. Depletion of USP15 downregulates total NDUF proteins, although presumably a mitochondrial fraction separate from ubiquitin-mediated regulation could be sufficient for Complex I formation and function. This could suggest that USP15 knockdown alone is not sufficient to limit expression or mitochondrial localisation of NDUF proteins. To account for potential compensatory actions of DUBs a broader DUB inhibition may lead to catastrophic loss of NUDF proteins and demonstrate Complex I dysfunction.

Importantly, the work presented here was performed in high glucose media. Under basal condition demand for ubiquitin-dependent regulation of NDUF proteins is not detrimental to Complex I assembly and function. The efficiency of ubiquitin-dependent regulation of NDUF proteins of Complex I may be exacerbated by cellular signalling or stressors. The conditions that require more stringent regulation of ubiquitin-dependent regulation of NDUF protein levels could also provide novel insight into the activity of E3 ligases. Additionally, the consequences of reduced NDUF proteins may affect other mitochondrial functions that have not been assessed by this methodology, such as the production or response to reactive oxygen species.

5.3.2 Potential Mechanisms of DUB Mediated Regulation of Mitochondrial Function and Proteins

Here, I will outline the role for ubiquitin-dependent regulation of mitochondrial function and briefly discuss the mechanisms and any supporting evidence for DUBs and/or USP15 in this process.

Nuclear and cytosolic functions of DUBs can influence mitochondria function through regulation of signalling. These effects can be through modulation of TF activity (Chapter 1, Section 7), or regulation of the mitochondrial processes. For example, USP30 opposes Parkin-mediated ubiquitylation at the mitochondrion that regulates mitophagy (Liang et al., 2015). Interestingly, a recent paper has suggested that the regulation of calcium-induced apoptosis can be modulated by the function of the DUB, BAP1, through regulation of the inositol-3-phosphate receptor (IP3R) (Bononi et al., 2017a). Additionally, germline mutation of BAP1 was shown to reduce mitochondrial respiratory function and promote glycolysis (Bononi et al., 2017b). These data demonstrate the range of possible mechanisms by which DUBs are known to regulate mitochondrial function. These recent papers demonstrate a developing niche in the study of ubiquitin-mediated regulation by DUBs on mitochondrial function.

Unlike recent papers, the preliminary data generated in this thesis promotes a theory that nuclear-encoded mitochondrial proteins could be regulated in a ubiquitin-dependent manner, which may occur at four main stages of the protein lifecycle: (1) transcriptional regulation, (2) co-translational degradation (3) mitochondrial targeting and import (4) protein degradation.

5.3.2.1 DUB-mediated Regulation of Transcription and Upstream Signalling

USP15 regulation of NDUFB6 could occur by modulating signalling that controls NDUF protein expression. In general, the co-ordinated expression of nuclear and mitochondrial genes is dependent upon mitochondrion-

localisation of nuclear TFs. Such dual nuclear and mitochondrial TFs include NF-kB, p53 and STAT3 that act as co-ordinators of regulation (Szczepanek et al., 2012). Interestingly, these TFs are also known to be regulated by USP15 and other DUBs (Table 1.1 & Chapter 1, Section 6.2.3). The transcription factor Nrf2, regulated by Keap1 and USP15 (Villeneuve et al., 2013), is a master regulator of cellular redox homeostasis that influences mitochondrial function (Dinkova-Kostova and Abramov, 2015, Holmström et al., 2016). Mechanistically deubiquitylation of these TFs and signalling pathways, could allow DUBs to modulate bi-organelle transcription.

Co-ordination of nuclear expression and ER positioning could be regulated by the NRF2 pathway. Nrf2 increases expression of genes through antioxidant response elements (ARE), which can regulate proteins involved in the regeneration of NADH. The dysregulation of Nrf2 has been implicated in reduced mitochondrial membrane potential and reduction of the NADH pool. USP15 was shown to regulate the expression of Nrf2, through modulation of the E3 ligase Keap1 (Villeneuve et al., 2013). Recently SQSTM1, a regulator of Nrf2, was implicated in the regulation of mitochondrial membrane potential (Bartolome et al., 2017). Disruption of the ER-mitochondrial positioning, could potentially reduce NDUF protein levels through mislocalisation and ubiquitin-dependent degradation. Additionally, positioning could simultaneously alter the concentration of ionic signalling between organelles. Interestingly, SQSTM1 was markedly reduced in proteomic analysis of USP15 depleted cells (Chapter 4, Supplementary Table 1), and was previously shown to be a target of USP15-mediated activity (Jongsma et al., 2016). Together these data may suggest that ubiquitylation and deubiquitylation, by USP15 and perhaps other DUBs, might play an important role in the co-ordination of inter-organelle signalling through the influence of the Nrf2 pathway.

5.3.2.2 USP15 Regulation of Protein Localisation

As USP15 has previously been associated with the co-translational regulation of REST, USP15 might be involved in quality control of the nascent

NDUF proteins prior to import across the membrane. Ubiquitylation is known to regulate cellular localisation and organisation into cellular compartments. Together these data demonstrate DUBs, including USP15, as regulators of time/signal dependent protein synthesis and translocation. These data are important as they demonstrate that the regulation of ubiquitylation, by E3 ligases or DUBs, could provide drugable targets for translocating proteins. The regulation of translocating proteins provides a unique interface for signalling to elicit broad ranging effects on protein function and compartmentally separated substrates.

5.3.2.3 Ubiquitylation of Mitochondrial Proteins

A proportion of USP15 has previously been shown to localise to, although not presumed to be incorporated into, the mitochondria (Cornelissen et al., 2014, Urbé et al., 2012). Importantly, there are reports of MS-identified ubiquitylation of NDUFB4 and NDUFB6 (www.phosphosite.org). These data suggest that NDUFB6 protein can be directly regulated by ubiquitin allowing for USP15 deubiquitylation of the substrate. USP15-regulation of NDUFB6 ubiquitylation could be assessed by *in vitro* incubation with active or catalytically inactive USP15. Cellular rescue of NDUFB6 protein levels following USP15-depletion could be attempted with exogenous expression of siRNA-resistant active and inactive USP15. In theory, as it has been shown that USP15 can locate to the exterior of mitochondrion, deubiquitylation may occur at the site of import into the mitochondrion. The data presented here represent the first suggestion that USP15 may deubiquitylate a nuclear encoded mitochondrial protein involved in the ETC.

5.3.2.4. DUBs and Mitochondrial Protein Quality Control and Degradation

Once inside the mitochondrion, NDUF proteins would appear to be exempt from ubiquitin-proteasome degradation due to the absence of internal mitochondrial ubiquitylation. The degradation of some mitochondrial proteins does not require the actions of the proteasome, due to the presence of mitochondrial proteases. These proteases are also involved in the cleavage of

localisation peptides sequences (Yogev and Pines, 2011). Interestingly, however, retrograde trans-localisation of mitochondrial proteins for proteasome degradation has been suggested as a possible mechanism of protein control (Bragoszewski et al., 2015). Alternatively, degradation of mitochondrial proteins might occur through mitochondrial derived vesicles (Sugiura et al., 2014). The role of ubiquitylation and deubiquitylation in these process remains to be determined. It is presumed that ubiquitin-dependent regulation of mitochondrial proteins could control the flux of proteins into the mitochondrion. Dysfunction of these processes could lead to cytosolic accumulation of mitochondrial proteins, reduced mitochondrial function and contribute to the onset of mitophagy.

This chapter attempts to develop upon the known regulation of mitochondrial proteins by inducing protein changes through the absence of USP15. Although downregulation of Complex I proteins is observed, the consequences of ubiquitin-dependent regulation and its requirement for cellular function remains to be determined.

CHAPTER 6: DISCUSSION

6.1 The Influence of REST Expression on Neuroendocrine Lung Cancer

REST is a context dependent tumour suppressor or oncogene and is differentially expressed in a range of cancers (Coulson, 2005, Negrini et al., 2013). As a tumour suppressor, the consequences of REST dysregulation or dysfunction influences cancerous growth and migration (Westbrook et al., 2005, Chang et al., 2017, Lim et al., 2017). REST also regulates access to NE specific genes and phenotypes (Chapter 1, Section 4.1.3). This differential expression of REST was predicted to produce prognostic indicators. The NE phenotype produces secreted protein biomarkers; somatostatin or serotonin for carcinoid syndrome and immunohistochemistry of neurosecretory proteins including synaptophysin and chromogranins for poorly differentiated NE tumours (Rickman et al., 2017). These NE biomarkers are used to assist the classification of the tumours when presenting with the NE morphology, whilst these techniques fail to accurately describe poorly differentiated NE tumours. The lack of veracity for secreted protein biomarkers for accurate lung NE tumour classification is complicated as only a small population, less than 10%, possess functional secretion and that high-grade tumours may express NE biomarkers, but lack NE morphology (Hendifar et al., 2017). It is well established that REST depletion or loss-of-function can promote a distinctive transcriptomic profile, a feature that can be utilised to identify mRNAs in circulating tumour cells as an alternative source of prognostic markers (Moss et al., 2009). Persistent questions remain; (1) how do these REST-dependent RNA changes influence the cellular proteome and pathways, (2) how these changes contribute to prognosis and (3) can these changes be used as cancer-specific prognostic markers, when used in combination with mRNA changes indicative of REST status. To address the first question requires a proteomic approach to REST-depletion (Chapter 4).

Just prior to the start of this thesis, the laboratory had shown that USP15 regulates nascent REST protein expression (Faronato et al., 2013). As an

enzymatic regulator of REST, it was prudent to investigate the relationship between these proteins in thoracic cancers (Chapter 3).

The consequences of REST1 depletion, and REST4 expression, in NE tumours contributes to broad transcriptional reprogramming, and as such, is relatively understudied at the protein level. Similarly, USP15 activity is influenced by the cellular context, access to substrates, interacting partners and regulators, as such the broad consequences of its activity is relatively understudied. To provide specificity to USP15 function, previous USP15-regulated cellular pathways tend to utilise stimulation and rescue with catalytically active or inactive isoforms (Buus et al., 2009). Here, I hypothesised that USP15-depletion could promote dysregulation of REST in early G1, and that this temporal REST dysregulation may lead to inadvertent REST-dependent RNA and protein changes. Assuming REST1 expression helps maintain non-NE status, these data should help elucidate the contribution of USP15 to NE differentiation through shared protein changes with REST-depletion, representing a USP15-REST axis. Importantly, USP15-specific pathway regulation could be inferred from proteins that were uniquely responsive to USP15 depletion.

Previously, USP7 was shown to counter $SCF^{\beta\text{-}TrCP}$-mediated degradation of REST during neuronal differentiation, thus maintaining the neuronal progenitor cells (Huang et al., 2011). My hypothesis shares a parallel in that DUB regulation of REST may be required to maintain a distinct population of cells. Evidence that supports USP15-regulated REST on the cellular proteome would highlight the importance of DUBs in the regulation of differentiation-restricting transcription factors. The logic for studying USP15, and the post-mitotic re-expression of REST, instead of USP7-regulation of REST, is based upon the identification of USP15 as the most prominent regulatory DUB from an unbiased siRNA screen in A549 NSCLC cells (Faronato et al., 2013). Theoretically, successful mitotic division and the concurrent absence of mature REST presents a logical time-point for a

differentiation checkpoint. Interestingly, Huang and colleagues demonstrate that REST depletion during neuronal differentiation is gradual, which theoretically can be achieved by reduced USP15 activity against REST in differentiating non-NE cells. If USP15-depletion produces a biologically significant dysregulation of REST, this should result in a loss of REST-regulated RNA and protein homeostasis. Although not addressed in this thesis, further experiments will be required to definitively demonstrate that prolonged USP15 or REST depletion can produce the NE phenotype from non-NE cells, and that reduced USP15 activity towards REST acts as a differentiation decision checkpoint.

6.1.1 Outstanding Questions

The outstanding question of how REST-dependent RNA changes influence the cellular proteome and pathways requires further investigation. In parallel, the recent identification of USP15 as a REST regulating DUB requires further study to investigate the extent of USP15 influence upon REST-dependent outcomes. The broad aim of this thesis was to investigate the expression and relationship of REST and USP15 in lung cancer cells. Specifically, I set out to (1) quantify REST and USP15 splicing/expression in thoracic cancers and explore any dynamic changes during the cell cycle, (2) use quantitative proteomic analysis to delineate the cellular response to loss of USP15 and/or REST1 function.

6.2 REST Isoform Expression in Thoracic Cancers and During the Cell Cycle

Alternative splicing of REST to produce C-terminal truncated REST4 was first shown in neuronal cells, neuroblastoma and in SCLC where it was linked with an NE-phenotype (Palm et al., 1999, Coulson et al., 2000). More recently, the extent of REST alternative splicing has been investigated in a variety of tissues, diseases and cancer cell types (Chen and Miller, 2013, Chen et al., 2017). In Chapter 3, I confirm that the loss of REST1 and gain in expression of REST4 is confined to NE lung cancers, and is not seen in other

thoracic cancer cell lines including mesothelioma (Figure 3.2), reiterating the importance of this event in the biology of NE cancer. In contrast the REST-E5 does not appear to be significantly upregulated in NE cells, as such there does not appear to be a concordant with REST4 splicing. A greater understanding of the contribution of REST splicing in restricting the NE cancer phenotype, and its regulation in context, may improve cancer diagnostics and influence therapeutic avenues for disease management.

The origins of the NE phenotype are usually derived from endogenous NE cells, which produce carcinoid tumours and whilst SCLCs share the NE phenotype they display more rapid proliferation and anchorage-independence. Lung cancers can form a heterogeneous tumour cell population through tumour plasticity or co-operation with surrounding cells. The proposed survival benefits of the NE phenotype include increased protein synthesis capacity and reduced apoptosis. In addition, NE cells accumulate and form endogenous niches, perhaps assisted by autocrine signalling and modulation of the microenvironment could promote metastasis. Recently, loss of the NE phenotype from SCLCs, caused by Notch signalling has been shown to reprogram cells to provide a co-operative cell niche that has greater chemoresistance (Lim et al., 2017). Importantly, Lim and colleagues demonstrate that a transition from NE to non-NE cell types could be induced by the exogenous expression of REST. These findings again suggest that regulated REST expression could be a key contributor to the differentiation status of the cell. The proposed pivot role of REST, is supported by recent predictions that suggest it acts as a common regulator of NE and non-NE/mesenchymal networks in SCLC heterogeneity (Udyavar et al., 2017). If REST regulation of NE and non-NE networks is determined by the alternative splicing and expression of REST, evidence of this would further support the proposed role in regulating the transition from non-NE to NE phenotypes and the hypothesis that REST dysregulation influences lung cancer outcomes.

In additional to examining asynchronous cell populations, I also monitored the expression of REST through the cell cycle in A549, a non-NE lung cancer cell line. My protein level data agree with previous reports that REST1 is acutely degraded at the onset of mitosis (Guardavaccaro et al., 2008, Faronato et al., 2013). In contrast, several regulators of REST that I investigated (SRRM4, USP7 and USP15) did not change expression through the cell cycle (Figure 3.11). Interestingly however, REST4 but not REST1 mRNA expression was increased during the mitotic phase of the cell cycle in A549 cells (Chapter 3, Figure 12). Other studies in neuronal and SCLC cells have shown that expression of REST4 requires the splicing factor SRRM4 (Raj et al., 2011, Shimojo et al., 2013). However, in my experiments, SRRM4 was undetectable in A549 cells, even at mitosis when REST4 transcript levels peaked (Figure 3.13). These data suggest that alternative REST splicing at mitosis may be independent of SRRM4, although another mechanism remains to be determined.

It is intriguing to speculate that the expression of REST4 prior to cell division in non-NE cells may play a role in maintaining repression of REST target genes as cells exit mitosis and enter G1, prior to re-expression of REST1. In common with the REST-FS mutant (Guardavaccaro et al., 2008), REST4 lacks the C-terminal phosphodegrons of REST1, and so is predicted to be spared from mitotic degradation. However, it should be noted that protein expression of REST4 was not confirmed in my experiments. In future, it would be desirable to design a gene-editing strategy so that expression of an endogenous tagged REST4 isoform could be monitored to confirm periodic REST4 expression during the cell cycle. Assuming REST4 is expressed at the protein level during mitosis, this truncated transcription factor could potentially act as a “bookmark” at RE1-restricted genes. Pioneer transcription factors are usually associated with bookmarking DNA for post-mitotic regulation (Zaret, 2014), that may be important for retaining cell differentiation programs or pluripotency. In the case of the transcriptional repressor REST however,

REST4 may instead be required to bookmark and limit exposure of neuronal gene subsets of RE-1 sequences in early G1.

6.2 USP15 Isoform Expression in Thoracic Cancer and During the Cell Cycle

In Chapter 3, I investigated the expression of USP15 and its isoforms in thoracic cancer cell lines. The different isoforms of USP15 are known to exhibit similar cellular localisation (Fielding et al., manuscript in preparation), but diversification of USP15 isoform function may arise through isoform-specific phosphorylation (Fielding et al., manuscript in preparation) or substrate interaction affinities (Kotani et al., 2017). The consequences of differential USP15 isoform expression in cancer is currently unstudied. The equivalent expression of isoform 1 and isoform 2 I observed in normal lung cells could suggest that no selective pressure is placed on the expression of either isoform. However, although expression of USP15 isoform 1 was seen across all thoracic cancers, its expression was generally higher in NE cell lines. Despite the preferential expression of USP15 isoform 1 in NE cells, this was not correlated to the expression level of SRRM4. The potential splicing factors that regulate USP15 isoform expression were not investigated further in this thesis. However, the intron inclusion splicing of USP15 isoform 1 may be due to RNA Pol II pausing (Gowher et al., 2012), which is a co-transcriptional regulation of RNA Pol II activity due to TF inhibition of progression. Gowher and colleagues demonstrated that inclusion splicing of USP15 isoform 1 was related to expression profile of vascular endothelial ZF 1 (VEZF1). Future experiments could explore the expression profile of VEZF1 across this cell panel.

The data presented here demonstrate that mRNA expression of USP15 does not change during the cell cycle (Fig 3.11). As a DUB, however, USP15 function is dependent upon both its expression and its catalytic activity, which may be dynamically regulated *in vivo*. Therefore, expression analysis alone of USP15 may be insufficient to provide mechanistic correlation with a

phenotype. Recently, techniques utilising ubiquitin probes that interact irreversibly with DUB catalytic sites have been developed to measure both expression and activity of DUBs (Ritorto et al., 2014). These techniques currently depend upon cellular protein extraction and in vitro incubation with the probe to provide a measure of the catalytic on-rate. The total amount of a given DUB from the sample that has bound to the probe can be calculated using biochemical techniques such as western blotting or mass spectrometry. Whilst isoform-specific DUB analysis could be challenging with these techniques, an obvious future direction of this project would be to incorporate DUB activity/expression analysis of the USP15 isoforms.

6.3 A Proteomic Approach to Investigating New Roles for USP15 and REST in Lung Cancer

I assumed that the loss of REST1 in non-NE cells could potentially mimic the onset of the NE differentiation programme when depleted by siRNA. If true, this assumption would demonstrate that subsequent loss of REST-dependent repression, in the absence of splicing regulators that promote the intron inclusion of REST4, could significantly contribute to the development of NE-like phenotype. Previously, transcriptome analysis of REST depleted cells had demonstrated upregulation of transcripts encoding neuropeptides and elements of the secretory machinery (Coulson et al, unpublished). Translation of REST-regulated transcripts that are definitively related to the secretory NE cell physiology, either intracellular proteins, secretory vesicles composition or machinery, or membrane localised proteins, stimuli sensing or ionic permeability, following knockdown of REST, has not been clearly demonstrated in cancer cells. Thus, the influence of REST in the pathophysiology of NE cancers is not as clear as first thought.

The multitude of REST regulated genes are not limited to those involved in NE lineage control and REST depletion may alter the ability of cells to regulate pathways that are not apparent from transcriptome analysis. As such, analysis of changes in protein levels, and the cellular pathways they regulate,

may provide greater insight into the effects of REST-depletion on the biology of the cells than analysis of RE-1 site occupancy or the transcriptome. To define the influence of REST on cancers, previous studies have relied upon comparisons of REST-positive to REST-negative cells or transcriptomic analysis of REST depletion (Neumann et al., 2004, Gurrola-Diaz et al., 2003, Kreisler et al., 2010, Coulson, Unpublished). In Chapter 4, I took an alternative approach by using SILAC-mass spectrometry to investigate the effect of REST-depletion on the cellular proteome. I chose a SILAC approach that allows for quantitative multiplex analysis, which has the advantage of including a third sample of USP15 knockdown, which should consequently limit REST expression during early G1 (Faronato et al., 2013). A proteomic approach has the advantage of reporting a combination of direct and indirect actions of REST, which is vital for studying the consequences of REST activity upon homeostatic feedback loops (Chapter 1, Section 3.2). In addition, it has been reported that only ~30% of transcripts correlate with protein expression levels (Maier et al., 2009) and so a REST-dependent proteome should better reflect the physiological changes of the cells by providing proteins and pathways that are disrupted by its absence. In this thesis, I suggest that gene ontology analysis of protein changes following REST depletion is generally not reflective of previous transcriptomic studies. Instead, REST-dependent proteins changes are primarily associated with the actin cytoskeleton. Interestingly, USP15-dependent protein changes were also associated with this term. The similarities between REST and USP15 knockdown conditions is consistent with my hypothesis that USP15-depletion in general produces protein changes that are shared with REST-depletion and potentially are due to its role in regulating REST. It is important to note that EGFR downregulation has been reported as an off-target effect of the initial control siRNA used (product information, Table 2.3), and that my proteomics data relate only to A549 cells. Follow up experiments for selected proteins should be confirmed using extra control and target siRNAs, and/or knockout models to improve confidence in on-target effects of REST and USP15 depletion.

The proteins that responded to both REST and USP15 depletion were analysed by gene ontology analysis and were shown to demonstrate enrichment for actin and cytoskeletal terms. Through involvement in the structure and migration of cells this collection of proteins has the potential to relate the activity of USP15 and REST to a cancerous trait. Previous studies have proposed that both USP15 and REST can regulate signalling pathways. USP15 regulates HGF-induced MEK-ERK signalling (Buus et al., 2009), and the tumour suppressive function of REST has been associated with PI3K and MAPK signalling (Westbrook et al., 2005). The general increase in the expression of actin cytoskeletal proteins fits with the tumour suppressive and migratory regulation roles of REST and USP15, respectively. Amongst the most prominent changes identified by proteomic analysis was EGFR and VCL, however, these were not validated by deconvolution of USP15 or REST siRNAs (Chapter 4, Figure 12).

Here, I demonstrated that REST-depletion increases the protein level of ITGB1, as confirmed by independent SILAC-MS experiment and with multiple REST siRNAs by immunoblotting. The mechanism by which REST could regulate ITGB1 expression remains untested, however it is interesting to note that ITGB1 is one of the few overlapping genes between my proteome dataset and the transcriptome response to REST depletion in NCI-H460 lung adenocarcinoma cells (Coulson, Unpublished). The effect of ITGB1 expression changes suggests that the regulation of cellular adhesion complexes could a downstream consequence of REST depletion. REST regulation of integrin expression has not previously been described, although REST is known to regulate expression of neuronal cellular adhesion molecule (NCAM)(Neumann et al., 2004). This hypothesis would appear to relate to previous literature that showed REST1-deficient cells are prone to anchorage-independent growth (Westbrook et al., 2005, Lim et al., 2017). The increase in ITGB1 expression I have identified in response to REST depletion will require further studies of the effects on localisation, activation and substrate migration to determine the functional significance for cancers that lack REST1. I propose

that invadapodia, which can be dependent upon ITGB1 (Di Martino et al., 2016), may be increased in REST-depleted cells. Quantification of cellular morphological changes or cellular migration potential and speed would be required to investigate this hypothesis.

Future investigation into mechanistic roles of REST or USP15 via modulating these proteins could include studies of focal adhesion complexes and stimulation modulated signalling. Such studies would include multiple cellular migration and invasion assays that could be used to investigate USP15 or REST depletion, requiring more time than available at the conclusion of my PhD to elucidate the specific pathways at play. It was therefore my decision to focus follow-up investigations on a USP15-specific role, as the study of ubiquitin regulated proteins due to both the novelty of the data and the wealth of expertise available to help determine DUB-regulated activities.

6.4 USP15-Regulation of Mitochondrial Complex I

The complexity of USP15 function is a consequence of its transient associations with substrates and binding partners that likely defines its disperse nature. To gain further insight into this complexity I used whole proteome analysis to investigate the proteins and pathways that were regulated by the depletion of USP15. The data suggest that this broad approach of monitoring protein expression level changes can be useful for the identification of cellular pathways that are regulated by DUBs. In addition to the findings described in this thesis, data generated by analysis of the USP15-dependent proteome identified topoisomerase II (TOP2A) as a potential USP15 target that underpins genomic instability in USP15-deficient cells (Fielding et al., manuscript in preparation). This proteomic approach also initiated studies in this thesis to investigate a novel role of USP15 at the mitochondrion (Chapter 5). The data generated from proteomic analysis had demonstrated a robust downregulation of certain mitochondrial proteins in response to USP15 depletion. In Chapter 5, I focused on two of these proteins, NDUFB4 and NDUFB6, and showed that downregulation of these NDUF

proteins could be recapitulated with different siRNA strategies. To ensure that this was not due to off-target effects of the siRNAs, USP15 knockout MEF cells were used to independently demonstrate that NDUF downregulation was seen in cells deficient for USP15. The mechanism by which USP15 regulates these mitochondrial proteins is yet to be elucidated and was discussed in more detail earlier (Chapter 5, Section 3).

In my opinion the regulation of nuclear-encoded mitochondrial proteins and their influence on mitochondrial function and cellular physiology has not received enough attention. In this thesis, the data on USP15 regulated expression of NDUF proteins highlights the possibility that nuclear-encoded mitochondrial proteins are subject to ubiquitylation-mediated degradation, which may ultimately influence electron transport chain function. Although the mechanism is not definitive at this time, the regulation of mitochondrial targeted proteins by DUBs raises the question of how this affects cellular behaviour. Here, the mitochondrial stress test was unable to identify a distinct change in the oxygen consumption profile. Alternative experimental conditions or techniques could in future be used to evaluate the contribution of ubiquitylation and DUB activity in the regulation of mitochondrial protein expression and the effects this has on mitochondrial function and cellular metabolism.

Several DUBs, including USP15, have been shown to oppose the activity of the mitochondrial targeted E3-ligase Parkin, that regulates mitophagy (Cornelissen et al., 2014, Liang et al., 2015, Durcan et al., 2014). I speculate that the broader regulation of mitochondrial functions, however, is not limited to the current handful of E3s and DUBs with many more still to be discovered. Understandably, most of the ubiquitin pathway enzymes currently associated with mitochondrial function are found to co-localise with the organelle. E3 ligases and DUBs, however, could also modulate signalling from afar, potentially regulating mitochondrial-targeted proteins, mitochondrial size, shape and location as well as altering enzymatic activities that control

concentration ratios and influence metabolism. A recent example of DUB-regulation of mitochondrial function from afar has been described with BRAC1-associated protein (BAP1) regulation of IP3R and metabolites (Bononi et al., 2017a, Bononi et al., 2017b). These data demonstrate that ubiquitylation and deubiquitylation may regulate cellular energetics, an emerging hallmark of cancer (Hanahan and Weinberg, 2011). To determine the extent of DUBs function towards the mitochondria combinations of metabolome and proteome strategies are obvious candidates for future experiments. Whilst, microscopy and spectrometry techniques could be used to demonstrate any influence on mitochondrial depletion, fusion/fission, membrane potential and oxygen consumption rate.

The data generated in this thesis demonstrate that (1) REST and USP15 show differential expression and isoform profiles amongst thoracic cancers or during the cell cycle, and (2) deficiency of USP15 or REST results in protein changes that could contribute to the pro-metastatic phenotype of cancers by altering the internal cytoskeletal profile of the cell and modulating subcellular organelle functions. Notably, I discovered that the REST4 splice variant is expressed at mitosis in non-NE cells, and hypothesise this may play a role in maintaining repression of REST target genes in dividing cells. I also demonstrated that USP15 could act to regulate the expression of mitochondrial proteins, predominantly Complex I subunits. These data lead to the hypothesis that ubiquitin-dependent regulation and the action of DUBs, specifically USP15, could be modulators of cellular metabolism. Further investigations would need to be performed to demonstrate a genuine and specific change in the production of ATP or mitochondrial capacity to cope with alternative fuel sources.

Bibliography

ABDUL REHMAN, S. A., KRISTARIYANTO, Y. A., CHOI, S.-Y. Y., NKOSI, P. J., WEIDLICH, S., LABIB, K., HOFMANN, K. & KULATHU, Y. 2016. MINDY-1 Is a Member of an Evolutionarily Conserved and Structurally Distinct New Family of Deubiquitinating Enzymes. *Molecular Cell,* 63**,** 146-155.

ABRAJANO, J. J., QURESHI, I. A., GOKHAN, S., ZHENG, D., BERGMAN, A. & MEHLER, M. F. 2009. REST and CoREST modulate neuronal subtype specification, maturation and maintenance. *PLOS ONE,* 4**,** e7936.

ABRAMOVITZ, L., SHAPIRA, T., BEN-DROR, I., DROR, V., GRANOT, L., ROUSSO, T., LANDOY, E., BLAU, L., THIEL, G. & VARDIMON, L. 2008. Dual role of NRSF/REST in activation and repression of the glucocorticoid response. *The Journal of Biological Chemistry,* 283**,** 110-119.

AFFAR, E. B., GAY, F., SHI, Y., LIU, H., HUARTE, M., WU, S., COLLINS, T., LI, E. & SHI, Y. 2006. Essential dosage-dependent functions of the transcription factor yin yang 1 in late embryonic development and cell cycle progression. *Molecular and Cellular Biology,* 26**,** 3565-3581.

AKUTSU, M., DIKIC, I. & BREMM, A. 2016. Ubiquitin chain diversity at a glance. *Journal of Cell Science,* 129**,** 875-880.

ALLEN, B. L. & TAATJES, D. J. 2015. The Mediator complex: a central integrator of transcription. *Nature Reviews Molecular Cell Biology,* 16**,** 155-166.

ALLFREY, V. G., FAULKNER, R. & MIRSKY, A. E. 1964. Acetylation and methylation of histones and their possible role in the regulation of RNA synthesis. *Proceedings of the National Academy of Sciences of the United States of America,* 51**,** 786-794.

ALSTON, C. L., ROCHA, M. C., LAX, N. Z., TURNBULL, D. M. & TAYLOR, R. W. 2017. The genetics and pathology of mitochondrial disease. *The Journal of Pathology,* 241**,** 236-250.

ALTSCHUL, S. F., GISH, W., MILLER, W., MYERS, E. W. & LIPMAN, D. J. 1990. Basic local alignment search tool. *Journal of Molecular Biology,* 215**,** 403-410.

ANDRÉS, M. E., BURGER, C., PERAL-RUBIO, M. J., BATTAGLIOLI, E., ANDERSON, M. E., GRIMES, J., DALLMAN, J., BALLAS, N. & MANDEL, G. 1999. CoREST: a functional corepressor required for regulation of neural-specific gene expression. *Proceedings of the National Academy of Sciences of the United States of America,* 96**,** 9873-9878.

ANGELATS, C., WANG, X. W., JERMIIN, L. S., COPELAND, N. G., JENKINS, N. A. & BAKER, R. T. 2003. Isolation and characterization of the mouse ubiquitin-specific protease Usp15. *Mammalian Genome,* 14**,** 31-46.

AOKI, H., HARA, A., ERA, T., KUNISADA, T. & YAMADA, Y. 2012. Genetic ablation of Rest leads to in vitro-specific derepression of neuronal genes during neurogenesis. *Development,* 139**,** 667-677.

ATOUF, F., CZERNICHOW, P. & SCHARFMANN, R. 1997. Expression of neuronal traits in pancreatic beta cells Implication of neuron-restrictive silencing factor/repressor element silencing transcription factor, a neuron-restrictive silencer. *Journal of Biological Chemistry,* 272**,** 1929-1934.

BAILLIE-JOHNSON, H., TWENTYMAN, P. R., FOX, N. E., WALLS, G. A., WORKMAN, P., WATSON, J. V., JOHNSON, N., REEVE, J. G. & BLEEHEN, N. M. 1985. Establishment and characterisation of cell lines from patients with lung cancer (predominantly small cell carcinoma). *British Journal of Cancer,* 52**,** 495-504.

BAIULA, M., CARBONARI, G., DATTOLI, S. D., CALIENNI, M., BEDINI, A. & SPAMPINATO, S. 2012. REST is up-regulated by epidermal growth factor in HeLa cells and inhibits apoptosis by influencing histone H3 acetylation. *Biochimica et Biophysica Acta,* 1823**,** 1252-1263.

BAKER, J. L., CELIK, E. & DELISA, M. P. 2013. Expanding the glycoengineering toolbox: the rise of bacterial N-linked protein glycosylation. *Trends in Biotechnology,* 31**,** 313-23.

BAKER, R. T., WANG, X. W., WOOLLATT, E., WHITE, J. A. & SUTHERLAND, G. R. 1999. Identification, functional characterization, and chromosomal localization of USP15, a novel human ubiquitin-specific protease related to the UNP oncoprotein, and a systematic nomenclature for human ubiquitin-specific proteases. *Genomics,* 59**,** 264-274.

BALDELLI, P. & MELDOLESI, J. 2015. The transcription repressor REST in adult neurons: physiology, pathology, and diseases. *eNeuro,* 2**,** e0010-15.

BALLAS, N., BATTAGLIOLI, E., ATOUF, F., ANDRES, M. E., CHENOWETH, J., ANDERSON, M. E., BURGER, C., MONIWA, M., DAVIE, J. R., BOWERS, W. J., FEDEROFF, H. J., ROSE, D. W., ROSENFELD, M. G., BREHM, P. & MANDEL, G. 2001. Regulation of neuronal traits by a novel transcriptional complex. *Neuron,* 31**,** 353-365.

BALLAS, N., GRUNSEICH, C., LU, D. D., SPEH, J. C. & MANDEL, G. 2005. REST and its corepressors mediate plasticity of neuronal gene chromatin throughout neurogenesis. *Cell,* 121**,** 645-657.

BANNISTER, A. J. & KOUZARIDES, T. 2005. Reversing histone methylation. *Nature,* 436**,** 1103-1106.

BARTOLOME, F., ESTERAS, N., MARTIN-REQUERO, A., BOUTOLEAU-BRETONNIERE, C., VERCELLETTO, M., GABELLE, A., LE BER, I., HONDA, T., DINKOVA-KOSTOVA, A. T., HARDY, J., CARRO, E. & ABRAMOV, A. Y. 2017. Pathogenic p62/SQSTM1 mutations impair energy metabolism through limitation of mitochondrial substrates. *Scientific Reports,* 7**,** 1666.

BATTAGLIOLI, E., ANDRÉS, M. E., ROSE, D. W., CHENOWETH, J. G., ROSENFELD, M. G., ANDERSON, M. E. & MANDEL, G. 2002. REST

repression of neuronal genes requires components of the hSWI.SNF complex. *The Journal of Biological Chemistry,* 277**,** 41038-41045.
BEPLER, G., KOEHLER, A., KIEFER, P., HAVEMANN, K., BEISENHERZ, K., JAQUES, G., GROPP, C. & HAEDER, M. 1988. Characterization of the state of differentiation of six newly established human non-small-cell lung cancer cell lines. *Differentiation,* 37**,** 158-171.
BESSIS, A., CHAMPTIAUX, N., CHATELIN, L. & CHANGEUX, J. P. 1997. The neuron-restrictive silencer element: a dual enhancer/silencer crucial for patterned expression of a nicotinic receptor gene in the brain. *Proceedings of the National Academy of Sciences of the United States of America,* 94**,** 5906-5911.
BESTWICK, M. L. & SHADEL, G. S. 2013. Accessorizing the human mitochondrial transcription machinery. *Trends in Biochemical Sciences,* 38**,** 283-291.
BINOTTI, B., JAHN, R. & CHUA, J. J. 2016. Functions of Rab Proteins at Presynaptic Sites. *Cells,* 5**,** 7.
BIRNEY, E., STAMATOYANNOPOULOS, J. A., DUTTA, A., GUIGÓ, R., GINGERAS, T. R., MARGULIES, E. H., WENG, Z., SNYDER, M., DERMITZAKIS, E. T. & THURMAN, R. E. 2007. Identification and analysis of functional elements in 1% of the human genome by the ENCODE pilot project. *Nature,* 447**,** 799-816.
BONONI, A., GIORGI, C., PATERGNANI, S., LARSON, D., VERBRUGGEN, K., TANJI, M., PELLEGRINI, L., SIGNORATO, V., OLIVETTO, F., PASTORINO, S., NASU, M., NAPOLITANO, A., GAUDINO, G., MORRIS, P., SAKAMOTO, G., FERRIS, L. K., DANESE, A., RAIMONDI, A., TACCHETTI, C., KUCHAY, S., PASS, H. I., AFFAR, E. B., YANG, H., PINTON, P. & CARBONE, M. 2017a. BAP1 regulates IP3R3-mediated Ca(2+) flux to mitochondria suppressing cell transformation. *Nature,* 546**,** 549-553.
BONONI, A., YANG, H., GIORGI, C., PATERGNANI, S., PELLEGRINI, L., SU, M., XIE, G., SIGNORATO, V., PASTORINO, S., MORRIS, P., SAKAMOTO, G., KUCHAY, S., GAUDINO, G., PASS, H. I., NAPOLITANO, A., PINTON, P., JIA, W. & CARBONE, M. 2017b. Germline BAP1 mutations induce a Warburg effect. *Cell Death and Differentiation***,** 1-11.
BRAGOSZEWSKI, P., WASILEWSKI, M., SAKOWSKA, P., GORNICKA, A., BÖTTINGER, L., QIU, J., WIEDEMANN, N. & CHACINSKA, A. 2015. Retro-translocation of mitochondrial intermembrane space proteins. *Proceedings of the National Academy of Sciences of the United States of America,* 112**,** 7713-7718.
BREMM, A. & KOMANDER, D. 2011. Emerging roles for Lys11-linked polyubiquitin in cellular regulation. *Trends in Biochemical Sciences,* 36**,** 355-363.
BRUCE, A. W., KREJCÍ, A., OOI, L., DEUCHARS, J., WOOD, I. C., DOLEZAL, V. & BUCKLEY, N. J. 2006. The transcriptional repressor REST is a critical regulator of the neurosecretory phenotype. *Journal of Neurochemistry,* 98**,** 1828-1840.

BRUCE, A. W., LOPEZ-CONTRERAS, A. J., FLICEK, P., DOWN, T. A., DHAMI, P., DILLON, S. C., KOCH, C. M., LANGFORD, C. F., DUNHAM, I., ANDREWS, R. M. & VETRIE, D. 2009. Functional diversity for REST (NRSF) is defined by in vivo binding affinity hierarchies at the DNA sequence level. *Genome Research,* 19**,** 994-1005.

BUCKLEY, N. J., JOHNSON, R., SUN, Y.-M. M. & STANTON, L. W. 2009. Is REST a regulator of pluripotency? *Nature,* 457**,** E4-E5.

BUUS, R., FARONATO, M., HAMMOND, D. E., URBÉ, S. & CLAGUE, M. J. 2009. Deubiquitinase activities required for hepatocyte growth factor-induced scattering of epithelial cells. *Current Biology,* 19**,** 1463-1466.

CALARCO, J. A., SUPERINA, S., O'HANLON, D., GABUT, M., RAJ, B., PAN, Q., SKALSKA, U., CLARKE, L., GELINAS, D., VAN DER KOOY, D., ZHEN, M., CIRUNA, B. & BLENCOWE, B. J. 2009. Regulation of vertebrate nervous system alternative splicing and development by an SR-related protein. *Cell,* 138**,** 898-910.

CALDERONE, A., JOVER, T., NOH, K., TANAKA, H., YOKOTA, H., LIN, Y., GROOMS, S. J., REGIS, R., BENNETT, M. V. L. & ZUKIN, R. S. 2003. Ischemic insults derepress the gene silencer REST in neurons destined to die. *Journal of Neuroscience,* 23**,** 2112-2121.

CANZONETTA, C., MULLIGAN, C., DEUTSCH, S., RUF, S., O'DOHERTY, A., LYLE, R., BOREL, C., LIN-MARQ, N., DELOM, F., GROET, J., SCHNAPPAUF, F., DE VITA, S., AVERILL, S., PRIESTLEY, J. V., MARTIN, J. E., SHIPLEY, J., DENYER, G., EPSTEIN, C. J., FILLAT, C., ESTIVILL, X., TYBULEWICZ, V. L., FISHER, E. M., ANTONARAKIS, S. E. & NIZETIC, D. 2008. DYRK1A-dosage imbalance perturbs NRSF/REST levels, deregulating pluripotency and embryonic stem cell fate in Down syndrome. *American Journal of Human Genetics,* 83**,** 388-400.

CARBONARI, G. 2012. *Identification of the N-linked Glycosylation Sites of the Transcription Factor REST and Effect of Glycosylation on DNA Binding and Transcriptional Activity.* Universita' Di Bologna.

CHANG, P. C., WANG, T. Y., CHANG, Y. T., CHU, C. Y., LEE, C. L., HSU, H. W., ZHOU, T. A., WU, Z., KIM, R. H., DESAI, S. J., LIU, S. & KUNG, H. J. 2014. Autophagy pathway is required for IL-6 induced neuroendocrine differentiation and chemoresistance of prostate cancer LNCaP cells. *PLOS ONE,* 9**,** e88556.

CHANG, Y. T., LIN, T. P., CAMPBELL, M., PAN, C. C., LEE, S. H., LEE, H. C., YANG, M. H., KUNG, H. J. & CHANG, P. C. 2017. REST is a crucial regulator for acquiring EMT-like and stemness phenotypes in hormone-refractory prostate cancer. *Scientific Reports,* 7**,** 42795.

CHEN, G.-L. & MILLER, G. M. 2013. Extensive Alternative Splicing of the Repressor Element Silencing Transcription Factor Linked to Cancer. *PLOS ONE,* 8**,** e62217.

CHEN, G.-L. L., MA, Q., GOSWAMI, D., SHANG, J. & MILLER, G. M. 2017. Modulation of nuclear REST by alternative splicing: a potential therapeutic target for Huntington's disease. *Journal of Cellular and Molecular Medicine***,** 10.1111/jcmm.13209.

CHEN, Z. F., PAQUETTE, A. J. & ANDERSON, D. J. 1998. NRSF/REST is required in vivo for repression of multiple neuronal target genes during embryogenesis. *Nature Genetics,* 20**,** 136-142.
CHONG, J. H. A., TAPIARAMIREZ, J., KIM, S., TOLEDOARAL, J. J., ZHENG, Y. C., BOUTROS, M. C., ALTSHULLER, Y. M., FROHMAN, M. A., KRANER, S. D. & MANDEL, G. 1995. REST - A mammalian silencer protein that restricts sodium-channel gene-expression to neurons. *Cell,* 80**,** 949-957.
CIECHANOVER, A., HELLER, H., ELIAS, S., HAAS, A. L. & HERSHKO, A. 1980. ATP-dependent conjugation of reticulocyte proteins with the polypeptide required for protein degradation. *Proceedings of the National Academy of Sciences of the United States of America,* 77**,** 1365-1368.
CLAGUE, M. J., BARSUKOV, I., COULSON, J. M., LIU, H., RIGDEN, D. J. & URBÉ, S. 2013. Deubiquitylases from genes to organism. *Physiological Reviews,* 93**,** 1289-1315.
CLAGUE, M. J., COULSON, J. M. & URBÉ, S. 2012. Cellular functions of the DUBs. *Journal of Cell Science,* 125**,** 277-286.
CLERICI, M., LUNA-VARGAS, M. P., FAESEN, A. C. & SIXMA, T. K. 2014. The DUSP-Ubl domain of USP4 enhances its catalytic efficiency by promoting ubiquitin exchange. *Nature Communications,* 5**,** 5399.
COHN, M. A., KOWAL, P., YANG, K., HAAS, W., HUANG, T. T., GYGI, S. P. & D'ANDREA, A. D. 2007. A UAF1-containing multisubunit protein complex regulates the Fanconi anemia pathway. *Molecular Cell,* 28**,** 786-797.
CONSORTIUM, E. P., BIRNEY, E., STAMATOYANNOPOULOS, J. A., DUTTA, A., GUIGO, R., GINGERAS, T. R., MARGULIES, E. H., WENG, Z., SNYDER, M., DERMITZAKIS, E. T., THURMAN, R. E., KUEHN, M. S., TAYLOR, C. M., NEPH, S., KOCH, C. M., ASTHANA, S., MALHOTRA, A., ADZHUBEI, I., GREENBAUM, J. A., ANDREWS, R. M., FLICEK, P., BOYLE, P. J., CAO, H., CARTER, N. P., CLELLAND, G. K., DAVIS, S., DAY, N., DHAMI, P., DILLON, S. C., DORSCHNER, M. O., FIEGLER, H., GIRESI, P. G., GOLDY, J., HAWRYLYCZ, M., HAYDOCK, A., HUMBERT, R., JAMES, K. D., JOHNSON, B. E., JOHNSON, E. M., FRUM, T. T., ROSENZWEIG, E. R., KARNANI, N., LEE, K., LEFEBVRE, G. C., NAVAS, P. A., NERI, F., PARKER, S. C., SABO, P. J., SANDSTROM, R., SHAFER, A., VETRIE, D., WEAVER, M., WILCOX, S., YU, M., COLLINS, F. S., DEKKER, J., LIEB, J. D., TULLIUS, T. D., CRAWFORD, G. E., SUNYAEV, S., NOBLE, W. S., DUNHAM, I., DENOEUD, F., REYMOND, A., KAPRANOV, P., ROZOWSKY, J., ZHENG, D., CASTELO, R., FRANKISH, A., HARROW, J., GHOSH, S., SANDELIN, A., HOFACKER, I. L., BAERTSCH, R., KEEFE, D., DIKE, S., CHENG, J., HIRSCH, H. A., SEKINGER, E. A., LAGARDE, J., ABRIL, J. F., SHAHAB, A., FLAMM, C., FRIED, C., HACKERMULLER, J., HERTEL, J., LINDEMEYER, M., MISSAL, K., TANZER, A., WASHIETL, S., KORBEL, J., EMANUELSSON, O., PEDERSEN, J. S., HOLROYD, N., TAYLOR, R., SWARBRECK, D.,

MATTHEWS, N., DICKSON, M. C., THOMAS, D. J., WEIRAUCH, M. T., et al. 2007. Identification and analysis of functional elements in 1% of the human genome by the ENCODE pilot project. *Nature,* 447**,** 799-816.
CORMACK, B. P. & STRUHL, K. 1992. The TATA-binding protein is required for transcription by all three nuclear RNA polymerases in yeast cells. *Cell,* 69**,** 685-96.
CORNELISSEN, T., HADDAD, D., WAUTERS, F., VAN HUMBEECK, C., MANDEMAKERS, W., KOENTJORO, B., SUE, C., GEVAERT, K., DE STROOPER, B., VERSTREKEN, P. & VANDENBERGHE, W. 2014. The deubiquitinase USP15 antagonizes Parkin-mediated mitochondrial ubiquitination and mitophagy. *Human Molecular Genetics,* 2**3,** 5227-5242.
COULSON, J. M. 2005. Transcriptional regulation: Cancer, neurons and the REST. *Current Biology,* 15**,** R665-R668.
COULSON, J. M. Unpublished.
COULSON, J. M., EDGSON, J. L., WOLL, P. J. & QUINN, J. P. 2000. A splice variant of the neuron-restrictive silencer factor repressor is expressed in small cell lung cancer: A potential role in derepression of neuroendocrine genes and a useful clinical marker. *Cancer Research,* 60**,** 1840-1844.
COULSON, J. M., FISKERSTRAND, C. E., WOLL, P. J. & QUINN, J. P. 1999a. Arginine vasopressin promoter regulation is mediated by a neuron-restrictive silencer element in small cell lung cancer. *Cancer Research,* 59**,** 5123-5127.
COULSON, J. M., STANLEY, J. & WOLL, P. J. 1999b. Tumour-specific arginine vasopressin promoter activation in small-cell lung cancer. *British Journal of Cancer,* 80**,** 1935-1944.
COVEY, M. V., STREB, J. W., SPEKTOR, R. & BALLAS, N. 2012. REST regulates the pool size of the different neural lineages by restricting the generation of neurons and oligodendrocytes from neural stem/progenitor cells. *Development,* 139**,** 2878-2890.
COWAN, J. M., POWERS, J. & TISCHLER, A. S. 1996. Assignment of the REST gene to 4q12 by fluorescence in situ hybridization. *Genomics,* 34**,** 260-262.
COX, J. & MANN, M. 2008. MaxQuant enables high peptide identification rates, individualized p.p.b.-range mass accuracies and proteome-wide protein quantification. *Nature Biotechnology,* 2**6,** 1367-1372.
COX, J., NEUHAUSER, N., MICHALSKI, A., SCHELTEMA, R. A., OLSEN, J. V. & MANN, M. 2011. Andromeda: a peptide search engine integrated into the MaxQuant environment. *Journal of Proteome Research,* 10**,** 1794-1805.
CROWE, S. O., PHAM, G. H., ZIEGLER, J. C., DEOL, K. K., GUENETTE, R. G., GE, Y. & STRIETER, E. R. 2016. Subunit-Specific Labeling of Ubiquitin Chains by Using Sortase: Insights into the Selectivity of Deubiquitinases. *Chembiochem,* 17**,** 1525-1531.
D'ALESSANDRO, R., KLAJN, A. & MELDOLESI, J. 2009. Expression of dense‐core vesicles and of their exocytosis are governed by the

repressive transcription factor NRSF/REST. *Annals of the New York Academy of Sciences,* 1152**,** 194-200.
D'ALESSANDRO, R., KLAJN, A., STUCCHI, L., PODINI, P., MALOSIO, M. L. & MELDOLESI, J. 2008. Expression of the neurosecretory process in PC12 cells is governed by REST. *Journal of Neurochemistry,* 105**,** 1369-1383.
DAS, C. M., TAYLOR, P., GIREUD, M., SINGH, A., LEE, D., FULLER, G., JI, L., FANGUSARO, J., RAJARAM, V., GOLDMAN, S., EBERHART, C. & GOPALAKRISHNAN, V. 2013. The deubiquitylase USP37 links REST to the control of p27 stability and cell proliferation. *Oncogene,* 32**,** 1691-1701.
DATTA, M. & BHATTACHARYYA, N. P. 2011. Regulation of RE1 Protein Silencing Transcription Factor (REST) Expression by HIP1 Protein Interactor (HIPPI). *Journal of Biological Chemistry,* 286**,** 33759-33769.
DAVE, K. A., NORRIS, E. L., BUKREYEV, A. A., HEADLAM, M. J., BUCHHOLZ, U. J., SINGH, T., COLLINS, P. L. & GORMAN, J. J. 2014. A comprehensive proteomic view of responses of A549 type II alveolar epithelial cells to human respiratory syncytial virus infection. *Molecular & Cellular Proteomics,* 13**,** 3250-3269.
DI MARTINO, J., HENRIET, E., EZZOUKHRY, Z., GOETZ, J. G., MOREAU, V. & SALTEL, F. 2016. The microenvironment controls invadosome plasticity. *Journal of Cell Science,* 129**,** 1759-1768.
DIETRICH, N., LERDRUP, M., LANDT, E., AGRAWAL-SINGH, S., BAK, M., TOMMERUP, N., RAPPSILBER, J., SÖDERSTEN, E. & HANSEN, K. 2012. REST-mediated recruitment of polycomb repressor complexes in mammalian cells. *PLOS Genetics,* 8**,** e1002494.
DINKOVA-KOSTOVA, A. T. & ABRAMOV, A. Y. 2015. The emerging role of Nrf2 in mitochondrial function. *Free Radical Biology and Medicine,* 88**,** 179-188.
DOBSON, T. H. W. H. W., HATCHER, R. J., SWAMINATHAN, J., DAS, C. M., SHAIK, S., TAO, R.-H. H., MILITE, C., CASTELLANO, S., TAYLOR, P. H., SBARDELLA, G. & GOPALAKRISHNAN, V. 2017. Regulation of USP37 Expression by REST-Associated G9a-Dependent Histone Methylation. *Molecular Cancer Research,* 15**,** 1073-1084.
DOMINGUEZ, D., TSAI, Y.-H. H., WEATHERITT, R., WANG, Y., BLENCOWE, B. J. & WANG, Z. 2016. An extensive program of periodic alternative splicing linked to cell cycle progression. *eLife,* 5**,** e10288.
DOUMA, S., VAN LAAR, T., ZEVENHOVEN, J., MEUWISSEN, R., VAN GARDEREN, E. & PEEPER, D. S. 2004. Suppression of anoikis and induction of metastasis by the neurotrophic receptor TrkB. *Nature,* 430**,** 1034-1039.
DURCAN, T. M. & FON, E. A. 2013. Ataxin-3 and its E3 partners: implications for Machado–Joseph disease. *Frontiers in Neurology,* 4**,** 46.

DURCAN, T. M. & FON, E. A. 2015. The three 'P's of mitophagy: PARKIN, PINK1, and post-translational modifications. *Genes & Development,* 29**,** 989-999.
DURCAN, T. M., TANG, M. Y., PERUSSE, J. R., DASHTI, E. A., AGUILETA, M. A., MCLELLAND, G. L., GROS, P., SHALER, T. A., FAUBERT, D., COULOMBE, B. & FON, E. A. 2014. USP8 regulates mitophagy by removing K6-linked ubiquitin conjugates from parkin. *The EMBO Journal,* 33**,** 2473-2491.
DUTTLER, S., PECHMANN, S. & FRYDMAN, J. 2013. Principles of cotranslational ubiquitination and quality control at the ribosome. *Molecular Cell,* 50**,** 379-393.
EICHHORN, P. J., RODÓN, L., GONZÀLEZ-JUNCÀ, A., DIRAC, A., GILI, M., MARTÍNEZ-SÁEZ, E., AURA, C., BARBA, I., PEG, V., PRAT, A., CUARTAS, I., JIMENEZ, J., GARCÍA-DORADO, D., SAHUQUILLO, J., BERNARDS, R., BASELGA, J. & SEOANE, J. 2012. USP15 stabilizes TGF-β receptor I and promotes oncogenesis through the activation of TGF-β signaling in glioblastoma. *Nature Medicine,* 18**,** 429-435.
ELLIOTT, P. R., LIU, H., PASTOK, M. W., GROSSMANN, G. J. J., RIGDEN, D. J., CLAGUE, M. J., URBÉ, S. & BARSUKOV, I. L. 2011. Structural variability of the ubiquitin specific protease DUSP-UBL double domains. *FEBS Letters,* 585**,** 3385-3390.
EMMERICH, C. H., ORDUREAU, A., STRICKSON, S., ARTHUR, J. S., PEDRIOLI, P. G., KOMANDER, D. & COHEN, P. 2013. Activation of the canonical IKK complex by K63/M1-linked hybrid ubiquitin chains. *Proceedings of the National Academy of Sciences of the United States of America,* 110**,** 15247-15252.
FARONATO, M., PATEL, V., DARLING, S., DEARDEN, L., CLAGUE, M. J., URBE, S. & COULSON, J. M. 2013. The deubiquitylase USP15 stabilizes newly synthesized REST and rescues its expression at mitotic exit. *Cell Cycle,* 12**,** 1964-77.
FARONATO, M., URBE, S. & COULSON, J. M. 2011. USP15 (ubiquitin specific peptidase 15). *Atlas Genet Cytogenet Oncol Haematol,* 15**,** 645-651.
FELDMANN, A., IVANEK, R., MURR, R., GAIDATZIS, D., BURGER, L. & SCHUBELER, D. 2013. Transcription factor occupancy can mediate active turnover of DNA methylation at regulatory regions. *PLOS Genetics,* 9**,** e1003994.
FERLAY, J., SOERJOMATARAM, I., DIKSHIT, R., ESER, S., MATHERS, C., REBELO, M., PARKIN, D. M., FORMAN, D. & BRAY, F. 2015. Cancer incidence and mortality worldwide: sources, methods and major patterns in GLOBOCAN 2012. *International Journal of Cancer,* 136**,** 86.
FIELDING, A. B., DARLING, S., CONCANNON, M. & COULSON, J. M. manuscript in preparation.
FORMISANO, L., GUIDA, N., LAUDATI, G., BOSCIA, F., ESPOSITO, A., SECONDO, A., DI RENZO, G. & CANZONIERO, L. M. 2015. Extracellular signal-related kinase 2/specificity protein 1/specificity

protein 3/repressor element-1 silencing transcription factor pathway is involved in Aroclor 1254-induced toxicity in SH-SY5Y neuronal cells. *Journal of Neuroscience Research,* 93**,** 167-177.

FRANKEL, A. D., BERG, J. M. & PABO, C. O. 1987. Metal-dependent folding of a single zinc finger from transcription factor IIIA. *Proceedings of the National Academy of Sciences of the United States of America,* 84**,** 4841-4845.

FUKAGAI, K., WAKU, T., CHOWDHURY, A. M. M., KUBO, K., MATSUMOTO, M., KATO, H., NATSUME, T., TSURUTA, F., CHIBA, T., TANIGUCHI, H. & KOBAYASHI, A. 2016. USP15 stabilizes the transcription factor Nrf1 in the nucleus, promoting the proteasome gene expression. *Biochemical and Biophysical Research Communications,* 478**,** 363-370.

FULLER, G. N., SU, X., PRICE, R. E., COHEN, Z. R., LANG, F. F., SAWAYA, R. & MAJUMDER, S. 2005. Many human medulloblastoma tumors overexpress repressor element-1 silencing transcription (REST)/neuron-restrictive silencer factor, which can be functionally countered by REST-VP16. *Molecular Cancer Therapeutics,* 4**,** 343-349.

GARRIDO, C., GALLUZZI, L., BRUNET, M., PUIG, P. E., DIDELOT, C. & KROEMER, G. 2006. Mechanisms of cytochrome c release from mitochondria. *Cell Death and Differentiation,* 13**,** 1423-1433.

GAZDAR, A. F. & MINNA, J. D. 1996. NCI series of cell lines: an historical perspective. *Journal of Cellular Biochemistry Supplement,* 24**,** 1-11.

GERLACH, B., CORDIER, S. M., SCHMUKLE, A. C., EMMERICH, C. H., RIESER, E., HAAS, T. L., WEBB, A. I., RICKARD, J. A., ANDERTON, H., WONG, W. W., NACHBUR, U., GANGODA, L., WARNKEN, U., PURCELL, A. W., SILKE, J. & WALCZAK, H. 2011. Linear ubiquitination prevents inflammation and regulates immune signalling. *Nature,* 471**,** 591-596.

GIAMPAZOLIAS, E. & TAIT, S. W. 2016. Mitochondria and the hallmarks of cancer. *The FEBS Journal,* 283**,** 803-814.

GIARD, D. J., AARONSON, S. A., TODARO, G. J., ARNSTEIN, P., KERSEY, J. H., DOSIK, H. & PARKS, W. P. 1973. In vitro cultivation of human tumors: establishment of cell lines derived from a series of solid tumors. *Journal of the National Cancer Institute,* 51**,** 1417-1423.

GILMORE, A. P. 2005. Anoikis. *Cell Death and Differentiation,* 12**,** 1473-1477.

GOLDKNOPF, I. L. & BUSCH, H. 1977. Isopeptide linkage between nonhistone and histone 2A polypeptides of chromosomal conjugate-protein A24. *Proceedings of the National Academy of Sciences of the United States of America,* 74**,** 864-868.

GOLDSTEIN, G., SCHEID, M., HAMMERLING, U., SCHLESINGER, D. H., NIALL, H. D. & BOYSE, E. A. 1975. Isolation of a polypeptide that has lymphocyte-differentiating properties and is probably represented universally in living cells. *Proceedings of the National Academy of Sciences of the United States of America,* 72**,** 11-15.

GOWHER, H., BRICK, K., CAMERINI-OTERO, R. D. & FELSENFELD, G. 2012. Vezf1 protein binding sites genome-wide are associated with pausing of elongating RNA polymerase II. *Proceedings of the National Academy of Sciences of the United States of America,* 109**,** 2370-2375.

GREENWAY, D. J., STREET, M., JEFFRIES, A. & BUCKLEY, N. J. 2007. RE1 Silencing transcription factor maintains a repressive chromatin environment in embryonic hippocampal neural stem cells. *Stem Cells,* 25**,** 354-363.

GRIMES, J. A., NIELSEN, S. J., BATTAGLIOLI, E., MISKA, E. A., SPEH, J. C., BERRY, D. L., ATOUF, F., HOLDENER, B. C., MANDEL, G. & KOUZARIDES, T. 2000. The co-repressor mSin3A is a functional component of the REST-CoREST repressor complex. *The Journal of Biological Chemistry,* 275**,** 9461-9467.

GRISS, J., MARTÍN, M., O'DONOVAN, C., APWEILER, R., HERMJAKOB, H. & VIZCAÍNO, J. A. 2011. Consequences of the discontinuation of the International Protein Index (IPI) database and its substitution by the UniProtKB "complete proteome" sets. *Proteomics,* 11**,** 4434-4438.

GUAN, H. & RICCIARDI, R. P. 2012. Transformation by E1A oncoprotein involves ubiquitin-mediated proteolysis of the neuronal and tumor repressor REST in the nucleus. *Journal of Virology,* 86**,** 5594-602.

GUARDAVACCARO, D., FRESCAS, D., DORRELLO, N. V., PESCHIAROLI, A., MULTANI, A. S., CARDOZO, T., LASORELLA, A., IAVARONE, A., CHANG, S., HERNANDO, E. & PAGANO, M. 2008. Control of chromosome stability by the beta-TrCP-REST-Mad2 axis. *Nature,* 452**,** 365-369.

GUI, J.-F., LANE, W. S. & FU, X.-D. 1994. A serine kinase regulates intracellular localization of splicing factors in the cell cycle. *Nature,* 369**,** 678-682.

GURROLA-DIAZ, C., LACROIX, J., DIHLMANN, S., BECKER, C.-M. & DOEBERITZ, M. 2003. Reduced expression of the neuron restrictive silencer factor permits transcription of glycine receptor 1 subunit in small-cell lung cancer cells. *Oncogene,* 22**,** 5636-5645.

HAKIMI, M. A., BOCHAR, D. A., CHENOWETH, J., LANE, W. S., MANDEL, G. & SHIEKHATTAR, R. 2002. A core–BRAF35 complex containing histone deacetylase mediates repression of neuronal-specific genes. *Proceedings of the National Academy of Sciences of the United States of America,* 99**,** 7420-7425.

HAMMOND-MARTEL, I., YU, H. & AFFAR, E. B. L. B. 2012. Roles of ubiquitin signaling in transcription regulation. *Cellular Signalling,* 24**,** 410-421.

HANAHAN, D. & WEINBERG, R. A. 2011. Hallmarks of Cancer: The Next Generation. *Cell,* 144**,** 646-674.

HARPER, S., BESONG, T. M., EMSLEY, J., SCOTT, D. J. & DREVENY, I. 2011. Structure of the USP15 N-terminal domains: a β-hairpin mediates close association between the DUSP and UBL domains. *Biochemistry,* 50**,** 7995-8004.

HAYES, S. D., LIU, H., MACDONALD, E., SANDERSON, C. M., COULSON, J. M., CLAGUE, M. J. & URBE, S. 2012. Direct and Indirect Control of Mitogen-activated Protein Kinase Pathway-associated Components, BRAP/IMP E3 Ubiquitin Ligase and CRAF/RAF1 Kinase, by the Deubiquitylating Enzyme USP15. *Journal of Biological Chemistry,* 287**,** 43007-43018.

HEIDEKER, J. & WERTZ, I. E. 2015. DUBs, the regulation of cell identity and disease. *The Biochemical Journal,* 465**,** 1-26.

HENDIFAR, A. E., MARCHEVSKY, A. M. & TULI, R. 2017. Neuroendocrine Tumors of the Lung: Current Challenges and Advances in the Diagnosis and Management of Well-Differentiated Disease. *Journal of Thoracic Oncology,* 12**,** 425-436.

HEPPELL-PARTON, A. C., NACHEVA, E., CARTER, N. P., BERGH, J., OGILVIE, D. & RABBITTS, P. H. 1999. Elucidation of the mechanism of homozygous deletion of 3p12-13 in the U2020 cell line reveals the unexpected involvement of other chromosomes. *Cancer Genetics and Cytogenetics,* 111**,** 105-110.

HERHAUS, L., AL-SALIHI, M. A., DINGWELL, K. S., CUMMINS, T. D., WASMUS, L., VOGT, J., EWAN, R., BRUCE, D., MACARTNEY, T., WEIDLICH, S., SMITH, J. C. & SAPKOTA, G. P. 2014. USP15 targets ALK3/BMPR1A for deubiquitylation to enhance bone morphogenetic protein signalling. *Open Biology,* 4**,** 140065.

HERNANDEZ-VALLADARES, M., ARAN, V. & PRIOR, I. A. 2014. Quantitative proteomic analysis of compartmentalized signaling networks. *Methods in Enzymology,* 535**,** 309-325.

HERNANDEZ-VALLADARES, M. & PRIOR, I. A. 2015. Comparative proteomic analysis of compartmentalised Ras signalling. *Scientific Reports,* 5**,** 17307.

HERSHKO, A., CIECHANOVER, A., HELLER, H., HAAS, A. L. & ROSE, I. A. 1980. Proposed role of ATP in protein breakdown: conjugation of protein with multiple chains of the polypeptide of ATP-dependent proteolysis. *Proceedings of the National Academy of Sciences of the United States of America,* 77**,** 1783-1786.

HETFELD, B. K., HELFRICH, A., KAPELARI, B., SCHEEL, H., HOFMANN, K., GUTERMAN, A., GLICKMAN, M., SCHADE, R., KLOETZEL, P.-M. M. & DUBIEL, W. 2005. The zinc finger of the CSN-associated deubiquitinating enzyme USP15 is essential to rescue the E3 ligase Rbx1. *Current Biology,* 15**,** 1217-1221.

HOEGE, C., PFANDER, B., MOLDOVAN, G.-L. L., PYROWOLAKIS, G. & JENTSCH, S. 2002. RAD6-dependent DNA repair is linked to modification of PCNA by ubiquitin and SUMO. *Nature,* 419**,** 135-141.

HOHL, M. & THIEL, G. 2005. Cell type‐specific regulation of RE‐1 silencing transcription factor (REST) target genes. *European Journal of Neuroscience,* 22**,** 2216-2230.

HOLMSTRÖM, K. M., KOSTOV, R. V. & DINKOVA-KOSTOVA, A. T. 2016. The multifaceted role of Nrf2 in mitochondrial function. *Current Opinion in Toxicology,* 1**,** 80-91.

HOSPENTHAL, M. K., MEVISSEN, T. E. & KOMANDER, D. 2015. Deubiquitinase-based analysis of ubiquitin chain architecture using Ubiquitin Chain Restriction (UbiCRest). *Nature Protocols,* 10**,** 349-361.
HUANG, D. W., SHERMAN, B. T. & LEMPICKI, R. A. 2009a. Bioinformatics enrichment tools: paths toward the comprehensive functional analysis of large gene lists. *Nucleic Acids Research,* 37**,** 1-13.
HUANG, D. W., SHERMAN, B. T. & LEMPICKI, R. A. 2009b. Systematic and integrative analysis of large gene lists using DAVID bioinformatics resources. *Nature Protocols,* 4**,** 44-57.
HUANG, X., LANGELOTZ, C., HETFELD-PECHOC, B. K., SCHWENK, W. & DUBIEL, W. 2009c. The COP9 signalosome mediates beta-catenin degradation by deneddylation and blocks adenomatous polyposis coli destruction via USP15. *Journal of Molecular Biology,* 391**,** 691-702.
HUANG, Y., MYERS, S. J. & DINGLEDINE, R. 1999. Transcriptional repression by REST: recruitment of Sin3A and histone deacetylase to neuronal genes. *Nature Neuroscience,* 2**,** 867-872.
HUANG, Z., WU, Q., GURYANOVA, O. A., CHENG, L., SHOU, W., RICH, J. N. & BAO, S. 2011. Deubiquitylase HAUSP stabilizes REST and promotes maintenance of neural progenitor cells. *Nature Cell Biology,* 13**,** 142-U91.
HUNT, L. T. & DAYHOFF, M. O. 1977. Amino-terminal sequence identity of ubiquitin and the nonhistone component of nuclear protein A24. *Biochemical and Biophysical Research Communications,* 74**,** 650-655.
HUSCHTSCHA, L. I. & HOLLIDAY, R. 1983. Limited and unlimited growth of SV40-transformed cells from human diploid MRC-5 fibroblasts. *Journal of Cell Science,* 63**,** 77-99.
INUI, M., MANFRIN, A., MAMIDI, A., MARTELLO, G., MORSUT, L., SOLIGO, S., ENZO, E., MORO, S., POLO, S., DUPONT, S., CORDENONSI, M. & PICCOLO, S. 2011. USP15 is a deubiquitylating enzyme for receptor-activated SMADs. *Nature Cell Biology,* 13**,** 1368-1375.
JACOBS, J. P., JONES, C. M. & BAILLE, J. P. 1970. Characteristics of a human diploid cell designated MRC-5. *Nature,* 227**,** 168-170.
JAKOBS, H. H., MIKULA, M., HAVEMEYER, A., STRZALKOWSKA, A., BOROWA-CHMIELAK, M., DZWONEK, A., GAJEWSKA, M., HENNIG, E. E., OSTROWSKI, J. & CLEMENT, B. 2014. The N-reductive system composed of mitochondrial amidoxime reducing component (mARC), cytochrome b5 (CYB5B) and cytochrome b5 reductase (CYB5R) is regulated by fasting and high fat diet in mice. *PLOS ONE,* 9**,** e105371.
JENUWEIN, T. & ALLIS, C. D. 2001. Translating the histone code. *Science,* 293**,** 1074-1080.
JIANG, L., YAO, M., SHI, J., SHEN, P., NIU, G. & FEI, J. 2008. Yin yang 1 directly regulates the transcription of RE‐1 silencing transcription factor. *Journal of Neuroscience Research,* 86**,** 1209-1216.
JOHNSON, D. S., MORTAZAVI, A., MYERS, R. M. & WOLD, B. 2007. Genome-wide mapping of in vivo protein-DNA interactions. *Science,* 316**,** 1497-1502.

JOHNSON, R., GAMBLIN, R. J., OOI, L., BRUCE, A. W., DONALDSON, I. J., WESTHEAD, D. R., WOOD, I. C., JACKSON, R. M. & BUCKLEY, N. J. 2006. Identification of the REST regulon reveals extensive transposable element-mediated binding site duplication. *Nucleic Acids Research,* 34**,** 3862-3877.

JOHNSON, R., RICHTER, N., BOGU, G. K., BHINGE, A., TENG, S. W., CHOO, S. H., ANDRIEUX, L. O., DE BENEDICTIS, C., JAUCH, R. & STANTON, L. W. 2012. A genome-wide screen for genetic variants that modify the recruitment of REST to its target genes. *PLOS Genetics,* 8**,** e1002624.

JOHNSON, R., TEH, C. H., KUNARSO, G., WONG, K. Y., SRINIVASAN, G., COOPER, M. L., VOLTA, M., CHAN, S. S., LIPOVICH, L., POLLARD, S. M., KARUTURI, R. K., WEI, C.-L. L., BUCKLEY, N. J. & STANTON, L. W. 2008. REST regulates distinct transcriptional networks in embryonic and neural stem cells. *PLOS Biology,* 6**,** e256.

JOHNSON, R., TEH, C. H.-L., JIA, H., VANISRI, R. R., PANDEY, T., LU, Z.-H., BUCKLEY, N. J., STANTON, L. W. & LIPOVICH, L. 2009. Regulation of neural macroRNAs by the transcriptional repressor REST. *RNA,* 15**,** 85-96.

JONGSMA, M. L., BERLIN, I., WIJDEVEN, R. H., JANSSEN, L., JANSSEN, G. M., GARSTKA, M. A., JANSSEN, H., MENSINK, M., VAN VEELEN, P. A., SPAAPEN, R. M. & NEEFJES, J. 2016. An ER-Associated Pathway Defines Endosomal Architecture for Controlled Cargo Transport. *Cell,* 166**,** 152-166.

JØRGENSEN, H. F., CHEN, Z.-F. F., MERKENSCHLAGER, M. & FISHER, A. G. 2009a. Is REST required for ESC pluripotency? *Nature,* 457**,** E4-E5.

JØRGENSEN, H. F., TERRY, A., BERETTA, C., PEREIRA, C. F., LELEU, M., CHEN, Z.-F. F., KELLY, C., MERKENSCHLAGER, M. & FISHER, A. G. 2009b. REST selectively represses a subset of RE1-containing neuronal genes in mouse embryonic stem cells. *Development,* 136**,** 715-721.

KAISER, S. E., RILEY, B. E., SHALER, T. A., TREVINO, R. S., BECKER, C. M., SCHULMAN, H. & KOPITO, R. R. 2011. Protein standard absolute quantification (PSAQ) method for the measurement of cellular ubiquitin pools. *Nature Methods,* 8**,** 691-696.

KALLUNKI, P., EDELMAN, G. M. & JONES, F. S. 1998. The neural restrictive silencer element can act as both a repressor and enhancer of L1 cell adhesion molecule gene expression during postnatal development. *Proceedings of the National Academy of Sciences of the United States of America,* 95**,** 3233-3238.

KANEKO, N., HWANG, J.-Y., GERTNER, M., PONTARELLI, F. & ZUKIN, R. 2014. Casein Kinase 1 Suppresses Activation of REST in Insulted Hippocampal Neurons and Halts Ischemia-Induced Neuronal Death. *The Journal of Neuroscience,* 34**,** 6030-6039.

KARLIN, K. L., MONDAL, G., HARTMAN, J. K., TYAGI, S., KURLEY, S. J., BLAND, C. S., HSU, T. Y., RENWICK, A., FANG, J. E., MIGLIACCIO, I., CALLAWAY, C., NAIR, A., DOMINGUEZ-VIDANA, R., NGUYEN,

D. X., OSBORNE, C. K., SCHIFF, R., YU-LEE, L.-Y. Y., JUNG, S. Y., EDWARDS, D. P., HILSENBECK, S. G., ROSEN, J. M., ZHANG, X. H., SHAW, C. A., COUCH, F. J. & WESTBROOK, T. F. 2014. The oncogenic STP axis promotes triple-negative breast cancer via degradation of the REST tumor suppressor. *Cell Reports,* 9**,** 1318-1332.

KELDER, T., VAN IERSEL, M. P., HANSPERS, K., KUTMON, M., CONKLIN, B. R., EVELO, C. T. & PICO, A. R. 2012. WikiPathways: building research communities on biological pathways. *Nucleic Acids Research,* 40**,** 7.

KEMP, D. M., LIN, J. C. & HABENER, J. F. 2003. Regulation of Pax4 paired homeodomain gene by neuron-restrictive silencer factor. *The Journal of Biological Chemistry,* 278**,** 35057-35062.

KENT, W. J. 2002. BLAT--the BLAST-like alignment tool. *Genome Research,* 12**,** 656-664.

KENT, W. J., SUGNET, C. W., FUREY, T. S., ROSKIN, K. M., PRINGLE, T. H., ZAHLER, A. M. & HAUSSLER, D. 2002. The human genome browser at UCSC. *Genome Research,* 12**,** 996-1006.

KERSEY, P. J., DUARTE, J., WILLIAMS, A., KARAVIDOPOULOU, Y., BIRNEY, E. & APWEILER, R. 2004. The International Protein Index: an integrated database for proteomics experiments. *Proteomics,* 4**,** 1985-1988.

KLEIN, M. E., LIOY, D. T., MA, L., IMPEY, S., MANDEL, G. & GOODMAN, R. H. 2007. Homeostatic regulation of MeCP2 expression by a CREB-induced microRNA. *Nature Neuroscience,* 10**,** 1513-1514.

KLUG, A. 2010. The discovery of zinc fingers and their applications in gene regulation and genome manipulation. *Annual Review of Biochemistry,* 79**,** 213-231.

KOENIGSBERGER, C., CHICCA, J. J., AMOUREUX, M. C., EDELMAN, G. M. & JONES, F. S. 2000. Differential regulation by multiple promoters of the gene encoding the neuron-restrictive silencer factor. *Proceedings of the National Academy of Sciences of the United States of America,* 97**,** 2291-2296.

KOJIMA, T., MURAI, K., NARUSE, Y., TAKAHASHI, N. & MORI, N. 2001. Cell-type non-selective transcription of mouse and human genes encoding neural-restrictive silencer factor. *Molecular Brain Research,* 90**,** 174-186.

KOMANDER, D. 2010. Mechanism, specificity and structure of the deubiquitinases. *Sub-cellular Biochemistry,* 54**,** 69-87.

KOMANDER, D., CLAGUE, M. J. & URBÉ, S. 2009. Breaking the chains: structure and function of the deubiquitinases. *Nature Reviews Molecular Cell Biology,* 10**,** 550-563.

KOMANDER, D. & RAPE, M. 2012. The ubiquitin code. *Annual Review of Biochemistry,* 81**,** 203-229.

KORRODI-GREGÓRIO, L., SOTO-CERRATO, V., VITORINO, R., FARDILHA, M. & PÉREZ-TOMÁS, R. 2016. From Proteomic Analysis to Potential Therapeutic Targets: Functional Profile of Two Lung

Cancer Cell Lines, A549 and SW900, Widely Studied in Pre-Clinical Research. *PLOS ONE,* 11**,** e0165973.
KOTANI, Y., MORITO, D., SAKATA, K., AINUKI, S., SUGIHARA, M., HATTA, T., IEMURA, S.-I. I., TAKASHIMA, S., NATSUME, T. & NAGATA, K. 2017. Alternative exon skipping biases substrate preference of the deubiquitylase USP15 for mysterin/RNF213, the moyamoya disease susceptibility factor. *Scientific Reports,* 7**,** 44293.
KOUZARIDES, T. 2007. Chromatin modifications and their function. *Cell,* 128**,** 693-705.
KREISLER, A., STRISSEL, P. L., STRICK, R., NEUMANN, S. B., SCHUMACHER, U. & BECKER, C. M. M. 2010. Regulation of the NRSF/REST gene by methylation and CREB affects the cellular phenotype of small-cell lung cancer. *Oncogene,* 29**,** 5828-5838.
KUMAR, S., TOMOOKA, Y. & NODA, M. 1992. Identification of a set of genes with developmentally down-regulated expression in the mouse brain. *Biochemical and Biophysical Research Communications,* 185**,** 1155-1161.
KUTMON, M., RIUTTA, A., NUNES, N., HANSPERS, K., WILLIGHAGEN, E. L., BOHLER, A., MÉLIUS, J., WAAGMEESTER, A., SINHA, S. R., MILLER, R., COORT, S. L., CIRILLO, E., SMEETS, B., EVELO, C. T. & PICO, A. R. 2016. WikiPathways: capturing the full diversity of pathway knowledge. *Nucleic Acids Research,* 44**,** 94.
KUTMON, M., VAN IERSEL, M. P., BOHLER, A., KELDER, T., NUNES, N., PICO, A. R. & EVELO, C. T. 2015. PathVisio 3: An Extendable Pathway Analysis Toolbox. *PLOS Computational Biology,* 11**,** e1004085.
LAN, F., COLLINS, R. E., CEGLI, D. R., ALPATOV, R., HORTON, J. R., SHI, X., GOZANI, O., CHENG, X. & SHI, Y. 2007. Recognition of unmethylated histone H3 lysine 4 links BHC80 to LSD1-mediated gene repression. *Nature,* 448**,** 718-722.
LANNING, N. J., LOOYENGA, B. D., KAUFFMAN, A. L., NIEMI, N. M., SUDDERTH, J., DEBERARDINIS, R. J. & MACKEIGAN, J. P. 2014. A mitochondrial RNAi screen defines cellular bioenergetic determinants and identifies an adenylate kinase as a key regulator of ATP levels. *Cell Reports,* 7**,** 907-917.
LAUWERS, E., JACOB, C. & ANDRÉ, B. 2009. K63-linked ubiquitin chains as a specific signal for protein sorting into the multivesicular body pathway. *The Journal of Cell Biology,* 185**,** 493-502.
LAWINGER, P., VENUGOPAL, R., GUO, Z. S., IMMANENI, A., SENGUPTA, D., LU, W., RASTELLI, L., MARIN DIAS CARNEIRO, A., LEVIN, V., FULLER, G. N., ECHELARD, Y. & MAJUMDER, S. 2000. The neuronal repressor REST/NRSF is an essential regulator in medulloblastoma cells. *Nature Medicine,* 6**,** 826-831.
LECHNER, J. F., TOKIWA, T., LAVECK, M., BENEDICT, W. F., BANKS-SCHLEGEL, S., YEAGER, H., BANERJEE, A. & HARRIS, C. C. 1985. Asbestos-associated chromosomal changes in human mesothelial cells. *Proceedings of the National Academy of Sciences of the United States of America,* 82**,** 3884-3888.

LEE, J. H., SHIMOJO, M., CHAI, Y. G. & HERSH, L. B. 2000. Studies on the interaction of REST4 with the cholinergic repressor element-1/neuron restrictive silencer element. *Molecular Brain Research,* 80**,** 88-98.

LEE, N. S., EVGRAFOV, O. V., SOUAIAIA, T., BONYAD, A., HERSTEIN, J., LEE, J. Y., KIM, J., NING, Y., SIXTO, M., WEITZ, A. C., LENZ, H.-J. J., WANG, K., KNOWLES, J. A., PRESS, M. F., SALVATERRA, P. M., SHUNG, K. K. & CHOW, R. H. 2015. Non-coding RNAs derived from an alternatively spliced REST transcript (REST-003) regulate breast cancer invasiveness. *Scientific Reports,* 5**,** 11207.

LEICHTER, M. & THIEL, G. 1999. Transcriptional repression by the zinc finger protein REST is mediated by titratable nuclear factors. *The European Journal of Neuroscience,* 11**,** 1937-1946.

LEPAGNOL-BESTEL, A.-M., ZVARA, A., MAUSSION, G., QUIGNON, F., NGIMBOUS, B., RAMOZ, N., IMBEAUD, S., LOE-MIE, Y., BENIHOUD, K., AGIER, N., SALIN, P. A., CARDONA, A., KHUNG-SAVATOVSKY, S., KALLUNKI, P., DELABAR, J.-M., PUSKAS, L. G., DELACROIX, H., AGGERBECK, L., DELEZOIDE, A.-L., DELATTRE, O., GORWOOD, P., MOALIC, J.-M. & SIMONNEAU, M. 2009. DYRK1A interacts with the REST/NRSF-SWI/SNF chromatin remodelling complex to deregulate gene clusters involved in the neuronal phenotypic traits of Down syndrome. *Human Molecular Genetics,* 18**,** 1405-1414.

LI, Y., DONMEZ, N., SAHINALP, C., XIE, N., WANG, Y., XUE, H., MO, F., BELTRAN, H., GLEAVE, M., WANG, Y., COLLINS, C. & DONG, X. 2017. SRRM4 Drives Neuroendocrine Transdifferentiation of Prostate Adenocarcinoma Under Androgen Receptor Pathway Inhibition. *European Urology,* 71**,** 68-78.

LIAKOPOULOS, D., DOENGES, G., MATUSCHEWSKI, K. & JENTSCH, S. 1998. A novel protein modification pathway related to the ubiquitin system. *The EMBO Journal,* 17**,** 2208-2214.

LIANG, H., STUDACH, L., HULLINGER, R. L., XIE, J. & ANDRISANI, O. M. 2014. Down-regulation of RE-1 silencing transcription factor (REST) in advanced prostate cancer by hypoxia-induced miR-106b~ 25. *Experimental Cell Research,* 320**,** 188-199.

LIANG, J.-R. R., MARTINEZ, A., LANE, J. D., MAYOR, U., CLAGUE, M. J. & URBÉ, S. 2015. USP30 deubiquitylates mitochondrial Parkin substrates and restricts apoptotic cell death. *EMBO Reports,* 16**,** 618-627.

LIM, J. S., IBASETA, A., FISCHER, M. M., CANCILLA, B., O'YOUNG, G., CRISTEA, S., LUCA, V. C., YANG, D., JAHCHAN, N. S., HAMARD, C., ANTOINE, M., WISLEZ, M., KONG, C., CAIN, J., LIU, Y.-W. W., KAPOUN, A. M., GARCIA, K. C., HOEY, T., MURRIEL, C. L. & SAGE, J. 2017. Intratumoural heterogeneity generated by Notch signalling promotes small-cell lung cancer. *Nature,* 545**,** 360-364.

LIU, Z., LIU, M., NIU, G., CHENG, Y. & FEI, J. 2009. Genome-wide identification of target genes repressed by the zinc finger transcription factor REST/NRSF in the HEK 293 cell line. *Acta Biochimica Et Biophysica Sinica,* 41**,** 1008-1017.

LONG, L., THELEN, J. P., FURGASON, M., HAJ-YAHYA, M., BRIK, A., CHENG, D., PENG, J. & YAO, T. 2014. The U4/U6 recycling factor SART3 has histone chaperone activity and associates with USP15 to regulate H2B deubiquitination. *The Journal of Biological Chemistry,* 289**,** 8916-8930.

LORINCZ, M. C., SCHÜBELER, D. & GROUDINE, M. 2001. Methylation-mediated proviral silencing is associated with MeCP2 recruitment and localized histone H3 deacetylation. *Molecular and Cellular Biology,* 21**,** 7913-7922.

LOUBLIER, S., BAYOT, A., RAK, M., EL-KHOURY, R., BÉNIT, P. & RUSTIN, P. 2011. The NDUFB6 subunit of the mitochondrial respiratory chain complex I is required for electron transfer activity: a proof of principle study on stable and controlled RNA interference in human cell lines. *Biochemical and Biophysical Research Communications,* 414**,** 367-372.

LU, M., ZHENG, L., HAN, B., WANG, L., WANG, P., LIU, H. & SUN, X. 2011. REST regulates DYRK1A transcription in a negative feedback loop. *The Journal of Biological Chemistry,* 286**,** 10755-10763.

LU, T., ARON, L., ZULLO, J., PAN, Y., KIM, H., CHEN, Y., YANG, T.-H. H., KIM, H.-M. M., DRAKE, D., LIU, X. S., BENNETT, D. A., COLAIÁCOVO, M. P. & YANKNER, B. A. 2014. REST and stress resistance in ageing and Alzheimer's disease. *Nature,* 507**,** 448-454.

LUNYAK, V. V., BURGESS, R., PREFONTAINE, G. G., NELSON, C., SZE, S. H., CHENOWETH, J., SCHWARTZ, P., PEVZNER, P. A., GLASS, C., MANDEL, G. & ROSENFELD, M. G. 2002. Corepressor-dependent silencing of chromosomal regions encoding neuronal genes. *Science,* 298**,** 1747-1752.

MAHAMDALLIE, S. S., HANKS, S., KARLIN, K. L., ZACHARIOU, A., R PERDEAUX, E., RUARK, E., SHAW, C. A., RENWICK, A., RAMSAY, E., YOST, S., ELLIOTT, A., BIRCH, J., CAPRA, M., GRAY, J., HALE, J., KINGSTON, J., LEVITT, G., MCLEAN, T., SHERIDAN, E., RENWICK, A., SEAL, S., STILLER, C., SEBIRE, N., WESTBROOK, T. F. & RAHMAN, N. 2015. Mutations in the transcriptional repressor REST predispose to Wilms tumor. *Nature Genetics,* 47**,** 1471-1474.

MAIER, T., GÜELL, M. & SERRANO, L. 2009. Correlation of mRNA and protein in complex biological samples. *FEBS Letters,* 583**,** 3966-3973.

MALEC, V., COULSON, J. M., URBÉ, S. & CLAGUE, M. J. 2015. Combined Analyses of the VHL and Hypoxia Signaling Axes in an Isogenic Pairing of Renal Clear Cell Carcinoma Cells. *Journal of Proteome Research,* 14**,** 5263-5272.

MANDEL, G., FIONDELLA, C. G., COVEY, M. V., LU, D. D., LOTURCO, J. J. & BALLAS, N. 2011. Repressor element 1 silencing transcription factor (REST) controls radial migration and temporal neuronal specification during neocortical development. *Proceedings of the National Academy of Sciences of the United States of America,* 108**,** 16789-16794.

MARTIN, D., ALLAGNAT, F., CHAFFARD, G., CAILLE, D., FUKUDA, M., REGAZZI, R., ABDERRAHMANI, A., WAEBER, G., MEDA, P.,

MAECHLER, P. & HAEFLIGER, J. A. 2008. Functional significance of repressor element 1 silencing transcription factor (REST) target genes in pancreatic beta cells. *Diabetologia,* 51**,** 1429-1439.
MARTIN, D., ALLAGNAT, F., GESINA, E., CAILLE, D., GJINOVCI, A., WAEBER, G., MEDA, P. & HAEFLIGER, J. A. 2012. Specific silencing of the REST target genes in insulin-secreting cells uncovers their participation in beta cell survival. *PLOS ONE,* 7**,** e45844.
MAUE, R. A., KRANER, S. D., GOODMAN, R. H. & MANDEL, G. 1990. Neuron-specific expression of the rat brain type II sodium channel gene is directed by upstream regulatory elements. *Neuron,* 4**,** 223-231.
MCDOWELL, G. S. & PHILPOTT, A. 2013. Non-canonical ubiquitylation: mechanisms and consequences. *The International Journal of Biochemistry & Cell Biology,* 45**,** 1833-1842.
MCGANN, J. C., OYER, J. A., GARG, S., YAO, H., LIU, J., FENG, X., LIAO, L., YATES, J. R. & MANDEL, G. 2014. Polycomb- and REST-associated histone deacetylases are independent pathways toward a mature neuronal phenotype. *eLife,* 3**,** e04235.
MCGOURAN, J. F., GAERTNER, S. R., ALTUN, M., KRAMER, H. B. & KESSLER, B. M. 2013. Deubiquitinating enzyme specificity for ubiquitin chain topology profiled by di-ubiquitin activity probes. *Chemistry & Biology,* 20**,** 1447-1455.
MEYER, H.-J. J. & RAPE, M. 2014. Enhanced protein degradation by branched ubiquitin chains. *Cell,* 157**,** 910-921.
MIWA, S., JOW, H., BATY, K., JOHNSON, A., CZAPIEWSKI, R., SARETZKI, G., TREUMANN, A. & VON ZGLINICKI, T. 2014. Low abundance of the matrix arm of complex I in mitochondria predicts longevity in mice. *Nature Communications,* 5**,** 3837.
MOGI, M., TOGARI, A., KONDO, T., MIZUNO, Y., KOMURE, O., KUNO, S., ICHINOSE, H. & NAGATSU, T. 1999. Brain-derived growth factor and nerve growth factor concentrations are decreased in the substantia nigra in Parkinson's disease. *Neuroscience Letters,* 270**,** 45-48.
MOSS, A. C., JACOBSON, G. M., WALKER, L. E., BLAKE, N. W., MARSHALL, E. & COULSON, J. M. 2009. SCG3 Transcript in Peripheral Blood Is a Prognostic Biomarker for REST-Deficient Small Cell Lung Cancer. *Clinical Cancer Research,* 15**,** 274-283.
MU, J.-J. J., WANG, Y., LUO, H., LENG, M., ZHANG, J., YANG, T., BESUSSO, D., JUNG, S. Y. & QIN, J. 2007. A proteomic analysis of ataxia telangiectasia-mutated (ATM)/ATM-Rad3-related (ATR) substrates identifies the ubiquitin-proteasome system as a regulator for DNA damage checkpoints. *The Journal of Biological Chemistry,* 282**,** 17330-17334.
MULLIGAN, P., WESTBROOK, T. F., OTTINGER, M., PAVLOVA, N., CHANG, B., MACIA, E., SHI, Y.-J., BARRETINA, J., LIU, J., HOWLEY, P. M., ELLEDGE, S. J. & SHI, Y. 2008. CDYL Bridges REST and Histone Methyltransferases for Gene Repression and Suppression of Cellular Transformation. *Molecular Cell,* 32**,** 718-726.

MURAI, K., NARUSE, Y., SHAUL, Y., AGATA, Y. & MORI, N. 2004. Direct interaction of NRSF with TBP: chromatin reorganization and core promoter repression for neuron-specific gene transcription. *Nucleic Acids Research,* 32**,** 3180-3189.

NAKAGAWA, T. & NAKAYAMA, K. 2015. Protein monoubiquitylation: targets and diverse functions. *Genes to Cells,* 20**,** 543-562.

NARIMATSU, T., MATSUURA, K., NAKADA, C., TSUKAMOTO, Y., HIJIYA, N., KAI, T., INOUE, T., UCHIDA, T., NOMURA, T., SATO, F., SETO, M., TAKEUCHI, I., MIMATA, H. & MORIYAMA, M. 2015. Downregulation of NDUFB6 due to 9p24.1-p13.3 loss is implicated in metastatic clear cell renal cell carcinoma. *Cancer Medicine,* 4**,** 112-124.

NECHIPORUK, T., MCGANN, J., MULLENDORFF, K., HSIEH, J., WURST, W., FLOSS, T. & MANDEL, G. 2016. The REST remodeling complex protects genomic integrity during embryonic neurogenesis. *eLife,* 5**,** e09584.

NEGRINI, S., PRADA, I., D'ALESSANDRO, R. & MELDOLESI, J. 2013. REST: an oncogene or a tumor suppressor? *Trends in Cell Biology,* 23**,** 289-295.

NESTI, E., CORSON, G. M., MCCLESKEY, M., OYER, J. A. & MANDEL, G. 2014. C-terminal domain small phosphatase 1 and MAP kinase reciprocally control REST stability and neuronal differentiation. *Proceedings of the National Academy of Sciences of the United States of America,* 111**,** 36.

NEUMANN, S. B., SEITZ, R., GORZELLA, A., HEISTER, A., DOEBERITZ, M. V. & BECKER, C. M. 2004. Relaxation of glycine receptor and onconeural gene transcription control in NRSF deficient small cell lung cancer cell lines. *Molecular Brain Research,* 120**,** 173-181.

NEVE, E. P., NORDLING, A., ANDERSSON, T. B., HELLMAN, U., DICZFALUSY, U., JOHANSSON, I. & INGELMAN-SUNDBERG, M. 2012. Amidoxime reductase system containing cytochrome b5 type B (CYB5B) and MOSC2 is of importance for lipid synthesis in adipocyte mitochondria. *The Journal of Biological Chemistry,* 287**,** 6307-6317.

NISHI, R., WIJNHOVEN, P., LE SAGE, C., TJEERTES, J., GALANTY, Y., FORMENT, J. V., CLAGUE, M. J., URBÉ, S. & JACKSON, S. P. 2014. Systematic characterization of deubiquitylating enzymes for roles in maintaining genome integrity. *Nature Cell Biology,* 16**,** 1016.

NISHIHARA, S., TSUDA, L. & OGURA, T. 2003. The canonical Wnt pathway directly regulates NRSF/REST expression in chick spinal cord. *Biochemical and Biophysical Research Communications,* 311**,** 55-63.

NORTHCOTT, P. A., NAKAHARA, Y., WU, X., FEUK, L., ELLISON, D. W., CROUL, S., S., M., KONGKHAM, P. N., PEACOCK, J., DUBUC, A., RA, Y. S., ZILBERBERG, K., MCLEOD, J., SCHERER, S. W., RAO, J. S., EBERHART, C. G., GRAJKOWSKA, W., GILLESPIE, Y., LACH, B., GRUNDY, R., POLLACK, I. F., HAMILTON, R. L., VAN METER, T., CARLOTTI, C. G., BOOP, F., BIGNER, D., GILBERTSON, R. J., RUTKA, J. T. & TAYLOR, M. D. 2009. Multiple recurrent genetic

events converge on control of histone lysine methylation in medulloblastoma. *Nature Genetics,* 41**,** 465-472.

ONG, S.-E. E., BLAGOEV, B., KRATCHMAROVA, I., KRISTENSEN, D. B., STEEN, H., PANDEY, A. & MANN, M. 2002. Stable isotope labeling by amino acids in cell culture, SILAC, as a simple and accurate approach to expression proteomics. *Molecular & Cellular Proteomics,* 1**,** 376-386.

OOI, L., BELYAEV, N. D., MIYAKE, K., WOOD, I. C. & BUCKLEY, N. J. 2006. BRG1 chromatin remodeling activity is required for efficient chromatin binding by repressor element 1-silencing transcription factor (REST) and facilitates REST-mediated repression. *The Journal of Biological Chemistry,* 281**,** 38974-38980.

OTTO, S. J., MCCORKLE, S. R., HOVER, J., CONACO, C., HAN, J.-J. J., IMPEY, S., YOCHUM, G. S., DUNN, J. J., GOODMAN, R. H. & MANDEL, G. 2007. A new binding motif for the transcriptional repressor REST uncovers large gene networks devoted to neuronal functions. *The Journal of Neuroscience,* 27**,** 6729-6739.

PACKER, A. N., XING, Y., HARPER, S. Q., JONES, L. & DAVIDSON, B. L. 2008. The bifunctional microRNA miR-9/miR-9* regulates REST and CoREST and is downregulated in Huntington's disease. *The Journal of Neuroscience,* 28**,** 14341-14346.

PALM, K., BELLUARDO, N., METSIS, M. & TIMMUSK, T. 1998. Neuronal expression of zinc finger transcription factor REST/NRSF/XRB gene. *Journal of Neuroscience,* 18**,** 1280-1296.

PALM, K., METSIS, M. & TIMMUSK, T. 1999. Neuron-specific splicing of zinc finger transcription factor REST/NRSF/XBR is frequent in neuroblastomas and conserved in human, mouse and rat. *Molecular Brain Research,* 72**,** 30-39.

PANCE, A., LIVESEY, F. J. & JACKSON, A. P. 2006. A role for the transcriptional repressor REST in maintaining the phenotype of neurosecretory-deficient PC12 cells. *Journal of Neurochemistry,* 99**,** 1435-1444.

PAQUETTE, A. J., PEREZ, S. E. & ANDERSON, D. J. 2000. Constitutive expression of the neuron-restrictive silencer factor (NRSF)/REST in differentiating neurons disrupts neuronal gene expression and causes axon pathfinding errors in vivo. *Proceedings of the National Academy of Sciences,* 97**,** 12318-12323.

PARK, K. C., CHOI, E. J., MIN, S. W., CHUNG, S. S., KIM, H., SUZUKI, T., TANAKA, K. & CHUNG, C. H. 2000. Tissue-specificity, functional characterization and subcellular localization of a rat ubiquitin-specific processing protease, UBP109, whose mRNA expression is developmentally regulated. *Biochemical Journal,* 349**,** 443-453.

PATEL, P. D., BOCHAR, D. A., TURNER, D. L., MENG, F., MUELLER, H. M. & PONTRELLO, C. G. 2007. Regulation of Tryptophan Hydroxylase-2 Gene Expression by a Bipartite RE-1 Silencer of Transcription/Neuron restrictive Silencing Factor (REST/NRSF) Binding Motif. *Journal of Biological Chemistry,* 282**,** 26717-26724.

PAVLETICH, N. P. & PABO, C. O. 1991. Zinc finger-DNA recognition: crystal structure of a Zif268-DNA complex at 2.1 A. *Science,* 252**,** 809-817.
PERERA, A., EISEN, D., WAGNER, M., LAUBE, S. K., KÜNZEL, A. F., KOCH, S., STEINBACHER, J., SCHULZE, E., SPLITH, V., MITTERMEIER, N., MÜLLER, M., BIEL, M., CARELL, T. & MICHALAKIS, S. 2015. TET3 is recruited by REST for context-specific hydroxymethylation and induction of gene expression. *Cell Reports,* 11**,** 283-294.
PINTO-FERNANDEZ, A. & KESSLER, B. M. 2016. DUBbing Cancer: Deubiquitylating Enzymes Involved in Epigenetics, DNA Damage and the Cell Cycle As Therapeutic Targets. *Frontiers in Genetics,* 7**,** 133.
POLIANSKYTE, Z., PEITSARO, N., DAPKUNAS, A., LIOBIKAS, J., SOLIYMANI, R., LALOWSKI, M., SPEER, O., SEITSONEN, J., BUTCHER, S., CEREGHETTI, G. M., LINDER, M. D., MERCKEL, M., THOMPSON, J. & ERIKSSON, O. 2009. LACTB is a filament-forming protein localized in mitochondria. *Proceedings of the National Academy of Sciences,* 106**,** 18960-18965.
PONTEN, J., JENSEN, F. & KOPROWSKI, H. 1963. Morphological and virological investigation of human tissue cultures transformed with SV40. *Journal of Cellular and Comparative Physiology,* 61**,** 145-163.
RAJ, B., IRIMIA, M., BRAUNSCHWEIG, U., STERNE-WEILER, T., O'HANLON, D., LIN, Z.-Y. Y., CHEN, G. I., EASTON, L. E., ULE, J., GINGRAS, A.-C. C., EYRAS, E. & BLENCOWE, B. J. 2014. A global regulatory mechanism for activating an exon network required for neurogenesis. *Molecular Cell,* 56**,** 90-103.
RAJ, B., O'HANLON, D., VESSEY, J. P., PAN, Q., RAY, D., BUCKLEY, N. J., MILLER, F. D. & BLENCOWE, B. J. 2011. Cross-regulation between an alternative splicing activator and a transcription repressor controls neurogenesis. *Molecular Cell,* 43**,** 843-850.
RAMOS, A. H., DUTT, A., MERMEL, C., PERNER, S., CHO, J., LAFARGUE, C. J., JOHNSON, L. A., STIEDL, A. C., TANAKA, K. E., BASS, A. J., BARRETINA, J., WEIR, B. A., BEROUKHIM, R., THOMAS, R. K., MINNA, J. D., CHIRIEAC, L. R., LINDEMAN, N. I., GIORDANO, T., BEER, D. G., WAGNER, P., WISTUBA, I. I., RUBIN, M. A. & MEYERSON, M. 2009. Amplification of chromosomal segment 4q12 in non-small cell lung cancer. *Cancer Biology & Therapy,* 8**,** 2042-2050.
RAVACHE, M., WEBER, C., MÉRIENNE, K. & TROTTIER, Y. 2010. Transcriptional activation of REST by Sp1 in Huntington's disease models. *PLOS ONE,* 5**,** e14311.
RAVANPAY, A. C., HANSEN, S. J. & OLSON, J. M. 2010. Transcriptional inhibition of REST by NeuroD2 during neuronal differentiation. *Molecular and Cellular Neuroscience,* 44**,** 178-189.
REDDEL, R. R., KE, Y., GERWIN, B. I., MCMENAMIN, M. G., LECHNER, J. F., SU, R. T., BRASH, D. E., PARK, J. B., RHIM, J. S. & HARRIS, C. C. 1988. Transformation of human bronchial epithelial cells by infection with SV40 or adenovirus-12 SV40 hybrid virus, or transfection via strontium phosphate coprecipitation with a plasmid

containing SV40 early region genes. *Cancer Research,* 48**,** 1904-1909.
REDDY, B. Y., GRECO, S. J., PATEL, P. S., TRZASKA, K. A. & RAMESHWAR, P. 2009. RE-1-silencing transcription factor shows tumor-suppressor functions and negatively regulates the oncogenic TAC1 in breast cancer cells. *Proceedings of the National Academy of Sciences,* 106**,** 4408-4413.
REN, X. & KERPPOLA, T. K. 2011. REST interacts with Cbx proteins and regulates polycomb repressive complex 1 occupancy at RE1 elements. *Molecular and Cellular Biology,* 31**,** 2100-2110.
REYES-TURCU, F. E., VENTII, K. H. & WILKINSON, K. D. 2009. Regulation and cellular roles of ubiquitin-specific deubiquitinating enzymes. *Annual Review of Biochemistry,* 78**,** 363-397.
RICKMAN, D. S., BELTRAN, H., DEMICHELIS, F. & RUBIN, M. A. 2017. Biology and evolution of poorly differentiated neuroendocrine tumors. *Nature Medicine,* 2**3,** 1-10.
RITORTO, M. S., EWAN, R., PEREZ-OLIVA, A. B., KNEBEL, A., BUHRLAGE, S. J., WIGHTMAN, M., KELLY, S. M., WOOD, N. T., VIRDEE, S., GRAY, N. S., MORRICE, N. A., ALESSI, D. R. & TROST, M. 2014. Screening of DUB activity and specificity by MALDI-TOF mass spectrometry. *Nature Communications,* 5**,** 4763.
ROCKOWITZ, S., LIEN, W.-H. H., PEDROSA, E., WEI, G., LIN, M., ZHAO, K., LACHMAN, H. M., FUCHS, E. & ZHENG, D. 2014. Comparison of REST cistromes across human cell types reveals common and context-specific functions. *PLOS Computational Biology,* 10**,** e1003671.
RODENAS-RUANO, A., CHÁVEZ, A. E. E., COSSIO, M. J., CASTILLO, P. E. & ZUKIN, R. S. 2012. REST-dependent epigenetic remodeling promotes the developmental switch in synaptic NMDA receptors. *Nature Neuroscience,* 15**,** 1382-1390.
ROOPRA, A., QAZI, R., SCHOENIKE, B., DALEY, T. J. & MORRISON, J. F. 2004. Localized domains of G9a-mediated histone methylation are required for silencing of neuronal genes. *Molecular Cell,* 14**,** 727-738.
ROOPRA, A., SHARLING, L., WOOD, I. C., BRIGGS, T., BACHFISCHER, U., PAQUETTE, A. J. & BUCKLEY, N. J. 2000. Transcriptional repression by neuron-restrictive silencer factor is mediated via the Sin3-histone deacetylase complex. *Molecular and Cellular Biology,* 20**,** 2147-2157.
SACCO, J. J., COULSON, J. M., CLAGUE, M. J. & URBÉ, S. 2010. Emerging roles of deubiquitinases in cancer-associated pathways. *IUBMB Life,* 62**,** 140-157.
SAEED, A. I., BHAGABATI, N. K., BRAISTED, J. C., LIANG, W., SHAROV, V., HOWE, E. A., LI, J., THIAGARAJAN, M., WHITE, J. A. & QUACKENBUSH, J. 2006. TM4 microarray software suite. *Methods in Enzymology,* 411**,** 134-193.
SAHTOE, D. D. & SIXMA, T. K. 2015. Layers of DUB regulation. *Trends in Biochemical Sciences,* 40**,** 456-467.

SCHEFFNER, M., HUIBREGTSE, J. M., VIERSTRA, R. D. & HOWLEY, P. M. 1993. The HPV-16 E6 and E6-AP complex functions as a ubiquitin-protein ligase in the ubiquitination of p53. *Cell,* 75**,** 495-505.
SCHEFFNER, M., WERNESS, B. A., HUIBREGTSE, J. M., LEVINE, A. J. & HOWLEY, P. M. 1990. The E6 oncoprotein encoded by human papillomavirus types 16 and 18 promotes the degradation of p53. *Cell,* 63**,** 1129-1136.
SCHMITTGEN, T. D. & LIVAK, K. J. 2008. Analyzing real-time PCR data by the comparative C(T) method. *Nature Protocols,* 3**,** 1101-1108.
SCHOENHERR, C. J. & ANDERSON, D. J. 1995. The neuron-restrictive silencer factor (NRSF) - a coordinate repressor of multiple neuron-specific genes. *Science,* 267**,** 1360-1363.
SCHOENHERR, C. J., PAQUETTE, A. J. & ANDERSON, D. J. 1996. Identification of potential target genes for the neuron-restrictive silencer factor. *Proceedings of the National Academy of Sciences of the United States of America,* 93**,** 9881-9886.
SCHRÒCK, E., THIEL, G., LOZANOVA, T., DU MANOIR, S., MEFFERT, M. C., JAUCH, A., SPEICHER, M. R., NURNBERG, P., VOGEL, S., JANISCH, W., DONIS-KELLER, H., REID, T., WITKOWSKI, R. & CREMER, T. 1994. Comparative genomic hybridization of human malignant gliomas reveals multiple amplification sites and nonrandom chromosomal gains and losses. *The American Journal of Pathology,* 144**,** 1203-1218.
SCHWANHÄUSSER, B., BUSSE, D., LI, N., DITTMAR, G., SCHUCHHARDT, J., WOLF, J., CHEN, W. & SELBACH, M. 2011. Global quantification of mammalian gene expression control. *Nature,* 473**,** 337-342.
SCHWEITZER, K., BOZKO, P. M., DUBIEL, W. & NAUMANN, M. 2007. CSN controls NF-kappaB by deubiquitinylation of IkappaBalpha. *The EMBO Journal,* 26**,** 1532-1541.
SETH, K. A. & MAJZOUB, J. A. 2001. Repressor element silencing transcription factor/neuronrestrictive silencing factor (REST/NRSF) can act as an enhancer as well as a repressor of corticotropin-releasing hormone gene transcription. *Journal of Biological Chemistry,* 276**,** 13917-13923.
SHERWOOD, R. I., HASHIMOTO, T., O'DONNELL, C. W., LEWIS, S., BARKAL, A. A., VAN HOFF, J. P., KARUN, V., JAAKKOLA, T. & GIFFORD, D. K. 2014. Discovery of directional and nondirectional pioneer transcription factors by modeling DNase profile magnitude and shape. *Nature Biotechnology,* 32**,** 171-178.
SHI, Y., LAN, F., MATSON, C., MULLIGAN, P., WHETSTINE, J. R., COLE, P. A., CASERO, R. A. & SHI, Y. 2004. Histone demethylation mediated by the nuclear amine oxidase homolog LSD1. *Cell,* 119**,** 941-953.
SHIMOJO, M. 2006. Characterization of the nuclear targeting signal of REST/NRSF. *Neuroscience Letters,* 398**,** 161-166.
SHIMOJO, M. 2008. Huntingtin regulates RE1-silencing transcription factor/neuron-restrictive silencer factor (REST/NRSF) nuclear

trafficking indirectly through a complex with REST/NRSF-interacting LIM domain protein (RILP) and dynactin p150 Glued. *The Journal of Biological Chemistry,* 283**,** 34880-34886.
SHIMOJO, M. & HERSH, L. B. 2003. REST/NRSF-interacting LIM domain protein, a putative nuclear translocation receptor. *Molecular and Cellular Biology,* 23**,** 9025-9031.
SHIMOJO, M. & HERSH, L. B. 2006. Characterization of the REST/NRSF-interacting LIM domain protein (RILP): localization and interaction with REST/NRSF. *Journal of Neurochemistry,* 96**,** 1130-1138.
SHIMOJO, M., LEE, J. H. & HERSH, L. B. 2001. Role of zinc finger domains of the transcription factor neuron-restrictive silencer factor/repressor element-1 silencing transcription factor in DNA binding and nuclear localization. *Journal of Biological Chemistry,* 276**,** 13121-13126.
SHIMOJO, M., SHUDO, Y., IKEDA, M., KOBASHI, T. & ITO, S. 2013. The small cell lung cancer-specific isoform of RE1-silencing transcription factor (REST) is regulated by neural-specific Ser/Arg repeat-related protein of 100 kDa (nSR100). *Molecular Cancer Research,* 11**,** 1258-1268.
SINGH, S. K., KAGALWALA, M. N., PARKER-THORNBURG, J., ADAMS, H. & MAJUMDER, S. 2008. REST maintains self-renewal and pluripotency of embryonic stem cells. *Nature,* 453**,** 223-U11.
SMITH, L. M. & KELLEHER, N. L. 2013. Proteoform: a single term describing protein complexity. *Nature Methods,* 10**,** 186-187.
SMITH, M. H., PLOEGH, H. L. & WEISSMAN, J. S. 2011. Road to ruin: targeting proteins for degradation in the endoplasmic reticulum. *Science,* 334**,** 1086-90.
SOBOLEVA, T. A., JANS, D. A., JOHNSON-SALIBA, M. & BAKER, R. T. 2005. Nuclear-cytoplasmic shuttling of the oncogenic mouse UNP/USP4 deubiquitylating enzyme. *Journal of Biological Chemistry,* 280**,** 745-752.
SONG, E. J., WERNER, S. L., NEUBAUER, J., STEGMEIER, F., ASPDEN, J., RIO, D., HARPER, J. W., ELLEDGE, S. J., KIRSCHNER, M. W. & RAPE, M. 2010. The Prp19 complex and the Usp4Sart3 deubiquitinating enzyme control reversible ubiquitination at the spliceosome. *Genes & Development,* 24**,** 1434-1447.
SOWA, M. E., BENNETT, E. J., GYGI, S. P. & HARPER, J. W. 2009. Defining the human deubiquitinating enzyme interaction landscape. *Cell,* 138**,** 389-403.
SPITZ, F. & FURLONG, E. E. M. 2012. Transcription factors: from enhancer binding to developmental control. *Nature Reviews Genetics,* 13**,** 613-626.
STADLER, M. B., MURR, R., BURGER, L., IVANEK, R., LIENERT, F., SCHOLER, A., VAN NIMWEGEN, E., WIRBELAUER, C., OAKELEY, E. J., GAIDATZIS, D., TIWARI, V. K. & SCHUBELER, D. 2011. DNA-binding factors shape the mouse methylome at distal regulatory regions. *Nature,* 480**,** 490-495.
STEGMEIER, F., RAPE, M., DRAVIAM, V. M., NALEPA, G., SOWA, M. E., ANG, X. L., MCDONALD III, E. R., LI, M. Z., HANNON, G. J.,

SORGER, P. K., KIRSCHNER, M. W., HARPER, J. W. & ELLEDGE, S. J. 2007. Anaphase initiation is regulated by antagonistic ubiquitination and deubiquitination activities. *Nature,* 446**,** 876-881.
SU, X., GOPALAKRISHNAN, V., STEARNS, D., ALDAPE, K., F. LANG, F., FULLER, G., SNYDER, E., EBERHART, C. G. & MAJUMDER, S. 2006. Abnormal expression of REST/NRSF and Myc in neural stem/progenitor cells causes cerebellar tumors by blocking neuronal differentiation. *Molecular and Cellular Biology,* 26**,** 1666-1678.
SUGIURA, A., MCLELLAND, G.-L. L., FON, E. A. & MCBRIDE, H. M. 2014. A new pathway for mitochondrial quality control: mitochondrial-derived vesicles. *The EMBO Journal,* 33**,** 2142-2156.
SWATEK, K. N. & KOMANDER, D. 2016. Ubiquitin modifications. *Cell Research,* 26**,** 399-422.
SZCZEPANEK, K., LESNEFSKY, E. J. & LARNER, A. C. 2012. Multi-tasking: nuclear transcription factors with novel roles in the mitochondria. *Trends in Cell Biology,* 22**,** 429-437.
TACHIBANA, M., SUGIMOTO, K., FUKUSHIMA, T. & SHINKAI, Y. 2001. Set domain-containing protein, G9a, is a novel lysine-preferring mammalian histone methyltransferase with hyperactivity and specific selectivity to lysines 9 and 27 of histone H3. *Journal of Biological Chemistry,* 276**,** 25309-25317.
TAPIA-RAMÍREZ, J., EGGEN, B. J., PERAL-RUBIO, M. J., TOLEDO-ARAL, J. J. & MANDEL, G. 1997. A single zinc finger motif in the silencing factor REST represses the neural-specific type II sodium channel promoter. *Proceedings of the National Academy of Sciences of the United States of America,* 94**,** 1177-1182.
TATENO, M., UKAI, W., HASHIMOTO, E., IKEDA, H. & SAITO, T. 2006. Implication of increased NRSF/REST binding activity in the mechanism of ethanol inhibition of neuronal differentiation. *Journal of Neural Transmission,* 113**,** 283-293.
TAWADROS, T., MARTIN, D., ABDERRAHMANI, A., LEISINGER, H. J., WAEBER, G. & HAEFLIGER, J. A. 2005. IB1/JIP-1 controls JNK activation and increased during prostatic LNCaP cells neuroendocrine differentiation. *Cellular Signalling,* 17**,** 929-939.
TERASAKI, T., MATSUNO, Y., SHIMOSATO, Y., YAMAGUCHI, K., ICHINOSE, H., NAGATSU, T. & KATO, K. 1994. Establishment of a human small cell lung cancer cell line producing a large amount of anti-diuretic hormone. *Japanese Journal of Cancer Research,* 85**,** 718-722.
THIEL, G., EKICI, M. & RÖSSLER, O. G. 2015. RE-1 silencing transcription factor (REST): a regulator of neuronal development and neuronal/endocrine function. *Cell and Tissue Research,* 359**,** 99-109.
THIEL, G., LIETZ, M. & CRAMER, M. 1998. Biological activity and modular structure of RE-1-silencing transcription factor (REST), a repressor of neuronal genes. *The Journal of Biological Chemistry,* 273**,** 26891-26899.
TIMANI, K. A., LIU, Y., SUVANNASANKHA, A. & HE, J. J. 2014. Regulation of ubiquitin-proteasome system-mediated Tip110 protein degradation

by USP15. *The International Journal of Biochemistry & Cell Biology,* 54**,** 10-19.
TIMMUSK, T., PALM, K., LENDAHL, U. & METSIS, M. 1999. Brain-derived neurotrophic factor expression in vivo is under the control of neuron-restrictive silencer element. *The Journal of Biological Chemistry,* 274**,** 1078-1084.
TODI, S. V., SCAGLIONE, K. M., BLOUNT, J. R., BASRUR, V., CONLON, K. P., PASTORE, A., ELENITOBA-JOHNSON, K. & PAULSON, H. L. 2010. Activity and cellular functions of the deubiquitinating enzyme and polyglutamine disease protein ataxin-3 are regulated by ubiquitination at lysine 117. *Journal of Biological Chemistry,* 285**,** 39303-39313.
TODI, S. V., WINBORN, B. J., SCAGLIONE, K. M., BLOUNT, J. R., TRAVIS, S. M. & PAULSON, H. L. 2009. Ubiquitination directly enhances activity of the deubiquitinating enzyme ataxin‐3. *The EMBO Journal,* 28**,** 372-382.
TORRE, L. A., BRAY, F., SIEGEL, R. L., FERLAY, J., LORTET-TIEULENT, J. & JEMAL, A. 2015. Global cancer statistics, 2012. *CA: A Cancer Journal for Clinicians,* 65**,** 87-108.
TORRE, S., POLYAK, M. J., LANGLAIS, D., FODIL, N., KENNEDY, J. M., RADOVANOVIC, I., BERGHOUT, J., LEIVA-TORRES, G. A., KRAWCZYK, C. M., ILANGUMARAN, S., MOSSMAN, K., LIANG, C., KNOBELOCH, K.-P. P., HEALY, L. M., ANTEL, J., ARBOUR, N., PRAT, A., MAJEWSKI, J., LATHROP, M., VIDAL, S. M. & GROS, P. 2017. USP15 regulates type I interferon response and is required for pathogenesis of neuroinflammation. *Nature Immunology,* 18**,** 54-63.
TSAI, M. C., MANOR, O., WAN, Y., MOSAMMAPARAST, N., WANG, J. K., LAN, F., SHI, Y., SEGAL, E. & CHANG, H. Y. 2010. Long noncoding RNA as modular scaffold of histone modification complexes. *Science,* 329**,** 689-693.
TYANOVA, S., TEMU, T., SINITCYN, P., CARLSON, A., HEIN, M. Y., GEIGER, T., MANN, M. & COX, J. 2016. The Perseus computational platform for comprehensive analysis of (prote)omics data. *Nature Methods,* 13**,** 731-740.
UDYAVAR, A. R., WOOTEN, D. J., HOEKSEMA, M., BANSAL, M., CALIFANO, A., ESTRADA, L., SCHNELL, S., IRISH, J. M., MASSION, P. P. & QUARANTA, V. 2017. Novel Hybrid Phenotype Revealed in Small Cell Lung Cancer by a Transcription Factor Network Model That Can Explain Tumor Heterogeneity. *Cancer Research,* 77**,** 1063-1074.
URBÉ, S., LIU, H., HAYES, S. D., HERIDE, C., RIGDEN, D. J. & CLAGUE, M. J. 2012. Systematic survey of deubiquitinase localization identifies USP21 as a regulator of centrosome- and microtubule-associated functions. *Molecular Biology of the Cell,* 23**,** 1095-1103.
VAN IERSEL, M. P., KELDER, T., PICO, A. R., HANSPERS, K., COORT, S., CONKLIN, B. R. & EVELO, C. 2008. Presenting and exploring biological pathways with PathVisio. *BMC Bioinformatics,* 9**,** 399.

VAQUERIZAS, J. M., KUMMERFELD, S. K., TEICHMANN, S. A. & LUSCOMBE, N. M. 2009. A census of human transcription factors: function, expression and evolution. *Nature Reviews Genetics,* 10**,** 252-263.

VENTII, K. H. & WILKINSON, K. D. 2008. Protein partners of deubiquitinating enzymes. *Biochemical Journal,* 414**,** 161-175.

VILLENEUVE, N. F., TIAN, W., WU, T., SUN, Z., LAU, A., CHAPMAN, E., FANG, D. & ZHANG, D. D. 2013. USP15 negatively regulates Nrf2 through deubiquitination of Keap1. *Molecular cell,* 51**,** 68-79.

VLASSCHAERT, C., XIA, X., COULOMBE, J. & GRAY, D. A. 2015. Evolution of the highly networked deubiquitinating enzymes USP4, USP15, and USP11. *BMC Evolutionary Biology,* 15**,** 230.

VOLVERT, M.-L. L., PRÉVOT, P.-P. P., CLOSE, P., LAGUESSE, S., PIROTTE, S., HEMPHILL, J., ROGISTER, F., KRUZY, N., SACHELI, R., MOONEN, G., DEITERS, A., MERKENSCHLAGER, M., CHARIOT, A., MALGRANGE, B., GODIN, J. D. & NGUYEN, L. 2014. MicroRNA targeting of CoREST controls polarization of migrating cortical neurons. *Cell Reports,* 7**,** 1168-1183.

VOS, R. M., ALTREUTER, J., WHITE, E. A. & HOWLEY, P. M. 2009. The ubiquitin-specific peptidase USP15 regulates human papillomavirus type 16 E6 protein stability. *Journal of Virology,* 83**,** 8885-8892.

WAGONER, M. P., GUNSALUS, K. T., SCHOENIKE, B., RICHARDSON, A. L., FRIEDL, A. & ROOPRA, A. 2010. The transcription factor REST is lost in aggressive breast cancer. *PLOS Genetics,* 6**,** e1000979.

WALLS, G. A. & TWENTYMAN, P. R. 1985. Cloning of human lung cancer cells. *British Journal of Cancer,* 52**,** 505-513.

WANG, F., DURFEE, L. A. & HUIBREGTSE, J. M. 2013. A cotranslational ubiquitination pathway for quality control of misfolded proteins. *Molecular Cell,* 50**,** 368-378.

WEI, N., SERINO, G. & DENG, X. W. 2008. The COP9 signalosome: more than a protease. *Trends in Biochemical Sciences,* 33**,** 592-600.

WESTBROOK, T. F., HU, G., ANG, X. L., MULLIGAN, P., PAVLOVA, N. N., LIANG, A., LENG, Y., MAEHR, R., SHI, Y., HARPER, J. W. & ELLEDGE, S. J. 2008. SCF beta-TRCP controls oncogenic transformation and neural differentiation through REST degradation. *Nature,* 452**,** 370-U11.

WESTBROOK, T. F., MARTIN, E. S., SCHLABACH, M. R., LENG, Y. M., LIANG, A. C., FENG, B., ZHAO, J. J., ROBERTS, T. M., MANDEL, G., HANNON, G. J., DEPINHO, R. A., CHIN, L. & ELLEDGE, S. J. 2005. A genetic screen for candidate tumor suppressors identifies REST. *Cell,* 121**,** 837-848.

WILKINSON, K. D., URBAN, M. K. & HAAS, A. L. 1980. Ubiquitin is the ATP-dependent proteolysis factor I of rabbit reticulocytes. *The Journal of Biological Chemistry,* 255**,** 7529-7532.

WILLERT, J., EPPING, M., POLLACK, J. R., BROWN, P. O. & NUSSE, R. 2002. A transcriptional response to Wnt protein in human embryonic carcinoma cells. *BMC Developmental Biology,* 2**,** 8.

WOLFE, S. A., NEKLUDOVA, L. & PABO, C. O. 2000. DNA recognition by Cys2His2 zinc finger proteins. *Annual Review of Biophysics and Biomolecular Structure,* 29**,** 183-212.
WU, J. & XIE, X. 2006. Comparative sequence analysis reveals an intricate network among REST, CREB and miRNA in mediating neuronal gene expression. *Genome Biology,* 7**,** R85.
XU, M., SKAUG, B., ZENG, W. & CHEN, Z. J. 2009a. A ubiquitin replacement strategy in human cells reveals distinct mechanisms of IKK activation by TNFalpha and IL-1beta. *Molecular Cell,* 36**,** 302-314.
XU, M., TAKANASHI, M., OIKAWA, K., TANAKA, M., NISHI, H., ISAKA, K., KUDO, M. & KURODA, M. 2009b. USP15 plays an essential role for caspase-3 activation during Paclitaxel-induced apoptosis. *Biochemical and Biophysical Research Communications,* 388**,** 366-371.
YAU, R. & RAPE, M. 2016. The increasing complexity of the ubiquitin code. *Nature Cell Biology,* 18**,** 579-586.
YE, Y., SCHEEL, H., HOFMANN, K. & KOMANDER, D. 2009. Dissection of USP catalytic domains reveals five common insertion points. *Molecular BioSystems,* 5**,** 1797-1808.
YEO, M., BERGLUND, K., AUGUSTINE, G. & LIEDTKE, W. 2009. Novel repression of Kcc2 transcription by REST–RE-1 controls developmental switch in neuronal chloride. *Journal of Neuroscience,* 29**,** 14652-14662.
YEO, M., LEE, S.-K., LEE, B., RUIZ, E. C., PFAFF, S. L. & GILL, G. N. 2005. Small CTD phosphatases function in silencing neuronal gene expression. *Science,* 307**,** 596-600.
YEO, M., LIN, P. S., DAHMUS, M. E. & GILL, G. N. 2003. A novel RNA polymerase II C-terminal domain phosphatase that preferentially dephosphorylates serine 5. *The Journal of Biological Chemistry,* 278**,** 26078-26085.
YOGEV, O. & PINES, O. 2011. Dual targeting of mitochondrial proteins: mechanism, regulation and function. *Biochimica et Biophysica Acta,* 1808**,** 1012-1020.
ZARET, K. S. 2014. Genome reactivation after the silence in mitosis: recapitulating mechanisms of development? *Developmental Cell,* 29**,** 132-134.
ZHANG, D., WU, B., WANG, P., WANG, Y., LU, P., NECHIPORUK, T., FLOSS, T., GREALLY, J. M., ZHENG, D. & ZHOU, B. 2017. Non-CpG methylation by DNMT3B facilitates REST binding and gene silencing in developing mouse hearts. *Nucleic Acids Research,* 45**,** 3102-3115.
ZHANG, L., ZHOU, F. F., DRABSCH, Y., GAO, R., SNAAR-JAGALSKA, B. E., MICKANIN, C., HUANG, H., SHEPPARD, K. A., PORTER, J. A., LU, C. X. & TEN DIJKE, P. 2012. USP4 is regulated by AKT phosphorylation and directly deubiquitylates TGF-[beta] type I receptor. *Nature Cell Biology,* 14**,** 717-726.
ZHANG, Q., HARDING, R., HOU, F., DONG, A., WALKER, J. R., BTEICH, J. & TONG, Y. 2016. Structural Basis of the Recruitment of Ubiquitin-specific Protease USP15 by Spliceosome Recycling Factor SART3. *The Journal of Biological Chemistry,* 291**,** 17283-17292.

ZHANG, X., COLEMAN, I. M., BROWN, L. G., TRUE, L. D., KOLLATH, L., LUCAS, J. M., LAM, H. M., DUMPIT, R., COREY, E., CHERY, L., LAKELY, B., HIGANO, C. S., MONTGOMERY, B., ROUDIER, M., LANGE, P. H., NELSON, P. S., VESSELLA, R. L. & MORRISSEY, C. 2015. SRRM4 expression and the loss of REST activity may promote the emergence of the neuroendocrine phenotype in castration-resistant prostate cancer. *Clinical Cancer Research,* 21**,** 4698-4708.

ZHENG, D., ZHAO, K. & MEHLER, M. F. 2009. Profiling RE1/REST-mediated histone modifications in the human genome. *Genome Biology,* 10**,** R9.

ZHU, J., VINOTHKUMAR, K. R. & HIRST, J. 2016. Structure of mammalian respiratory complex I. *Nature,* 536**,** 354-358.

ZHU, Y., LIU, C., CUI, Y., NADIMINTY, N., LOU, W. & GAO, A. C. 2014. Interleukin-6 induces neuroendocrine differentiation (NED) through suppression of RE-1 silencing transcription factor (REST). *The Prostate,* 74**,** 1086-1094.

ZONG, W.-X. X., RABINOWITZ, J. D. & WHITE, E. 2016. Mitochondria and Cancer. *Molecular Cell,* 61**,** 667-676.

ZOU, Q., JIN, J., HU, H., LI, H. S., ROMANO, S., XIAO, Y., NAKAYA, M., ZHOU, X., CHENG, X., YANG, P., LOZANO, G., ZHU, C., WATOWICH, S. S., ULLRICH, S. E. & SUN, S.-C. C. 2014. USP15 stabilizes MDM2 to mediate cancer-cell survival and inhibit antitumor T cell responses. *Nature Immunology,* 15**,** 562-570.

ZUCCATO, C., TARTARI, M., CROTTI, A., GOFFREDO, D., VALENZA, M., CONTI, L., CATAUDELLA, T., LEAVITT, B. R., HAYDEN, M. R., TIMMUSK, T., RIGAMONTI, D. & CATTANEO, E. 2003. Huntingtin interacts with REST/NRSF to modulate the transcription of NRSE-controlled neuronal genes. *Nature Genetics,* 35**,** 76-83.